FACULTY OF TECHNOLOGY

HYDROTHERMAL ALTERATION AND HOST ROCK COMPOSITION OF THE PYHÄSALMI VOLGANOGENIC MASSIVE SULPHIDE DEPOSIT, CENTRAL FINLAND

Jesse Sakari Hettula

MASTER'S PROGRAMME IN GEOSCIENCES

Master's thesis

2019

TIIVISTELMÄ
OPINNÄYTETYÖSTÄ Oulun yliopisto Teknillinen tiedekunta

Koulutusohjelma (kandidaatintyö, diplomityö) Geologian ja mineralogian koulutusohjelma	Pääaineopintojen ala (lisensiaatintyö)
Tekijä Hettula, Jesse Sakari	Työn ohjaaja yliopistolla Strand, K., professori, Holger, P., professori

Työn nimi

Pyhäsalmen vulkanogeenisen massiivisen sulfidimalmin isäntäkiven hydroterminen muuntuminen ja koostumus, Keski-Suomi

Opintosuunta	Työn laji	Aika	Sivumäärä
Geotieteet	Pro Gradu	Marraskuu 2019	68

Tiivistelmä

Pyhäsalmen vulkanogeeninen massiivinen sulfidi – esiintymä (VMS) alkaa maan pinnalta ja yltää 1420 m syvyyteen. Muodoltaan esiintymä koostuu ensimmäisen 1050 m matkalta pitkästä tasomaisesta rakenteesta, mudostaen hieman länteen ja jyrkästi alaspäin suuntautuvan, pohjois-etelä suunnassa tasomaisen massiivisen sulfidiesiintymän, joka kapenee syvyyden kasvaessa. Välillä 1050 – 1420 m, esiintymän rakenne muistuttaa muodoltaan perunaa, joka on vain pieneltä alalta kosketuksissa sen yläpuolella olevaan esiintymään. Malmimuotojen perusteella Pyhäsalmen VMS on jaettu ylempään malmiin ja syvämalmiin. Ylempi ja syvämalmi ovat malmikerrostumaltaan huomattavan erilaiset, vaikka molempiin on rikastunut Zn ja Cu. VMS esiintymälle tyypillistä hydrotermistä muuntumista ilmenee esiintymän itäpuolella, mikä tarkoittaa, että se oli esiintymän muodostumishetkellä jalkapuoli. Esiintymän hydrotermisesti muuntumaton länsipuoli on taas vastaavasti kattopuoli. Sekä jalka että kattopuolta dominoi massiivisen sulfidi - esiintymän läheisyydessä homogeeninen ja hienorakeinen felsinen kivilajiyksikkö, joka on hydrotermisesti muuntunut jalkapuolessa serisiittiseksi liuskeeksi. Paikoin dominoiva kivilaji on maafinen, mutta vain syvemmällä jalkapuolessa ja korkeammalla kattopuolella. Jalkapuolessa ilmenee useampia vanhoja intruusioita kuin kattopuolessa, mutta molemmissa ilmenee viimeisimpien tektonisten tapahtumien seuraamuksesta tuoreempia pegmatiittisia graniittijuonia. Lähestulkoon kaikki kivilajit ovat joko/sekä hydrotermisen tai/ja metamorfisen muuntumisen yhteydessä muuntuneet niin voimakkaasti, että kaikki primääriset rakenteet ovat tuhoutuneet.

Pyhäsalmen VMS esiintymästä kerättiin dataa vuoden 2017 kesänä seitsemästä eri kairansydämestä, jotka yhdessä edustavat kattavasti esiintymän jalka ja kattopuolta sekä syvämalmia. Pyhäsalmi Mine Oy luovutti kaiken aikaisemmin kerätyn geokemiallisen ja geofysikaalisen datan tätä tutkielmaa varten, mikä oli jo kerätty ennen tämän tutkielman alkua näistä kairansydämistä. Suurin osa tästä datasta kuvasi jalkapuolta ja kairansydämmissa esiintyvän massiivisen sulfidien perusmetallien pitoisuuksia. Tämän lisäksi, kattopuolesta ja syvämalmin silikaattisista inkluusioista kerättiin lisää geokemiallista dataa ja ohuthieitä paremman kokonaisuuden hahmottamiseksi. Tämän datan lisäksi nämä seitsemän kairansydäntä logattiin, valokuvattiin ja säännöllisin väliajoin niiden geofysikaaliset ominaisuudet, kuten ominaispaino ja susceptibiliteetti, mitattiin. Jälkeenpäin 55 ohuthiettä valittiin, jotka näyttävät esiintymän pääasialliset kivilajit ja asteittaisen hydrotermisen muuntumisen voimakkuuden kasvun.

Tämän tutkielman tarkoitus on kuvata oleellisimpia Pyhäsalmen VMS esiintymän piirteitä ja sen isäntäkiven ominaisuuksia, käyttäen näitä seitsemää kairansydäntä ja niistä kerättyä tietoa. Geokemialliset tutkimukset ovat osoittautuneet korvaamattomaksi työkaluksi esiintymän isäntäkiven litologian selvittämiseen, hydrothermisen muuntumisen intensiivisyyden mittaamiseen ja hydrotermisen muuntumisen yhteydessä tapahtuvan massasiirtymisen arvioimiseen. Jalkapuolen isäntäkivi koostuu kahdesta kemiallisesti toisistaan poikkeavista felsisistä vulkaanisesta kivilajista, jotka on täällä nimetty Ryoliitti 1:ksi ja 2:ksi. Litologisesti Ryoliitti 2 on 1:sen yläpuolella, ja jalkapuolessa Ryoliitti 2 assosioidaan hydrotermisen muuntumisen kanssa. Kattopuolen felsinen vulkaaninen isäntäkivi koostuu yksinomaan Ryoliitti 2:sta. Vastaavasti, lukuisat mafiset intruusiot ja kerrostumat jakautuivat geokemiallisesti kolmeen pääryhmään, joista Andesiittit ja Basalttiset andesiitit kuuluvat jalkapuoleen, ja Basaltti kuulluu yksinomaan kattopuoleen. Geofysikaalisen datan käytännön hyödyllisyyttä on myös arvioitu kivilajiluokittelun yhteydessä käytettäväksi työkaluksi ja hydrotermisen muuntumisen voimakkuuden arvioimista varten. Ominaispaino osoittautui hyödyllisimmäksi geofysikaaliseksi ominaisuudeksi kaiken kaikkiaan, mutta se pystyi parhaillaan vain osoittamaan oikean vastauksen suuntaan niissä tehtävissä missä sitä testattiin.

Muita tietoja

Asiasanat: Pyhäsalmi, VMS, vulkaaniset kivet, hydroterminen muuntuminen, intruusio, paleoproterotsooinen

ABSTRACT
FOR THESIS

University of Oulu Faculty of Technology

Degree Programme (Bachelor's Thesis, Master's Thesis)	Major Subject (Licentiate Thesis)
Degree programme in Geology and Mineralogy	
Author	**Thesis Supervisor**
Hettula, Jesse Sakari	Strand, K., Professor, Holger, P., Professor

Title of Thesis

Hydrohermal altreration and host rock composition of the Pyhäsalmi volganogenic massive sulphide deposit, Central Finland

Major Subject	Type of Thesis	Submission Date	Number of Pages
Geosciences	Masters's Thesis	November 2019	68

Abstract

The Pyhäsalmi volcanogenic massive sulphide (VMS) deposit begins at ground level and reaches a depth of 1420 m. For the first 1050 m, the massive sulphide is formed of long a long conical sheet-like structure, which is slightly sloping to the west and steeply downward, forming a north – south planar massive sulphide deposit that narrows with increasing depth. Between 1050 and 1420 m, the structure of the deposit resembles the shape of a potato, which is connected to the upper deposit by a small contact area in between these two shapes. The upper and deep ore bodies are significantly different in shape, but both are enriched with Zn and Cu. VMS related hydrothermal alteration is present on the eastern side of the deposit, meaning that the east was, at the time of deposit formation, the footwall. Similarly, hydrothermally unaltered western side of the deposit is the hangingwall. Both the footwall and hangingwall are dominated by a homogeneous and aphanitic felsic rock unit, which has hydrothermally altered in the footwall into sericite schist. In both footwall and in hanginwall, mafic units are more common with increasing distance from massive sulphide. In total, when compared to hangingwall, the footwall has older and more numerous mafic intrusions, but both share pegmatitic granite intrusions in equal measure, which are a byproduct of latest local tectonic event. Nearly all the rock types have undergone severe alteration due to hydrothermal or/and metamorphic events, leaving no primary textures intact.

During the summer of 2017, all the data relevant to this study was collected from seven drillcores which collectively represent the footwall, hangingnwall and deep massive sulphide itself. Pyhäsalmi Mine Oy provided all their previously collected geochemical and geophysical data from these drillcores. Most of this data portray the footwall rock units and massive sulphide base metal content. In addition, whole-rock geochemical data and thin sections were collected from the hangingwall and from silicic inclusions in deep ore body for better overall view of the deposit. These seven drillcores were also logged, photographed and systematically measured for their geophysical properties, such as specific gravity and susceptibility. Subsequently, 55 thin sections were selected from collection of samples, which display the relevant major rock types and gradual increase in hydrothermal alteration intensity in host rock.

The purpose of this thesis is to describe most relevant properties of Pyhäsalmi VMS deposit and its host rock, based on the seven drillcores and data collected from them. As a result, geochemical studies have proven to be and irreplaceable tool for clarifying the host lithology and drillcore logging, measuring the intensity of hydrothermal alteration and estimating absolute mass transfer during hydrothermal alteration. It is evident that the footwall felsic host rock consists of two chemically different felsic volcanic units, which are named here Rhyolite 1 and 2. Lithologically Rhyolite 2 is atop Rhyolite 1, and it is also associated with massive sulphide related hydrothermal alteration. In hangingwall, the felsic host rock is solely composed of unaltered Rhyolite 2. Similarly, numerous mafic intrusion and layers are geochemically divided into three major groups, of which Andesites and Basaltic andesites belong to the footwall, whereas the third group, Basalt, belongs exclusively to hangingwall. The practical utility of geophysical data for ore exploration, measuring hydrothermal alteration intensity and rock type identification was also estimated. It seems that specific gravity was most useful of the three properties, however it could only indicate correct answers in all studied categories.

Additional Information

Key words: Pyhäsalmi, VMS, volcanic rock, hydrothermal alteration, intrusion, Paleoproterozoic

Contents

1. INTRODUCTION

The purpose of this thesis is to describe most properties of Pyhäsalmi volganogenic massive sulphide (VMS) deposit, Central Finland. Timo Mäki, the Chief geologist at Pyhäsalmi Mine Oy, provided seven drillcores and all raw geochemical and geophysical data related to these drillcores, for Oulu University. These seven drillcores were selected in order to display different aspects of volcanogenic massive sulphide and its host rock, for this MSc thesis work. This initial description of these drillcores would then be used for educational purposes in the Oulu university.

This thesis work was first initiated by professor Holger Paulick, and by agreement of Timo Mäki, data collection began in summer 2017. In three months, drillcore logs and other data acquisition were done, which includes 31 additional whole-rock geochemical assays and 55 thin sections in addition to data provided by Pyhäsalmi Mine Oy.

This work first describes the basic characteristics of typical VMS model, after which introduction to the Pyhäsalmi VMS deposit is provided. Lastly, it is displayed how and by what methods lithological units were identified, how they have been hydrothermally altered and what typical trends were found in hydrothermal alteration and in massive sulphide metal zonation.

A more advanced geochemical tools are also used for identifying mass transfer during hydrothermal alteration, as well as Alteration Box plot and its interpretation. A great amount of geophysical data was also collected, namely specific gravity and susceptibility. Some electric resistivity measurements were also performed.

All relevant raw data and information is presented in Appendices All calculations were performed on Excel, and they can be acquired by asking the author or Oulu Mining School staff in Oulu University. The main source of reference for how to describe volcanic rocks and their hydrothermal alteration in VMS setting is from Gifkins et al., (2005).

2. VOLGANOGENIC MASSIVE SULPHIDE (VMS) DEPOSIT

Volcanogenic massive sulphide (VMS) deposits are stratabound or stratiform massive bodies of sulphide minerals and other accessory minerals, which form just at or slightly below seafloor surface. VMS deposits can develop in several different marine volcanic settings, usually in zones of extension and active volcanism along mid-ocean ridges, island arcs, back-arc basins and fore-arc troughs (Hannington, 2014).

VMS formation is driven by convective fluid circulation above deep heat source. The convective fluids are derived mostly from seawater, which has seeped down into permeable seafloor as pore water. Footwall fluid flow may be enhanced by structural control, such as faults or otherwise highly permeable footwall characteristics. Enhanced fluid flow in constrained structures develops a pathway for up to 400 °C hydrothermal fluids to move back up towards the seafloor. When hot hydrothermal fluids mix with cold seawater, sulphides will begin to precipitate due to lowering fluid temperature and form a massive sulphide mound (Robb, 2005).

Seawater is cold (2 °C), alkaline, neutral (pH 7 - 8), oxidizing, rich in SO_4 and poor in metals. As seawater fluids begin to circulate in hydrothermal system due to increased heat, the fluids will scavenge metals from the host rock. The source of sulfur for hydrothermal fluid is the sulfate component of the seawater itself with reduction of sulfate to sulfide during fluid-rock interaction prior to venting. As the hydrothermal fluids are flowing through footwall, the footwall composition will also change. This change is referred to as hydrothermal alteration, and the altered rock area is referred to as the alteration zone (Robb, 2005).

Interaction between footwall and hydrothermal fluids change the composition of both. These interactions are very complex and vary based on the footwall composition. However, as a general result, high temperature fluids (>300 °C) are saline (7 wt. % NaCl), acidic (pH 4 - 6), reducing, rich in H_2S and metals such as Fe, Mn, Pb, Zn and Cu. Low temperature hydrothermal fluids have salinities up to twice that of modern

seawater (3,2 wt. % NaCl). Footwall composition also dictates how much metal is available for scavenging, and what kind of alteration hydrothermal fluid interaction produces (Robb, 2005). As an indication of hydrothermal activity, regional synvolcanic semi-conformable alteration zone can be seen up to 20 km laterally and 2 – 4 km deep below the venting site. Alteration strength intensifies at closer proximity to hydrothermal venting site.

2.1 VMS classification

VMS deposits have been classified by base metal content (Solomon, 1976; Franklin et al., 1981; Large 1992), host rock textures (Morton and Franklin, 1987), host rock lithology (Sangster and Scott, 1976), tectonic setting (Sawkins, 1976) and host rock composition (Barrie and Hannington, 1997; Franklin et al., 2005; Galley et al., 2007). Since most of the metals in VMS deposits are derived from leaching of the footwall rock (Large, 1992), and the footwall composition commonly reflects to tectonic setting, there tends to be some overlap and common agreement between these classification schemes.

The most common classification method is based on the base metal content of the VMS deposit. This classification splits the VMS deposits into three groups; Cu-Zn, Zn-Pb-Cu and Pb-Zn according to their contained ratios of these three metals (Figure 1).

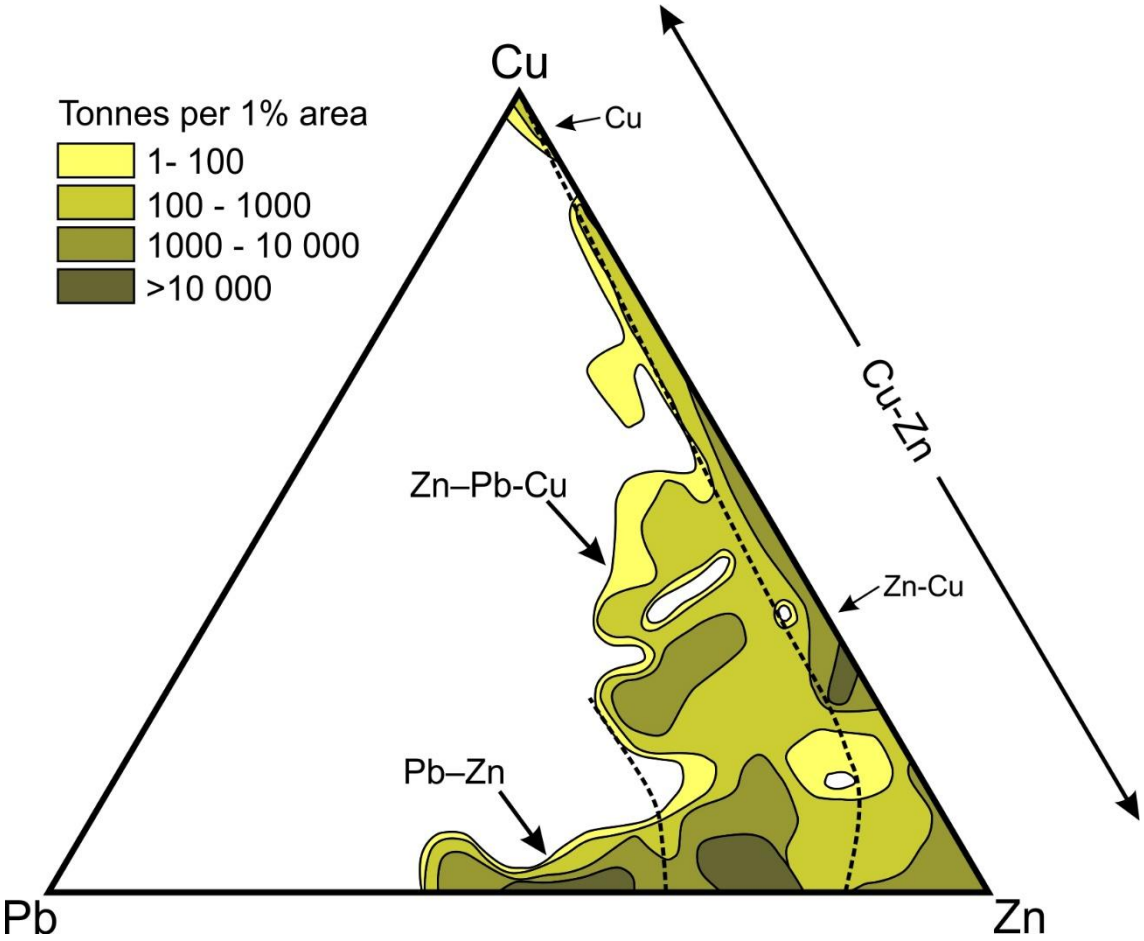

Figure 1*. VMS classification system which is based on base metal content of the deposit. The three main groups are Cu-Zn, Zn-Pb-Cu and Pb-Zn (modified from Franklin et al. 1981).*

The latest VMS classification system was first introduced by Barrie and Hannington (1999), and later modified by Franklin et al. (2005). It consists of five groups, and the upgraded names and definitions are as follows:

1. Back-arc mafic type. Host rock is predominantly mafic, which was formed in back-arc setting. Stratigraphic succession contains ophiolites, dominated by pillowed and massive tholeiitic basalt flows. Back-arc mafic type is Cu rich and

Zn poor, small deposits and size. Found almost exclusively in Phanerozoic rocks.

2. Bimodal-mafic type. Basalt dominated host rock that can contain less than 25% felsic strata. However, deposits are often hosted by felsic rocks. Tectonic setting is most commonly primitive arc or primitive Figvolcanic arc. Predominates in Late Archean and Early Proterozoic rocks, and they are the most common of VMS deposit types. Bimodal mafic types have the second highest Cu content of these five groups.
3. Pelitic-mafic type. Sub-equal propositions of mafic volcanic or intrusive rocks and sedimentary rock, while felsic rocks are minor or absent. Middle Proterozoic and younger in mature back arc-settings. Less numerous than the other types of deposits, but they have the second highest average tonnage.
4. Bimodal-felsic type. Dominated by felsic volcanic rocks and accompanied by basalts (20-50%) and terrigenous sedimentary rocks (~10%). Forms in continental margin arcs and related back-arc settings. Most abundant in Phanerozoic rock, but also occurs in Late Archean and Early Proteroizoic rocks. Bimodal-felsic type deposits are second-most numerous, and on average contain the most Zn and Ag.
5. Felsic-siliciclastic type. Dominated by felsic rocks, most often by siliciclastic felsic rocks which are sometimes accompanied by minor amounts mafic volcanic rock. Forms in mature continental back-arc settings, of which majority is dated to Phanerozoic age. Felsic-siliciclastic type has the greatest tonnage of the VMS types, the lowest average Cu content and the highest average Pb content of the five deposit types.

Galley et al. (2007) later added a sixth group:

6. Hybrid bimodal-felsic type. This group was added to present a cross between VMS and shallow-water epithermal mineralization. They resemble bimodal-felsic type deposits, but contain shallow-water epithermal features, such as aluminous alteration assemblages and precious metal enrichment.

2.2 Deep regional altered zones

Deep, regional and synvolcanic semi-conformable altered zones consist of vertically stacked, sub-horizontal altered zones that are distinctively different from each other. Although, in many VMS systems only two or one of these zones are recognized since both diagenesis and deep regional hydrothermal alteration involve reactions between seawater (or modified seawater) and volcanic successions at increasing temperatures and depths. Identifying these regional altered zones from diagenetic and metamorphic facies is problematic since diagenesis and burial metamorphism are also regionally extensive, vertically stacked altered zones with similar mineral assemblages. However, although the process of diagenesis and deep regional hydrothermal alteration are very similar, regional alteration can be identified by timing of the alteration, temperatures, fluid-rock ratios and inconsistencies within the diagenetic metamorphic system (fig. 2) (Gifkins et al., 2005; Gibson et al., 1983; Galley et al., 2007).

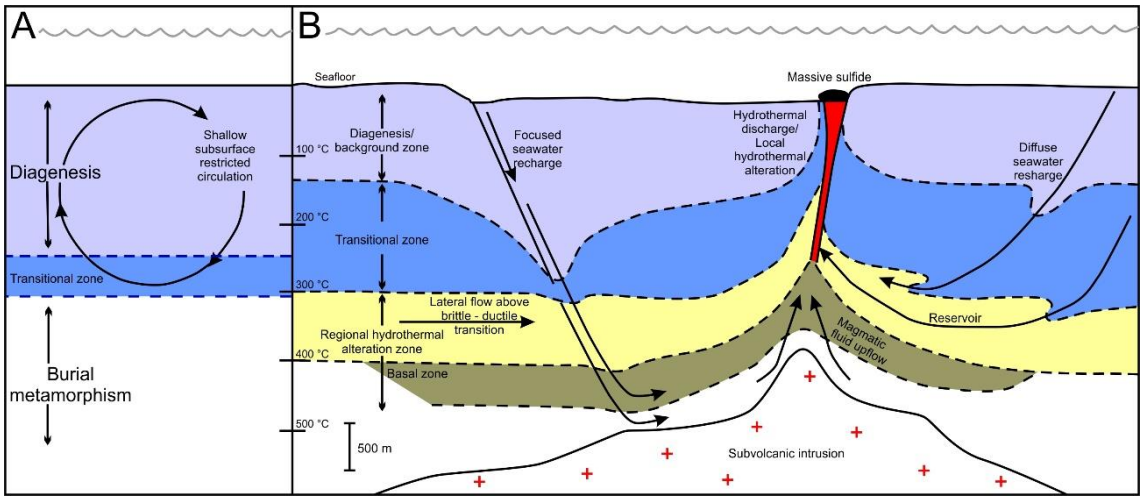

Figure 2. *Model of a deep, regional hydrothermal alteration related to volcanic intrusions in seafloor. A) Diagenetic-metamorphic system, where diagenesis progresses to isochemical metamorphism with increasing temperature and depth. B) Diagenetic-hydrothermal system beneath rift basin, where subsurface intrusion drives fluid circulation. Transition from one alteration zone to another is dependent on temperature gradients and fluid circulation. Modified from Gifkins et al., (2005).*

The uppermost altered zone is referred to as upper background K-Mg metasomatic zone, which consists mostly of zeolite-clay and related diagenetic sub-greenschist mineral assemblages, such as K-Mg-rich smectites, mixed-later chlorites, and K-feldspar. In felsic rocks these minerals include adularia and Mg-smectite, whereas in mafic rocks they are dominated by zeolites and Mg-smectite. Descending seawater becomes enriched in Si, Fe^{3+}, Mn and lesser amounts of Ca, Mg and sulfur.

Increasing stratigraphic depth and temperature (between 140°C and 200°C) promotes a replacement from K-rich metasomatism to Na-rich metasomatism. At moderate temperatures (140-300°C), metasomatic reactions between modified seawater and the volcanic successions result in Na-Mg alteration assemblages, which is referred to as the transition zone. Regardless of the rock type, high temperature alteration mineral assemblages in transition zone include Mg-smectite + chlorite + quartz + albite, gaining Na_2O and MgO and losing CaO, Zn and Cu (Gifkins et al., 2005).

The central altered zone is typically silicified, with assemblages of quartz + plagioclase or albite, overprinting regional albite zones. If the parent rock composition was originally mafic, then the central altered zone may be sericitic, dominated by sericite + quartz ± chlorite. Alteration intensity increases with closer proximity to subvolcanic intrusions, marked by increased net gains in SiO_2 and Na_2O, due to the precipitation of silica within pore spaces and albitization, and increased net losses in FeO_2, MgO, CaO, K_2O, MnO and other metals, which have been transported away.

The basal zone mineral assemblages are dependent on the host rock composition and porosity. Felsic rocks are typically altered to sericite or chlorite zones, whereas mafic rocks are altered to clinozoisite or epidote + quartz zones. In either case, high temperature interaction between modified seawater and the host rocks in the basal zone is interpreted to represent the final phase of metal rich hydrothermal fluid formation. Hence, it could also represent the reservoir of up-welling fluid discharge zones, which can potentially form local hydrothermal alteration zones and related massive sulphides (Skirrow and Franklin, 1994).

2.3 Local hydrothermal alteration haloes

Pipe-like hydrothermal altered zones are globally the most typical shape related to VMS deposits, even if in certain VMS districts, such as the Mount Read province, Mount Windsor Subprovince and several others, sheet-like stratabound altered zones are more common. Altered hangingwall zones are also identified in some deposits, but since hangingwall alteration is rare and alteration intensity is weak in comparison to the footwall hydrothermal alteration, hangingwall altered zones are not as well-known as footwall hydrothermal zones (Gifkins et al., 2005).

Hellyer VMS deposit in the Mount Read province (Gemmell and Large, 1992) is the most common example when describing VMS associated footwall hydrothermal alteration. The Hellyer deposit will also be used as an example here, since the massive sulphide and its host rock are only slightly metamorphosed or otherwise altered after VMS mineralization, and because Hellyer footwall hosts wide range of different VMS related hydrothermal zones (Fig. 3). Starting from the center of the pipe outwards, an ideal pipe-like footwall hydrothermal alteration includes the following zones: siliceous core zone, chlorite zone, sericite zone and albite zone.

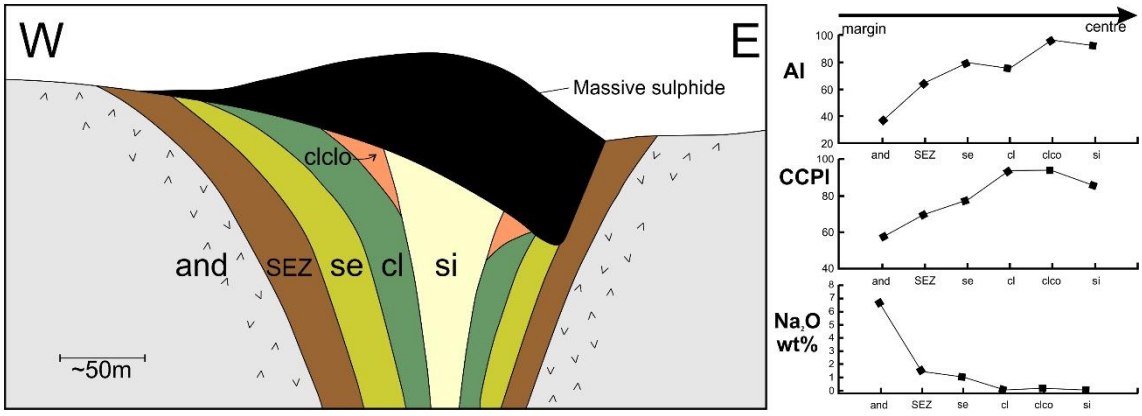

Figure 3. *Cross section of idealized Hellyer VMS mineralization and alteration zonation in the footwall of the massive sulphide (modified after Gemmell and Large, 1992). AI (Alteration Index), CCPI (Chlorite-Carbonate-Pyrite Index) and Na2O wt% represent the chemical alteration of host rock that occurs during hydrothermal fluid flow. si = quartz-chlorite ± sericite, clco = chlorite > dolomite, cl = chlorite ± pyrite ± quartz, se = strong sericite-chlorite ± pyrite, SEZ = weak sericite ± chlorite, And = least altered andesite (modified from Large 2001a).*

Siliceous core zone is mainly composed of quartz + pyrite and quartz + pyrite + sericite ± chlorite assemblages. Siliceous core represents the zone of maximum hydrothermal fluid flow and highest temperatures and it hosts the most intensely altered rocks, which are commonly intersected by networks of pyrite + chalcopyrite stringer veins. All primary textures are likely to have destroyed.

Chlorite zones are dominated by chlorite (>50 wt% and commonly >80wt%), with subordinate quartz + pyrite + sericite ± carbonate, where pyrite + chalcopyrite veins are common. Typically, chlorite zones appear as fine-grained, dark and massive, exhibiting no volcanic or sedimentary textures. Some chlorite zones exhibit a general increase of Fe/Mg ratio from inner chlorite zone to the outer edge of sericite zone (Riverin and Hodgson, 1980), but the reverse trend has also been observed (Gifkins, et al. 2005).

Sericite zones are characterized by assemblages of sericite + chlorite + quartz + carbonate + pyrite. Since sericite zones alteration strength varies from weak to strong, relict textures are likely to be sparse. In most cases the alteration intensity decreases towards the outer margin, where altered rocks grades into least altered footwall rocks. Sericite zones may be laterally extensive.

Albite zones are described as weakly altered zones of albite + chlorite ± sericite that surround the main sericite zones. Primary volcanic textures are well preserved, and so albite zones may be difficult to identify from the background diagenetic alteration facies. However, identifying albite zone is worth the effort, since it can be an important factor during ore exploration.

2.4 Metal zonation in massive sulphide

The most critical factor for VMS metal zonation formation is the temperature evolution through hydrothermal system life cycle. Hydrothermal system circulation begins as a

deep heat source presents itself. Fluid circulation slowly increases as fluid temperatures gradually rise until it reaches a thermal maximum, and then diminishes as fluid temperatures decline. Since the major ore minerals have a strong temperature-solubility relationship, gradually increasing and then degreasing thermal regime has a critical control on base and precious metal transport and deposition. Large (1992) described the metal zonation process to have four stages:

Stage 1: Low-temperature (150°C – 250°C) hydrothermal fluids are discharged onto the seafloor with the precipitation of galena, sphalerite, anhydrite and barite to form a small porous sulphide mound.

Stage 2: The temperature of the hydrothermal fluid input rises to the range of 250-300°C. Hotter fluids introduce significant copper into the footwall stringer system and into the base of developing sulphide mound. As copper is being precipitated due to lowering temperature effect of cold seawater, galena and sphalerite are dissolved from the base and later precipitated onto top layers of developing sulphide mound.

Stage 3: Continued input of high temperature fluids (300°C – 350°C) promotes further precipitation of chalcopyrite to the stringer zone and in the basal part of the mound. Hotter fluids also transport Cu-rich metal zone further up by first dissolving them from base and then precipitating at upper levels where temperatures are lower. If the input hydrothermal fluid temperature rises as high as 400°C, all sulphides that have bound base metals will be dissolved from the base of the mound and later precipitated at colder upper zones, leaving only massive pyrite to the base of the mound.

Stage 4: After thermal maximum, the input hydrothermal fluid temperature will eventually decline. As a result, colder late-stage hydrothermal fluids will somewhat overprint earlier metal zones by precipitating sphalerite, galena, barite and carbonates.

Figure 4 represent a rough temperature estimates for the various zones of the classic massive sulphide mound. These temperatures will vary according to the pH, salinity and f_{O2} of the fluid.

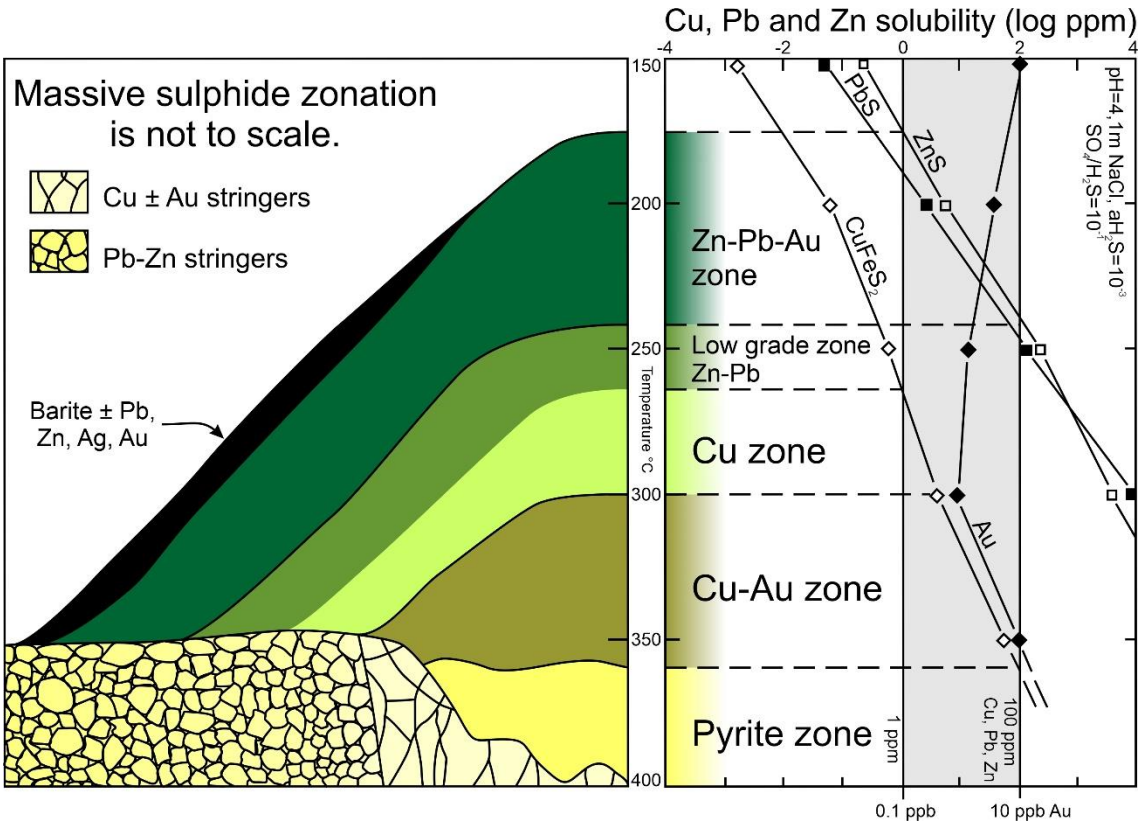

Figure 4. *Solubility-temperature plot for the major ore minerals in equilibrium with pyrite, assuming a constant fluid chemistry during controlled temperature-f_{O2} decrease from 400°C to 150°C parallel to the pyrite-hematite boundary, but within the pyrite field. The gray zone at right is the metal composition range for a typical VMS ore fluid. Above the range fluids are grossly undersaturated in metals and below the range they carry insufficient metals to produce ore grades. Gold solubilities need to be multiplied by a factor of 10^{-4} (modified from Large, 1992).*

Besides hydrothermal fluid chemistry and fluid temperature, there are several other major factors that will produce a spectrum of VMS deposit styles. Reasons for departure of the classic mound style VMS deposit (Fig. 3 and 4) has to do with seawater depth variation, permeability and composition of footwall volcanic rock in addition to before mentioned fluid chemistry and temperature variation (Large, 1992).

3. GEOLOGICAL SETTING

Paleoproterozoic initial island arc formed 1.93-1.92 Ga in ocean located on the western side of the Finnish Archean basement complex (3.1-2.6 Ga) and later collided against that Archean basement. As a result, a northwest-southeast trending major thrust zone formed, which is referred to as Raahe-Ladoga zone (RLZ) (Laine et al., 2015). To the west of RLZ, there is currently Ylivieska-type metavolcanic and metavolcaniclastic sediments that are younger than the rocks in RLZ (Fig. 5) (Korsman et al., 1997 in Mäki et al., 2015). Beyond the Ylivieska group, further to the southwest, is the Svecofennian Central Finland Granitoid Complex (1.89-1.87 Ga) (Kousa et al. 2013).

Supracrustal rocks along the RLZ are for the most part turbiditic metasedimentary rocks with minor metavolcanic interlayers and locally abundant graphite-bearing schists. This sequence is defined as the Näläntöjärvi suite. The VMS mineralizations in RLZ are genetically related to the Paleoproterozoic island arc and they are in distinct lithostratigraphical units along northwestern parts of RLZ. Two apparently separate VMS related lithostratigraphical groups are hosted in metavolcanic rocks and they have been defined as Vihanti group and Pyhäsalmi group (Fig. 5) (Mäki, et al., 2015).

The Vihanti group (1.89-1.87 Ga) is dominated by intermediate and felsic metavolcanics rocks where mafic metavolcanics rocks are minor and sparsely distributed. It hosts several VMS related mineralizations: The Vihanti deposit (28.1 Mt @ 0.5% Cu, 5.1% Zn, 0.4% Pb, 0.5g/t Au, 25g/t Ag) with two satellite deposits; Kuuhkamo (0.15Mt @ 4 % Zn) and Näsälänperä (0.1Mt @ 2% Zn, 15g/t Ag), and uneconomic Kokkoneva mineralization. (Mäki, et al., 2015)

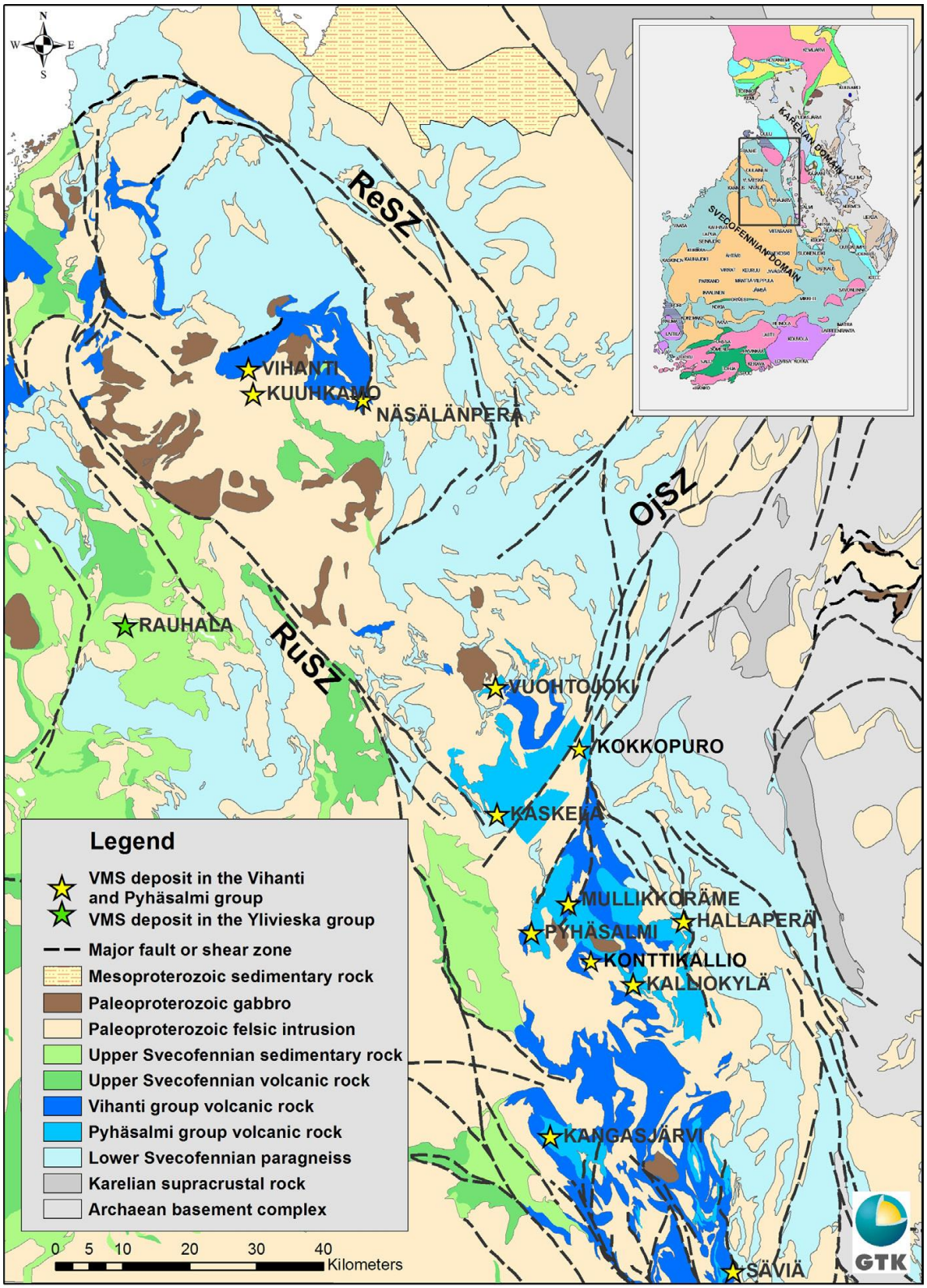

Figure 5. *Regional geology of the Vihanti - Pyhäsalmi belt. Most important Zn-Cy deposits of the are shown with stars and major shear systems are expressed as by black dashed lines (Mäki et al., 2015) (OjSZ = Oulujärvi shear zone, ReSZ = Revonneva shear zone, RuSZ = Ruhaperä shear zone). (with permission: Mäki, et al., 2015)*

The Pyhäsalmi group protolith is interpreted to be slightly older of the two groups, based on lithostratigraphy succession. Host rock is constructed of bimodal felsic-mafic metavolcanics rocks, but a wider range of volcanic compositions exists. It hosts several VMS related mineralizations: The Pyhäsalmi deposit (with total reserves of 58.3 Mt @ Cu 0.9 %, Zn 2.4 %, S 37.8 %, Au 0.4 g/t and Ag 14 g/t), two satellite deposits; Kangasjärvi (0.8 Mt @ 0.1% Cu, 5.4% Zn, 38% S) and Ruostesuo (0.24 Mt @ 0.4% Cu, 2.7% Zn, 30% S, 0.3g/t Au, 10g/t Ag), and uneconomic Hallaperä, Vuohtojoki and Kokkopuro satellite mineralizations.

Mullikkoräme satellite deposit (1.148 Mt @ 0.3% Cu, 6.1% Zn, 0.9% Pb, 1g/t Au, 45g/t Ag) is located 8 km to the northeast of Pyhäsalmi. Despite its proximity to the Pyhäsalmi deposit, stratigraphically the Mullikkoräme deposit belongs to the Vihanti group. (Mäki, et al., 2015)

The two stratigraphical units are separated by one major southwest-northeast and two major southeast-nortwest trending shear zones, respectively Oulujärvi (OjSZ), Revonneva (ReSZ) and Ruhaperä (RuSZ) shear zones. These shear zones further broke down the Vihanti and Pyhäsalmi districts into smaller fault-bounded blocks with internally different structural and metamorphic histories (Mäki and Puustjärvi, 2003). In general, the regional metamorphic grade in the Vihanti-Pyhäsalmi belt ranges from lower amphibolite facies to upper amphibolite facies (Korsman et al., 1997 in Mäki et al., 2015).

3.1 Structural evolution

The structural evolution of the Vihanti-Pyhäsalmi area is divided into two major compressional phases that are separated by extensional phase. (Laine et al., 2015)
The first compressional phase begins with D1 stage and ends with D3 stage. D1 started 1.91 Ga by thrusting and flat lying folding of island arc epicontinental sediments

towards the Archean basement in NE. During D1-D2 volcanic island arc most probably collided against the Archean basement, which produced the major thrust fault zone (RLZ) in between these units. D2-D3 stage (1.89 Ga) coeval magmatism produced large volumes of tonalitic migmatites related to high temperature, low pressure metamorphism which peaked at 670-800°C and 5kb (Korja et al., 1994).

During D3 stage, SW-NE compression continued, which caused crust thickening and refolding the earlier flat lying structures into upright position along the RLZ. At the later stage of D3, folding changed to ductile shearing. This change in deformation style caused large scale dextral SE trending strike-slip faults and initiated a major fragmentation in the crust along the RLZ. Dextral Ruhaperä (RuSZ) is one example of these shear zones (Mäki and Puustjärvi, 2003).

The first compressional phase ended around 1.89 Ga, after which the volcanic arc went through a short progressive extensional phase (1.89-1.85 Ga). This phase caused uplift of granulite facies metamorphic block along the earlier shear zones.

The second compressional phase, which solely includes D4 stage, began 1.82-1.79 Ga. During this phase, the earlier SW-NE compression shifted to N-S direction, producing a new set of SW-NE trending large scale F4 folds that also refolded previous D3 folds in the RLZ. The D4 stage also created the crustal scale, sinstral, SW-NE trending Oulujärvi shear zone (OjSZ) and easily recognizable D3-D4 basin and dome interference structure in the Vihanti and Pyhäsalmi areas. The horsetail system, which extends from the OjSZ (Fig. 5), caused intense shearing in the Pyhäsalmi area. The shearing caused remobilization of the massive sulphide ores and reactivation of the Archean craton shear zones. This was accompanied by large amounts of late granites and pegmatite intrusions close to the major shear zones between 1.82 and 1.79 Ga. Granite intrusions are also present at close contact with the Pyhäsalmi deposit.

3.2 Volcanic stratigraphy of the Pyhäsalmi mine area

Turbiditic metasedimentary rocks of the Näläntöjärvi suite are interpreted to be the depositional basement for both Vihanti and Pyhäsalmi groups island arc volcanic rocks. According to Kousa et al. (2013), the youngest part of Näläntöjärvi suite before the Vihanti-Pyhäsalmi related volcanism is around 1924±3 Ma old, which serves as reliable constraint for the said volcanism. The zircon U-Pb from Riitavuori metarhyolite (1921±2 Ma) and metarhyolite at the Mullikkoräme mine area (1925±4 Ma) are both from Mullikkoräme formation, which is stratigraphically on top of Pyhäsalmi group, and thus younger the Pyhäsalmi group rocks. The zircon U-Pb analyze results indicate that both the Vihanti group and Pyhäsalmi group formed in just few million years (Fig. 6). (Kousa et al., 2013)

The volcanic rocks around the Pyhäsalmi mine area belong to the Ruotanen formation. The lower part of the Ruotanen formation lithostratigraphy is primarily low- to medium-K rhyolitic and transitional between the tholeiitic and calc-alkaline trends while the upper part of the formation is tholeiitic (Fig. 6). (Kousa et al., 2013)

Geochemical analysis of the mines drill-core samples has identified several distinct rhyolite units, the Pyhäsalmi (Rhyolite A and Rhyolite B units) and the Arttu horizon (Rhyolite X). The alteration zone associated with the Pyhäsalmi ore deposit is predominantly altered rhyolite A and B, of which Rhyolite B has gone through more intense hydrothermal alteration. Rhyolites A and B also include altered mafic sills of the Mafic A-2 (Lehto Fm) intrusion. (Mäki et al., 2015; Imaña, et al., 2013; Laitela, 2015)

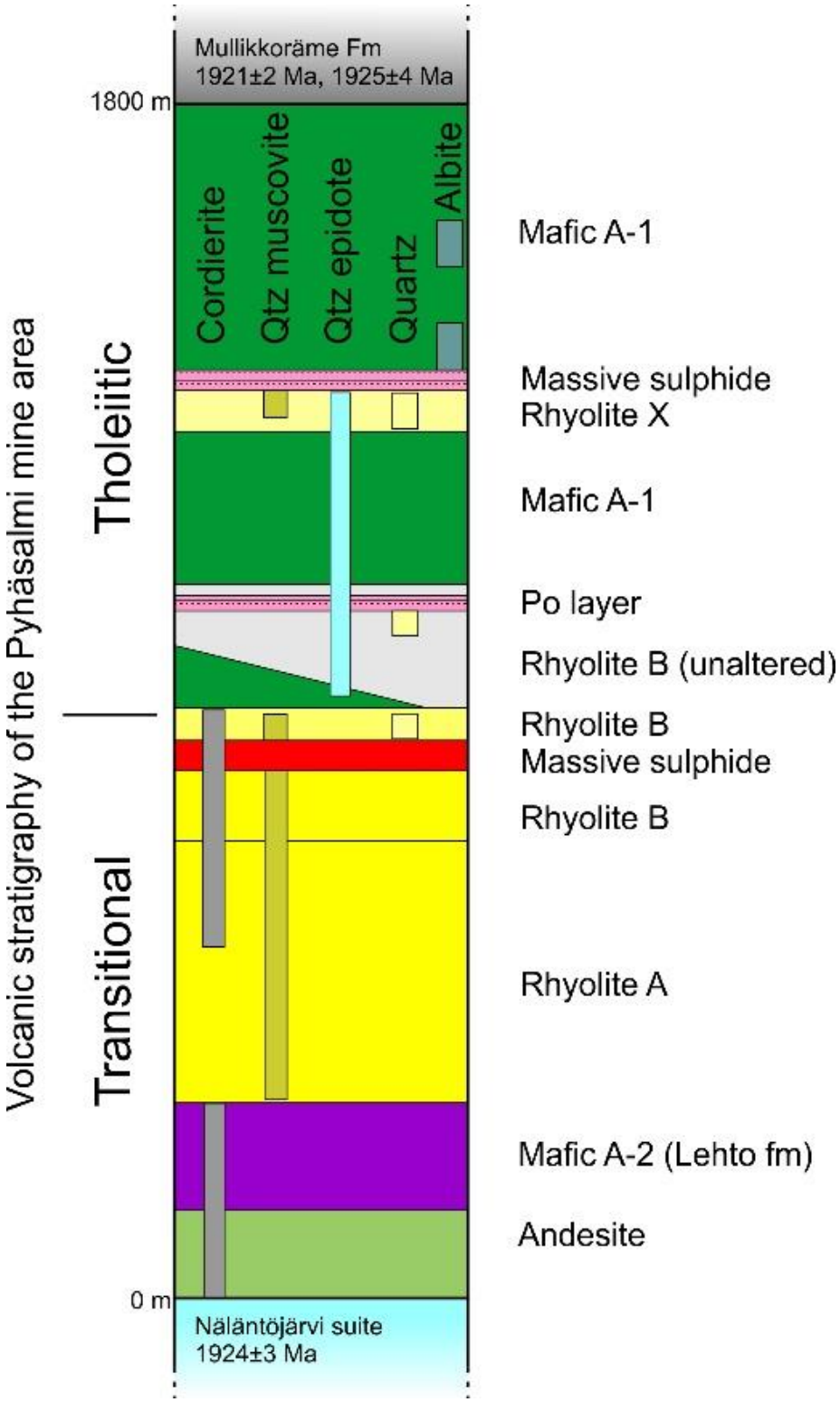

Figure 6. *Chemostratigraphy and alteration of the Pyhäsalmi mine area. Näläntöjäjrvi suite age at the bottom and Mullikkoräme formation ages at the top. (Modified from Mäki et al., 2015)*

At some point above the alteration zone, the volcanic sequence changes from predominantly rhyolitic to basic in character. The upper part of the Ruotanen formation contains predominantly mafic rocks (Mafic A-1) with few felsic horizons (Rhyolite X and Rhyolite X-1) and a late calc-alkaline trend composed of rhyolites, andesites and mafic rocks. (Imaña, et al., 2013; Mäki, et al., 2015)

The Arttu ore horizon is a thin tholeiitic rhyolite unit that sits within a package of mafic tholeiitic rocks. Locally, the Arttu horizon is well mineralized, containing Zn and Pb sulphides with predominance of pyrrhotite gangue (Laitala, 2015). Though, when compared to Rhyolite B ore horizon, Rhyolite X shows lower-temperature hydrothermal alteration (Mäki, et al., 2015)

3.3 Pyhäsalmi VMS deposit

The Pyhäsalmi deposit extends vertically from surface to depth of 1420 m. The massive sulphide body has been divided into two parts, upper ore body and deep ore body. The upper body has a steeply dipping, elongated conical shape which extends from surface to 1100m depth and is surrounded by tectonically foliated alteration zone. The upper ore body does not have identifiable metal zonation due to intense deformation and post-VMS tectonic shaking of different parts of the original massive sulphide lens. (Mäki et al., 2015)

The deep mine ore body extends out from 1100 m downward into a potato shaped blob which ends at the depth of 1420 m. It has a typical sulphide zonation pattern, which consists of a massive inner part composed of barren massive pyrite, followed by pyrite-chalcopyrite, pyrite-chalcopyrite-sphalerite and pyrite-sphalerite zones. Cu-rich ores are around the periphery of the deep orebody, with a skin of Zn-rich ore on the outside layers, surrounding both Cu-rich ore and massive pyrite. The Zn-rich ore surrounds the deep ore body on all sides except the top. Similarly, the deep ore body also displays

typical gangue zonation: from calcite and calcite-dolomite adjacent to the massive pyrite core, and then quartz-calcite-barite, barite-calcite and barite zones towards the Zn-rich layer. (Imaña, 2003)

Based on the metal zonation in the massive sulphide and hydrothermally unaltered rocks of western side of the massive sulphide, the west has been interpreted to be the hangingwall of the deposit. It consists of mostly unaltered and partly altered Rhyolite B and Mafic A-1, which also hosts Rhyolite X. The Rhyolite X effectively separates the unaltered Rhyolite B from Mafic A-1 (Figure 7). (Lickorish, 2012)

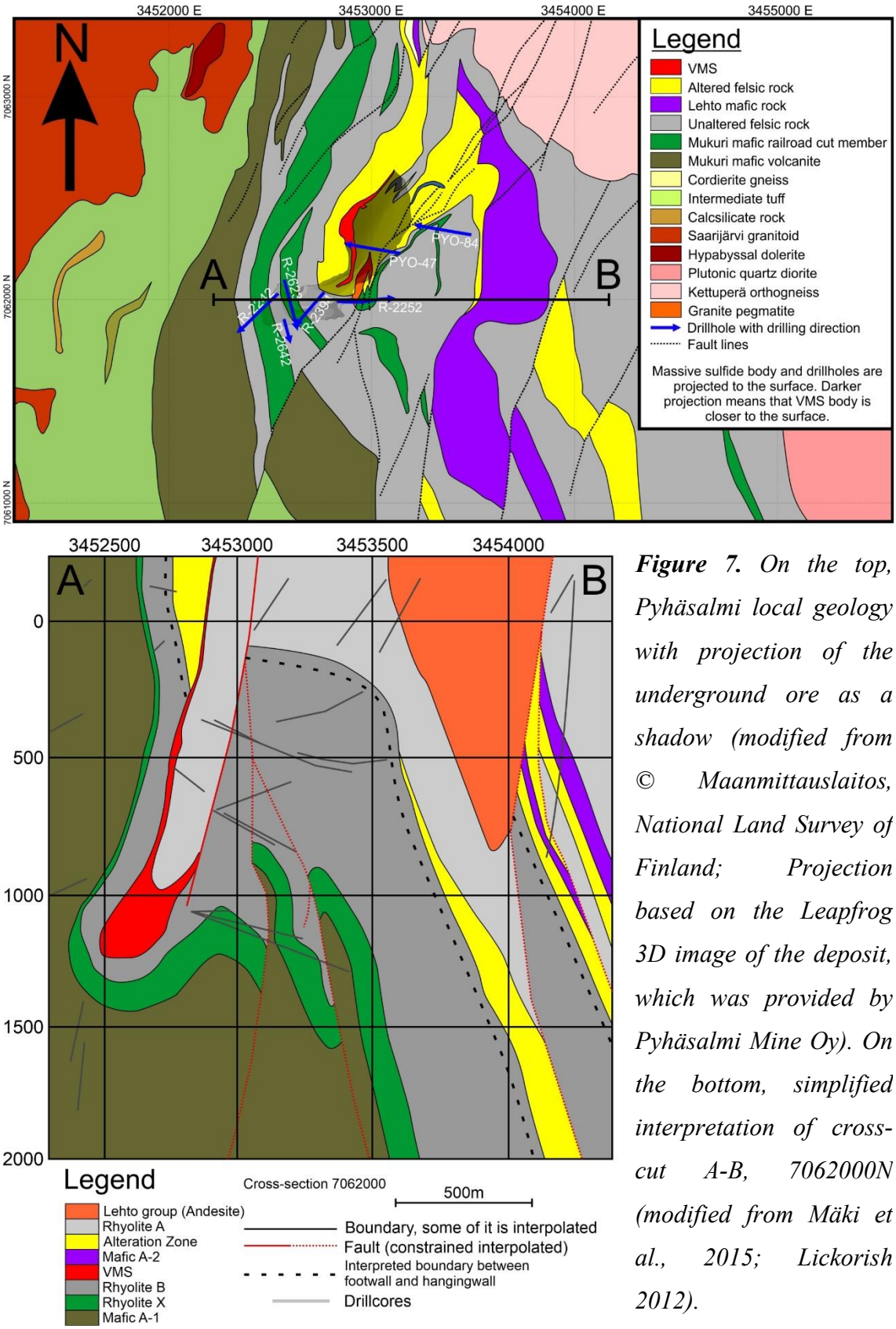

Figure 7. *On the top, Pyhäsalmi local geology with projection of the underground ore as a shadow (modified from © Maanmittauslaitos, National Land Survey of Finland; Projection based on the Leapfrog 3D image of the deposit, which was provided by Pyhäsalmi Mine Oy). On the bottom, simplified interpretation of cross-cut A-B, 7062000N (modified from Mäki et al., 2015; Lickorish 2012).*

Since the eastern side of massive sulphide has hydrothermally altered zones, the east has been interpreted to be the original footwall of the deposit. At shallow levels, hydrothermally altered rhyolite A is dominant. Beyond that, there is also andesites that are mapped as part of Lehto group. Granite pegmatites, although present throughout the area, are particularly abundant in the immediate footwall of the deposit. (Mäki et al., 2015; Lickorish, 2012)

Due to folding of stratigraphy round the nose of the mineral deposit, deep sections of the eastern side of the massive sulphide is composed of the same hangingwall stratigraphy which is seen in the west (Fig. 7), hosting rhyolite B, basaltic flows and mafic dykes, and Rhyolite X bed. (Lickorish, 2012)

3.4 Pyhäsalmi ore formation model

The current structure of Pyhäsalmi deposit is composed of a subvertical, strongly sheared, inverted anticline structure with a sheath fold at its lower end. The sheath fold formed because of continuous high strain deformation of folded material of contrasting competency along a shear zone (Fig. 8D). Anomalous structure such as massive sulphide forms a singularity in the stratigraphy that has concentrated strain, producing a higher amplitude structure that, by continual deformation, would have stretched out to form a sheath fold localized on the massive sulphide.

Sheath folding transported the deep ore body onto less altered hangingwall mafic volcanic rocks, separating the deposit from its original hydrothermal venting site. With ensuing folding and tilting of the surrounding hangingwall, the massive sulphide deposit was enclosed in unaltered rocks. In addition to large-scale synform structure in the deep ore body, there appears to be some smaller scale folding inside the ore body (Miettinen, 2011).

By studying the geochemistry of local footwall metal enrichment and hydrothermal alteration, it was found that the alteration and metal enrichment of altered units are

stronger in the northernmost parts of the Pyhäsalmi system, which are located more than 2 km away from the actual ore body position. This too would suggest that the massive sulphide was detached from the original position by thrusting and deformation.

The Pyhäsalmi deposit is hosted by felsic volcanic rocks, which are interpreted to represent lapilli tuff and coherent lava flow units. The massive sulphide itself hosts relicts of altered host rock (Rhyolite B) within the Cu-enriched zone. The altered enclaves are not present in the Zn ores of the massive sulphide, so it is conceivable that the Zn-rich sulphides formed by direct venting onto the seafloor (Miettinen, 2011).

Imaña (2003) also concluded in his ore petrography studies that inner massive pyrite and Cu-zone were formed by syngenetic sub-seafloor replacement and Zn ores formed by deposition near the palaeo-seafloor (Fig. 8A). Since the ore body was formed because of sulphides replacing a part of the hosting volcanic Rhyolite B rocks, the fact that the ore body is currently hosted by this same rhyolite, albeit not in contact with its alteration zone, indicates that the deep ore body has been displaced from its primary position along the same lithological horizon (Miettinen, 2011).

Pyhäsalmi district also hosts pyrrhotite horizons that exhibit anomalous base metal contents. These horizons could be related to the VMS formation, or alternatively to the later geological evolution base metals were remobilized from nearby VMS deposits during metamorphism. It is also possible that pyrrhotite horizons were deposited in the time-stratigraphic intervals that are not related to the major VMS forming phase. The occurrence of pyrrhotite as the primary iron sulphide phase in the pyrrhotite horizons could indicate that the environment (sea floor), where the deposition took place, was reducing but sulphur-poor, thus causing the predominance of pyrrhotite over pyrite (Fig. 8C). (Laitala, 2015)

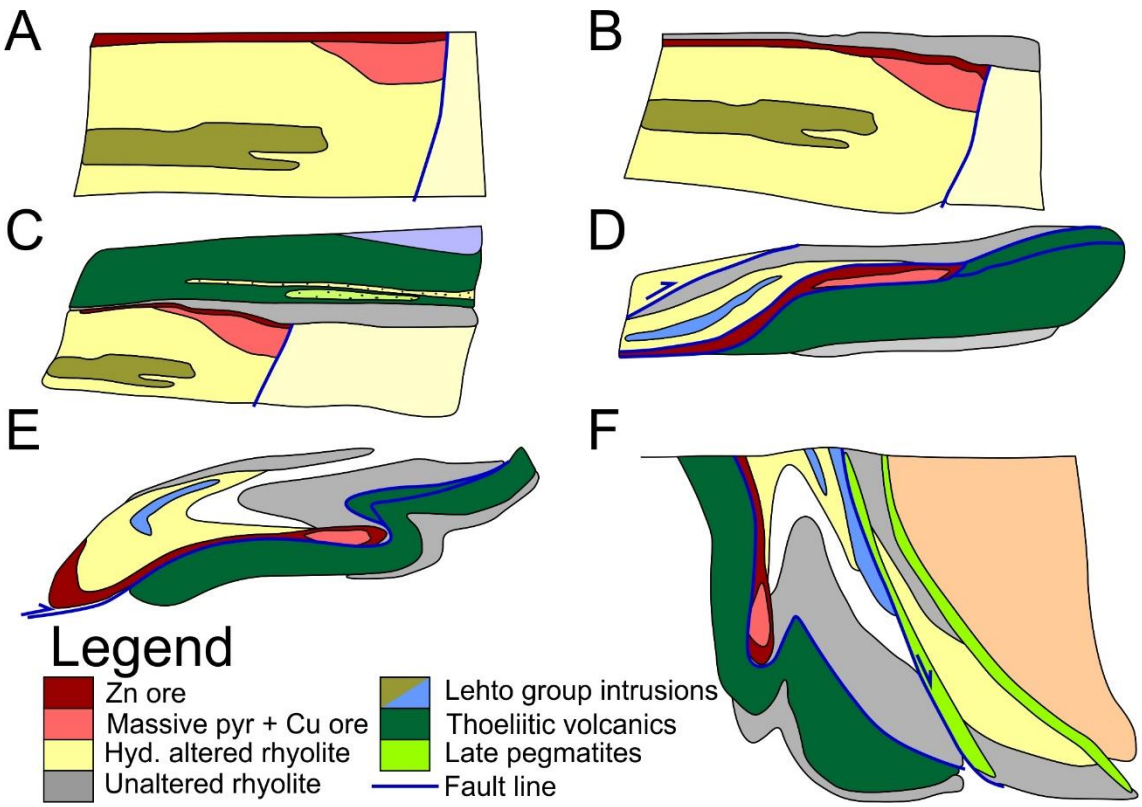

Figure 8. *One possible evolution model of Pyhäsalmi deposit. A-F represent the evolution stages chronologically. This model assumes that each lithostratigraphical unit originated from single body, but now appears separate due to over-thrust, which is shown in picture D (modified from Imaña et al., 2013).*

4. DRILLCORES, THEIR POSITION AND GEOLOGY

Seven drillcores was selected around the Pyhäsalmi mine area to display the main lithostratigraphical units around the deposit. All of the drillcores have been projected to the surface in Figure 7A, and more detailed profile pictures are represented as they are discussed.

PYO-47 (Fig. 11) and PYO-84 (Fig. 12) were drilled during the year 1989 from ground level, at eastern side of the upper ore body in slight angle towards west. Both begin

from unaltered felsic rocks and pierce hydrothermally altered felsic rocks that exhibit sericite schistosity. From these two drillcores, only PYO-47 pierces the upper ore body.

The remaining five drillcores belong to R-series, indicating that they have been drilled underground around or through the deep ore body. R-2242 (Fig.15) and R-2252 (Fig. 16) start from the near vicinity of the deep ore body and drill away from the ore body to SW and east, respectively. Both R-2394 and R-2623 start from the hangingwall of the deep ore body, pierce through the massive sulphide and end at the other side of the ore body. R-2642 begins at the outer layers of deep ore body, drilling away from the center of the deep ore body and continues a bit further away into the hangingwall than R-2394 and R-2623 (Fig. 13).

5. DATA COLLECTION PROCEDURE

Data collection was carried out in June 2017 – August 2017. During that time, seven drillcores were logged, measured, collected samples from and lastly photographed. Logging was performed using the same symbols and methods that were discussed in Gifkins et al (2005). The drillcore logs can be found in Appendix 1.

PYO-47 and PYO-84 drillcores have been subjects of previous lithogeochemical studies, where these drillcores were analyzed by taking 10 cm long samples every 1 m and combining them as composite samples, representing no more than 5m of core length. The contacts between the rock types were considered when determining composite samples. The samples were analyzed at Geological Laboratory of Outokumpu Exploration for SiO_2, TiO_2, FeO (total), MgO, CaO, Na_2O, K_2O, Ba, Sr, Zr, Cr, As, and P by using XRF. Ore samples were analyzed at Pyhäsalmi Mine for Zn, Cu, Ni, Co, Pb, Ag, Fe, Mn and Cd by using AAS (Mäki, 1986). PYO-47 (432 m) has 146 whole-rock geochemical assays and PYO-84 (483 m) has 195 whole-rock geochemical assays.

R-2394, R-2623 and R-2642 also have pre-existing geochemical assays on massive sulphide body. Maximum sample length for massive sulphides was 2 m. The samples were processed at the Pyhäsalmi Mine by crushing and grinding, and then analyzed at Pyhäsalmi Mine by using AAS, the same method as for the PYO- series.

Prior to this study, all seven drillcores had some pre-existing geochemical data, and all of it will be considered in this thesis, and they are available in Appendix 4. In addition to the old data, a total of 140 thin section samples and 104 geochemical samples were collected by sawing the drillcore in half in lengthwise direction, one half going either to analysis while the other half was placed back to drillcore box. From 140 thin section samples, 32 regular thins sections and 23 polished thins sections were produced in the end (a total of 55 thin sections) and the unused samples were placed in storage. All thin sections have corresponding whole-rock geochemical data. Since PYO- series drillcores already had pre-existing whole-rock geochemical assays, 31 whole-rock geochemical samples were analyzed from R- series drillcores silicate rocks. These samples were sent to Bureau Veritas Minerals for XRF Whole Rocks and ICP-MS Trace Elements analysis, and they are also available in Appendix 3. These new thin sections and geochemical data produced for this thesis work, are numbered as JSH-17001 – JSH-17140, and the selected samples are referred to as JSH-series samples.

From all these drillcores, non-destructive geophysical measurement was also collected. Specific gravity (kg/dm^3), magnetic susceptibility (SI-units) and electric resistance was measured by using common scale with measurement accuracy of 0.1g, handheld SATISGEO KT-6 with sensitivity of 10-5 SI units and custom-made electrical resistance meter made by Outokumpu with measurement scale of 10^6 - 10^{-3} Ωm, respectively. These geophysical properties were measured from most representing section of each geochemical assay in PYO- series drillcores and for each meter in R-2394, R-2623 and R-2642 hangingwall and most representing measurement for each geochemical sample in massive sulphide of these drillcores. Drillcores R-2242 and R-2252 had pre-existing geophysical measurements for every 3rd meter. In the end, however, electric resistivity measurements were only performed for PYO-47, R-2242 and R-2252.

6. METHODS OF STUDY

Since almost all protolith textures have been destroyed in the host rocks around the Pyhäsalmi deposit, geochemical trends are the most reliable tools to interpret startigraphical layers. The tools used in this study include the Alteraton Box plot, immobile element ratios and an attempt to use single precursor absolute mass transfer calculations.

The Alteration box plot was introduced by Large et al. (2001a). It is used for mapping out alteration zones associated within VMS footwalls and to help distinguish hydrothermal alteration from regional diagenesis. It consists of x-y diagram that has Ishikawas Alteration Index (AI) plotted from 0 to 100 in horizontal axis and chlorite-carbonate-pyrite index (CCPI) plotted from 0 to 100 in vertical axis. Least altered volcanics plot towards the center of the diagram, and hydrothermally altered volcanics plot at varying positions around the center, depending on the principal hydrothermal minerals present. Figure 3 serves as example on how AI and CCPI behave independently in different alteration zones. Both AI and CCPI formulas are below:

$$AI = \frac{100\ (K_2O + MgO)}{(K_2O + MgO + Na_2O + CaO)}$$

$$CCPI = \frac{100\ (MgO + FeO)}{(MgO + FeO + Na_2O + K_2O}$$

Major element compositions can be used to classify volcanic rocks in terms of petrogenesis and tectonic setting, but since many of the major elements are relatively mobile during alteration, these major elements cannot be used for identifying hydrothermally altered rocks. Fortunately, several elements are chemically immobile during most types of alteration, meaning that they are neither added to, nor taken from the rock during alteration. Although the concentrations of immobile elements may change due to net mass changes in the system, the ratios of immobile elements remain the same. Barrett and MacLean (1994) introduced plotted incompatible-compatible bivariate plots which are used to identify hydrothermally altered volcanic rocks

precursors. Different rock units will exhibit different immobile element ratios in comparison to each other.

Immobile elements can also be used to calculate net mass transfer of mobile elements that resulted of hydrothermal alteration. There are several approaches to estimating mass transfer, of which MacLean and Barrett (1993) single precursor mass transfer technique is used here because of its simplistic calculation. This method calculates mass transfer for each element in each sample separately by using the following formulae:

$$\Delta^a = \left(\frac{Z^O}{Z^a} \times C^a\right) - C^O$$

where Δ^a is absolute mass trasnfer expressed in g/100g, C^a = wt% proportion of element in altered rock, C^O = wt% proportion of element in precursor, Z^a = proportion of immobile element in altered rock and Z^0 = proportion of immobile element in precursor. In this context, precursor refers to hydrothermally unaltered rock, which is used as geochemical baseline for calculating absolute mass transfer in altered rocks. Due to closure, also known as the constant sum effect, a single immobile element is selected to more accurately determine mass transfer. Otherwise closure could obscure mass changes in major elements which exist in high proportions in primary unaltered rocks. For example, intense silicification of felsic volcanic rocks might not be apparent in composition data.

The degree of element immobility is established by plotting potentially immobile elements on x-y bivariate diagrams with the origins at zero. If the selected elements are immobile, the data points for a single precursor system should align in a highly correlated linear trend, which goes through the origin and the least altered samples. The correlation of all reliable single precursor samples, including both altered and unaltered, should be higher than 0.85 for accurate absolute mass transfer calculations.

Geochemical data is often normalized to 100%, or in slightly altered rocks the data may have been recalculated to be volatile free. Here, however, normalization or any other kind of data recalculation was not performed due to strong hydrothermal alteration that has caused significant mass changes in major elements. Recalculations might

unpredictably falsify the net mass transfer calculations, depending on changes in H_20, CO_2 and other possibly significant elements which were not measured. In addition, if the major elements were to be recalculated, the same should be done to trace elements. Failure to similarly adjust the trace element ratios could lead to small inconsistencies in immobile element ratios. And, even if recalculations were performed correctly, it would not affect immobile ratios anyway, and so there is no value in adding complications.

Geophysical properties will also be displayed and compared with geochemical data by using correlation, and major trends will be highlighted. Thin sections are used to determine mineral composition and rock texture for each sampled rock unit. The increase of hydrothermal alteration strength in the footwall is also observed and described in thin section reports. Drillcore logs and pictures are used as reference to verify geochemical calculation results, and for checking sampling integrity in PYO-series drillcores.

7. HYDROTHERMAL ALTERATION ZONE

The hydrothermal alteration zone can be seen most clearly in PYO-47 and PYO-84, and at certain small sections in R-2394, R-2623 and R-2252. Both PYO-series drillcores begin with white aphanitic footwall rhyolite, which has been regularly intersected by mafic veins and granite pegmatite veins. Both drillcores enter the footwall hydrothermal alteration zone.

At around Pyhäsalmi VMS deposit, the hydrothermal alteration typically exhibits sericite ± pyrite + quartz alteration, forming sericite schist. The alteration strength varies from weak, rhyolite dominated units with selective sericite alteration, to pervasive strong sericite alteration, where sericite schist has sulphides and quartz as additional main minerals. In footwall, alteration strength increases at proximity to the

massive sulphides, and is most reliably identified by the increase of disseminated sulphides.

Hydrothermal alteration also appears in some of the R-series drillcores, which explore the massive sulphide and the surrounding hangingwall host rocks. Most intense alteration is found within the massive sulphide body, and some weaker sericite alteration is found to the east from the deep massive sulphide body, where the drillcore R-2252 starts from hangingwall and heads towards east.

The footwall rhyolite consists of two geochemically separate units, which have been identified in TiO_2-Zr bivariate plot (Fig. 9B). They have been named in this thesis work as Rhyolite 1 and Rhyolite 2, and they are visible in Figure 9B as orange and gray groupings, respectively. Stratigraphically Rhyolite 1 is below Rhyolite 2, but their contact is interfingering. Rhyolite 2 is associated with massive sulphide body and more intense hydrothermal alteration. PYO-47 exhibits more hydrothermally altered rock than PYO-84, and it also hosts more Rhyolite 2 than PYO-84.

Absolute mass transfer calculations were performed on PYO-47 for Rhyolite 2 and on PYO-84 for Rhyolite 1. Zr, TiO_2 and Al_2O_3 are the only immobile elements available for PYO- series drillcores geochemical calculations. TiO_2-Zr, Al_2O_3-Zr and TiO_2-Al_2O_3 ratios (Fig. 9) have only average correlation.

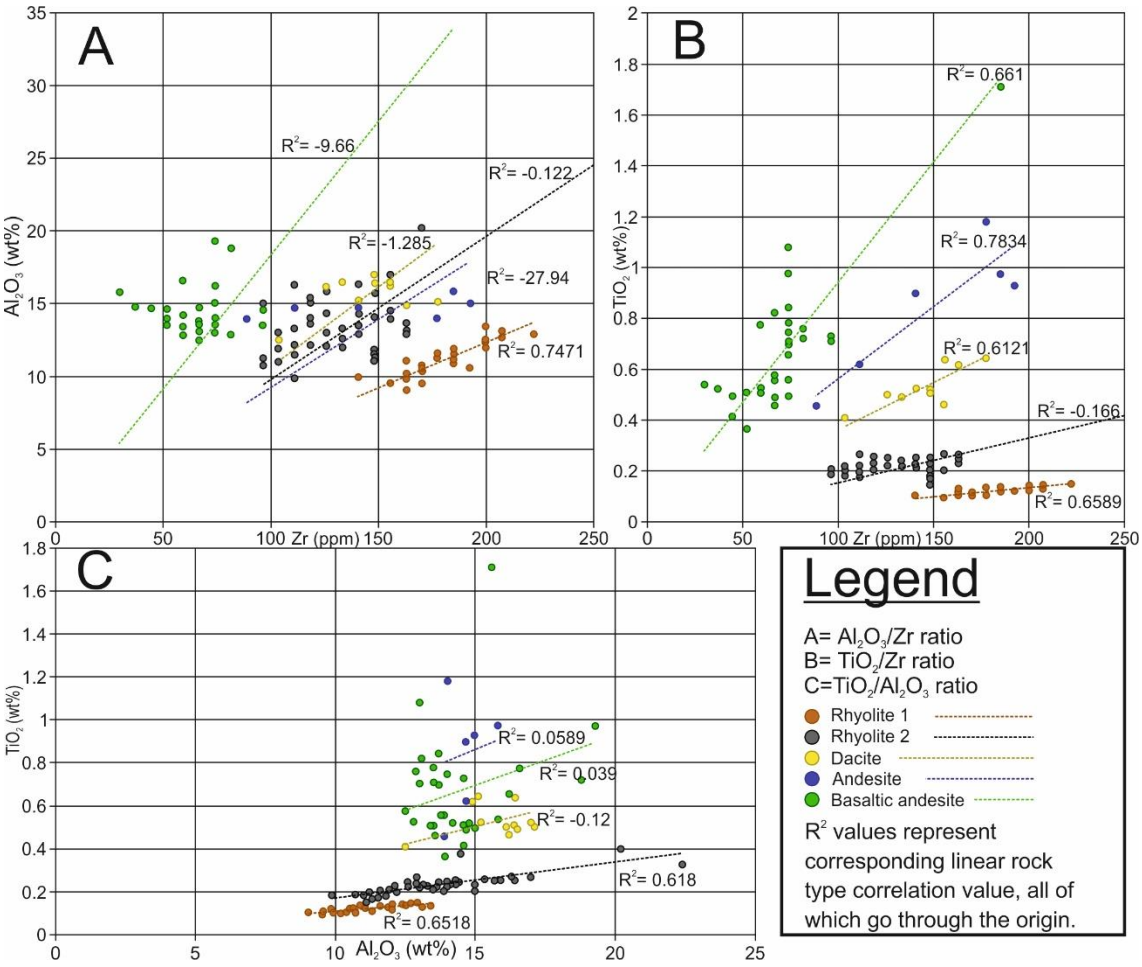

***Figure 9**. PYO-47 immobile element ratios in footwall. Different rock types should be identifiable by looking at sample groups. Chart B separates different groups most clearly. Thus, chart B was used to identify different rock types, and it has deemed reliable when the TiO2-Zr based classification was compared to drillcore logs and pictures, even in hydrothermally altered zones. Diagram C has the highest correlation values for rhyolitic rock units. Based on these charts, both Al_2O_3 and Zr would be a good candidate for absolute mass transfer calculations.*

Immobility of available immobile elements was also tested on new JSH-series geochemical samples collected from R-series drillcores in hangingwall. These elements include Zr, TiO_2, Al_2O_3, Nb and Y. Based on the correlation values in Figure 10, Zr, Al_2O_3 and Nb are most immobile, but Al_2O_3 seems to be more reliable on rhyolitic rock units specifically, whereas Zr could be applied to all rock types. Neither of them reaches the immobility standards set by Barrett and MacLean (1994), but Al_2O_3 is nevertheless

selected as the most immobile element for calculating mass transfer in rhyolitic units, since the general trend of mass transfer should still be available.

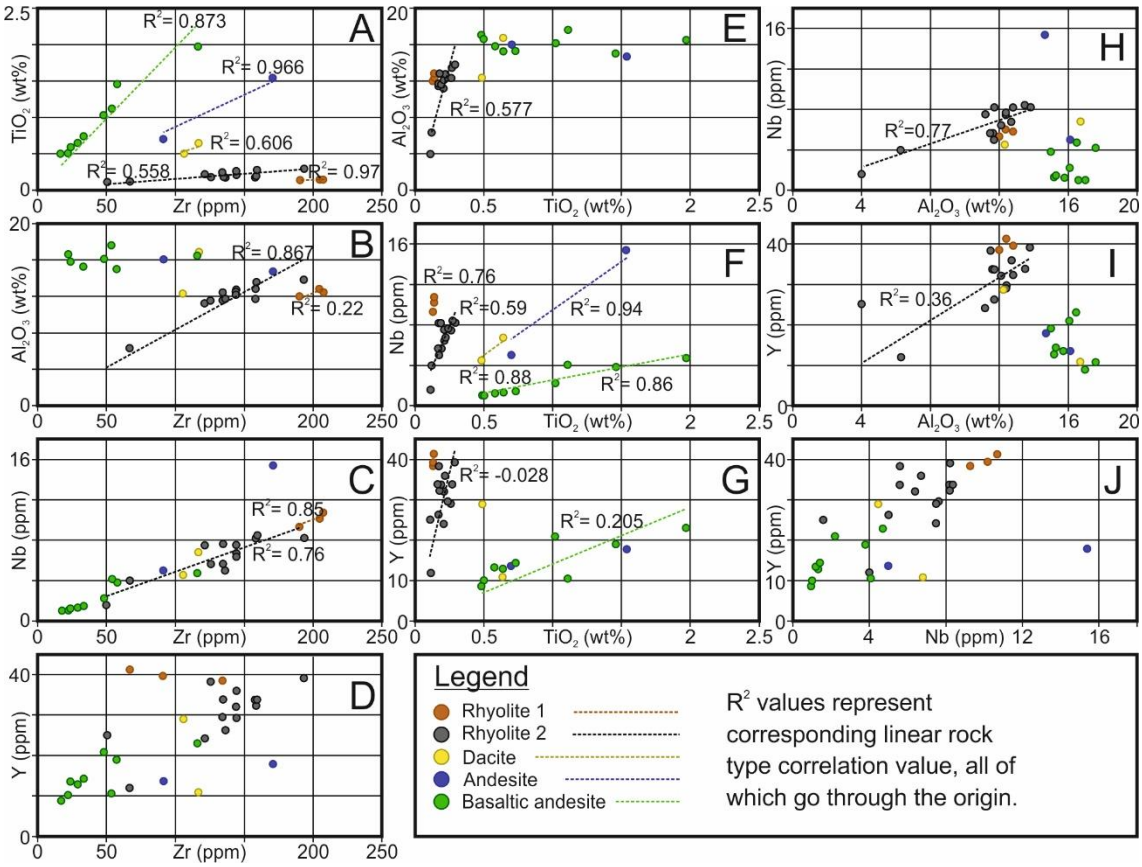

Figure 10. *Different immobile element ratios from R-series drillcores in hangingwall. A = TiO_2/Zr, B = Al_2O_3/Zr, C = Nb/Zr, D = Y/Zr, E = Al_2O_3/TiO_2, F = Nb/TiO_2, G = Y/TiO_2, H = Nb/Al_2O_3, I = Y/Al_2O_3 and Y/Nb. Charts B, C and H provides highest correlation values for Rhyolite 2 rock type. Rhyolite 1, Dacite and Andesite rock type correlation values are not reliable because there are not enough samples.*

The least altered sample, e.g. the protolith for Rhyolite 2 was selected to be an average of three least altered samples at the end of PYO-47 (415.2 m – 416.38 m, 421.52 m – 422.38 m and 425.95 m – 427.98 m). By the same logic, three samples were also selected to represent protolith for Rhyolite 1 from the very beginning of PYO-84 (16,6m – 20,3m, 20,3 – 22,4m and 22,77 – 23,27m). Precursor geochemical data is displayed in the table 1 below.

Table 1. *Rhyolite 1 and 2 precursors and their major oxides, Zr and S content. These values serve as a comparison point for absolute mass transfer calculations.*

Drill core	Precursor	SiO_2 %	TiO_2 %	Al_2O3 %	Fe_2O_3 %	MnO %	MgO %	CaO %	Na_2O %	K_2O %	P_2O_5 %	S %	Zr ppm
PYO-47	Rhyolite 2	73.97	0.0107	12.1	4.09	0.064	0.36	3.107	1.267	3.5	0.0237	0.1	152.93
PYO-84	Rhyolite 1	75.58	0.1335	11.75	2.9151	0.0745	0.55	1.9	4.5175	1.165	0.0138	0.1	173.9

7.1 PYO-47

Hydrothermal alteration is mostly absent up to 215.1 m of the drillcore. The very first few centimeters after 215.1 m are massive sulphide, after which the host rock is mainly composed of strongly altered sericite schist. Prior to the short massive sulphide section, the drillcore consist of fine-grained hydrothermally unaltered intermediate intrusion, which started at 206.3 m. Unfortunately, this intrusion destroyed the contact between sericite schist and hydrothermally unaltered rhyolitic rock unit that precedes the intrusion.

After 215.1 m, the host rock is mostly sericite schist, which has occasional biotite rich sections and increasing amounts of pyrite veins. The host rock has been metamorphosed at least once after hydrothermal activity ceased, recrystallizing sericite and quartz and occasionally forming cordierite. TiO_2-Zr ratios (Fig. 9B and 11) indicate that all the

sericite schist in this drillcore was originally Rhyolite 2 rock unit, which is geochemically slightly different from the unaltered Rhyolite 1 (Table 1), which is the dominant host rock up to 215.1 m mark (Fig. 11).

Sericite schist also hosts unaltered and moderately to strongly hydrothermally altered mafic veins and unaltered granite pegmatites. Unaltered mafic veins have intruded after hydrothermal alteration and the contacts between unaltered mafic veins and sericite schist exhibit biotite alteration. Hydrothermally altered mafic veins commonly appear as sericite - biotite schist. Hydrothermally altered mafic sections are not obvious during drillcore logging, but they are identifiable by comparing the immobile element ratios to PYO-47 drillcore logs (Fig. 11 and Appendix 1a, respectively). Most of the current sericite - biotite schists are altered of rock that more mafic, possibly andesitic in composition and was probably introduced to the host rock as an intrusion. Near the end of this drillcore (405.6 – 407.6 m), there is minor primary textures left of the altered mafic veins, where hydrothermal alteration intensity is not as strong. By studying thin section JSH-17045 (405.08 m), this rock can be described as cordierite-porphyroblastic biotite schist, which also has some sericite and chlorite alteration.

There are two main massive sulphide bodies in this drillcore, where the first one is thin (340 – 343.9 m) when compared to the second one (356.3 – 381.6 m). In between these units the host rock is mostly quartz rich sericite schist + pyrite veins. After the second main massive sulphide body (381.6 m), the host rock gradually changes from sericite schist into rhyolite that has weak sericite alteration and disseminated pyrite. The drillcore ends at 412.9 m.

Figure 11 displays TiO_2-Zr ratio along the whole drillcore length, which is used to identify all sampled rock types. This information is then applied to AI, CCPI, Alteration box plot and absolute mass transfer calculations.

Unaltered rhyolite, dacite and andesite/basalt fields are displayed in the Alteration box plot. If any samples map outside of their respective unaltered rock type fields, they are most probably hydrothermally altered. The further away each sample is from their respective unaltered field, the stronger the hydrothermal alteration has been.

Hydrothermal alteration trend is also visible in the Alteration box plot. For example, if originally rhyolitic unit is plotting a clear trend towards upper right corner of Alteration box plot, the hydrothermal alteration is expected to be chloritization. In Figure 11, Rhyolite 2 is clearly the most altered rock unit, while all other rock units are remained relatively unaltered. There are a few unaltered Rhyolite 2 samples, which can be seen in the unaltered rhyolite and dacite fields. The average values of these samples are used as a precursor for absolute mass transfer calculations in Rhyolite 2.

When looking at PYO-47 profile picture and the changes of hydrothermal alteration intensity in alteration index chart, it seems that the approximate contact between unaltered Rhyolite 1 and altered Rhyolite 2 just before 215.1 m, is a fault zone. Supportive argument for the fault zone hypothesis is that the adjacent Rhyolite 1 exhibits no hydrothermal alteration whatsoever, whereas Rhyolite 2 exhibits strong hydrothermal alteration just a few meters away from the unaltered Rhyolite 1, as is clearly displayed in AI and CCPI charts in Figure 11. It seems improbable that Rhyolite 1 would remain hydrothermally unaltered if it were in a proximity to Rhyolite 2 during such intense hydrothermal alteration. Therefore, this Rhyolite 1 rock unit was not near this Rhyolite 2 unit during hydrothermal alteration but are now next to each other due to tectonic event, which happened after hydrothermal alteration took place. Unfortunately, this hypothesis could not be verified from this drillcore alone due to the intrusion that has overprinted the hypothetical fault zone area.

This hypothetical fault zone, however, could explain what the small massive sulphide section is, which starts after 215.1m. The small massive sulphide could be connected to the deeper ore fan, which is visible in Figure 11 profile picture. The small massive sulphide section would be in that case a remnant of the bigger massive sulphide body, which has “dragged” and extended along the fault line as the main ore body has thrusted down. The small massive sulphide section could be currently connected to a larger massive sulphide body by this extension which follows the hypothetical fault zone. This hypothesis is supported by the fact that Rhyolite 2 rock unit surrounding the small massive sulphide section bears similar trends in Alteration index chart and absolute S% mass changes as the Rhyolite 2 rock units do, that surround the main massive sulphide bodies later in 340 – 343.9 m and 356.3 – 381.6 m (Fig. 11).

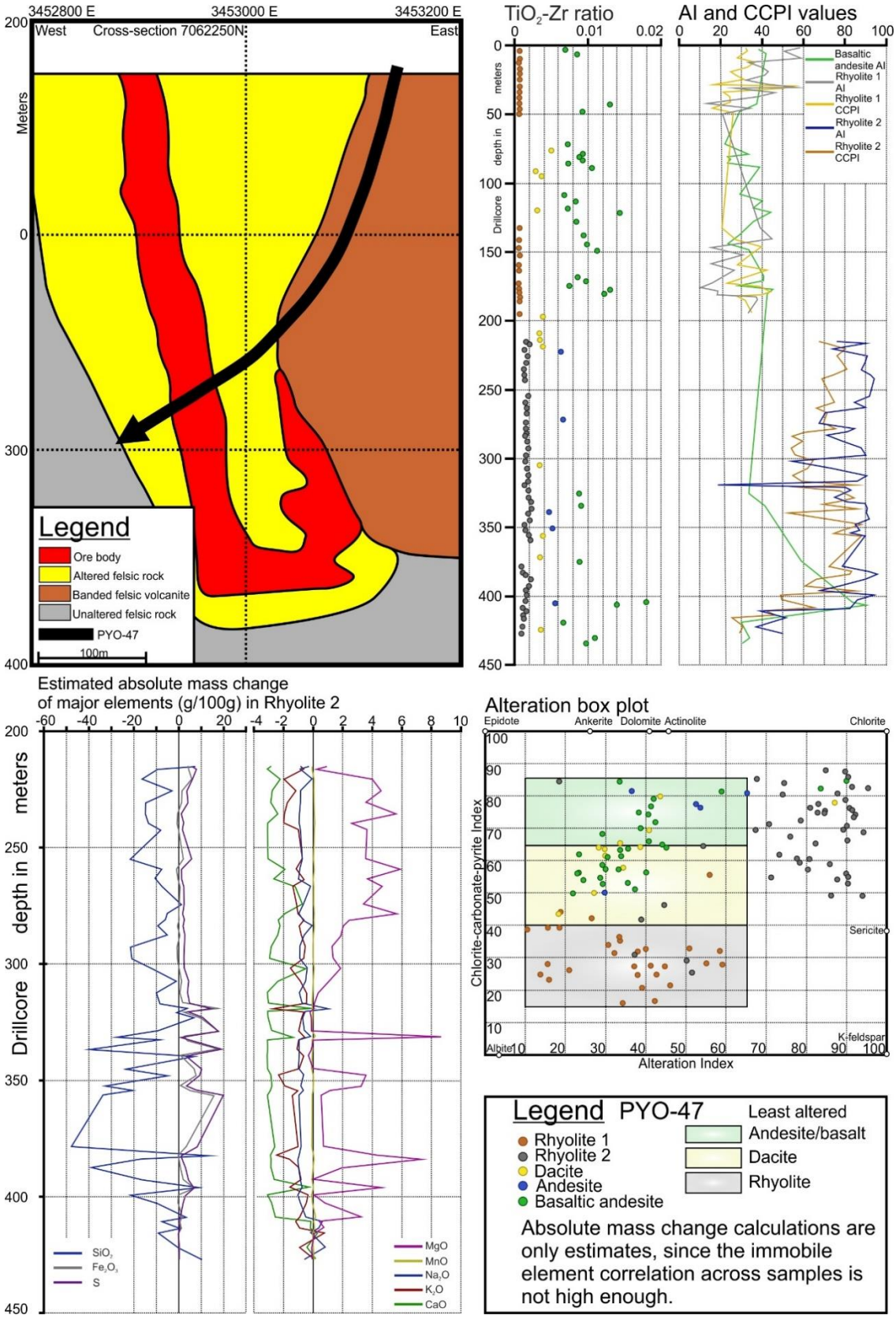

Figure 11. *PYO-47 profile and major geochemical trends. Al_2O_3 was used as immobile element and the least three altered samples in alteration box plot serve as precursor for absolute mass transfer calculations.*

7.2 PYO-84

Weak sericite alteration occurs infrequently up to 322 m, after which alteration intensity increases, and disseminated pyrite appears as an additional component in sericite schist. The strongest hydrothermal alteration is seen in 413.7 – 447 m, where sericite alteration is pervasive, and pyrite presents itself as strings. After 447 m, alteration intensity gradually degreases again and by the end of this drillcore (483.3 m), there is no indication of hydrothermal alteration.

In comparison to the hydrothermal alteration displayed in PYO-47, this drillcore shows lower tiers of hydrothermal alteration and no apparent faulting. In addition to that, the contacts between Rhyolite 1 and 2 are also seen in a few occasions, as is visible in TiO_2-Zr ratio in Figure 12. In the PYO-84 drillcore logs, Rhyolite 2 is described as dacite, because these drillcores were logged without prior to studies in immobile element ratios and because Rhyolite 2 appears to be a shade darker that Rhyolite 1. Rhyolite 2 is in small part present along with Rhyolite 1 whenever there are noticeable increases in hydrothermal alteration intensity.

When studying how different Alteration index and CCP index values affect the host rock, which is in this case Rhyolite 1, it was observed that when AI went above 40, it would reliably indicate that weak sericite alteration is noticeable in macroscale. Similarly, CCPI values above 40 indicate visible sulphide enrichment in sericite alteration. Determining these values was possible due to the spectrum of hydrothermal alteration intensity in Rhyolite 1. These observations are verifiable by comparing AI and CCPI values to drillcore logs and pictures. These tighter restrictions for unaltered Rhyolite 1 are also highlighted by red outline in the Alteration box plot and red lines in AI and CCPI charts in Figure 12.

By looking at SiO_2, MgO, MnO, Na_2O, K_2O and CaO mass changes alone, it is hard to distinguish hydrothermal alteration from diagenesis. In this regard, S% mass gains is the most reliable indicator of hydrothermal alteration, aside from AI and CCPI.

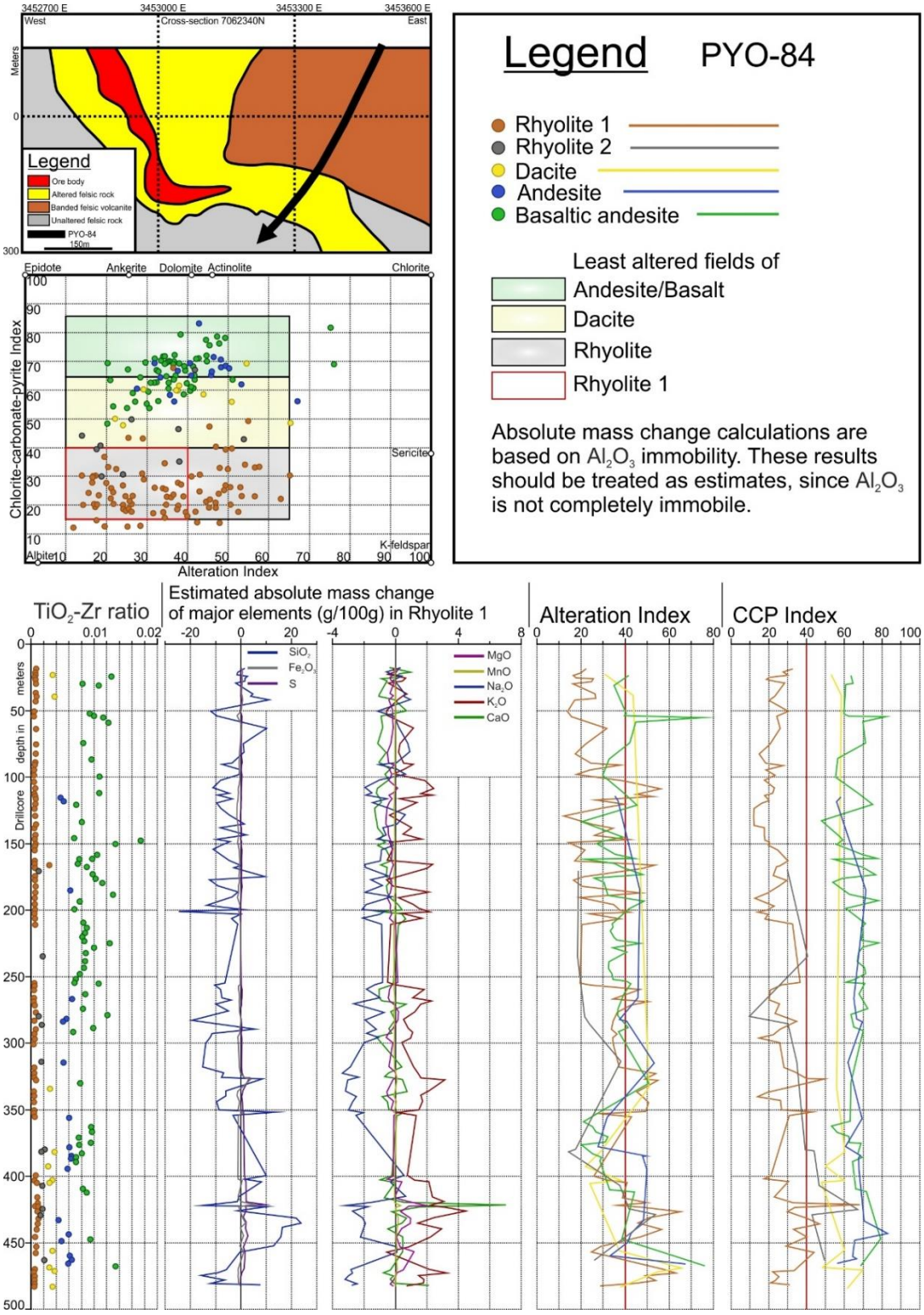

Figure 12. *PYO-84 profile and major geochemical trends. Unaltered field for Rhyolite1 has been constrained to the red box in Alteration box plot. Upper limits for this box is also highlighted in AI and CCPI charts as a red line.*

7.3 R-2623

This drillcore only has one small section that has been hydrothermally altered. It is in the middle of deep ore body (114.25 m – 117.47 m), and the sample of this interval, JSH-17010, is mostly composed of quartz + pyrite grains ± sericite, fibrous sillimanite and chalcopyrite infill. Based on absolute mass transfer calculations this section has gained 69% of SiO_2 and 16% of S. PYO-47 Rhyolite 2 precursor has been used as baseline, since it groups together with Rhyolite 2 in PYO-47 TiO_2-Zr chart (Fig. 14). AI is 73 and CCPI is 87. When this samples location in massive sulphide and the nature of the hydrothermal alteration is considered, this sample could represent the stringer zone of the Pyhäsalmi VMS deposit.

7.4 R-2394

The only hydrothermally altered sample in this drillcore is found closer to the edges of deep ore body (151.11 m - 151.72 m). In drillcore, it appeared to be a dacitic vein or clast, but proved to be unidentifiable in optical microscope (Appendix 2). The sample JSH-17082 is composed of large subhedral biotite crystals and fine-grained unidentified matrix. It also hosts pyrrhotite, chalcopyrite and some pyrite.

Based on TiO_2/Zr ratio, JSH-17082 is also Rhyolite 2. It has gained 83% SiO_2, 65% MgO, 33% CaO and 6% S when compared to PYO-47 Rhyolite 2 precursor. The unidentified matrix could be amphibolite group minerals, based on the abundance of MgO. AI value is 63 and CCPI is 98. When compared to the nature of hydrothermal alteration in JSH-17010, this sample is clearly not a part of the stringer zone.

7.5 R-2252

Possible weak hydrothermal alteration in 28.85 m – 35.78 m. This area has numerous pervasive epidote + quartz ± cordierite veins that cut through granular rhyolite.

The second altered area is located at 84.3 – 94 m. The host rock is rhyolite, which has strong pervasive sericite + chlorite + quartz hydrothermal alteration. This area has also been intruded by numerous small mafic veins which are not hydrothermally altered, but host disseminated pyrite.

Sample JSH-17129 was collected from 103.46 – 103.66 m, which is composed of smaller patch of sericite altered rhyolite, surrounded by mafic veins. Based on thin section studies, weak sericite alteration has been overprinted by later metamorphosis. The rock is sericite altered, diopside-epidote felsic gneiss. AI is 9 and CCPI is 87, and when this sample is mapped to the Alteration box plot and compared to unaltered rhyolite, the trend indicates the presence of epidote and calcite, both of which was found in thin section. (Large, et al. 2001a)

7.6 General aspects of alteration

The Alteration box plot in Figure 11 indicates that Rhyolite 2 should have experienced chlorite alteration, when looking at the general trend for Rhyolite 2 from unaltered to hydrothermally altered samples. Based on drillcore logs and thin section studies, this has clearly not been the case and instead sericite alteration has dominated. Equations 1 and 2 describe what happens during sericite and chlorite alteration, respectively:

$$3\,NaAlSi_3O_8 + K^+ + 2H^+ = KAl_3Si_3O_{10}(OH)_2 + 6SiO_2 + 3Na^+ \qquad Equation\ 1$$

Equation 1 involves a loss of Na_2O, from albite to the hydrothermal fluid, and gain of K_2O to sericite altered albite. During alteration, the hydrothermal fluids pH increases, and silica is conserved by the deposition of quartz (Gifkins et al., 2005). However, Rhyolite 2 has experienced losses in both Na_2O and K_2O in equal amounts.

$$2KAl_3Si_3O_{10}(OH)_2 + 3H_4SiO_4 + 9Fe^{2+} + 6Mg^{2+} + 18H_2O = 3Mg_2Fe_3Al_2Si_3O_{10}(OH)_8 + 2K^+ + 28H^+ \qquad Equation\ 2$$

During equation 2, the fluid becomes more acidic. As sericite alters to chlorite, it gains FeO and MgO and relinquishes K_2O, provided that Al_2O_3 remains constant. Al_2O_3 content may change if carbonate alteration is present (Large et al., 2001a), but no carbonate alteration was seen in hydrothermally altered Rhyolite 2 and, as has already been indicated, Al_2O_3 should be immobile. Some carbonate alteration is seen in biotite schists, which have mafic protolith.

Based on absolute mass transfer calculations (Fig. 11) and thin sections, sericite, FeO, MgO and H_2O should have been abundant when Rhyolite 2 was undergoing hydrothermal alteration, which would leave H_4SiO_4 as the only component which might have been lacking for chlorite alteration. This would mean that the hydrothermal fluid was not acidic enough or there was not enough SiO_2. The lack of SiO_2 is not the correct answer, since quartz is one of the main minerals in sericite schist, even when absolute mass transfer calculations might suggest otherwise. The lack of H^+ could be a possibility if the Rhyolite 2 protolith did not have high enough plagioclase and albite content to produce necessary sericite and H^+, both of which is needed for chlorite alteration.

The reason for these two seemingly contradicting observations of abundant quartz in thin sections and loss of SiO_2 in absolute mass transfer calculations could be that the mass transfer calculations are not correct. When some other immobile element than Al_2O_3 is used for absolute mass transfer calculations, these calculations show some

areas where there are SiO_2 gains. The overall SiO_2 gains and losses trend would still be similar to what is shown in Figure 11.

Considering the complexity of a hydrothermal system, there is too many unknown variables to make more than educated guesses on the nature of hydrothermal alteration in Rhyolite 2. The only thing that is safe to say is that even though absolute mass transfer calculations and Alteration box plot trends would imply that chlorite alteration should be the major chlorite alteration type around the massive sulphide, it is not. And that seems to be an anomaly.

8. MAIN CHARECTERISTICS OF PYHÄSALMI VMS DEPOSIT

There are several observable main characteristics about Pyhäsalmi VMS available in drillcores R-2394, R-2623, R-2642 and PYO-47; metal zonation and rock inclusions that are mafic intrusions, remnants of the host rock or carbonate veins.

Pyhäsalmi Mine has used Imaña's (2003) classification for the deep ore body ore types ever since it was developed, and the same classification is used here. Massive sulphide was not studied too closely for this thesis work, since Imaña has already described the textures, metal content, possible origins of each metal zone and other characteristics. A short summary of that classification can be found in Appendix 6.

8.1 Metal zonation in deep ore body

In drillcores R-2394, R-2623 and R-2642, the outer layer of the deep ore body always exhibits 10 – 25m thick layer of B Zinc ore (BZ), as can be seen in Figure 13. After BZ, the underlaying A Cu-Pyrite Ore (AP) seems to appear, in comparison to BZ, more often and at times larger bodies. Underneath the BZ layer, which also dominates the central parts of the deep ore body, is mostly Massive Pyrite (MP) or Spotty Massive Pyrite (SMP). These observations agree with Imaña's (2003) description of the massive sulphide, and also with general metal zonation model (Large, 1992).

The deep ore body also has other metals in smaller quantities, such as Pb, Au and Ag, all of which are clearly enriched in BZ, the outermost layers of massive sulphide. Au and Ag are also enriched together in small sections of SMP, MP and AP.

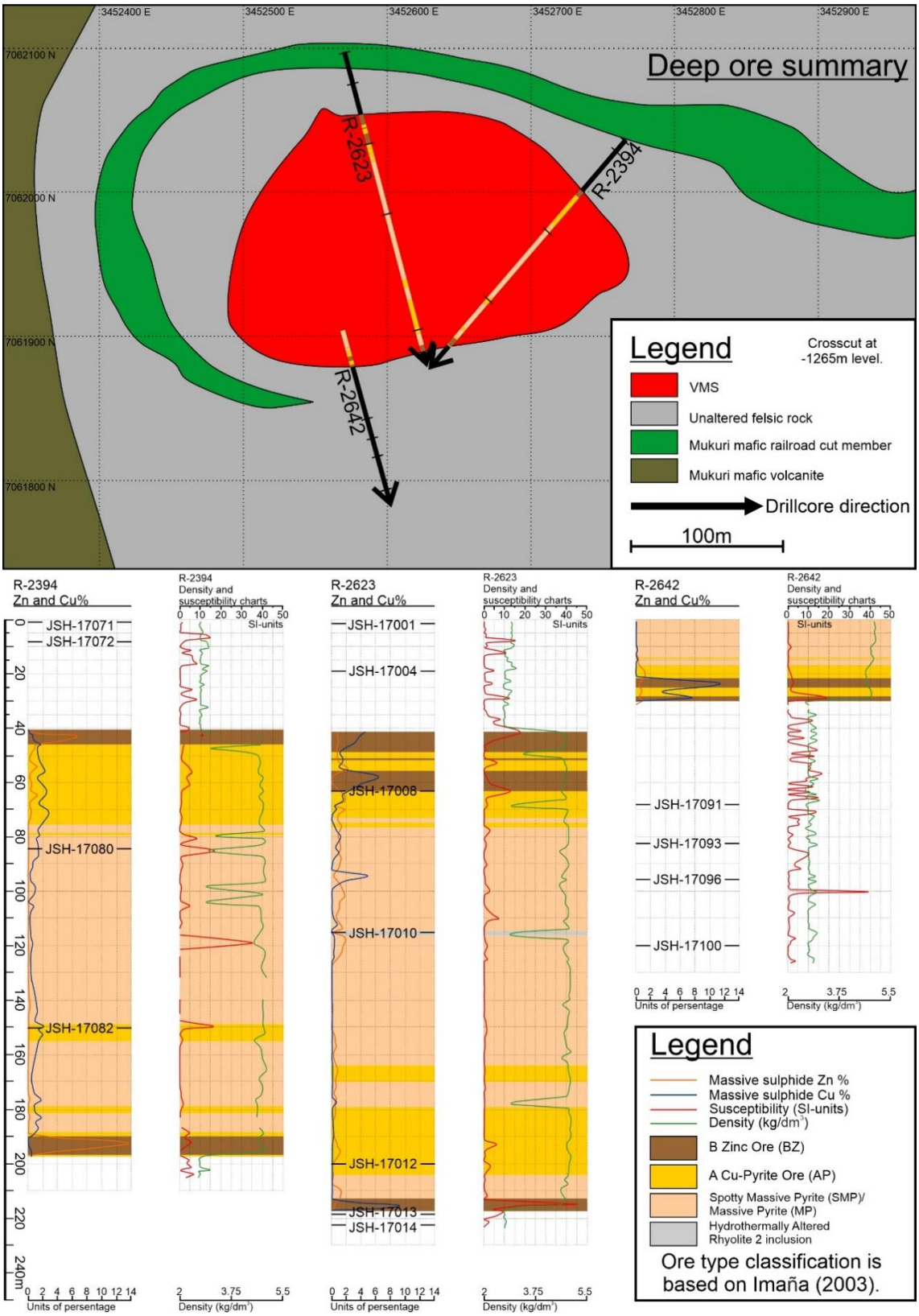

Figure 13. *Deep ore summary. These three drillcores have been projected to 1115 m level, ignoring depth and dip of the drillcores. Sharp declines in massive sulphide density values indicate the presence of silicic inclusions. Approximate selected JSH-series sample locations have been marked.*

8.1.1 A brief description of PYO-47 massive sulphide

PYO-47 also has some massive sulphides, but no clear metal zonation was observed. Zn values are overall high, varying from 0,7 to 8,8 wt% from the beginning (356 m) to the end (380 m) of the massive sulphide. Cu has enriched in smaller area in 370 – 376 m, where Cu content peaks around 375 ppm. Pb also peaks at specific point of 378,7 – 379.8 m, up to 13,4 wt%. However, this value is most probably a result of measurement or sampling error rather than actual Pb content, since the average Pb content is 192 ppm.

8.2 Rock inclusions in deep ore body

The deep ore body has numerous mafic intrusions. Three of these intrusions were sampled as JSH-17008 (63.61 - 63.82 m) and JSH-17012 (199.9 - 200.08 m) from R-2623, and JSH-17080 (85 - 85.21 m) from R-2394. All three samples map well within the unaltered mafic section in Alteration box plot and exhibit no hydrothermal alteration in thin sections either. However, all three samples seem to be enriched with disseminated pyrite and this is clearly seen in hand sample. Whole-rock geochemical data also shows that these intrusions are also enriched in Ag and Au (Appendix 3), but it is not clear by what method they have been enriched in these rare metals.

The deep ore body also hosts some felsic inclusions, such as the previously stated short hydrothermally altered section in the middle of massive pyrite and drillcore R-2623 (114.25 - 117.47 m), sampled as JSH-17010. It groups well with other Rhyolite 2 samples, when it is mapped in PYO-47 TiO_2-Zr chart. One other Rhyolite 2 unit was sampled JSH-17082 in R-2394 (151.2 - 151.3 m), in one of the earlier AP ore zones. (Fig. 13).

The massive sulphide also hosts other mineral groups, such as carbonates and sulfosalts. They appear as small mineralizations in massive sulphide, often with chalcopyrite, sphalerite and occasionally in larger areas in massive pyrite, but no samples were collected from these mineralizations. Their locations, however, are mapped in the drillcore logs (Appendices 1 e – g).

9. REVIEWED LITHOSTRATIGRAPHY

Lithostratigraphy is divided here to footwall and hangingwall for practical purposes. Footwall includes all the lithostratigraphical units that are in and under the massive sulphide and hangingwall includes all the rock mass that is above the topmost layer of massive sulphide, which is the B zinc ore layer.

According to VMS formation model, the hangingwall should be less altered than footwall or, more commonly, completely unaltered. For this reason, all hydrothermally altered rocks that are at near vicinity of the massive sulphide are also included to the footwall. In the case where there is no massive sulphide, the boundary between footwall and hangingwall goes between hydrothermally altered and unaltered rock units.

Figure 14 is a collection of all available samples in TiO2-Zr plot, classified by rock type and location. It is a useful summary, which is used to identify the main protoliths in both footwall and hangingwall. Chemical rock type classification is required, since it would be otherwise impossible to identify which rock is related to which protolith, due to hydrothermal alteration and metamorphic events.

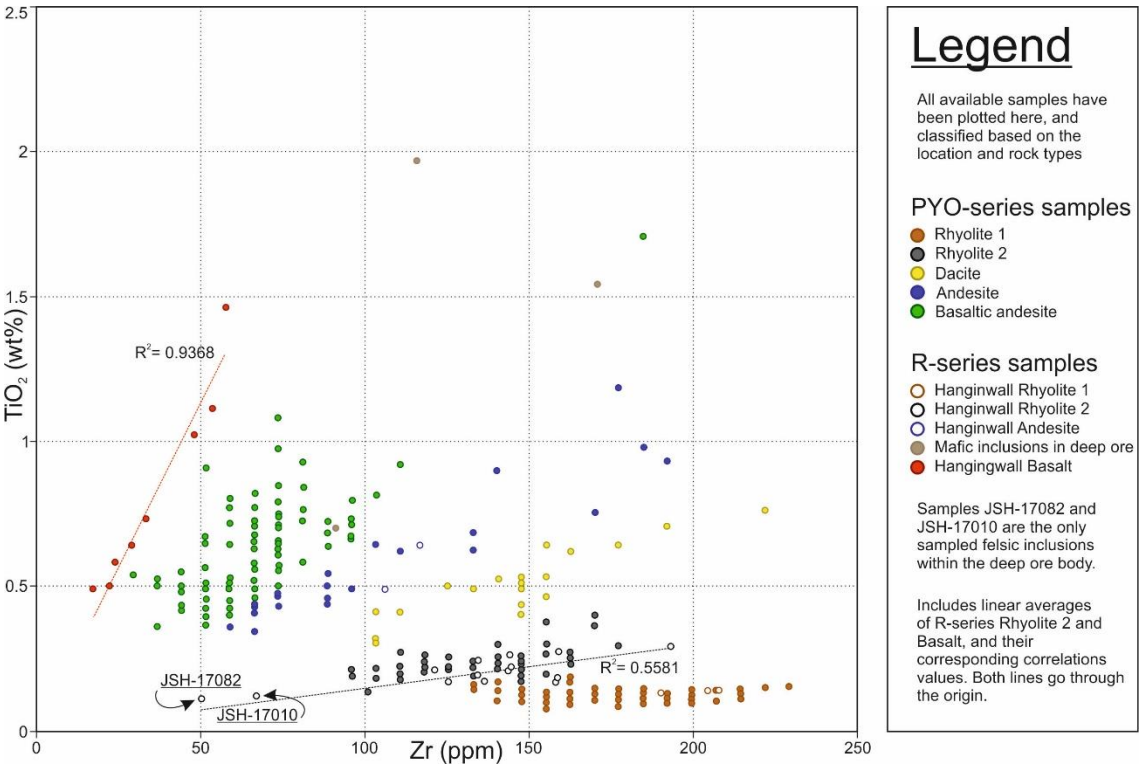

Figure 14. *TiO_2-Zr plot of all available samples. This figure is the main tool in this thesis work for identifying different rock types in and around the Pyhäsalmi VMS deposit.*

9.1 Footwall lithostratigraphy

Footwall lithostratigraphy can only be observed in PYO-series drillcores and in R-series massive sulphide inclusions. R-2252 advances towards the footwall lithologies from hangingwall but does not reach it.

PYO-47 breaches through the upper massive sulphide and stronger hydrothermal alteration zone whereas PYO-84 does not and exhibits weaker hydrothermal alteration. Beside these differences, both PYO-series drillcores show the same lithostratigraphical units in a similar order. Figure 14 shows all prominent rock types around Pyhäsalmi

deposit, excluding granite pegmatite veins. The veins are located and shortly described in drillcore logs (Appendix 1).

The general description of Pyhäsalmi VMS deposit lithostratigraphy in Figure 6 describes the footwall lithology in the same order as it is being described here, only the rock type names are different. Starting from the lowermost rock unit in Figure 6, the supracrustal Näläntöjärvi suite is not visible in PYO-series drillcores, and neither there are any Andesite or Mafic A-2 main magma bodies, but the following Rhyolite A is. Rhyolite A is equivalent to the rock unit that was named in this thesis work as Rhyolite 1. In this thesis work, Rhyolite 1 rock unit is overlaid by following Rhyolite 2 rock unit, just as Rhyolite A is overlaid by Rhyolite B in Figure 6. The contact between these two rock units is not a clear line but rather interfingering stratification between the two, as is seen in PYO-84.

The host rock for massive sulphide is Rhyolite 2 (which is equivalent to Rhyolite B in Fig. 6), where it appears as sericite schist with occasional sericite – biotite schist intervals. These sericite – biotite schist intervals are identified as hydrothermally altered Andesite rock type in TiO_2-Zr charts (Fig. 11 and 14). Sericite schist also hosts unaltered Basaltic andesite rock type veins. On these two observations, it is reasonable to assume that the footwall hosts two separate mafic bodies deeper in footwall, of which Andesite body is older of the two, and both have intruded into Rhyolite 1 and 2. Mäki et al. (2015) seem to have concluded the same since Andesite and Mafic A-2 are clearly separated in Figure 6, where Mafic A-2 is equivalent to Basaltic andesite. Figure 6, however, does not include Dacite rock unit, which was also identified in Figure 14. Dacite rock type seems to be one of the younger intrusions, since it is located just at the contact between Rhyolite 1 and 2 in PYO-47, where the hypothetical fault zone lies. There are also several unaltered gray Dacite veins in alteration zone itself, so it was not relevant during VMS formation process.

Hydrothermally altered Rhyolite 2 also seems to stratigraphically extend over massive sulphide around the upper ore body. The alteration intensity rapidly weakens with increasing distance above the massive sulphide. The deep ore body hosts minor felsic inclusions, such as samples JSH-17010 and JSH-17082, which have undergone intense

hydrothermal alteration, and they belong to Rhyolite 2 rock type (Fig. 14). Miettinen (2011) also concluded the same and showed additional evidence that these inclusions are indeed early relicts of an altered footwall host rock. Miettinen (2011) also observed that the Zn ore layer does not have any footwall relicts, and no contradicting evidence were found in this thesis work. Large et al., (2001b) explains that Zn metal layer often precipitate on top of the seafloor, whereas Cu ore layer and the other massive sulphide layers below usually replace the footwall rocks in certain types of VMS deposits.

Massive sulphide mafic inclusions JSH-17008, JSH-17012 and JSH-17080 groups with Basaltic andesite, which is a rock type that originates from deeper footwall and is visible in all other lithostratigraphical units as intrusions and does not exhibit any hydrothermal alteration. Since it appears as an inclusion in massive sulphide, this would indicate Basaltic andesite has intruded into massive sulphide as well, after hydrothermal alteration had ceased. The mafic inclusions have been marked in Figure 14.

In Figure 14, Basaltic andesite rock type has a wide spread of TiO_2-Zr ratios, which could be explained away with periodical intrusion from an evolving magma body. Andesites and Dacites have tighter, but longer spread along their alteration line, which reflects how these units intruded in shorter span of time.

Further away from the massive sulphide, Rhyolite 2 rock unit in PYO-84 appears as a much smaller and infrequent stratigraphical units in comparison to PYO-47. Even when Rhyolite 2 units are present, Rhyolite 1 dominates as most common rock type overall, as is seen in Figure 12, and continues as the dominant rock type upon entering the hangingwall. As a conclusion, the relationship between Rhyolite 1 and 2 rock units is more complicated further away from massive sulphide than how it is displayed in Figure 6. Rhyolite 2 may not be the dominant rock type in all areas along the footwall – hangingwall boundary.

9.2 Hangingwall lithostratigraphy

Only the R-series drillcores display hangingwall characteristics. Drillcores R-2623, R-2394 and R-2642 (Fig. 13) are only showing the immediate hangingwall after deep massive sulphide, and drillcores R-2242 (Fig. 15) and R-2252 (Fig. 16) show the lithostratigraphical units near the deep massive sulphide, and some distant hanginwall towards south-west and east, respectively.

The immediate hangingwall alternates between felsic dominated layers with additional thin mafic layers, where both rock type layers have oriented concordant to deep massive sulphides outer surface, enveloping the deep massive sulphide body on all sides. The immediate hanginwall has undergone intense metamorphism, leaving no primary textures. There is no hydrothermal alteration or even disseminated sulphides in mere centimeters after massive sulphide contact. Instead, felsic rocks have more commonly saturated by magnetite. Figure 13 shows all selected JSH- series samples in and around deep massive sulphide from R-2623, R-2394 and R-2642, and each thin section description is available in Appendix 2.

Samples JSH-17013 and JSH-17014 from R-2623 and JSH-17122 from R-2252 are the nearest to massive sulphide. These samples group as the hangingwall Rhyolite 1 in Figure 14. It seems that the first meters of the hangingwall chemically belong to Rhyolite 1 rock type, but the rock type changes quickly to Rhyolite 2, as samples JSH-17001 and JSH-17004 from R-2623, samples JSH-17071 and JSH-17072 from R-2394 and some other samples collected from drillcores R-2642, R-2242 and R-2252 show. These other samples were collected further away from massive sulphide, indicating that Rhyolite 2 unit extend further into hangingwall than Rhyolite 1.

Mäki et al., (2015) describes how the entire massive sulfide body has thrusted into the unaltered hanginwall (Fig. 8D). This would explain why the deep ore body is surrounded at all sides by hanginwall, and is one of the possible reasons why Rhyolite 1 currently appears to be the in the immediate hangingwall of the deep ore body, even though Rhyolite 1 is more commonly associated with deep footwall of the deposit.

Alternatively, as was stated in chapter 9.1, Rhyolite 1 is in some areas the dominant rock type at the footwall – hangingwall boundary.

Starting from the beginning of immediate hangingwall, the first few meters consist of Rhyolite 1, after which Rhyolite 2 becomes the dominant rock type for the next 40 – 50 m. After around 50 m, however, the dominant rock type changes into Basalt, as it has been identified in TiO_2-Zr chart (Fig. 14), but the contact with Basaltic rock type changes depending on which side of the deep ore body hangingwall is studied. Figure 13 profile picture shows a good summary of the immediate hangingwall. Basalt is also present as frequent thin mafic layers in 0 - 50 m range but was not yet dominant rock type.

In drillcore R-2252, however, dominant Basalt unit is first encountered on 120 m mark. This basaltic layer will continue until 165 m, followed again by a long section of Rhyolite 2 (Fig. 16). The apparently thicker stratigraphical units are to be expected, considering that R-2252 starts from near contact with massive sulphide in depth of 996 m and faces towards east in -35° dip, drilling along the plane boundary between footwall and hangingwall, which is similiarly dipping steeply towards east (Fig. 7B). This means that the rock unit widths in R-2252 are only apparent, and not the true thickness of the rock unit.

The same is also true for the first 140 m of drillcore R-2242 (Fig. 15), since its starting drilling direction is parallel with massive sulphide surface and with hosting rock units towards south-west. After 140 m, the general foliation of the host rock turns from south-west to south-east, and the apparent thickness is starting to be closer to the true thickness of the rock units.

Since R-2242 and R-2252 are the only drillcores that go beyond 100 m into hanginwall and in different directions in respect to deep massive sulphide (Fig. 7A), it is safer to only generalize that beyond the first major Basalt layer, Rhyolite 2 is again dominant. It is occasionally intersected by smaller basaltic layers and granite pegmatite intrusions. In R-2242, there are also some mafic intrusions which appeared around 250m depth, and were logged as “trachybasalt,” but no samples were analyzed from these rock units.

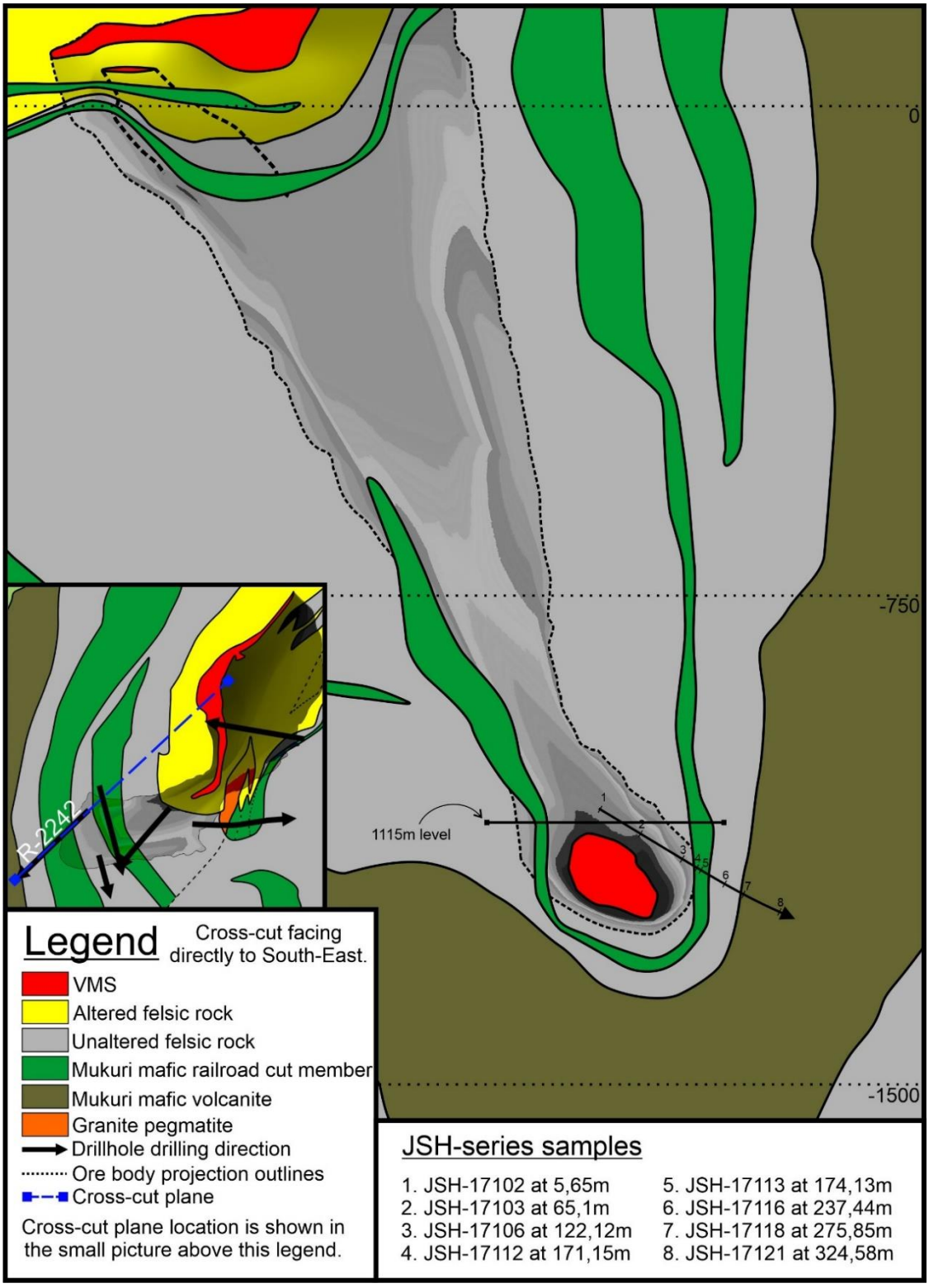

Figure 14 Drillcore R-2242 profile and approximate sample locations. Massive sulphide behind the cross-section has been projected as a shadow for clearer representation of the surrounding rock. Drillcore goes perpendicular with the massive sulphide outer surface up to 120 m, after which the alfa angle between drillcore and rock units starts to increase up to 56°.

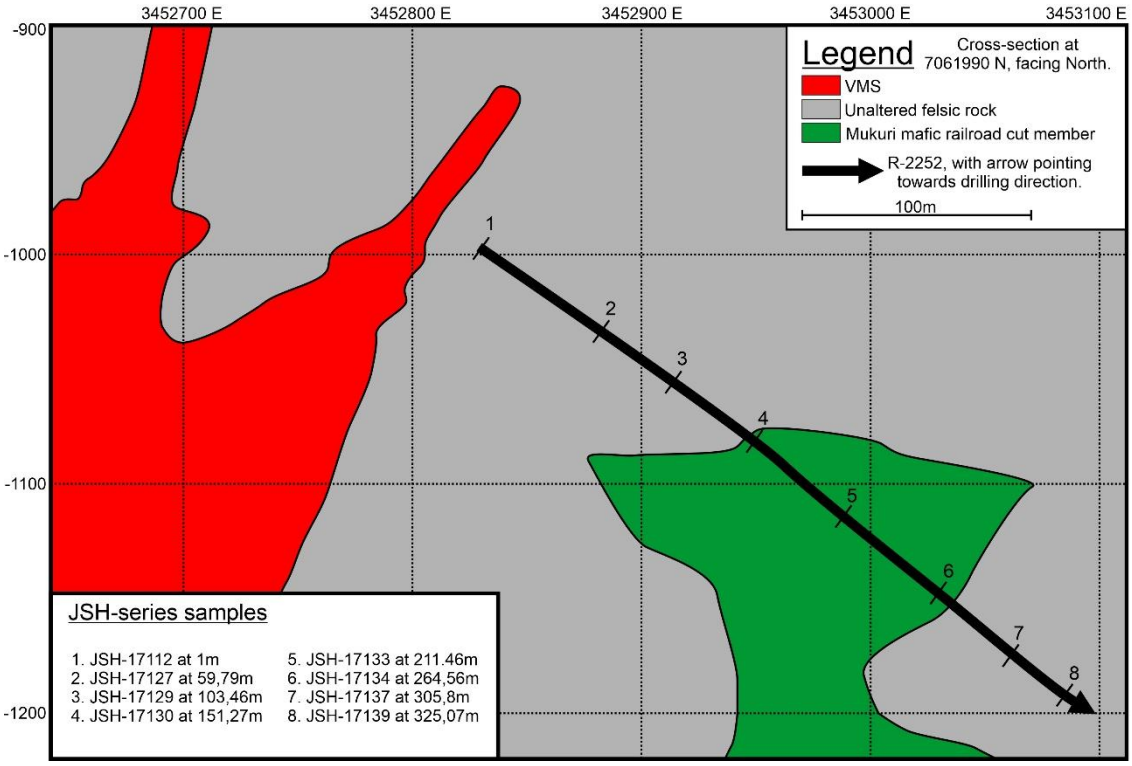

Figure 15 Drillcore R-2252 profile, and approximate sample locations.

10. GEOPHYSICS

In this chapter, specific gravity and susceptibility measurement values are evaluated on how useful they are for interpreting drillcores, and what limitations there are for using them.

Electric resistivity measurements did not produce any valuable data from silicic rocks, and no electric resistivity measurements were performed in massive sulphides since the measured values were not constant nor repeatable. The only thing worth mentioning about electric resistivity is that it is certainly much lower in massive sulphides than in the silicic rocks that surrounds it, which is useful during massive sulphide exploration.

10.1 Specific gravity

Of the 928 measured specific gravity values, 338 measurements have corresponding whole rock geochemical assays and 173 massive sulphide measurements with corresponding AAS geochemical assays. Most of the 338 specific gravity measurements with whole-rock geochemical assays come from PYO-series drillcores, and the rest are selected from JSH-series samples. These samples are plotted to SiO_2 - specific gravity (kg/dm^3) chart in Figure 17, where samples are divided by rock type.

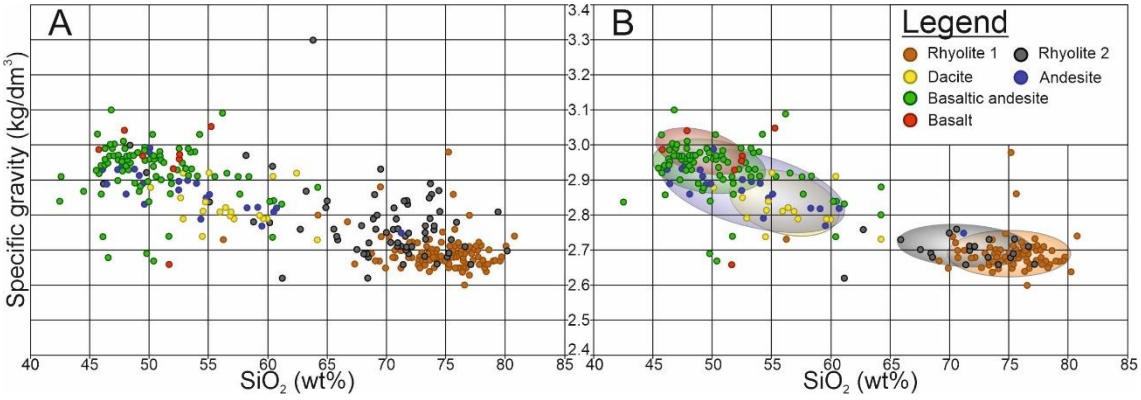

Figure 17. *SiO_2 - specific gravity charts. Chart A has all 338 samples, whereas in chart B, most of the altered samples has been removed. Chart B also has highlighted groupings, where Dacite, Andesite and Basalt groups are somewhat inaccurate due to low number of samples.*

There is quite a bit of overlap between different chemotratigraphical units in specific gravity axis. Overall, specific gravity values are not accurate enough in on itself to determine rock type, but specific gravity values are nevertheless useful tool during drillcore logging, if certain Pyhäsalmi deposit specific characteristics are kept in mind.

For one, keeping in mind where the drillcore in question is located. In unaltered footwall, the relevant rock types are unaltered Rhyolite 1, Dacite, Andesite and Basaltic andesite. In hydrothermally altered footwall, the relevant rock types are unaltered and altered Rhyolite 1, altered Rhyolite 2, Dacite, altered Andesite and Basaltic andesite. In hangingwall, the relevant rock types are unaltered Rhyolite 2 and Basalt. Taking note of the drillcore location may reduce the number of factors to the point that in first 100 m of

hangingwall, specific gravity values are enough for differentiating rock types, since there is only Rhyolite 2 and Basalt rock units. In footwall, however, there is so many different rock types that specific gravity measurements are not as useful as in immediate hangingwall.

Second, it is recommended to only measure unaltered samples when determining different rock types. Any type of alteration reduces accuracy, which is obvious when comparing Figure 17 A and B charts, especially on Rhyolite 2.

Most of these rock units are easy to differentiate by eye, but there are situations where additional information is useful. For example, if there are several Basaltic andesite veins that have a slightly different composition in the same area, or different layers of unaltered aphanitic Rhyolite 1 and Rhyolite 2 rock units, specific gravity measurements are useful on verifying on what point the rock unit changes, since around Pyhäsalmi deposit, the rock units are rather homogenous and do not change composition much in short intervals.

As was already stated, collecting specific gravity measurements from hydrothermally altered zone is less useful, if the purpose is to determine what rock type is in question. Instead, specific gravity measurements in hydrothermal alteration zones can be used as an additional estimation tool on whether massive sulphide is getting closer or further away in hydrothermal alteration zone. In order to see the increasing or decreasing trend properly, collecting frequent specific gravity measurements from the whole hydrothermal alteration zone is required. Figure 18 shows the correlation and possible equation for calculating S% from specific gravity for sericite altered Rhyolite 2. Other correlations were also tested, such as SiO_2 – specific gravity and Fe_2O_3 – specific gravity, but their correlations values were lower than 0.2 in both cases. The correlation between specific gravity and S% in all Rhyolite rock unit samples is 0.3401, which is still low. At the very least, if Rhyolite 2 rock unit specific density is higher than 2.7332 kg/dm^3, it has accumulated suplhides during hydrothermal alteration.

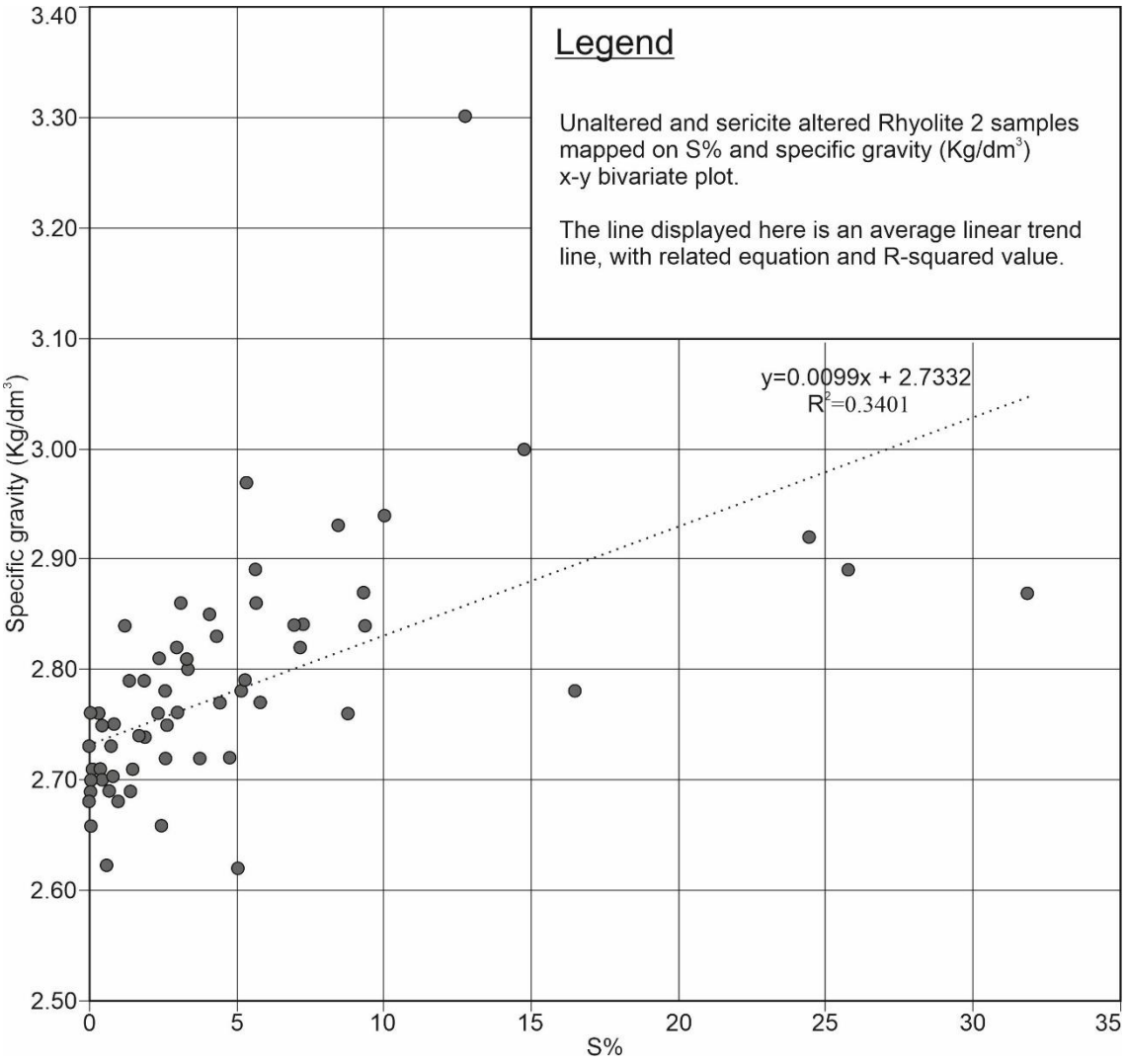

Figure 18. *Rhyolite 2 samples on specific gravity/S% chart. Unfortunately, the linear trend line correlation is too low for using the equation in the chart for calculating S% from specific gravity reliably. However, it seems that if the specific gravity of the sericite schist is higher than 2.7332, it has accumulated sulphides during hydrothermal alteration.*

In hydrothermally altered zones, the increases in specific gravity are related to increased sulfide content of the rock, i.e. closer proximity to massive sulphide. For increased accuracy, it is better to collect measurements only from sericite schist, ignoring sericite – biotite schist. Figures 19 and 20 serves as an example of increasing specific gravity per increasing S% in drillcore.

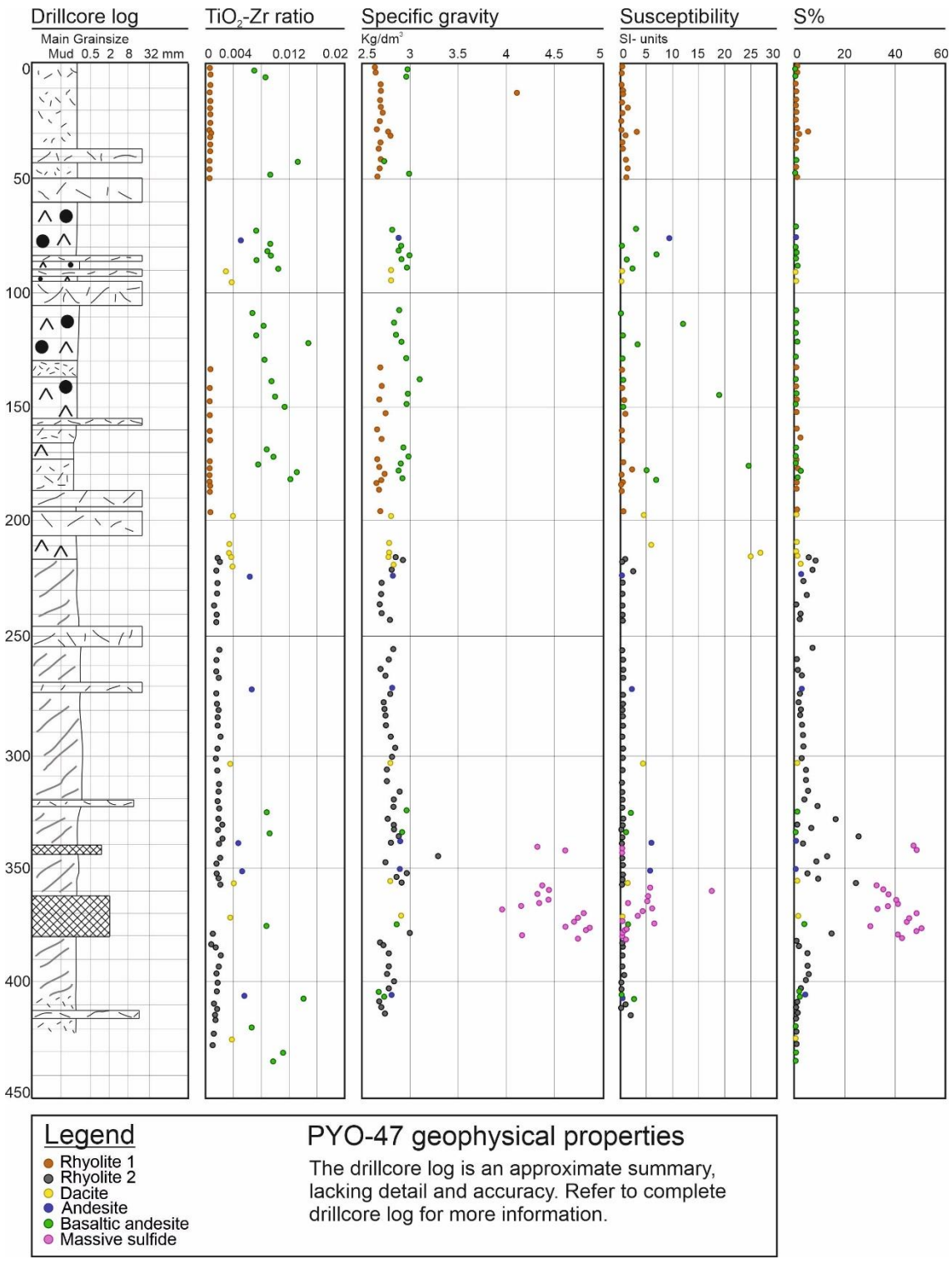

Figure 19. *PYO-47 geophysical properties and S% along drillcore length.*

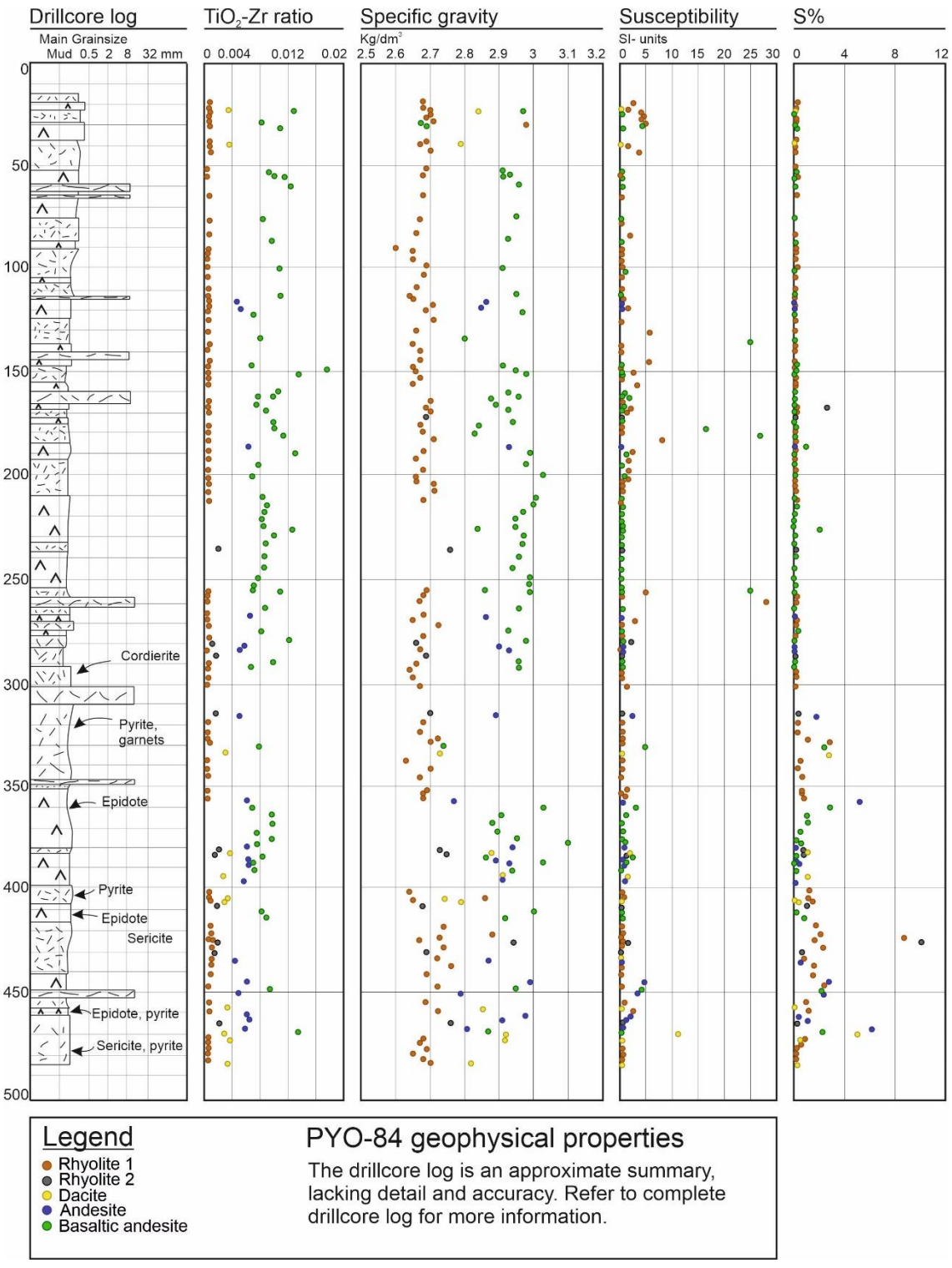

Figure 20. *PYO-84 geophysical properties and S% along drillcore length.*

10.2 Susceptibility

The increases in susceptibility are related to magnetic properties of the minerals in the drillcore. In silicic unaltered rocks, the random increases of susceptibility are more commonly related to the presence of magnetite. In hydrothermally altrered rocks, the increased susceptibility is more commonly related to the presence of pyrrhotite. These connections are hard to display on chart, since pyrrhotite can't be geochemically distinguished from pyrite, which has no magnetic properties. Instead, these connections can be found by comparing drillcore log to susceptibility measurements (Fig. 19 and 20, more drillcore log related details in Appendix 1).

For the same reason, it is also challenging to display the correlation between Zinc ore and susceptibility in Figure 13, which displays the deep ore metal zonation and related geophysical properties. When Zn wt% and corresponding susceptibility values are mapped in x-y diagram, R^2 is around 0.2, which is calculated from the average linear trend line. There is no correlation between Cu wt% and susceptibility.

The reason for increases in susceptibility around Zinc ore has not been investigated in this thesis work, but Imaña (2003) noted that "magnetite is a common mineral in the A zinc ore (1 – 4%), but is also present as an accessory mineral in other ore types (<1%)." Pyrrhotite is also a factor, but they are indistinguishable from magnetite by just looking at susceptibility measurements. In massive pyrite and spotty massive pyrite (MP and SMP), susceptibility is low and only spikes in association of inclusions and veins.

11. DISCUSSION FOR FURTHER STUDIES

The accuracy of the older PYO-series immobile element measurements was verified by comparing them to newer selected JSH-series measurements in Figure 14, where footwall and hangingwall Rhyolite 2 seems to align with each other well enough. Identifying the major rock units is easy when TiO_2-Zr ratios are available but, for example, identifying different Basaltic andesite intrusion sets is harder because immobile element measurement accuracy is not good enough in older whole-rock geochemical measurements.

The PYO-series geochemical measurements only include Al_2O_3, TiO_2 and Zr as available immobile elements, so determining the most immobile element with only these three is unreliable. A better conclusion of most immobile element was estimated by looking Al_2O_3, TiO_2, Zr, Y and Nb, which were available in selected JSH-series samples. Al_2O_3 was selected as best immobile element for rhyolitic rock units and Zr for all rock units, but neither of them is still not immobile enough for accurate absolute mass transfer calculations.

For comparison, absolute mass transfer calculations were performed on each immobile element, Al_2O_3, TiO_2 and Zr, separately and then the average of these results were calculated. The result of this average was that the trend appeared almost the same, only the total amounts of mass transfer increased when compared to solely Al_2O_3 based absolute mass transfer calculations. The average absolute mass transfer calculations are certainly inaccurate in some capacity, but not as much as when selecting wrong immobile element, so it is possible that this solution would have served this thesis work better.

There is also the possibility of selecting Rhyolite 2 protolith from hangingwall samples, which would certainly be unaltered. This was also tested, but since the differences between hangingwall precursor-based mass transfer calculations and footwall precursor-based mass transfer calculations were so small, the footwall precursor was nevertheless selected. Additional reasons for selecting the footwall precursor over hangingwall

precursor are that the footwall precursors location is nearer to hydrothermal alteration zone and because of that, it is most likely more representative of the true protolith for footwall Rhyolite 2. Additionally, the footwall precursor has been analyzed by the same method as the rest of samples in PYO-series, negating the possibility of resulting wrong calculation results due to different sampling and analyzing method.

Since the purpose of this thesis is to cover as wide field of subjects in some detail, there are quite a bit of topics left unexplored. Some of them are listed here:

1. The 55 thin sections (of which 23 are polished thin sections) have not been studied in any other way than by optical microscope, leaving room for later studies. What kind of hydrothermal alteration has happened to the unidentifiable sample JSH-17082, and what is its current mineralogy?
2. This study mainly used the immobile elements (Al_2O_3, TiO_2, Zr, Y and Nb) for calculating immobile ratios and mass transfer of major elements, and K_2O, Fe_2O_3, MgO, Na_2O and CaO for Alteration Index and CCP Index calculations. There are still many elements in the data sets that are unutilized.
3. In chapter 7.1 it was noted that the lack of chlorite alteration is an anomaly, since hydrothermal alteration trend in Figure 11 Alteration box plot indicates that geochemically speaking it should exist. Comparisons of Rhyolite 1 and 2 precursors could be made to other rhyolites in order to see if it is different in a way that could negate chlorite alteration.
4. There is also a possibility of finding better factors to correlate between geophysical and geochemical properties of the rocks. These seven drillcores provide three different main scenarios for study, unaltered silicic rock, hydrothermally altered silicic rock and massive sulphide, which are excellent for testing different geophysical ore exploration methods on.
5. Three of the seven drillcores also provide a good insight into volcanogenic massive sulphide ore zonation characteristics. Imaña (2003) has already provided a thorough interpretation and mineralogical description of these zones, but there is still room for more in-depth studies.

12. SUMMARY

The objective of this thesis work was to describe drillcores PYO-47, PYO-84, R-2242, R-2252, R-2623, R-2394 and R-2642. Together, they define footwall and hangingwall of the Pyhäsalmi deposit, hydrothermal alteration and the volcanogenic massive sulphide deposit setting in and around Pyhäsalmi VMS deposit.

Drillcores PYO-47 and PYO-84 are drilled in the footwall of the Pyhäsalmi VMS deposit, where host rock has been subjected to mafic intrusions before and after intense hydrothermal alteration took place. Later, the massive sulphide has been subjected to at least one tectonic event that has forced the massive sulphide body to intrude into hangingwall.

The footwall host rock is mainly homogenous and aphanitic rhyolite. Almost all primary textures have been destroyed due to metamorphism and hydrothermal alteration, leaving geochemical data as main tool for identifying the main rock types in area. By studying immobile element ratios, it is concluded that the footwall has two different rhyolitic units at the time of hydrothermal alteration. These units have been named here as Rhyolite 1 and 2. In previous studies equivalent rock units have been named as Rhyolite A and B, respectively.

Rhyolite 2 is slightly darker in color than Rhyolite 1, stratigraphically it is lying on top of Rhyolite 1 and it also has a closer association with hydrothermal alteration. Otherwise there is no visible difference between the two.

As Rhyolite 2 has hydrothermally altered into sericite schist, it has in average lost SiO_2, Na_2O, K_2O and Ca_2O, and gained MgO, Fe_2O_3 and S. Pyrite content increases near massive sulphide and SiO_2 mass transfer changes wildly, depending on location. Mass changes has been estimated by using MacLean and Barrett (1993) single precursor mass transfer technique, but it is important to note that the supposedly immobile elements used for single precursor mass transfer calculations were not immobile enough to reach the standards set by MacLean and Barrett (1993), hence the losses and gains of elements

during hydrothermal alteration are only estimates. The alteration intensity, however, can reliably be tracked by using Alteration Index and CCP Index (Large et al. 2001a) and by measuring S% content of the rock.

Later, during some metamorphic event, cordierite has occasionally formed in sericite schist. Chlorite alteration is only seen in association of mafic units, which have intruded both prior and after hydrothermal alteration. There are two different mafic intrusion types, which have been named Andesite and Basaltic andesite. In earlier studies, equivalent rock units have been named Andesite and Mafic A-2 (Lehto fm), respectively.

The Pyhäsalmi massive sulphide has been divided into two different sections, the old upper ore body and newer deep ore body. The upper ore body consists of steeply dipping, elongated conical shape of massive sulphide, where the metal zonation typical to VMS model is not clear, but it has been enriched in Cu and Zn nevertheless.

The deep ore body has a potato like shape, which is connected to upper ore body by a small contact area at the top of deep ore body. Drillcores R-2623, R-2394 and R-2642 clearly show how Cu and Zn rich layers are in all outer sides of the deep ore body and how the massive pyrite is concentrated in the middle of the deep ore body.

The host rock that surrounds the deep ore body is deemed as hangingwall, based on the metal zonation structure in the deep ore body and the fact that the host rock is hydrothermally unaltered. It consists of identical host rock in all sides of the deep ore body, mainly Rhyolite 2 with frequent small layers of mafic rock. However, the very first few meters around deep ore consists of Rhyolite 1 rock type. Based on immobile element ratios, hanginwall mafic rock is different from footwall mafic units, and it has been named Basalt. In previous studies, it has been referred to as Mafic A-1.

Drillcores R-2242 and R-2252 go deeper into the hanginwall, both starting from proximity to deep ore body. The first drillcore pierces into south-west and the latter straight to east. In both cases, the main rock types consist of unaltered Rhyolite 2 and Basalt, where Rhyolite 2 is dominant for the first 100m radius, after which starts a Basalt rich layer.

Geochemical techniques used, i.e. immobile element ratios, single precursor absolute mass transfer and Alteration box plot proved to be invaluable for verifying and correcting drillcore logs, which were done prior geochemical studies. Thin sections were mainly used to check mineralogy and texture. All thin section reports and drillcore logs are presented in Appendix.

928 specific gravity and susceptibility measurements were performed for this thesis work, all of which is also presented in Appendix. Of the measured geophysical properties, specific gravity proved to be most useful tool during drillcore logging. Measuring specific gravity does not take much time or resources, and it is great help when geologist is trying to differentiate different homogenous and aphanitic rhyolitic units. It can also be used to verify sulphide increases in hydrothermally altered rocks, providing additional information of nearby massive sulphide body. However, this requires that the geologist only takes sericite altered rocks, otherwise interpretation may be false, and there is no situation where it can be used as a sole factor for making for making conclusions.

Susceptibility measurements along drillcores mostly highlight the locations of magnetite and pyrrhotite and it does increase in hydrothermally altered rock slightly, but neither these observations provide any additional useful information during drillcore logging. Although, susceptibility values did increase in association with zinc-rich massive sulphide in deep ore, but this correlation is hard to prove numerically due to the abundance of Fe in massive sulphide.

13. ACKNOWLEDGEMENTS

First, I want to thank Chief Geologist Timo Mäki from Pyhäsalmi Mine Oy for generously providing drillcores required for this thesis work, contributing for additional whole-rock geochemical samples that I required and allowing me the access into their facilities and database during 2017. Also, great thanks to K.H. Relunds foundation for contributing on thin section expenses.

I would also like to offer my thanks to professor Holger Paulick for initiating this thesis subject. He and Timo Mäki both helped me out in the beginning, when I was still lacking experience on how to properly read and describe drillcore. For later support, my thanks to professors Eero Hanski and Kari Strand for giving me advice on how to properly structure pro gradu.

I am also grateful for the staff of Pyhäsalmi Mine oy, namely Kjell Kurten and Mikko Numminen, who showed great patience while I was trying to explain to myself aloud what happened to supposedly stratabound and stratiform VMS. Also, thanks to Pyhäsalmi Mine Oy geotechnicians Janne Kaijankoski, Toni Leskinen and special thanks for Topi Halonen, who worked at the time for Pyhäsalmi Mine Oy in summer job position. He was the one who performed most of the geophysical measurements, after all.

14. REFERENCES

Barrie, C. T., & Hannington, M. D., (1999). Classification of volcanic-associated massive sulfide deposits based on host-rock composition. Reviews in Economic Geology, v. 8, pp. 1 - 11.

Barrett, T. J., & Maclean, W. H., (1994). Mass changes in hydrothermal alteration zones associated with VMS deposits of the Noranda area. Exploration Mining Geology, v. 3, pp. 131 – 160.

Franklin, J. M., Sangster, D. M., Lydon, J.W., (1981). Volcanic-associated massive sulfide deposits: Economic Geology 75th Anniversary Volume, pp. 485 – 627.

Franklin, J. M., Gibson, H. L., Jonasson, I. R., Galley, A. G., (2005). Volcanogenic massive sulfide deposits. Economic Geology, v. 98, pp. 523 - 560.

Galley, A. G., Hannington, M. D., Jonasson, I. R., (2007). Volcanogenic massive sulphide deposits. Mineral Deposits of Canada: A Synthesis of Major Deposit-Types, District Metallogeny, the Evolution of Geological Provinces, and Exploration Methods. Geological Association of Canada, Mineral Deposits Division, Special Publication, v. 5, pp. 141 - 161.

Gemmell, J. B., & Large, R. R., (1992). Stringer system and alteration zones underlying the Hellyer volcanogenic massive sulfide deposit, Tasmania, Australia. Economic Geology, v. 87, pp. 620 – 649.

Gibson, H. L., Watkinson, D. H., Comba, C.D.A., (1983). Silicification: Hydrothermal alteration in an Archean geothermal system within the Amulet rhyolite formation, Noranda, Quebec. Economic Geology, v.78, pp. 954-971.

Gifkins, C. C., Herrmann, W., Large, R. R., (2005). Altered volcanic rocks: a guide to description and interpretation. University of Tasmania. Centre for Ore Deposit Research. Printing Authority of Tasmania. 275p.

Hannington, M. D., (2014). 13.18 - Volcanogenic Massive Sulfide Deposits. In: Turekian, K., K. & Holland, H., D. (ed.) Treatise on Geochemistry (Second Edition). Elsevier, Oxford, pp. 463 – 488.

Imaña, M., (2003). Petrography, mineralogy, geochemistry and 3D modelling of the A zinc ore in the Pyhäsalmi Zn-Cu VMS deposit, central Finland. Master's thesis, University of Turku, Department of Geology and Mineralogy, p. 72.

Imaña, M., Mäki, T., Heinonen, S., Häkkinen, T., Luukas, J., Kousa, J., Margaux Le Vaillant., Miettinen, E., Mäntylä, A., (2013). 3D modelling research activities 2009-2013 in the Pyhäsalmi district. Unpublished internal report for Pyhäsalmi Mine Oy, March 2013.

Korja, T., Luosto, U., Korman, K., Pajunen, M., (1994). Geophysical and metamorphic features of Paleoproterozoic Svecofennian orogeny and Palaeoproterozoic overprinting on Archaean crust. Geological Survey of Finland, Guide 37, pp. 11 – 20.

Kousa, J., Lukkas, J., Huhma, H., Mänttäri, I., (2013). Palaeoproterozoic 1.93-1.92 Ga Svecofennian rock units in the northwestern part of the Raahe-Lagoda zone, Central Finland. Hölttä, P., (ed.) Geological Survey of Finland, Report of Investigation 198.

Laine, E., Luukas, J., Mäki, T., Kousa, J., Ruotsalainen, A., Suppala, I., Imaña, M., Heinonen, S., Häkkinen, T., (2015). The Vihanti-Pyhäsalmi area. In: Weihed, P., (ed.) 3D, 4D and Predictive modelling of Major Mineral Belts in Europe. Springer International Publishing Switzerland 2015. Chap. 6, pp. 123 – 144.

Laitala, J., (2015). Mineralogy and geochemistry of the pyrrhotite horizons in the Pyhäsalmi district, central Finland. Master's Thesis, University of Turku, Department of Geography and Geology, p. 86.

Large, R. R., (1992). Australian Volcanic-Hosted Massive Sulfide Deposits: Features, Styles, and Genetic Models. Economic Geology, v. 87, pp. 471 – 510.

Large, R. R., Gemmell, J. B., Holger, P., (2001a). The Alteration Box Plot: A simple approach to understanding the relationship between alteration mineralogy and lithogeochemistry associated with volcanic-hosted massive sulfide deposits. Economic Geology, v. 96, pp. 957 – 971.

Large, R. R., McPhie, J., Gemmell, J. B., Herrman, W., Davidson, G. J., (2001b). The spectrum of ore deposit types, volcanic environments, alteration halos, and related exploration vectors in submarine volcanic successions: Some examples from Australia. Economic Geology, v. 96, pp. 913 – 938.

Lickorish, W. H., (2012). Structure of the Pyhäsalmi VMS deposit, Finland. Unpublished internal report for Pyhäsalmi mine Oy. p. 41.

MacLean, W. H., Barrett, T. J., (1993). Lithogeochemical techniques using immobile elements. Journal of Geochemical Exploration, v. 48, pp. 109 – 133.

Miettinen, E., (2011). Detailed geology of the level - 1275, Pyhäsalmi Mine, central Finland and genetic implications of rock inclusions within the ore body. Unpublished master's thesis, University of Helsinki, p. 67.

Morton, R. L., Franklin, J. M., (1987). Two-fold classification of Archean volcanic associated massive sulfide deposits: Economic Geology, v. 82, pp. 1057–1063.

Mäki, T., (1986). The Lithogeochemistry of the Pyhäsalmi Zn-Cu-Pyrite Deposit, Finland. In: Prospecting in areas of glaciated terrain symposium, Sept. 1 – 2, Kuopio. Finland. Institute of Mining and Metallurgy, London. pp. 69 – 82.

Mäki, T., Imaña, M., Kousa, J., Luukas, J., (2015). The Vihanti-Pyhäsalmi VMS Belt. In: Maier, W., Lahtinen, R., O´Brien, H., (Eds.) Mineral Deposits of Finland, 1st edition. Elsevier, Inc. Chap. 7, pp. 507 – 530.

Mäki, T., Puustjärvi, H., 2003. The Pyhäsalmi massive Zn-Cu-pyrite deposit, Middle Finland—a Paleoproterozoic VMS-class "giant." In: Ashton, J., et al. (Ed.) Europe's Major Base Metal Deposits. Irish Association for Economic Geology, Dublin. pp. 87 – 91.

Riverin, G., Hodgson, C.J., (1980). Wall-rock alteration at the Millenbach Cu-Zn mine, Noranda, Quebec. Economic Geology, v. 75, pp. 424 - 444.

Robb, L. J., (2005). Introduction to ore – forming processes. Blackwell Publishing, Blacwell Sicence LTD. 373p.

Sangster, D., Scott, S. D., (1976). Precambrian strata-bound massive Cu-Zn-Pb sulfide ores of North America, in Wolf, K.H., (ed.) Handbook of strata-bound and stratiform ore deposits: Amsterdam, Elsevier, pp. 129 – 222.

Sawkins, F. J., (1976). Massive sulphide deposits in relation to geotectonics: Geological Association of Canada Special Paper 14, pp. 221 - 240.

Skirrow, R. G., Franklin, J. M., (1994). Silicification and metal leaching in semicomformable alteration beneath the Chisel lake massive sulfide deposit, Snow Lake, Manitoba. Economic Geology, v. 89, pp. 31 - 50.

Solomon, M., (1976). Volcanic massive sulphide deposits and their host rocks: A review and an explanation, in Wolf, K.H., (ed.) Handbook of strata-bound and stratiform ore deposits, II: Regional studies and specific deposits: Amstedam, Elsevier, pp. 1307 – 1328.

APPENDICES

1. **Drillcore logs in following order:**
    a. **PYO-47**
    b. **PYO-48**
    c. **R-2242**
    d. **R-2252**
    e. **R-2394**
    f. **R-2623**
    g. **R-2642**
2. **Selected 55 thin sections from JSH-17001 – JSH-17140 samples in numerological order:**
3. **Selected 31 samples from JSH-17001 – JSH-17140 XRF / ICP-MS geochemical data in numerological order:**
4. **XRF/AAS whole rock geochemical data in following order, by courtesy of Pyhäsalmi Mine Oy:**
    a. **PYO-47 XRF/AAS whole-rock geochemical data**
    b. **PYO-84 XRF/AAS whole-rock geochemical data**
    c. **R-2394 AAS geochemical data**
    d. **R-2623 AAS geochemical data**
    e. **R-2642 AAS geochemical data**
5. **All available geophysical data in following order:**
    a. **PYO-47**
    b. **PYO-48**
    c. **R-2242**
    d. **R-2252**
    e. **R-2394**
    f. **R-2623**
    g. **R-2642**
6. **General features of main ore types in Pyhäsalmi VMS deposit (Imaña, 2003):**

APPENDIX 1.a. PYO-47 drillcore log.

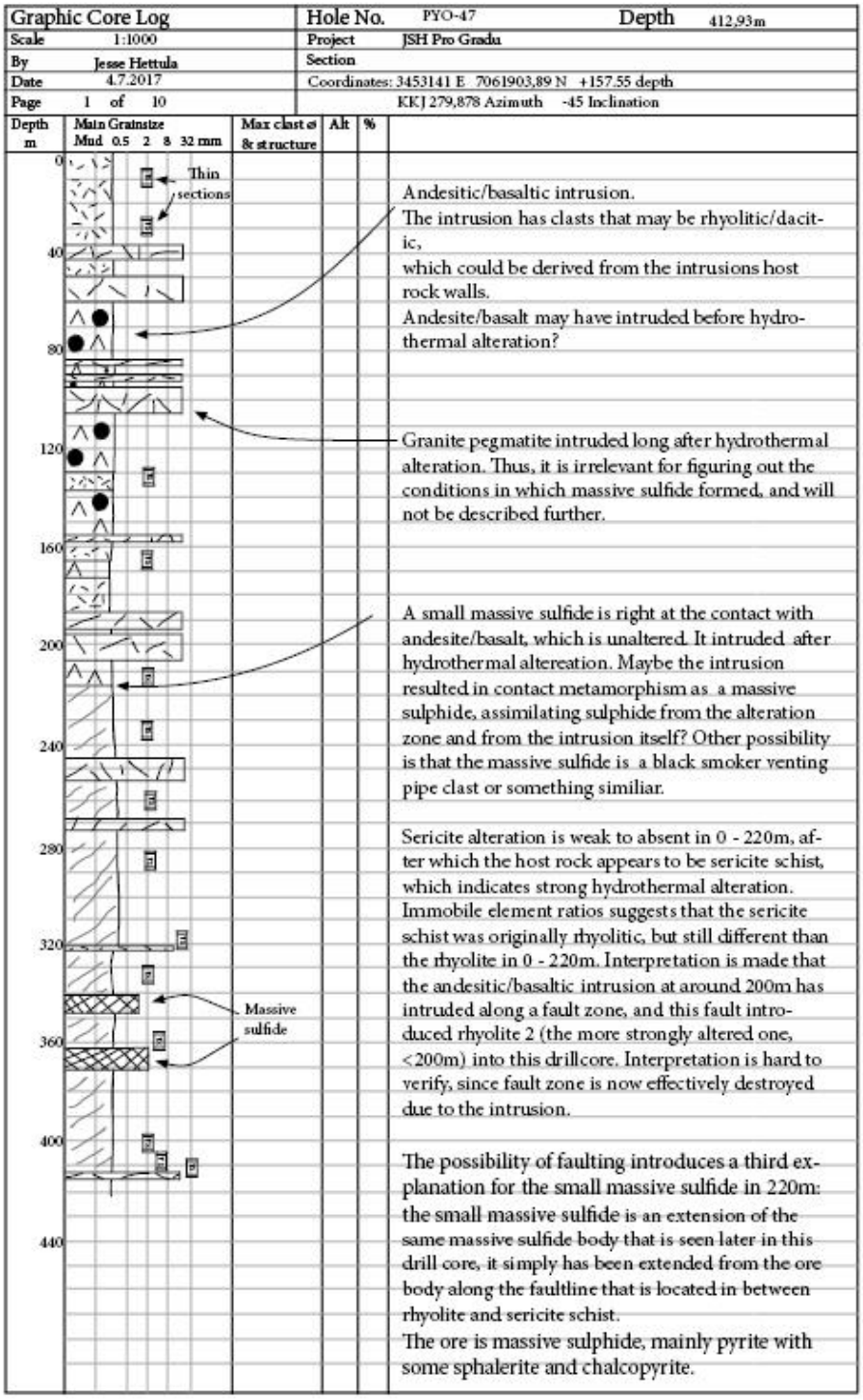

Graphic Core Log		Hole No. PYO-47	Depth 412,93m
Scale 1:100		Project JSH Pro Gradu	
By Jesse Hettula		Section	
Date 4.7.2017		Coordinates: 3453141 E 7061903,89 N +157.55 depth	
Page 2 of 10		KKJ 279,878 Azimuth -45 Inclination	

Depth m	Main Grainsize Mud 0.5 2 8 32 mm	Max clast ø & structure	Alt	%		
0		ø = 3 mm, qtz-nodules			Rhyolite, fine-grained matrix, slightly porphyritic texture (qtz nodules?)	
					Andesite, density is 2.9 kg/dm3.	2,41
					Same rhyolite as earlier	3,23
4						
					Spotty andesite, bigger grains than earlier.	5,50
		1.5 cm			Granite pegmatite	6,70
						7,81
8					Mostly massive fine-grained rhyolite. Some porphyritic textures (qtz-nodules) and alteration. Thin section JSH-17015 at 9,97m.	
12						
					Granite pegmatite	14,08
						14,99
16					Massive fine-grained rhyolite.	
20					No major changes. Some silicic alteration at bottom + pyrrhotite.	
					Granite pegmatite	22,46
24					Mostly massive rhyoltie. Some odd textures and intrusions by mafic unit.	23,79
					Granite pegmatite	26,39
28					Massive fine-grained rhyolite. Thin section JSH-17017 at 29,29m.	29,70
			mod. perv.	60-80%	Hydrothermally altered rhyolite, silicic + veins of pyrite and pyrrhotite. And then ...	29,62
32						32,35
			weak	10-15%	... back to massive rhyolite. This section has slight marks of hydrothermal alteration and disseminated pyrite.	
36						
		3 cm			Granite pegmatite	38,46
40						
					Massive rhyolite. At section 42.62m - 44.08m is a mafic intrusion (andesite?) with clear contact alteration in rhyolite.	41,78
						42,62
44						44,08
					Couple of thin granite pegmatite veins.	
48					Mafic intrusion into rhyolite.	47,30
					Massive rhyolite.	48,50
50						

Graphic Core Log		Hole No. PYO-47	Depth 412,93m
Scale	1:100	Project	JSH Pro Gradu
By	Jesse Hettula	Section	
Date	4.7.2017	Coordinates: 3453141 E 7061903,89 N +157,55 depth	
Page	3 of 10	KKJ 279,878 Azimuth -45 Inclination	

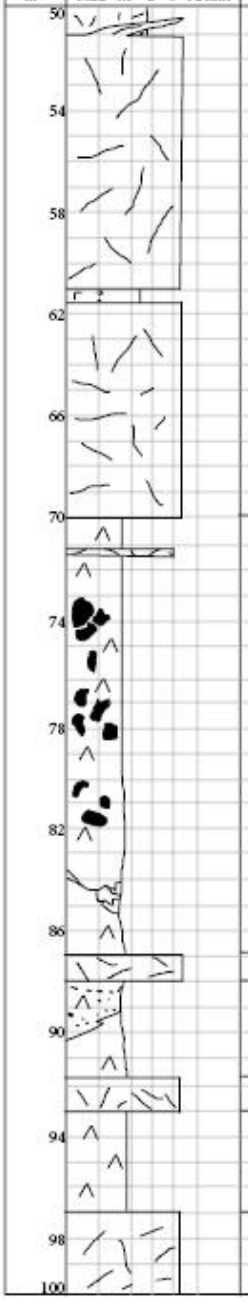

Max clast ø & structure	Alt	%		
				50,64
			Granite pegmatite	
3 cm				
Massive				
			Aphanitic dacite in middle of pegmatite intrusion. Density is 2.7.	
				69,80
			Aphanitic andesite/basalt matrix. Starting from 73.80 and ending at 78.12, the matrix supports sharp-edged rhyolite clasts (ø= 3 - 4 cm).	
			From 78.11 - 79.81 m, andesite/basalt has gone through epidote type alteration + silicic (pervasive, moderate).	
			From 83.95 - 86.9 m (geochemical sample 8336902), andesite has epidote alteration along fractures. Andesite then turns into gneiss near the granite pegmatite intrusion contact.	
				86,88
			Granite pegmatite	87,91
			Fine-grained andesite with 7% disseminated pyrrhotite in its matrix. It has a intersection with another andesite at 89.90 m (which has no pyrrhotite). The Zr values of these units are different.	
				91,75
			Granite pegmatite	92,99
			Fine-grained andesite wtih 7 % pyrrhotite in its matrix + pyrite veins along fractures. This andesite has the same Zr values as the one at other side of granite pegmatite intrusion (89.90 - 91.75 m)	
				96,80
			Granite pegmatite	

Graphic Core Log		Hole No. PYO-47	Depth 412,93m
Scale	1:100	Project	JSH Pro Gradu
By	Jesse Hettula	Section	
Date	4.7.2017	Coordinates: 3453141 E 7061903,89 N +157.55 depth	
Page	4 of 10	KKJ 279,878 Azimuth -45 Inclination	

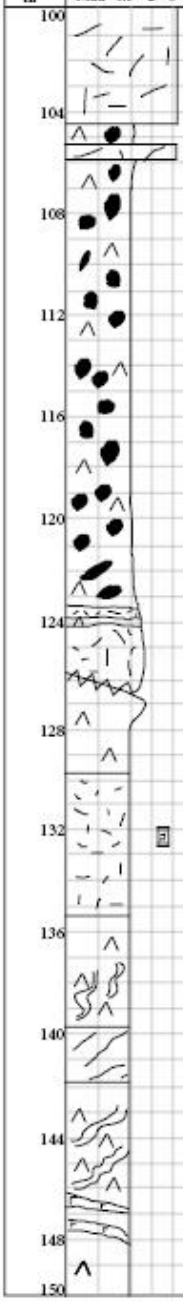

	Granite pegmatite
	Contact wit andesite is choppy. Massive pyrrhotite grains at contact (ø = 3 cm).
104,60	
105,76	
	Fine-grained basaltic andesite as a matrix, matrix supported felsic (rhyolitic?) clasts.
	Felsic clasts are more elongated near granite pegmatite vein. Further away, the clasts have sharper edges. The clasts are 3 cm in diameter or less. (more accurate value was not possible due to the drillcore diameter, which is 3 cm)
	Magnetite minerals in matrix
	Felsic clasts become bigger after 119.92 m, and more disseminated at edges.
119,92	
120,87	
123,49	
	Rhyolite with minor diesseminated pyrrhotite. At 123.95 m, a mafic vein with more concentrated pyrrhotite. The contact with wollowing andesite is dissiminated.
126,35	
	"Spotty" andesite/basalt. There is no magnetite, but instead there are more green minerals. Pyroxene? Pyrite is located in fractures.
129,98	
	Aphanitic massive dacite Thin section JSH-17024 at 132,2m
	Assimilated pyrrhotite at beginning (hydrothermal fluids?) Pyrrhotite amount is minor.
135,50	
	Mostly massive andesite/basalt.
	Starting from 137.28 m, moderate pervasive silicic + epidote hydrothermal alteration
139,91	
	Strong quartz + sericite hydrothermal alteration in presumably rhyolitic unit. Geochemical sample 8336917.
141,90	
	Mostly massive andesite/basalt with occasional hydrothermal fluid channel
146,40	
146,80	
	Two dacite intersections / veins at 149.4 - 146.8 m and 147.54 - 147.83m. The first ones geochemical sample id is 8336919.
147,54	
147,83	

Graphic Core Log		Hole No. PYO-47	Depth 412,93m
Scale 1:100		Project JSH Pro Gradu	
By Jesse Hettula		Section	
Date 5.7.2017		Coordinates: 3453141 E 7061903,89 N +157.55 depth	
Page 5 of 10		KKJ 279,878 Azimuth -45 Inclination	

Depth m	Main Grainsize Mud 0.5 2 8 32 mm	Max clast ø & structure	Alt	%		
150					Andesite/basalt with granite pegmatite vein.	150,07 – 150,21
					Rhyolite with disseminated pyrrhotite ± sphalerite.	151,03
154					Granite pegmatite	153,94
		Massive			Rhyolite with couple of andesite veins (157.49 - 157,89 m and 159.44 - 159.80 m).	157,13 – 157,49 – 157,89
158					Rhyolite is aphanitic, with a few magnetite minerals in between the andesite veins.	159,44 – 159,80
162		Fractures	Per.	7%	From 161.88 m onwards, increasing amount of disseminated pyrrhotite ± pyrite along with fractures.	
166	?				Two very similar basaltic units. Middle part is unaltered, whereas the edges are subjected to alteration (chlorite + (epidote?) ± pyrrhotite).	165,35 – 166,80
170					It might be that there is two different kinds of basaltic units here. The younger basalt might have intruded right in the middle (167,5-170,33m) of the older basalt, which are now observeable before and after the younger basalt. Thin section JSH-17026 at 166,9m.	170,33
					Rhyolite with clear edges.	172,38
174					Basaltic section with what seem to be two different intersecting basaltic units.	173,66
					Rhyolite. Its contacts with upper and lower basalt are disseminated.	175,11
					Basalt. Pyrite along with quartz veins.	177,16 – 177,92
178		Fractures, fault			Rhyolite. Some cracks and a fault + disseminated pyrite (10 %)	179,70
					Basalt. Pyrite along with quartz veins.	181,17
182					Rhyolite. Contact with upper basalt is disseminated, forming garnets in the matrix. Quartz content of the rock increases with depth and with lower grain size. At the end of this rhyolite section, moderate alteration + minor pyrite.	
186						187,44
					Granite pegmatite.	
190						193,48
194					Rhyolite + garnets + pyrite. Lower contact with andesite is blurred.	196,22
					Granite pegmatite.	
198						
200						

Graphic Core Log		Hole No.	PYO-47	Depth	412,93m
Scale	1:100	Project	JSH Pro Gradu		
By	Jesse Hettula	Section			
Date	5.7.2017	Coordinates:	3453141 E 7061903,89 N +157.55 depth		
Page	6 of 10		KKJ 279,878 Azimuth -45 Inclination		

Depth m	Main Grainsize Mud 0.5 2 8 32 mm	Max clast ø & structure	Alt	%		
200					Granite pegmatite.	
204						
						206,37
208					Fine-grained homogenous andesite/basalt matrix with felsic clasts.	
212					Orthoclase intrusion at 211 m. Garnets closer to sericite alteration zone below. The contact in between andesite/basalt and the alteration zone is messy because of ... (Thin section JSH-17029 at 213,5m.)	
						215,13
216			Ser		... Massive pyrite. Right after the massive pyrite comes sericite schist + pyrite ± biotite.	
						217,34
			Bio		Dominant biotite + pyrite schist structures in fine grained matrix.	
						219,42
220			Ser Qtz		Dark porphyroblasts in sericite + quartz schist + pyrite.	
						221,85
			Ser Bio		Starts as sericite schist, and soon turns into biotite schist + pyrrhotite	
						223,21
224					Moderately altered rhyolite 2? These may be primary structures.	
			???		In any case, rock is currently fine-grained Sericite schist. Overprinting that is a unknown mineral (cordierite?) + quartz + pyrite.	
228			K-feld spar ?	40	Alteration may have been selective (orange mineral). Grain size increases slightly with depth.	
					Upper contact has large grains (garnets + tourmaline?)	
232					Thin section JSH-17038 at 317,86m	
						234,58
236			Ser Bio	60	Protolith was something more mafic than earlier? This is seen as abrupt increase in sulphide content and biotite scihstosity.	
				80		237,74
			Ser	45	Primary textures vanish with depth. Rock turns more into sericite schist rather than biotite schist.	
240						240,93
					Gneissic primary structure right before granite pegmatite vein.	241,37
			Bio	80		
						243,43
244					Granite pegmatite.	
248						
250						

Graphic Core Log		Hole No. PYO-47	Depth 412,93m
Scale	1:100	Project	JSH Pro Gradu
By	Jesse Hettula	Section	
Date	6.7.2017	Coordinates: 3453141 E 7061903,89 N +157.55 depth	
Page	7 of 10	KKJ 279,878 Azimuth -45 Inclination	

Depth m	Main Grainsize Mud 0.5 2 8 32 mm	Max clast ø & structure	Alt	%		
250					Granite pegmatite.	
						253,25
254			Ser pyr	Moderate	Sericite schist with pyrite (15 - 20%) increasing porphyritic texture with depth.	
						256,61
258					Porphyritic texture disappears. At first sericite - biotite schist with carbonate veins. From 259m onwards weak sericite alteration. Less pyrite.	
262						
					Alteration strength is back to moderate-strong. Biotite - sericite schist with pyrite (20 %).	262,39
266					Weak - moderate alteration + carbonate veins, turns into strong near the pegmatite intrusion. Sericite - biotite schsit + pyrite.	265,34
						268,59
270					Granite pegmatite.	
					Biotite schist + pyrite (different rock type?)	271,47
						271,94
274					Sericite schist + biotite + pyrite and some carbonate veins. At times, rock looks a bit loke rhyolite. The first sphalerite at 275,55m, afterwards is seen with pyrite. Quartz veins or clasts?	
						276,97
278						
						280,00
282					Massive sericite schist. Pervastive strong alteration. 19 % pyrite qtz veins at 282,22 and 286,83 (clast?)	
						285,18
286					Massive sericite schist. Sulfides (pyrite + sphalerite) consentrated at fractures.	
						290,17
290					Sphalerite at 296,70m, next to pyrite.	
294						295,17
298						
300						

Graphic Core Log		Hole No. PYO-47	Depth 412,93m
Scale 1:100		Project JSH Pro Gradu	
By Jesse Hettula		Section	
Date 8.7.2017		Coordinates: 3453141 E 7061903,89 N +157.55 depth	
Page 8 of 10		KKJ 279,878 Azimuth -45 Inclination	

Depth m	Main Grainsize Mud 0.5 2 8 32 mm	Max clast ø & structure	Alt	%		
300					Sericite schist + pyrite. Biotite content increases with depth. Biotite consentration at 300 - 300,23m + qtz vein +pyrite.	300,17
304					This andesite seems to be similiar to 20,5 - 21,5m andesite (based on Zr value). Garnets and weak alteration.	303,74
308					Sericite schist with quartz + pyrite + dark mineral veins. Thickest one is 9 cm.	304,94
312						
316					Thin section JSH-17038 at 317,86m.	
320					Moderately altered sericite schist + pyrrhotite + pyrite in most silicic parts, couple of pyrite veins.	318,90
					Granite pegmatite	321,29
324					Sericite schist	321,82
					Vein of basaltic rock with silicic clasts which have some pyrite. Contact with surrounding rock has been biotite altered. This unit is similiar to 70 - 91m basalt (Zr value). How about the clasts?	324,48
328					Quartz - cordierite, some sericite sections and pyrite veins.	326,42
					Quartz - sericite surrounding 30 cm wide pyrite vein. Pyrite replasing sericite.	328,08
					Pure sericite schist.	330,29
					Biotite alteration. Mafic protolith?	331,19
332					Sericite schist with cordierite spots & pyrite veins. 5 cm thick.	331,77
					Basaltic intrusion where the middle part has porphyritic texture.	333,99
336					Sericite schist with thick veins of pyrite + chlorite? At some points sericite is being replased by quartz + quartz & pyrite.	334,90
					Porphyritic basalt intrusion	338,20
					Sericite shist with thick pyrite veins.	339,12
340					Massive sulfide (pyrite). Some patches of chalcopyrite at middle.	340,05
344					Sericite - quartz + very fine-grained pyrite veins (20 % pyrite).	343,95
348					Cordierite - mica schist. Pyrite veins (~20 %). Dark mineral (chlorite?).	346,40
350					Porous basaltic intrusion, porphyritic texture.	349,50

Graphic Core Log		Hole No. PYO-47	Depth 412,93m
Scale	1:100	Project	JSH Pro Gradu
By	Jesse Hettula	Section	
Date	7.7.2017	Coordinates: 3453141 E 7061903,89 N +157.55 depth	
Page	9 of 10	KKJ 279,878 Azimuth -45 Inclination	

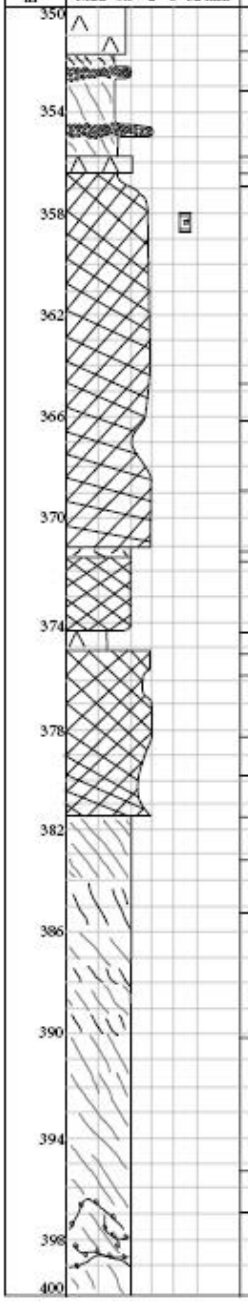

Same basaltic andesite intrusion as in 333,96 - 334,93m. Porphyritic texture. Porous at the start and at the end.		351,92
Sericite and biotite schist. ~20cm wide section of pyrite replasing sericite (+ qtz).		353,10
Sericite-quartz (cordierite?) schist with one major pyrite vein (quartz supported) and several minor ones.		355,84
Andesite intrusion. Some biotite alteration.		356,30
Sericite schist + quartz + cordierite with increasing pyrite content.		356,90
Spotty pyrite + sphalerite. Matrix is hard to determine - generally dark, has quartz + sulfosalts. Sulfosalts also form ~3 cm white patches in total of 3 different occasions. Rock varies in between sulfide and matrix supported structure. Thin section JSH-17042 at 358,47m		364,65
Sulfide supported. Pyrite becomes massive and oriented. No sphalerite.		366,30
Fine grained spotty pyrite + sphalerite in sulfosalt matrix. Even distribution.		368,84
Massive pyrite (70%). Some sphalerite. Matrix is sulphosalts.		371,12
Felsic unit. Intrusion? Clast? Disseminated pyrite + sphalerite. 30 - 80% pyrite. Matrix sulfosalts + quartz + unknown dark mineral.		371,38
Mafic intrusion, very fine-grained, some pyrite.		374,38
Spotty pyrite + sphalerite. Matrix supported.		375,11
Massive pyrite (> 70 %) + sphalerite. Sulphosalts.		375,55
First 33cm are sericite -qtz schist. Afterwards pyrite (60 - 70%) + sphalerite. Matrix varies in between schist and sulphosalts.		378,39
At first massive pyrite and sulfate (sulfosalt). Changes to schist matrix + sphalerite.		379,87
Felsic rock with weak alteration. Alteration increases to strong sericite + quartz. Gneissic texture?		381,67
Sericite + biotite + cordierite schist. Some white dots, quartz veins (+pyrite).		383,11
Two above mentioned compositons vary in turns. What kind of this was originally?		385,13
Sericite schist with pyrite veins and some quartz. Quartz may be either clasts or veins.		390,13
Schisous sericite + biotite + quartz. Fractures with pyrite infill.		395,28
Sericite schist.		396,92

Graphic Core Log		Hole No.	PYO-47	Depth	412,93m
Scale	1:100	Project	JSH Pro Gradu		
By	Jesse Hettula	Section			
Date	7.7.2017	Coordinates: 3453141 E 7061903,89 N +157.55 depth			
Page	10 of 10	KKJ 279,878 Azimuth -45 Inclination			

Depth m	Main Grainsize Mud 0.5 2 8 32 mm	Max clast ø & structure	Alt	%		
400					Sericite schist.	
						401,92
					Rhyolite, weak to strong sericite alteration.	
						403.75
404					Biotite schist with some primary structures?	
					Biotite + ser + cordierite + pyrite + odd clasts. TS JSH-17045	404.65
					Mafic protolith resulted in abundant biotite alteration. Some primary structures.	405.28
						407,63
408					Modearate alteration. Sericite + cordierite gneiss + disseminated pyrite. Primary clast at 408,47m? TS JSH-17046 at 408,13m.	
						409,85
					Rhyolitic unit with weak alteration. Garnet porphyry near granite pegmatite intrusion. Biotite edges. TS JSH-17047 at 411.3m.	
412					Granite pegmatite	411,52
						412.12
					Rhyolite. Weak sericite alterion + disseminated pyrite.	414,93
416						

APPENDIX 1.b. PYO-84 drillcore log.

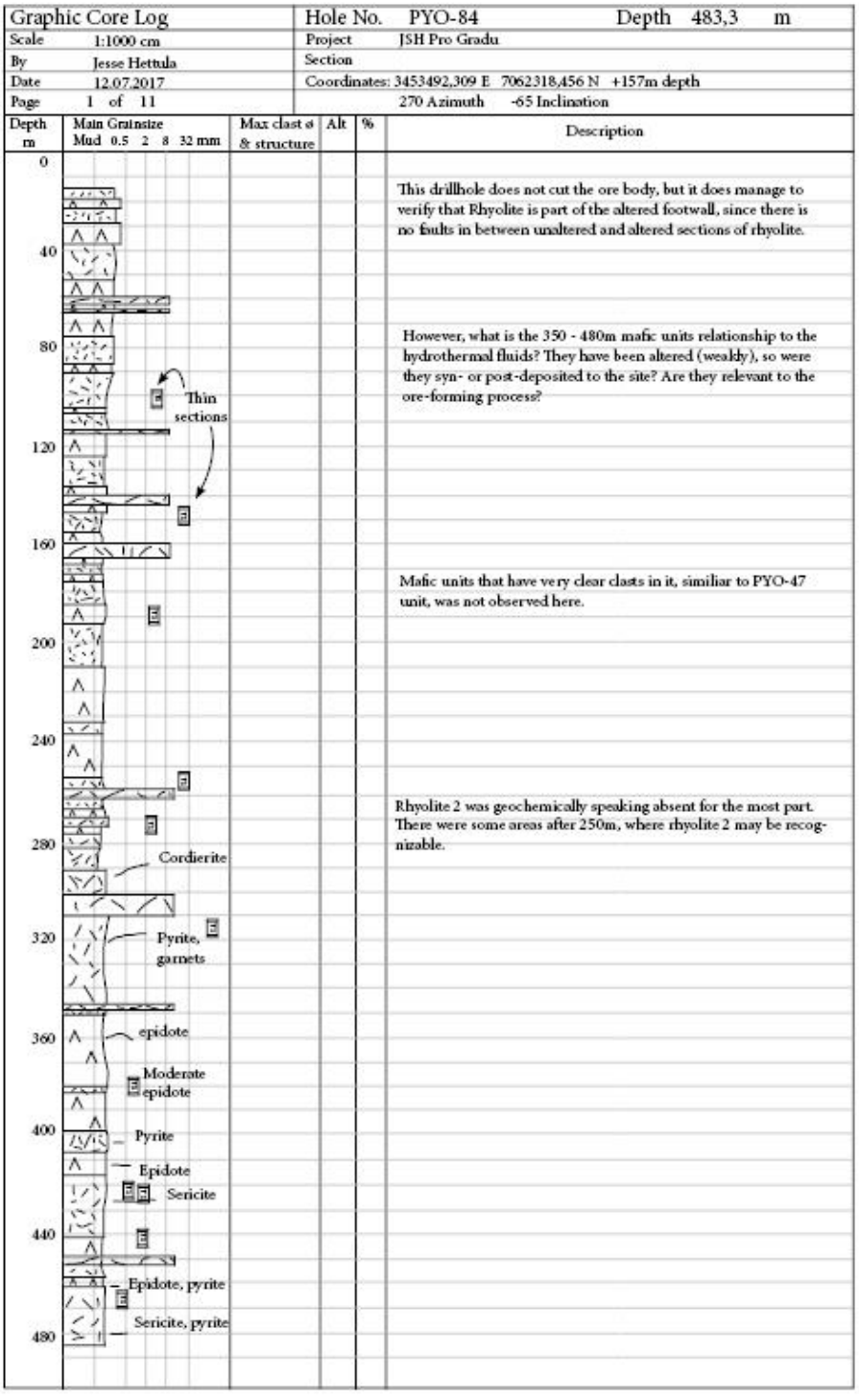

Graphic Core Log		Hole No.	PYO-84	Depth 483,3 m
Scale	1:100 cm	Project	JSH Pro Gradu	
By	Jesse Hettula	Section		
Date	12.07.2017	Coordinates: 3453492,309 E 7062318,456 N +157m depth		
Page	2 of 11	270 Azimuth -65 Inclination		

Depth m	Main Grainsize Mud 0.5 2 8 32 mm	Max clast ø & structure	Alt	%	Description	
0						
4						
8						
12						
16					Aphanitic massive rhyolite	15,30
					Mafic gneiss	15,69
					Aphanitic rhyolite + pyrite veins + some cordiorite - looking alteration (very weak and selective)	16,60
20						
			Ser	30	At 21.59m sericite alteration.	
					Basaltic andesite intrusion	22,41
					Rhyolite	22,77
					Basalt	23,27
24					At around 54m, quartz vein with sericite + orthoclase alteration	23,67
			Qtz Ser	50	in rhyolite. (Later editing: orthoclase alteration refers to apparent alteration of the rock, which resulted in red alteration. May be hematization.)	
					At 26.95m basaltic intrusion with qtz-clasts.	
28					Basalt intrusion.	28,04
						29,15
					Too much rock missing and the small clasts remaining probaply are not in their original position, so they have not been logged. There is however, more information available in geophysical and geochemical excel charts.	
32						
36						
40						
44						
48						
50						

Graphic Core Log		Hole No.	PYO-84	Depth	483,3	m
Scale	1:100 cm	Project	JSH Pro Gradu			
By	Jesse Hettula	Section				
Date	12.07.2017	Coordinates: 3453492,309 E 7062318,456 N +157m depth				
Page	3 of 11	270 Azimuth -65 Inclination				

Depth m	Main Grainsize Mud 0.5 2 8 32 mm	Max clast ø & structure	Alt	%	Description	
50						
					Too much rock missing and the small clasts remaining probaply are not in their original position, so they have not been logged. There is , however, more information available in geophysical and geochemical excel charts.	
54						
58						
62						
66						
70						
74						
78						
82					Rhyolite	
					Basaltic andesite	84,87
					Rhyolite	85,17
86					Basaltic andesite	85,74
					Rhyolite + pyrite (1 - 3%)	86,58
					Basaltic andesite	88,00
90					Rhyolite (higly fractured)	
					Granite pegmatite	91,58
					Rhyolite	91,78
94					Moderate pervasive silicic alteration	
98						
					Basaltic andesite intrusion, thin section JSH-17048 at 99m.	98,75
100					Rhyolite	99,75

Graphic Core Log		Hole No. PYO-84		Depth 483,3 m
Scale	1:100 cm	Project	JSH Pro Gradu	
By	Jesse Hettula	Section		
Date	12.07.2017	Coordinates: 3453492,309 E 7062318,456 N +157m depth		
Page	4 of 11	270 Azimuth -65 Inclination		

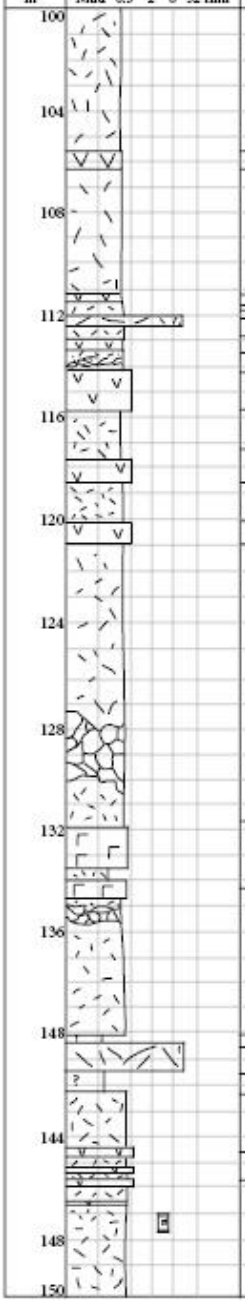

Depth m	Main Grainsize Mud 0.5 2 8 32 mm	Max clast ø & structure	Alt	%	Description
					Rhyolite
			Qtz	50	from weak to strong pervasive silicic + epidote/chlorite alteration
					+cordierite
					No pyrite.
					Basalt intrusion with clasts
					Rhyolite
					weak to moderate pervasive silicic alteration
					± chlorite?
					Basalt
					Granite pegmatite
					Rhyolite
					Basaltic andesite
					Rhyolite, fractures
					Basaltic andesite. Porphyritic texture.
					Rhyolite
					Basaltic andesite. Porphyritic texture.
					Rhyolite with minor basaltic intrusions.
					Basalt, porphyry pumice.
					Rhyolite
					Weak - moderate silicic alteration
					127.70 - 130m, thorougly fractured rock
					Dacite
					Garnets
					Rhyolite with occasional dacite intrusion.
					Weak - moderate quartz + chlorite alteration
					Contact metamorphism
					Granite pegmatite
					Contact metamorphism
					Rhyolite
					Series of andesite intrusions into rhyolite
					Rhyolite with occasional andesite or granite pegmatite intrusions.
					Weak - moderate pervasive quartz + chlorite alteration.
					Thin section JSH-17050 at 146,17m.

105,44
106,02
111,10
111,41
111,53
112,00
112,90
113,19
114,20
115,84
117,13
118,63
120,09
120,99
121,72
122,82
131,80
134,36
140,12
140,60
141,53
142,40
144,68
145,97

Graphic Core Log		Hole No.	PYO-84	Depth	483,3	m
Scale	1:100 cm	Project	JSH Pro Gradu			
By	Jesse Hettula	Section				
Date	13.07.2017	Coordinates: 3453492,309 E 7062318,456 N +157m depth				
Page	5 of 11	270 Azimuth -65 Inclination				

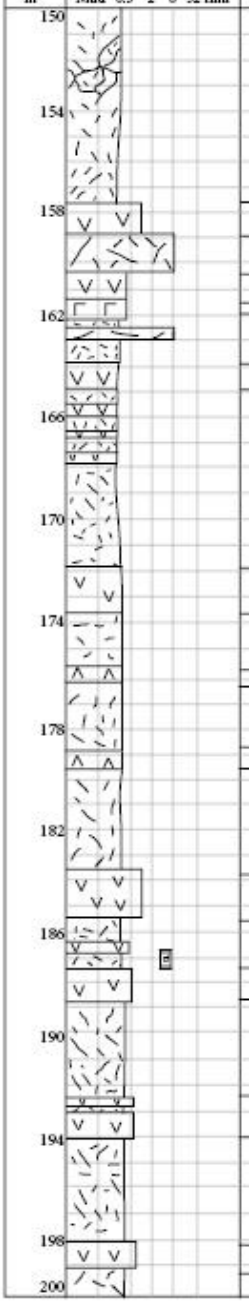

Depth m	Main Grainsize Mud 0.5 2 8 32 mm	Max clast ø & structure	Alt	%	Description
					Rhyolite Fractures that have orange/red alteration haloes. Otherwise weak silicic alteration. At 154,08m, thin mafic intrusion.
157,13					
					Basaltic andesite, porphyroblastic texture.
158,80					
					Granite pegmatite
160,30					
161,20					Porphyroblastic rhyolite. Biotite at contacts.
161,80					Dacite, which has intruded after basalt.
162,07					Rhyolite, which is the host rock. All mafic sections are intrusions
163,44					and so are the granite pegmatites, which are the newest intrusions.
163,80					Basaltic intrusion
164,90					Rhyolite with 3 basaltic intrusions.
171,80					Basalt intrusion
173,75					Rhyolite. Moderate pervasive quartz-chlorite alteration.
175,55					Andesite
176,13					Rhyolite. Too much vegetation on the drillcore to see textures properly.
178,76					Andesite. Too much vegetation.
179,60					Rhyolite. Too much vegetation on the drillcore to see textures properly.
183,85					Porphyritic basalt (possibly pyroxenes).
185,80					Rhyolite with mafic intrusion in the middle. Thin section JSH-17051 at 187,09m.
187,52					Basaltic andesite. No contact metamorphosis.
188,80					Aphanitic massive rhyolite.
192,30					Basaltic intrusion that has some rhyolite segments in middle.
194,00					Rhyolite with assimilated mafic rocks. Moderate silicic alteration.
198,15					Porphyritic basalt (no contact alteration).
199,15					Rhyolite, some silicic alteration.

Graphic Core Log		Hole No.	PYO-84	Depth 483,3 m
Scale	1:100 cm	Project	JSH Pro Gradu	
By	Jesse Hettula	Section		
Date	13.07.2017	Coordinates: 3453492,309 E 7062318,456 N +157m depth		
Page	6 of 11	270 Azimuth -65 Inclination		

Max clast ø & structure	Alt	%	Description	
			Rhyolite.	
			202 - 205m garnets.	
			Pervasive moderate quartz-chlorite alteration.	
			Either somewhat disseminated dacite intrusion or syndeposited seafloor sediment.	
			Aphanitic basaltic intrusion with small clasts.	208,95
			Rhyolite with small basalt intrusion.	209,95
			Basalt, few patches of rhyolite at beginning.	211,10
			Granite pegmatite	214,94
			Basalt	215,50
			Granite pegmatite	217,67
			Basalt	218,85
			Granite pegmatite	221,45
			Basalt.	221,98
			224,1 - 225,1 is basanite composition. This area has been somewhat epidote altered and fractured. Less green than the other basalts surroinding this area.	224,10 225,20
			Granite pegmatite intrusion, where the surrounfing rock appears to be dacite. Disseminated contact with basalt. Assimilated host rock and intrusion?	233,30
			Otherwise all this basalt is unchanging.	235,55
			Some fractures. At fractured areas, epidote alteration can be seen, but it is rare.	

Graphic Core Log		Hole No. PYO-84	Depth 483,3 m
Scale	1:100 cm	Project	JSH Pro Gradu
By	Jesse Hettula	Section	
Date	13.07.2017	Coordinates: 3453492,309 E 7062318,456 N +157m depth	
Page	7 of 11	270 Azimuth -65 Inclination	

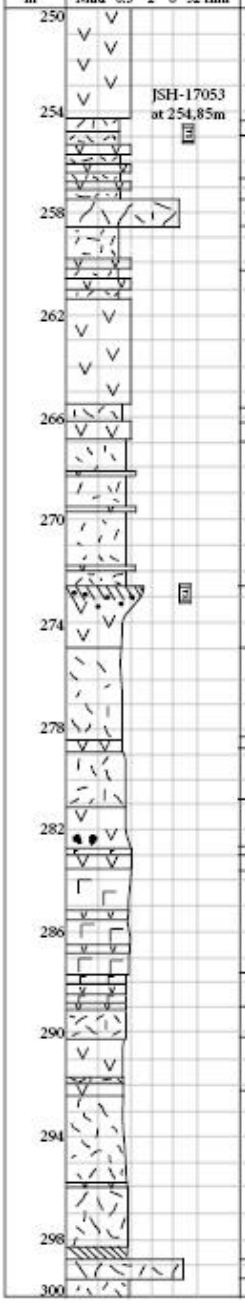

Description	
Aphanitic homogenous basalt.	
At end, more biotite.	251,78
Rhyolite wuth 1cm thick dacitic layers (>7)	254,35
Rhyolite and basalt layers in equal amounts.	254,78
Rhyolite, some patches of dark (biotite) layers.	256,49
Granite pegmatite	257,45
Unaltered, aphanitic homogenous rhyolite.	258,60
Unaltered, aphanitic homogenous basalt	260,17
Rhyolite, quartz- chlorite alteration.	256,60
Basalt + biotite.	266,10
Rhyolite.	266,70
Several mafic intrusions.	
Moderate pervasive quartz + chl alteration.	
Garnets.	
Basalt. upper contact is biotite schist with quartz clasts.	272,40
Thin section JSH-17054 at 272,83m.	
Rhyolite.	274,90
Moderate pervasive qtz + chl alteration.	
Fractures + some red alteration (hematization?)	
Basalt	278,09
Rhyolite	278,55
Basalt, at 262,28m big qtz clasts.	280,75
Dacite	282,47
Basalt	282,97
Dacite with occasional patch of basalt.	283,54
Resembles tuff.	
No alteration.	
Basalt / dacite	287,70
Mostly rhyolite. Looks like dacite.	289,00
Basalt with layers of dacite, rhyolite and quartz.	290,10
Rhyolite with some garnets.	292,20
Moderate pervasive qtz - chl alteration.	
Contact with pegmatite has intense biotite alteration.	
Granite pegmatite.	298,83
Rhyolite.	299,43

Graphic Core Log		Hole No. PYO-84	Depth 483,3 m
Scale	1:100 cm	Project	JSH Pro Gradu
By	Jesse Hettula	Section	
Date	14.07.2017	Coordinates: 3453492,309 E 7062318,456 N +157m depth	
Page	8 of 11	270 Azimuth -65 Inclination	

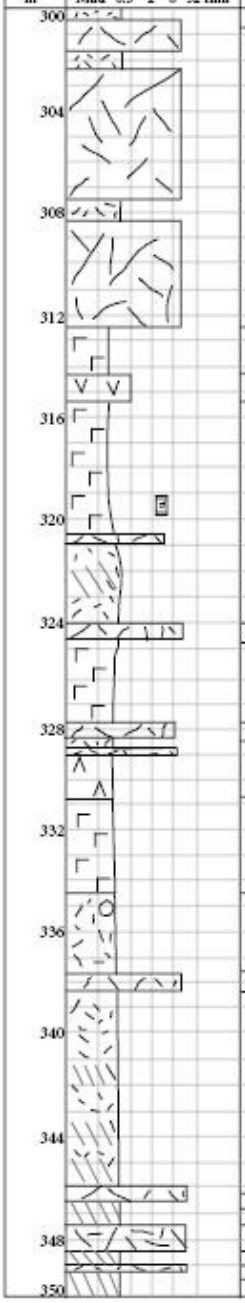

Depth m	Main Grainsize Mud 0.5 2 8 32 mm	Max clast ø & structure	Alt	%	Description	
					Rhyolite	300,70
					Granite pegmatite with two sections of original host rock:	301,80
					301,8 - 302,31m = Rhyolite	302,31
					307,77 - 308,02m = Rhyolite with biotite contacts.	307,77
						308,02
					Aphanitic massive dacite	312,48
					Trachybasalt, biotite alteration.	314,37
					Aphanitic massive dacite. No alteration. Thin section JSH-17055 at 319,50m.	315,19
					Rhyolite 8% of the rock has been sericite altered. Intrusion at contact (between dacitic and rhyolitic sections).	
					Granite pegmatite	324,00
					Dacite	324,80
					Granite pegmatite	327,90
					Andesite, and small granite pegmatite at 328.90m. Rhyolite at between two granite pegmatite intrusions.	328,43
					Dacite. Some biotite alteration. Pyrite veins. Resembles andesite.	330,91
					Rhyolite. No pyrite or sericite. ○ = partly carbonate rock	334,55
					Granite pegmatite	337,75
					Rhyolite. Slight sericite alteration (7%) + pyrite veins (1 - 2%). frequency increases with depth. Some garnets.	338,21
					Granite pegmatite.	346,18
					Rhyolite	346,76
					Granite pegmatite	347,60
					Rhyolite. Intense sericite alteration at contacts.	348,61
					Granite pegmatite.	349,04
					Rhyolite with sericite alteration.	349,40

Graphic Core Log		Hole No. PYO-84	Depth 483,3 m
Scale	1:100 cm	Project	JSH Pro Gradu
By	Jesse Hettula	Section	
Date	14.07.2017	Coordinates: 3453492,309 E 7062318,456 N +157m depth	
Page	9 of 11	270 Azimuth -65 Inclination	

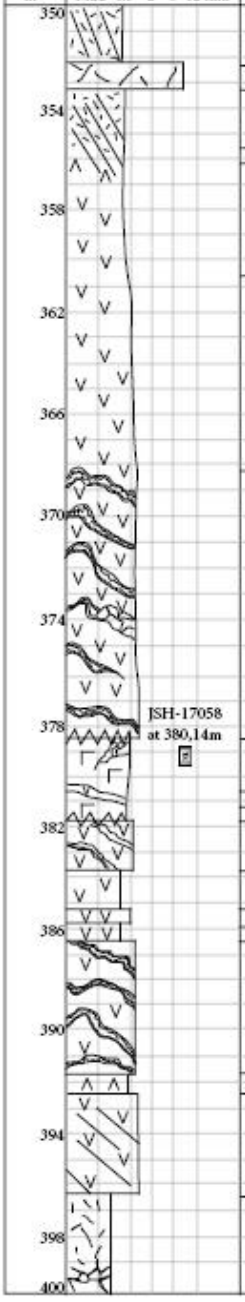

Alt	%	Description	
		Rhyolite + sericite alteration (8%)	
			352,37
		Granite pegmatite	359,13
		Rhyolite + sericite alteration (10-15%).	
			355,70
		Andesite	356,30
		Basaltic andesite + epidote alteration (10%) ± pyrite	
			360,70
		Porphyritic trachybasalt quartz nodules (could be clasts).	
			368,20
		Porphyritic basalt Alteration is common (epidote)	
		Some fractures with carbonate infill.	
		At times there seems to be clasts, but hard to say for sure.	
			378,50
		Dacite, somewhat fractured. Hard to say which which were deposited first: dacite or basalt because of disseminated contacts.	380,74
		Basalt.	381,15
		Dacite.	381,65
		Basalt. Moderate pervasive quartz+epidote+sericite ±pyrite alteration is common (50% of the rock is unaltered).	383,90
		Fine-grained homogenous trachybasalt.	385,15
		Basalt. Same describtion as 381,65 - 383,90m.	385,37
		Fine-grained homogenous trachybasalt.	386,41
		Basalt. Moderate pervasive quartz+epidote+sericite ±pyrite alteration is common (50% of the rock is unaltered). Some of the white felsic dots may be clasts.	
			381,78
		Andesite, porphyritic texture at middle of this section. Clasts?	392,33
		Biotite - basalt.	
			396,65
		Rhyolite (SiO_2=76,4%). Very white homogenous charecter. Disseminated pyrite (5 - 10%). No sericite. Fractured.	

Graphic Core Log		Hole No. PYO-84	Depth 483,3 m
Scale	1:100 cm	Project	JSH Pro Gradu
By	Jesse Hettula	Section	
Date	14.07.2017	Coordinates: 3453492,309 E 7062318,456 N +157m depth	
Page	10 of 11	270 Azimuth -65 Inclination	

Depth m	Main Grainsize Mud 0.5 2 8 32 mm	Max clast ø & structure	Alt	%	Description	
400					Rhyolite.	
					Quartz vein at 401,1m + pyrite	
					Mafic vein at 402,25m.	402,25
					Basaltic andesite	403,10
404					Rhyolite	403,80
					Andesite. Porphyritic texture at the end.	444,37
					Dacite with 4 mafic veins.	405,15
					Some fractures.	407,50
408					Basalt with dacite intrusion at 411,60m, where there is contact alteration in basalt.	
					Some alteration (20%), weak pervasive epidote + pyrite (3%).	
412					Quartz clasts, which seem to occur at near the alteration.	
						413,70
					At first, rhyolite which seamlessly turns into	
416					.... Dacite at 418m onwards.	
					Pyrite veins are most abundant at 413 - 427m.	
					Matrix is aphanitic and, at places, sericite altered, starting from 423,5m and ending at ... no specific point.	
420					Sericite alteration can be seen frequently from 423,5m onwards, but alteration is at it strongest in beginning (pervasive, strong).	
424					Thin section JSH-17062 and JSH-17063 at 423,82m and 424,28m, respectively.	
428					At 428m, 429,6m and 429,90m, mafic (basaltic andesite) veins, currently altered into somewhat biotitic composition.	
					Quartz veins frequent at 430 - 432m.	
432						433,00
					Basaltic andesite, similiar to earlier smaller intrusions.	433,45
					Dacite with moderate (50%) amount of sericite alteration + 10% pyrite veins.	
436						
440					Thin section JSH-17064 at 440,6m.	441,55
					Biotite schist at upper contact. Basaltic charecter and composition at middle and at the lower contact.	
444						444,85
					Rhyolite, sericite alteration at middle, no pyrite.	445,95
					Basaltic andesite composition, similiar to a the basalt above.	
448					Fractures with carbonate infill.	
						449,08
450					Granite pegmatite	

Graphic Core Log		Hole No. PYO-84	Depth 483,3 m
Scale	1:100 cm	Project	JSH Pro Gradu
By	Jesse Hettula	Section	
Date	17.07.2017	Coordinates: 3453492,309 E 7062318,456 N +157m depth	
Page	11 of 11	270 Azimuth -65 Inclination	

Depth m	Main Grainsize Mud 0.5 2 8 32 mm	Max clast ø & structure	Alt	%	Description	
450					Granite pegmatite	
					Rhyolite + pyrite (10%). No sericite.	450,85
454					Granite pegmatite.	
					Basaltic andesite, altered sections are biotite schist.	454,65
					Rhyolite, very obscure outlook.	456,75
458					Basalt Couple of epidote altered patches, but mostly unaltered.	457,50
					Basaltic andesite. Biotite alteration.	
462					Dacite.	462,15
					Disseminated contact with basenite. Increasingly mafic parts have more pyrite.	463,30
466					Thin section JSH-17067 at 466,48m.	
					Basanite. Pumice + pyrite (15%)	467,05
					Rhyolite. Some sericite (20%) and pyrite (5%).	467,50
470					At 471 - 471,24m, 471,41 - 471,52 and 473,04 - 473,24m basaltic andesite veins.	469,05
						471,00
474						
478					478,71 - 479,06m Granite pegmatite	
					Relatively unaltered rhyolite, porphyritic texture, looks like sediment.	
482					Basaltic andesite. Looks like intrusion.	482,30
					Zone in between dacite and more mafic unit, which would come next.	483,30
486						

APPENDIX 1.c. R-2242 drillcore log.

Graphic Core Log		Hole No.	R-2242	Depth	330,57
Scale	1:1000cm	Project	JSH Pro Gradu		
By	Jesse Hettula	Section			
Date	25.07.2017	Coordinates:	2252,567 E 8212,484 N -1226,88m depth, KKJ		
Page	1 of 8		220 ° Azimuth -32 ° Inclination		

Depth m	Main Grainsize Mud 0.5 2 8 32 mm	Max clast ø & structure	Alt	%	Description
0	Thin section	α = 7°			This drillcore starts from a underground tunnel wall and comes close to the massive sulfide in an angle, but does not come into contact with the deep massive sulfide body. The closest section to the sulphide body in this drillcore exhibits the typical strong metamorphosed mafic and felsic lamillae.
40		α = 10°			
		α = 5°			Because surrounding rock around the massive sulfide has wrapped around the sulfide body, it is to be expected that some rock units have been cut at least twice by the drillcore. If this is not the case, the above mentioned statement may not be completely correct.
80		α = 10°			
		α = 15°			
120		α = 25°			The α- angle increaces steadily from the start of the drillcore. The only expections appaer in some intrusion that has not used any specific stratigraphic unit as channelway.
		α = 25°			
160	Mafic and felsic lamillae	α = 35°			
		α = 40°			Observations: - Dacite is the dominant host rock in the near vinicinity to the massive sulfide. Most of the mafic units are intrusions. - This drillcore comes close to the massive sulfide.
200		α = 40°			
		α = 50°			
		α = 55°			
240		α = 50°			
280					
		α = 44°			
320		α = 56°			
360					

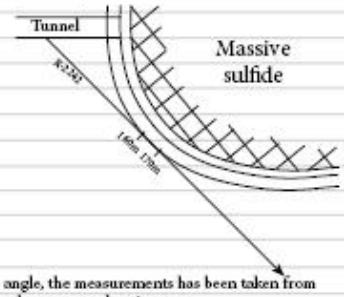

Note:
Due to the α- angle, the measurements has been taken from the first point where new rock unit starts.
Thus, rock unit thickness displayed here is not the true thickness.

Example:
Measurement points have been marked with circles.

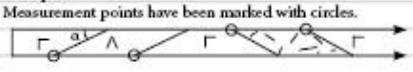

Graphic Core Log		Hole No. R-2242	Depth 330,57
Scale	1:100cm	Project	JSH Pro Gradu
By	Jesse Hettula	Section	
Date	25.07.2017	Coordinates:	2252,567 E 8212,484 N -1226,88m depth, KKJ
Page	2 of 8		220 ° Azimuth -32 ° Inclination

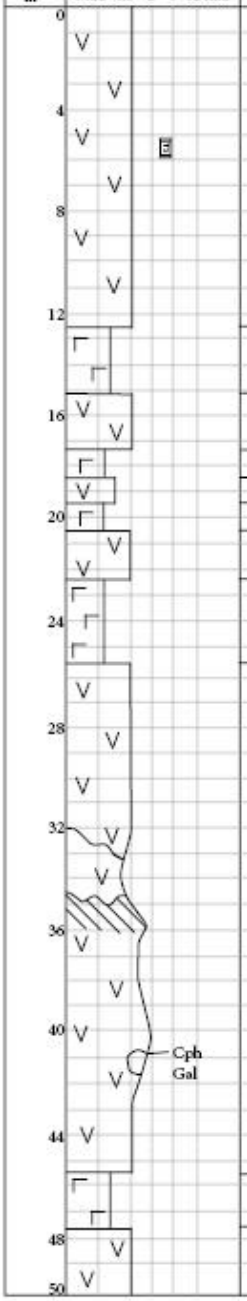

Depth m	Max clast ø & structure	Alt	%	Description
0				Fine grained mafic slate.
	α = 10°			Thin section JSH-17102 at 5,65m.
12				
12,44	α = 3-5°	Sil	20	Dacite with some silicic alteration + pyrite. Slightly laminated parallel to surrounding rock contacts.
15,05	α = 5°			Fine - grained mafic slate.
16				
17,35	α = 8°			Dacite with slaty structure.
18,50	α = 10°			Mafic slate.
19,20	α = 10°			Almost rhyolitic composition. Slate.
20				
20,61	α = 21°	Ep	60	Pervasive moderate epidote alteration + pyr in mafic rock.
22,43	α = 6°			Banded dacite with 7% pyrite in along bands and cracks.
24				
25,60	α = 1-5°			Fine-grained mafic slate.
28				
32		Ep		Strong pervasive epidote ± pyrite alteration, followed by unaltered and bigger grain-sized mafic slate.
36				
39,14				Even more mafic (ultramafic?) rock with some alteration (cph + gal). Increase of grain size.
40				
41,00				Mafic slate.
44				
44,25				
45,58	α = 4°			Very thin (4cm true thickness) dacitic section that has magnetite porphyritic texture.
47,67	α = 3°			
48				
50				Mafic slate.

Graphic Core Log		Hole No.	R-2242	Depth 330,57
Scale	1:100cm	Project	JSH Pro Gradu	
By	Jesse Hettula	Section		
Date	25.07.2017	Coordinates:	2252,567 E 8212,484 N -1226,88m depth, KKJ	
Page	3 of 8		220 ° Azimuth -32 ° Inclination	

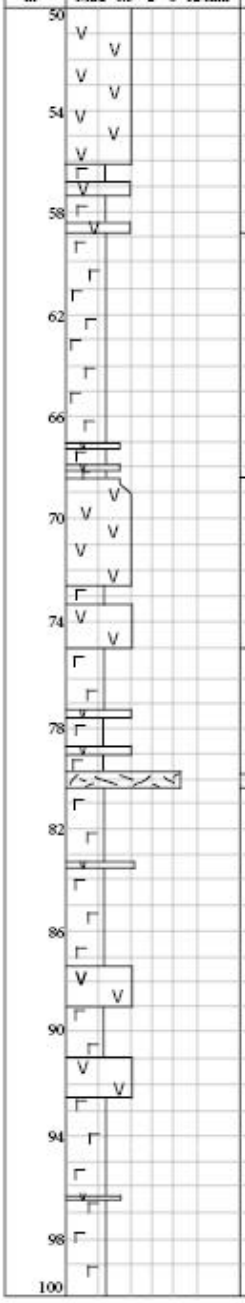

Max clast ø & structure	Alt	%	Description	
			Fine-grained mafic slate.	
			Contact with following dacite appears in three phases. Contacts are sharp in each one.	
α = 5°				56,10
α = 5°				56,85
α = 5°				57,60
				58,66
α = 10°				58,88
			At first, aphanitic massive dacite. After 61 m, lamillar structure (sericite?) and magnetite porphyry.	
			Contact with following mafic rock comes in several phases.	
				67,01
α = 9°				67,23
α = 10°				67,95
				68,16
α = 11°				68,45
			Fine-grained mafic schist. Quartz clast at 69,9m has pyrite (no hyd. alt.).	
α = 10°			Starting from 70,37m, 20% epidote alteration. Ends at contact	72,75
	Ep	20%	with quartz vein (72,75m).	73,33
α = 15°				75,00
α = 14°			Aphanitic dacite lamillae / slate? Magnetite porphyry.	
α = 9°			Some mafic veins.	77,20
				77,53
α = 13°				78,80
				79,05
α = 36°			Granite pegmatite.	79,41
				79,64
				80,55
α = 14°				83,55
			Aphanitic dacite lamillae / slate? Magnetite porphyry. Some mafic veins.	
α = 11°			Mafic vein at 98,54m has caused orange colored alteration (hematization?) in dacite	87,42
α = 15°			Dacite is the host rock rock for sure.	89,04
α = 17°				90,97
α = 17°				92,50
α = 21°				96,40
				96,54

Graphic Core Log		Hole No. R-2242	Depth 330,57
Scale	1:100cm	Project	JSH Pro Gradu
By	Jesse Hettula	Section	
Date	25.07.2017	Coordinates:	2252,567 E 8212,484 N -1226,88m depth, KKJ
Page	4 of 8		220 ° Azimuth -32 ° Inclination

Depth m	Main Grainsize Mud 0.5 2 8 32 mm	Max clast ø & structure	Alt	%	Description	
100					Aphanitic felsic slate.	101,57
						101,72
						101,80
						102,00
					Fine-grained mafic slate that has couple of controlled silicic alteration veins. Granite pegmatite intrusion at 101,90m - 102,00m.	
104						104,60
		α = 13°			Aphanitic dacite, somewhat slaty structure. Slate-planes cutting surfaces have almost a glas-like look, but fresh fractures show very fine-grained dacite.	
108						
		α = 21°				110,83
			Ep	20	Mafic slate with folding and epidote type alteration.	112,00
112		α = 11°			Aphanitic dacite. Increasingly slaty structure and metamorphism, where grain size increases. Some mafic veins.	
		α = 18°				113,92
						114,00
		α = 15°				115,00
						115,29
116						
					Interesting mafic vein at 124,7m - 125,3m.	
120						
		α = 20°			Thin section JSH-17106 at 122,04m.	121,21
		α = 18°				121,58
						122,19
						122,50
124						124,70
						125,30
128						
132		α = 20°				132,17
					This section has 15 mafic veins in total, and only some has been drawn and measured here. Instead, a representive draft is displayed. Host rock is dacite.	132,62
						133,06
						133,41
						133,69
						133,75
136		α = 21°				136,07
		α = 18°				137,13
						137,25
		α = 22°				138,10
						139,06
140					Dacite, which turns into highly metamorphosed dacite after what presumeably is a fault. Metamorphism gradually decreases, but slaty structure does not disappear. α- angle has been measured from the slate-planes at 142m.	
		α = 19°				
144		α = 22°				144,47
						144,62
		α = 26°				145,95
					Metamorphism strength increases again starting at 149m.	
148		α = 29°				148,80
		α = 26°				149,25
150						

Graphic Core Log		Hole No. R-2242	Depth 330,57
Scale	1:100cm	Project	JSH Pro Gradu
By	Jesse Hettula	Section	
Date	26.07.2017	Coordinates:	2252,567 E 8212,484 N -1226,88m depth, KKJ
Page	5 of 8		220 ° Azimuth -32 ° Inclination

Depth m	Main Grainsize Mud 0.5 2 8 32 mm	Max clast ø & structure	Alt	%	Description
150					Dacite that has increased grain size due to metamorphism.
154					Mafic intrusions grain size decreases and begins to blend into dacite, meaning that both rock units have gone through the same deformation / metamorpism phase.
158					
162					This section resembles the immediate hanging-wall rock of the ore.
166					Aphanitic felsic and mafic units appear in turns. Felsic rock is dominant. Some silicic + chlorite (?) alteration.
170					Mafic units have clastic and/or porphyritic textrure. At 164,5m and 171m, disseminated pyrite in felsic rock. Thin section JSH-17112 at 171,15m.
174		α = 38°			Thin section JSH-17113 at 174,13m. At first, aphanitic massive basalt with quartz nodules. At 174,40m - 174,75m intrusion of mafic biotite-schist, after which comes the aphanitic massive basalt with quartz nodules again. Biotite schist has caused contact metamorphosis host rock. Aphanitic massive basalt has schistous/slaty structure.
178	Alt.				At marked locations, the basalt has undergone epidote type alteration.
182	Alt.				At 181,65m - 182,10m, granite pegmatite.
186					
190	Alt.				
194					
198	Alt.				
200					

150,72
151,05
151,23
151,64
152,40
152,85
155,10
157,05
157,60
159,33
160,30
161,08
161,23
161,85
173,65
174,40
174,75
181,65
182,00
182,10

Graphic Core Log		Hole No. R-2242	Depth 330,57
Scale	1:100cm	Project	JSH Pro Gradu
By	Jesse Hettula	Section	
Date	26.07.2017	Coordinates:	2252,567 E 8212,484 N -1226,88m depth, KKJ
Page	6 of 8		220 ° Azimuth -32 ° Inclination

Depth m	Main Grainsize Mud 0.5 2 8 32 mm	Max clast ø & structure	Alt	%	Description
200	Alt				Basalt with qtz-nodules. some epidote alteration. Slaty structure.
					Host rock is andesite, schistous structure.
204					It might be that this is dacite with thin disseminated mafic veins, or it is simply gneiss.
208					Magnetite porphyry.
212					After the mafic intrusion at 212,52m - 213,95m, the host rock is stil dacite. At 216,00 - 218,32m; garnet porphyry.
216					Thin mafic intrusive veins are common, Thicker massive veins are unaltered.
220					Starting from 218,32m, dacite is aphanitic and massive, with only slight schostosity.
224					A long section of facite host rock veing intruded be numerous granite pegmatite veins.
228					
232					
236					235,00m seems to be intersections of two different kinds of dacite. the "new" one has more SiO2 in comparison.
					Thin section JSH-17116 at 237,44m.
240					Dacite schist has magnetite grains.
					Side note: thicker sections of granite pegmatite seems to favor mafic units.
244					
248					
250					Trachybasalt?

202,35
204,63
206,13
209,06
209,33
210,67
211,42
212,52
213,95
218,32
219,23
220,18
220,28
220,40
220,80
221,35
221,40
222,10
222,63
223,15
223,75
224,06
224,30
225,04
225,53
227,10
227,75
228,82
229,11
229,50
230,26
231,00
231,25
231,83
232,41
233,00
234,27
235,00
235,40
236,00
238,12
239,20
239,80
240,50
242,80
243,65
244,00
244,47
244,70
245,85
247,00
247,65
249,20

Graphic Core Log		Hole No. R-2242	Depth 330,57
Scale	1:100cm	Project	JSH Pro Gradu
By	Jesse Hettula	Section	
Date	26.07.2017	Coordinates:	2252,567 E 8212,484 N -1226,88m depth, KKJ
Page	7 of 8		220 ° Azimuth -32 ° Inclination

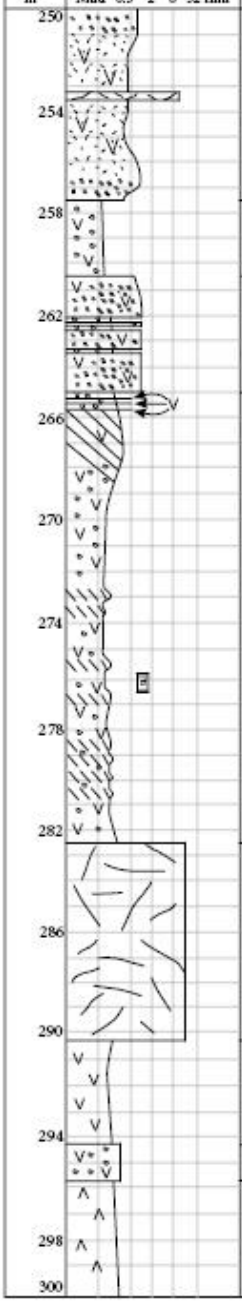

Description	
Porphyritic trachybasalt? Porhpyry grain size decreases around granite pegmatite intrusion.	253,11 – 253,61
Aphanitic basalt with occasional biotite schistosity and qtz-clasts.	269,55
"trovhybasalt" contact with above-mentioned unit is complex. It seems like trachybasalt is an intrsusion. There is sections of qtz-granular basalt in between.	260,53 – 262,20 – 262,40 – 263,40
	265,00 – 265,25 – 265,50 – 265,75
Complex section of mafic rock. It is hard to say if it is a single mafic unit or several because of alteration and metamorphism.	268,80
At times the rock appears as biotite schist, other places it is aphanitic basalt.	
Qtz-grains can be seen (altered and unaltered) often.	
Thin section JSH-17118 at 275,85m.	
It might be that "aphanitic basalt" sections are different rock unit. There is not a single qtz-clast in them.	
Granite pegmatite.	282,56
Aphanitic massive basalt.	290,25
Basaltic schist with elongated qtz -clasts.	294,29 – 295,00
Aphanitic massive basaltic andesite.	295,89 – 300,00

Graphic Core Log		Hole No. R-2242	Depth 330,57
Scale	1:100cm	Project	JSH Pro Gradu
By	Jesse Hettula	Section	
Date	26.07.2017	Coordinates:	2252,567 E 8212,484 N -1226,88m depth, KKJ
Page	8 of 8		220 ° Azimuth -32 ° Inclination

Depth m	Main Grainsize Mud 0.5 2 8 32 mm	Max clast ø & structure	Alt	%	Description
300					Aphanitic massive basaltic andesite.
304					Aphanitic massive dacite, at places alteration and metamorphism (garnets).
308					
312					"Trachybasalt." Basaltic schist, highly porphyritic,
316					"Trachybasalt" is an intrusion. It has been intruded by granite pegmatite.
320					
324					Host rock dacite.
328					A series of granite pegmatite intrusions into dacite. Thin section JSH-17121 at 324,58m.
332					Granite pegmatite.

300,50
300,81
301,27
302,89
303,30
311,80
315,57
316,78
320,89
321,15
322,68
323,18
324,58
324,82
325,28
325,50
325,86
326,64
326,80
327,28
330,57

APPENDIX 1.d. R-2252 drillcore log.

Graphic Core Log		Hole No.	R-2252	Depth	334,31m
Scale	1:1000cm	Project	JSH Pro Gradu		
By	Jesse Hettula	Section			
Date	27.07.2017	Coordinates:	3452829,131 E	7061989,429 N	- 996,317 Depth
Page	1 of 8		Az. 85 °	Incl. - 35 °	

Depth m	Main Grainsize Mud 0.5 2 8 32 mm	Max clast ø & structure	Alt	%	Description
0	Thin section				The drillcore goes to the east from east-side of the near massive sulfide body in -35° angle to horizontal. The purpose of this drillcore is to see what kind of lithostratigraphical units the massive sulfide has towards the east. Theory: The rock is hanging-wall at first, but turns into foot-wall at unknown point. Presumeably at around alteration zone. This drillhole is mostly dacitic. Dacite color gets darke with depth. The best way to interpret different rock units is by correlating immobile element ratios to other drillcores rock units and looking for repetative patterns.
40					
80					
120					
160					
200					
240					
280					
320					
360					

Graphic Core Log		Hole No.	R-2252	Depth 334,31m
Scale	1:100cm	Project	JSH Pro Gradu	
By	Jesse Hettula	Section		
Date	27.07.2017	Coordinates:	3452829,131 E 7061989,429 N - 996,317 Depth	
Page	2 of 8		Az. 85 ° Incl. - 35 °	

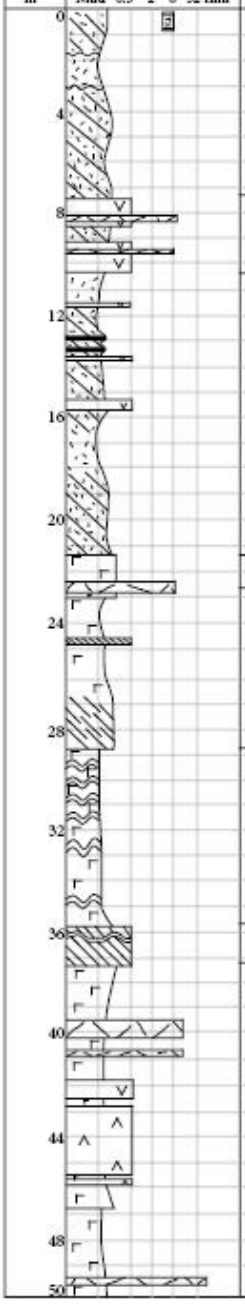

Max clast ø & structure	Alt	%	Description	
			Unaltared is aphanitic rhyolite. Altered rocks have gone tgrough metamorphism resulting in bigger grain-size mylonite with garnets and magnetite.	
			Thin section JSH-17112 at 1m.	
				7,3
			Two quartz intrusions that within mafic units, which are aphanitic and massive.	8,24
				9,10
				9,86
				10,00
				10,27
			Aphanitic rhyolite matrix and disseminated pyrite (5%), which are most seen in mylonitic serious (40%). Some magnetites and garnets.	11,55
				12,90
				13,20
				13,54
			A few mafic intrusions.	15,30
				15,60
				21,36
			Granite pegmatite, along fine-grained dacite.	22,30
				22,56
				22,70
			Aphanitic dacite with increasing biotite schistocity. At 25 - 26m, odd alteration veins.	23,10
				24,05
				24,55
			At 28,56m, biotite schist turns turns into dacite, green contact? Fault plane?	
				28,85
			Dacite / Rhyolite , quartz - granular texture. Numerous hydrothermal alteration veins. Strong pervasive epidote + quartz ± cordierite alteration. It is unusual to see epidote in silica-rich in rock. Mass inflow?	
				35,78
			Mafic biotite-scist with the same hyd. alt.	
				37,13
			Very messy dacite. Fine-grained, metamorphosed quartz veins, schistous.	39,50
				40,06
				40,85
			This unit is then intruded by "basaltic" and "andesite" intrusions that have similiar chorecter. Dacite at the other end seems much clearer - aphanitic massive.	41,80
				42,30
				42,73
				45,53
				45,63
				45,81
				46,63
				49,65
				49,96

Graphic Core Log		Hole No. R-2252	Depth 334,31m
Scale	1:100cm	Project	JSH Pro Gradu
By	Jesse Hettula	Section	
Date	27.07.2017	Coordinates:	3452829,131 E 7061989,429 N - 996,317 Depth
Page	3 of 8		Az. 85 ° Incl. - 35 °

Depth m	Main Grainsize Mud 0.5 2 8 32 mm	Max clast ø & structure	Alt	%	Description	
50					Aphanitic homogenous dacite. Some magnetite porphyry and slightly schsitous structure.	
54						54,28
					White granite pegmatite.	55,08
58					Aphanitic dacite with biotite schistosity + magnetite. Thin section JSH-17127 at 59,76m.	
62						61,50 61,78 62,26 62,60
						64,16
66					White granite pegmatite.	
70						
74						
						76,50
78					Biotite schist (basaltic) at contact.	78,28
					Fine-grained dacite with inner lamillae of pyrrhotite, magnetite, biotite.	79,30
					(Different color from dacite before granite pegmatite, < 64m)	80,30 80,60
82	Same color				Aphanitic massive dacite. (Different color from dacite before granite pegmatite, < 64m)	81,14
						84,30
86					Dacite which has strong pervasive sericte + chlorite + quartz alteration, and some orange colored alteration (hematization?).	86,70 87,20 87,75
					Clearly hydrothermally altered, but has the fluids come from basalt intrusions, or has the intrusions simply preferred altered rocks?	88,70 89,24 89,69
90					Basalt has dissemintaed pyrite, but no alteration.	91,08 91,30 91,87 92,16 92,82 93,07 93,32
94					Granite pegmatite intrusions in aphanitic massive dacite.	
						95,90 96,30 97,00 97,60
98						
100					Contact metamorphosis with andesite at 99,70m?	99,70

Graphic Core Log		Hole No. R-2252	Depth 334,31m
Scale	1:100cm	Project	JSH Pro Gradu
By	Jesse Hettula	Section	
Date	28.07.2017	Coordinates:	3452829,131 E 7061989,429 N - 996,317 Depth
Page	4 of 8		Az. 85 ° Incl. - 35 °

Depth m	Main Grainsize Mud 0.5 2 8 32 mm	Max clast ø & structure	Alt	%	Description
100					100,24
					100,86
					101,10
					Dominated by mafic units. One of them (porphyritic basalt) is an intrusion for sure.
					102,50
					102,62
	← Ser				The rest is harder to differentiate since the contacts are blurred.
104	← Intrusion				102,80
					The biggest unit has quartz nodules in the matrix. It also has moderate pervasive epidote alt + cph +galena.
					103,93
					104,27
					Thin section JSH-17129 at 103,46m.
					Dacite can be seen in between the mafic units. There is some sericite in these dacitic units.
108	Alt.				
	Alt. Cu Pb				
					102,37
					Dominated by felsic rock units (dacite, but may also be rhyolitic). Aphanitic and homogenous for the most part.
					110,55
112					112,07
					112,50
					Some schistous structures (= bigger grain size) and magnetite.
					114,30
116					
					Alteration halo near the mafic unit at around 120m.
120	Alt.				120,55
					120,83
	Alt.				A long section of single mafic unit. It has a granite pegmatite vein in the middle (142,30 - 147,05m).
124					
					Pervasive epidote + qtz altertation is frequent. Strength and alteration area varies.
	Sharp cont.				
					127,88m Biotite schist
128	Alt.				127,88
					Odd contact at 127,86m; Fault? Intrusion?
	Alt.				
132	Alt.				Qtz - nodules are almost everywhere.
136	Alt.				
	Alt.				
140	Alt.				
					142,30
144					White granite pegmatite.
					147,05
148					
150					

Graphic Core Log		Hole No. R-2252	Depth 334,31m
Scale	1:100cm	Project	JSH Pro Gradu
By	Jesse Hettula	Section	
Date	28.07.2017	Coordinates:	3452829,131 E 7061989,429 N - 996,317 Depth
Page	5 of 8		Az. 85 ° Incl. - 35 °

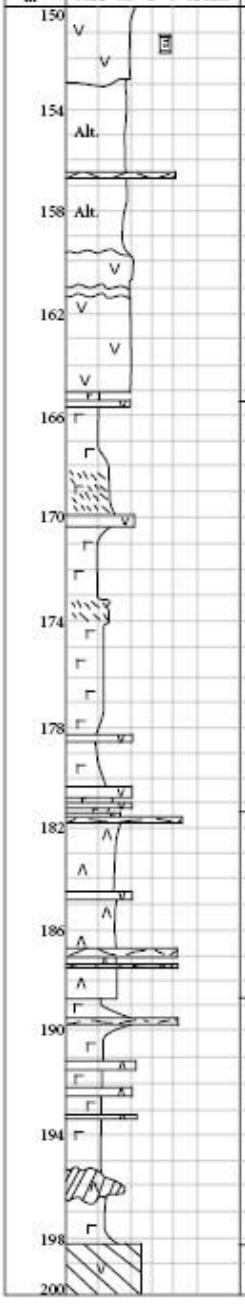

Max clast ø & structure	Alt	%	Description	
			Description in the previous page.	
			Thin section JSH-17130 at 151,27m.	
			Moderate - weak pervasive alteration. Small granite pegmatite vein at 156,5m.	
				156,50
				165,73
			Dacite with some altered sections (white with darker mica). Density remains the same, 2,66 - 2,67 kg/m3.	
			A few mafic intrusions.	
				170,95
				171,30
				173,05
				178,06
				178,32
				180,48
				180,84
				181,10
				181,40
			Homogenous andesite with some intrusions. (D=2,72 kg/m3)	181,80
				184,70
				186,72
				187,06
				187,37
				188,73
			Aphanitic dacite. Some minor mica schist at times. Magnetite in matrix.	189,70
				191,00
				191,45
				192,20
				193,08
				195,69
				195,36
				198,08
			Biotite schist.	

Graphic Core Log		Hole No. R-2252	Depth 334,31m
Scale	1:100cm	Project	JSH Pro Gradu
By	Jesse Hettula	Section	
Date	31.07.2017	Coordinates:	3452829,131 E 7061989,429 N - 996,317 Depth
Page	6 of 8		Az. 85 ° Incl. - 35 °

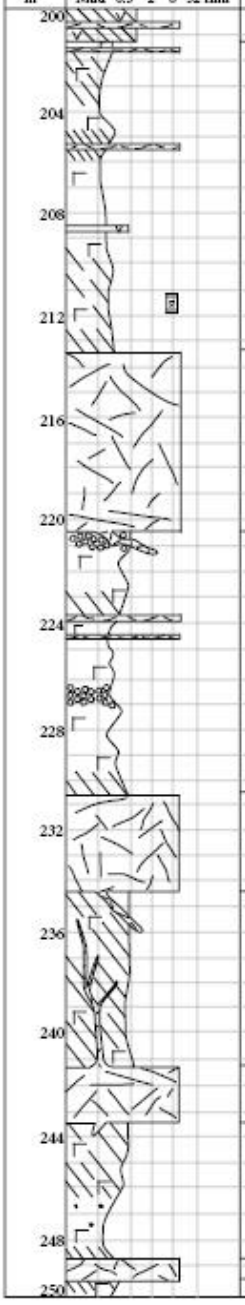

Max clast ø & structure	Alt	%	Description	
			Biotite schist with granite pegmatite intrusion + contact alteration.	201,26
				201,66
			Biotite - dacite.	
			Matrix is aphanitic massive.	
			Garnets and magnetite minerals.	205,30
			A few intrusions.	
				208,50
			Thin section JSH-17133 at 211,46m.	
				213,32
			Granite pegmatite.	
				220,44
			At granite pegmatite contact, granular texture, which turns aphanitic with distance from the intrusion. Recrystallization due to heat?	
			The original texture is massive aphanitic. All other textures are due to alteration, deformation and/or metamorphism.	223,84
				224,50
			At near intrusions, biotite dacite is common.	
			Garnets.	
				230,59
			Granite pegmatite.	
				234,35
			Mostly biotite-schist (dacite) with numerous thin granite pegmatite intrusions. The host rock is recrystallized almost completely.	
				241,10
			Granite pegmatite.	
				243,39
			Composition is at first similiar to 234,35 - 243,39 m, but changes into aphanitic massive dacite + garnets with distance.	
				248,80
			Granite pegmatite.	242,50
			Dacite	

Graphic Core Log		Hole No. R-2252	Depth 334,31m
Scale	1:100cm	Project	JSH Pro Gradu
By	Jesse Hettula	Section	
Date	31.07.2017	Coordinates:	3452829,131 E 7061989,429 N - 996,317 Depth
Page	7 of 8		Az. 85 ° Incl. - 35 °

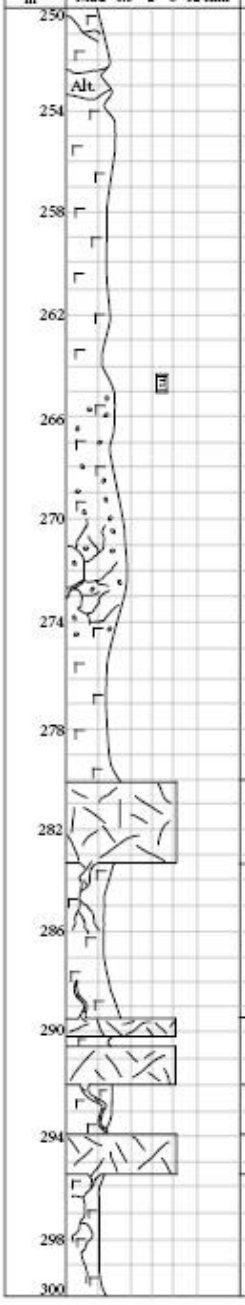

Depth m	Description
	Long section of aphanitic massive dacite.
252,75	The density (2,68 kg/m3) starts to increase at 268m and after (up to 2,72 kg/m3). The decrease of SiO2 content can be seen as darker dacite.
	Generally recrystallization caused by granite pegmatite increases the grain size of the host rock.
	Hydrothermal alteration generally decreases the grain size. Only one such case here (252,75m), which is possibly related to granite pegmatite vein. Moderate chlorite + cph alteration. Otherwise weak hematization anywhere where is granite pegmatite intrusions. Thin section JSH-17134 at 264,56 m.
	= Garnets, usually around intrusions.
280,00	Granite pegmatite.
283,30	Aphanitic massive dacite. The color of the rock is getting darker.
289,42	Granite pegmatite.
292,08	Dacite.
293,97	Granite pegmatite.
295,43	Dacite with granite pegmatite veins.

Graphic Core Log		Hole No.	R-2252	Depth 334,31m
Scale	1:100cm	Project	JSH Pro Gradu	
By	Jesse Hettula	Section		
Date	31.07.2017	Coordinates:	3452829,131 E 7061989,429 N - 996,317 Depth	
Page	8 of 8		Az. 85 ° Incl. - 35 °	

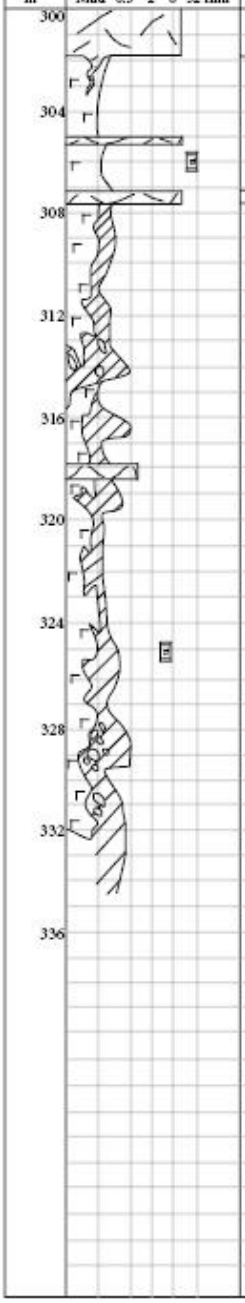

Description	
Granite pegmatite.	300,00
Aphanitic massive dacite (density = 2,7 kg/m3).	301,92
Thin section JSH-17137 at 305,8m	305,07
Granite pegmatite.	307,05 307,58
The rest of this drillcore is very confusing interplay between dacite host rock and mafic intrusion. The drillcore follows along the contact.	310,10 310,50
The intrusion is mostly biotite schist.	311,40
Some minor hydrothermal alteration at 323,35m. - Carbonates along fractures as infill. - Quartz vein.	317,85 318,35
Magnetite porphyry at around 328m.	
There is no contact metamorphism in dacite. It is possible that the mafic units are pillow lava. This is hard to verify, though, due to small diameter of the drillcore, since the pillows are typically very large in Pyhäsalmi area.	323,35
Thin section JSH-17139 at 325,07m.	

APPENDIX 1.e. R-2394 drillcore log.

Graphic Core Log		Hole No. R-2394	Depth 204,81m
Scale	1:500cm	Project	JSH Pro Gradu
By	Jesse Hettula	Section	
Date	19.07.2017	Coordinates: 345766,426 E 7062306,151 N - 1104,68m depth	
Page	1 of 6	KKJ 220,698 Azimuth 2,2 Inclination	

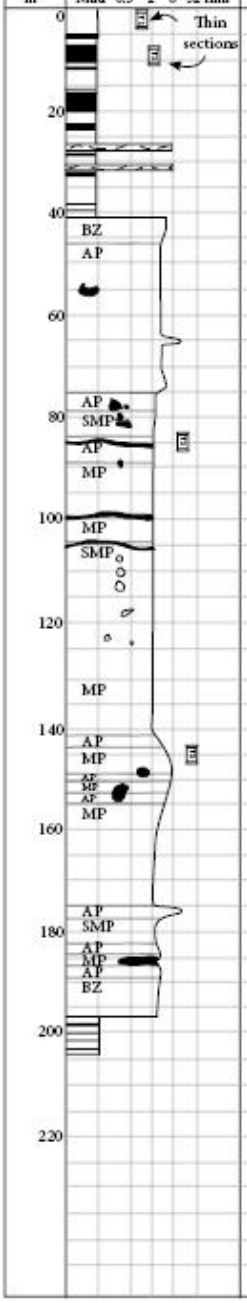

The hanging-walls are similiar to each other. Visit in the underground mine verified the fact that these layers surround the ore body in all fronts perpendicularly to the ore body surface. So it is not a suprise to see the same thing in this drillcore.

The ore body itself commonly has unaltered and (sericite) altered clasts, intrusions and talc (personal communication with Mikko Nummінen). However, sericite alteratin or talc were not observed in these drillcores.

"Stringer zone" (ref. R-2623) did not appear in this drillcore either.
Otherwise the base metal layers are observed as expected: Uppermost layer is zinc-rich, the layer below zinc is copper rich, after which the center is mostly massive pyrite, and then the increase of base metals occurs in reserve order.

There are several possible explanation for the clasts inside the massive sulfide:
- The clasts entered the massive sulfide during deposition as clasts, and remained unalterd through all different phases after that (unlikely).
- The clasts are remnants of broken dikes that ran through the ore body. If this is the case, the intrusions must have happened when the ore body was in several kilometers below seafloor or the sea is not anymore a factor during the intrusion, both of which would limit hydrothermal fluid activity. Thus the clasts remain unaltered. The dikes were then broken after cooling due to tectonic processess such as faulting and thrusting.

There can, of course, be other explanations that have not been considered yet. In any case, these clasts were identified by using following parameters:
- If the clast is bigger than average, and
- if the clast has no considerable amounts of disseminated pyrite in its matrix, then the clast is deemed as a intrusion or vein.

Ore terminology is based on earlier studies, made by Imaña (2003).
- AP = (A_Cu-pyrite ore). Py (90%) >> cpy, (sph)
- BZ = (B_Zinc). Porhpyroblastic py (90%) >> sph (>cpy)
- SMP = (Spotty massive pyrite). Py (80%) >> cpy >> sph. Pyrite content of the SMP is low because of the abundance of sulphosalts and carbonates.
- MP = (Massive pyrite).

Imaña, M (2003):
Petrography, mineralogy, geochemistry and 3D modelling of the A zinc ore in the Pyhäsalmi Zn-Cu VMS deposit, Central Finland. Master's thesis, University of Turku, Department of Geology and Mineralogy, p. 72.

Graphic Core Log		Hole No. R-2394	Depth 204,81m
Scale	1:100cm	Project	JSH Pro Gradu
By	Jesse Hettula	Section	
Date	19.07.2017	Coordinates: 345766,426 E 7062306,151 N - 1104,68m depth	
Page	2 of 6	KKJ 220,698 Azimuth 2,2 Inclination	

Depth m	Main Grainsize Mud 0.5 2 8 32 mm	Max clast ø & structure	Alt	%	Description
0		α=70°			In grainsize chart, felsic and matic sections are divided by black and white color.
4		Fractures			Felsic rock: Aphanitic, primarily white rock with minor mica, which form concordant layers (α=70° - 90°). Weak to moderate silicic + chlorite? + cordierite ± pyrite pervasive alteration at 1,10m; 2,17m; 2,30m; 2,60m; 5,47m; 7,28m - 7,85m and 12,12m - 13,66m.
8		α=75°			Dots in felsic units indicate magnetite minerals. Open dots indicate garnet porphyroblasts. Thin section JSH-17071 at 0,46m.
12					Mafic rock: Mostly aphanitic amphibolic rock with mica (hornblende - biotite?). Pyrite 0 - 3%. Quartz clasts from time to time. If altered, it is epidote alteration. Thin section JSH-17072 at 8,02m.
16					The α angle slowly turns into perdendicular.
		α=80°			
20					Felsic rock at 22m - 23,56m has gone through moderate silicic alteration. Mafic rocks in this area have increased pyrite at contacts and disseminated pyrite in matrix.
24					18m - 18,50m is problematic. It looks like porphyroblastic felsic rock + pyrite, but may also be mafic rock with strong pervasive silicic + chlorite(?) + pyrite alteration.
28		Cph			
32		Sph α=80°			With depth, contacts and contrast between felsic and mafic units become increasingly distinct due to increasing metamorphosis grade.
36		α=90°			
40		α=85°			
44	ZB Drillcore missing ZB Drillcore missing				Contact between the massive sulfide and hanging-wall is very sharp. The only indication of the massive sulfide is minor disseminated pyrite (3 - 5%) in 1m radius of the contact. Typical topmost structure of the VMS body. Zinc - bearing outer layer, followed by copper - bearing layer.
48	AP AP				Small felsic intrusion at 46,82m - 47,63m. Grainsize = pyrite grainsize.
50					

1,20 1,60 1,93 2,12 2,25 4,34 4,50 5,00 5,20 7,25 10,68 11,36 11,73 16,97 17,82 18,52 19,48 19,80 21,75 22,42 22,56 23,73 26,78 27,16 27,30 27,70 28,69 28,90 29,50 31,27 31,73 32,30 33,41 33,57 34,14 35,40 35,54 38,00 38,18 41,45 45,82 47,63

Graphic Core Log		Hole No. R-2394	Depth 204,81m
Scale	1:100cm	Project	JSH Pro Gradu
By	Jesse Hettula	Section	
Date	20.07.2017	Coordinates: 345766,426 E 7062306,151 N - 1104,68m depth	
Page	3 of 6	KKJ 220,698 Azimuth 2,2 Inclination	

Depth m	Main Grainsize Mud 0.5 2 8 32 mm	Max clast ø & structure	Alt	%	Description
50	AP				
	AP	Qtz -vein			Clast at 55,37m - 55,68m is aphanitic massive rhyolite - dacite with assimilated edges with surrounfing massive sulfide, and disseminated pyrite (3%) in matrix.
54					
58	SMP				
	AP				
62					
	AP				
66	+ asp				
	AP				
70					
74	MP				
78	AP				
	AP				
	MP				
82					
86	MP				
90					
94					
98	MP				
100					

Imaña, M (2003)

Ore types:	Sulphides:	Sulphide content:	Gangue:	Textures:
Massive pyrite (MP)	Py >> po, cpy	80 - 95%	Cal, tre, sec qtz	Massive, recrystallized
Spotty massive pyrite (SMP)	Py >> cpy >> sph	70 - 85%	cal, dol, tre, act, mt, ant	Colloform, crustified
A_Cu_Pyrite (AP)	Py >> sph, cpy	90%	Bar, cal, wol	Strongly cataclastic
A_Zinc (AZ)	Py, sph >> cpy	40 - 60%	Qtz, bar, mt, cal, grt, ank, ser	Dissemination, banded sulphides
B_Zinc (BZ)	Py > sph >> cpy	> 60%	Bar, cal, anh, sil,	Porphyroblastic breccia, banding
Remobilised sulphides (REM)	Cpy, po >> gn (asp, tet, py)	50 - 95%	qtz anh >> act, mt	Veins, veinlets, irregular segregation

52,00	
55,37	
55,68	
57,75	
58,70	
64,60	
66,30	
74,37	
76,33	
78,90	
79,68	
84,05	
85,60	
97,72	
98,39	

At 74,35m; silicic clast with 20% disseminated pyrite.

At 78,9m - 79,68m, propably andesite vein because the edge is not badly assimilated and because there is a clear inner halo which follows the contact with MP. Inner halo is porhyritic, which indicates slower cooling at some point. The outer halo is aphanitic.
Then again, it could also be a clast, and the rocks outer edge was altered during sulfide precipitation, though this is more unlikely case.

At 84,05 - 85,60m and 97,72m - 98,39m, both are similiar andesites or basaltic andesites with porphyritic textures. Amphiboles have bigger grain size than matrix.
Thin section JSH-17080 at 85m.

Graphic Core Log		Hole No. R-2394	Depth 204,81m
Scale	1:100cm	Project	JSH Pro Gradu
By	Jesse Hettula	Section	
Date	20.07.2017	Coordinates: 345766,426 E 7062306,151 N - 1104,68m depth	
Page	4 of 6	KKJ 220,698 Azimuth 2,2 Inclination	

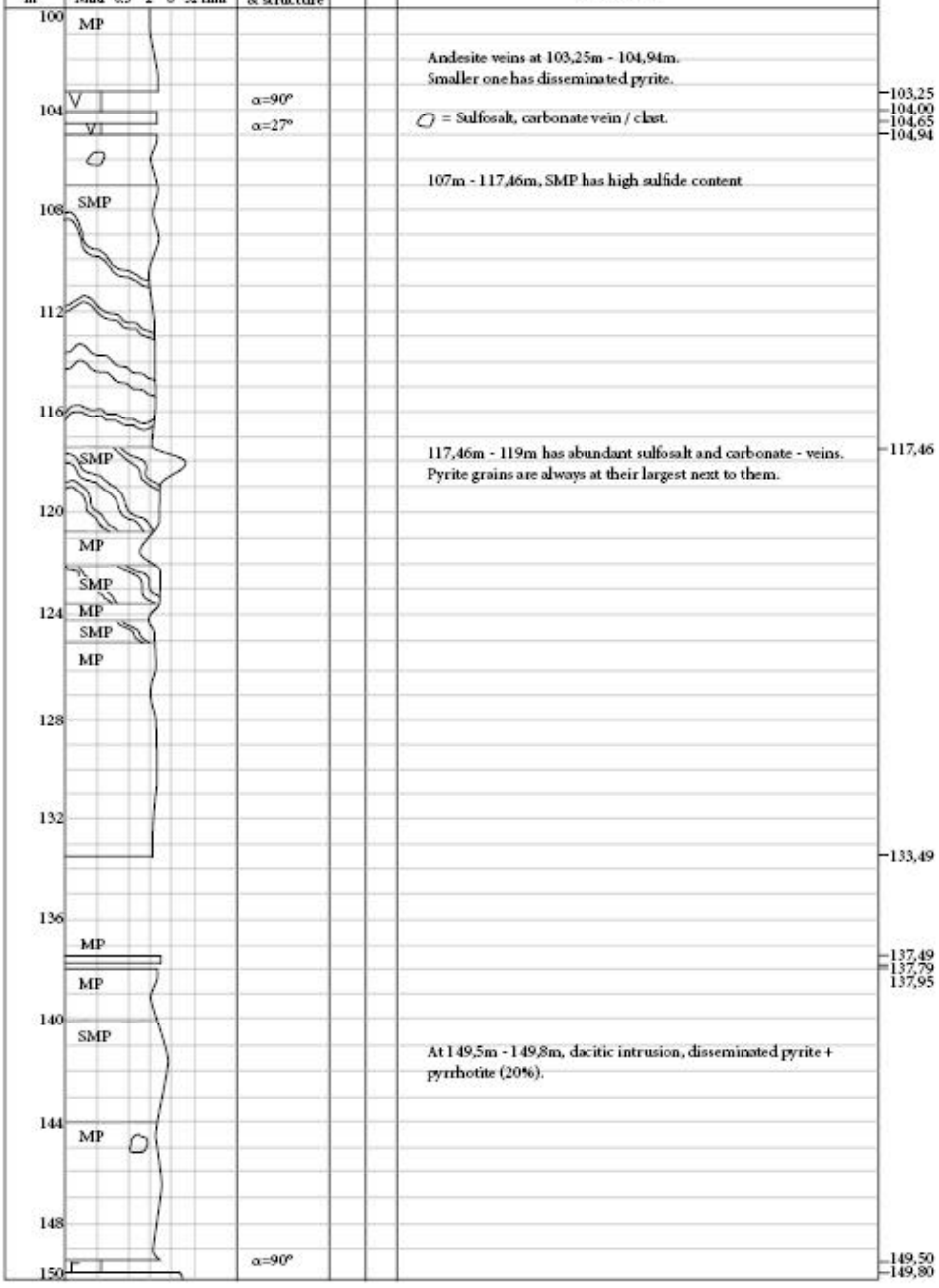

Graphic Core Log		Hole No. R-2394	Depth 204,81m
Scale	1:100cm	Project	JSH Pro Gradu
By	Jesse Hettula	Section	
Date	21.07.2017	Coordinates: 345766,426 E 7062306,151 N - 1104,68m depth	
Page	5 of 6	KKJ 220,698 Azimuth 2,2 Inclination	

Depth m	Main Grainsize Mud 0.5 2 8 32 mm	Max clast ø & structure	Alt	%	Description
150	AP				
					Dacitic vein at 151,11 - 151,72m. Sharp edges, very little or none disseminated pyrite. Thin section JSH-17082 at 151,15m.
	AP				
154					Clast at 152,7m has, however, 50% disseminated pyrite in its matrix. Clast at 153,17m is the same dacite as at the vein. 10% disseminated pyrite.
	MP				
	SMP				
158					
	MP				
162					
168					
170					
174	SMP				
178					
	AP				Andesite intrusion at 185,7 - 186,05m. Aphanitic, 8% disseminated pyrite.
	SMP				
182					
					Aphanitic dacite vein at 187,08 - 187,46m. Fractured, chalcopyrite and pyrite infill. Disseminated pyrite (10%).
186	MP	Carbonate vein			
	MP				
	AP				Contact with hanging-wall at 196,56m. Disseminated pyrite (15 - 17%) can be seen up to 197,10m. Amount decreases with distance from the massive sulfide contact.
190	BZ				
194					Wall rock is (again) made of two kinds of rocks: Mafic and felsic layers that are concordant to the massive sulfides outer surface. Mafic layers are composed mostly of mica, and felsic layers are aphanitic. Felsic layers have magnetite porphyry texture.
	AP? REM?				
198					
200					

151,11
151,72
152,70
153,17
163,44
165,09
183,26
185,68
185,70
186,05
187,08
187,46
196,56

Graphic Core Log		Hole No. R-2394	Depth 204,81m
Scale	1:100cm	Project	JSH Pro Gradu
By	Jesse Hettula	Section	
Date	21.07.2017	Coordinates: 345766,426 E 7062306,151 N - 1104,68m depth	
Page	6 of 6	KKJ 220,698 Azimuth 2,2 Inclination	

Depth m	Main Grainsize Mud 0.5 2 8 32 mm	Max clast ø & structure	Alt	%	Description
200					With increasing distance from the massive sulfide contact, the felsic rock has a more distinct texture. Magnetite is everywhere.
201		α=50°			
202					
203					
204					
205		α=45°			204,81

APPENDIX 1.f. R-2623 drillcore log.

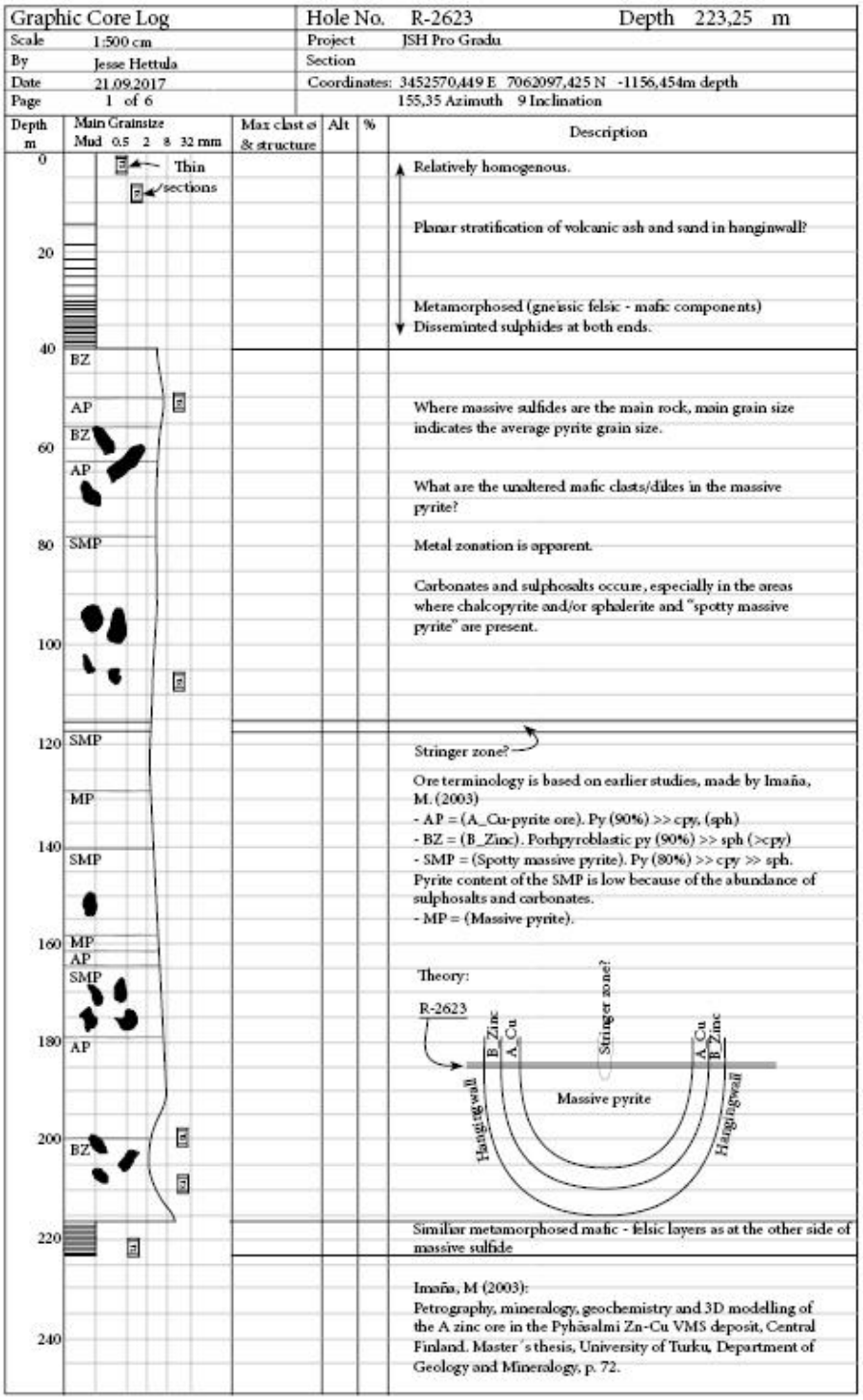

Graphic Core Log		Hole No. R-2623		Depth 223,25 m
Scale	1:100 cm	Project	JSH Pro Gradu	
By	Jesse Hettula	Section		
Date	21.09.2017	Coordinates:	3452570,449 E 7062097,425 N -1156,454m depth	
Page	2 of 6		155,35 Azimuth 9 Inclination	

Depth m	Main Grainsize Mud 0.5 2 8 32 mm	Max clast ø & structure	Alt	%	Description	
0					Relatively homogenous mafic rock. Small garnet - porphyroblasts ---> Metamorphic. Thin section JSH-17001 at 1.52m.	
					Thin sections of mud lamillae spaced in 7 - 10cm from each other.	2,00
4					Different compositions of mud lamillae with syndepositional clasts in between. Example at 6,72m, where silicic clasts have deformed into lenticular shape due to pressure (diagenesis). Some epidote alteration at 6,92m and 8,96m + Quartz clasts + garnet crystals.	3,00
8			Ep.	60		
			Ep.	80		
					Thick gray (ash?) lamillae as a repeating unit. Some alteration.	10,09
12					The ash lamillae has disappeared. Mostly silicic rock. At 13.50m, silicic clast with a diameter of 3cm. 	11,30
			Ep.	60		14,29
16					From 14,25m onward, mafic - felsic lamillae appear freguently in turns. Felsic lamillae are more common, thickness varying from 5,2cm to 1,2m. Average thickness for mafic sections is 8cm.	
			Ep.	70		
			Ep.	80		
20					Thin section JSH-17004 at 19,37m.	
					Metamorphism becomes more apparent with increasing depth.	
24						
					Also, there is a third unit of rock: fine-grained gray (ash?) lamillae, thickness varies from 3mm to 23mm. They are more common when closing in to the massive sulfide.	
28						
32					Epidote +qtz alteration at 16,69m, 17,35m and 17,87m.	
					Garnets can be seen everywhere, no size differentiations.	
36					Interesting clasts at 17,28 m; 18,10 m; 26,69 m; 17,73 m. 24,67 m - 24,90 m: ash lamillae with pyrite.	
40						40,26
	BZ				Transition from silicates to massive sulfide at 40,26 m is very sharp, cutting all pyrite grains in single plain.	
44					Pyrite porphyroblasts (>70%) >> sph > cph > pyrr. Gangue: barite and/or anhydrite. These charecteristics make this unit a B_Zinc (BZ)	
48						48,55
50	REM				Remobilized sulphides ---> REM Disseminated fine-grained pyrite in gangue matrix.	50,05

Graphic Core Log		Hole No. R-2623	Depth 223,25 m
Scale	1:100 cm	Project	JSH Pro Gradu
By	Jesse Hettula	Section	
Date	21.09.2017	Coordinates:	3452570,449 E 7062097,425 N -1156,454m depth
Page	3 of 6		155,35 Azimuth 9 Inclination

Depth m	Main Grainsize Mud 0.5 2 8 32 mm	Max clast ø & structure	Alt	%	Description
50	AP				Ore terminology is based on earlier studies, made by Imaña, M. (2003)
	BZ				- AP = (A_Cu-pyrite ore). Py (90%) >> cpy, (sph)
	AP				- BZ = (B_Zinc). Porhpyroblastic py (90%) >> sph (>cpy)
54					- SMP = (Spotty massive pyrite). Py (80%) >> cpy >> sph. Pyrite content of the SMP is low because of the abundance of sulphosalts and carbonates.
	BZ				- MP = (Massive pyrite).
58					At 57m: mafic clast/dike with edges altered to silica + carbonates ± sulfosalts.
					At 63,60m - 64m: representive sample for unaltered to weakly altered mafic clast/dike.
					= clast/dike (unaltered).
62					Thin section JSH-17008 at 63,61m.
	AP				AP changes slowly to Massive Pyrite (MP) which is also Spotty Massive Pyrite (SMP) at time (around the ⬡- spots)
66					
					⬡ = indicates sulphosalts + silica + carbonates.
	AP				
70					
					At 68,55m -68,83m: A clast with jigsaw - fit texture. Massive pyrite infill, pyrrhotite ± cph at contact.
	MP				
74					
	AP				At 74,85 - 76,8m: 5 clasts in total, fractures which has been intruded by pyrite. Otherwise disseminated pyrite in the matrix.
	SMP				
78					
82					
86					
90					
94					
					The clast at 95m has 30% of its volume replaced by fine-grained disseminated pyrite.
					At 96,90m: clast has clear edges, dis. pyr. 10%
98					At 99,90m: disseminated edges, dis. pyr. 10%
100					

Graphic Core Log		Hole No.	R-2623	Depth	223,25	m
Scale	1:100 cm	Project	JSH Pro Gradu			
By	Jesse Hettula	Section				
Date	21.09.2017	Coordinates:	3452570,449 E 7062097,425 N -1156,454m depth			
Page	4 of 6		155,35 Azimuth 9 Inclination			

Depth m	Main Grainsize Mud 0.5 2 8 32 mm	Max clast ø & structure	Alt	%	Description
100	SMP				The clast at 100,38m has a very fine grained disseminated pyrite (10%) within the matrix. Otherwise clean. Clean quartz vein above the clast.
104					At 104,18m: deformed small (Ø = 3cm) clast with diss. pyr (10%).
108					At 106,12m, Ø = 4cm, clear edge, 7% diss. pyr. At 109,67m, a clast. Very small piece.
112					At 113,56m, 113,56 clast with a very clear edges, rounded. Might be shear-edge. Disseminated pyrite (7%). At 113,95m, small clast with clay-like contact with massive pyrite. Sheared?
116	"Stringer zone?"				
120	SMP				Theoretical "stringer zone." Starts at 114,25m and ens at 117,47m (thin section JSH-17010 at 115,29m). It consists of similiar rock as the previous clasts (Density = 2,87), but more strongly altered (silicic). A single larger piece with pervasive pyrite veins. Pyrite grains seems to be more elongated at areas where fluid flux was higher.
124					At 121,65 - 122m: a clast that has disseminated pyrite. Similiar to "stringer zone."
128	MP				Right next to it: 122,07 - 122,67m a clast that is relatively unaltered at left. At right: Carbonate-sulfosalt composition. Right side of the clast and the middle section are more pyrite rich. Middle pyrite is disseminated into the clast. Right sides pyrite is precipitated.
132					
136					At 124,40m: Clast with disseminated pyrite (15%). Semiclear edges.
140	SMP				
144					
148					
150					

Graphic Core Log		Hole No. R-2623	Depth 223,25 m
Scale	1:100 cm	Project	JSH Pro Gradu
By	Jesse Hettula	Section	
Date	22.09.2017	Coordinates: 3452570,449 E 7062097,425 N -1156,454m depth	
Page	5 of 6	155,35 Azimuth 9 Inclination	

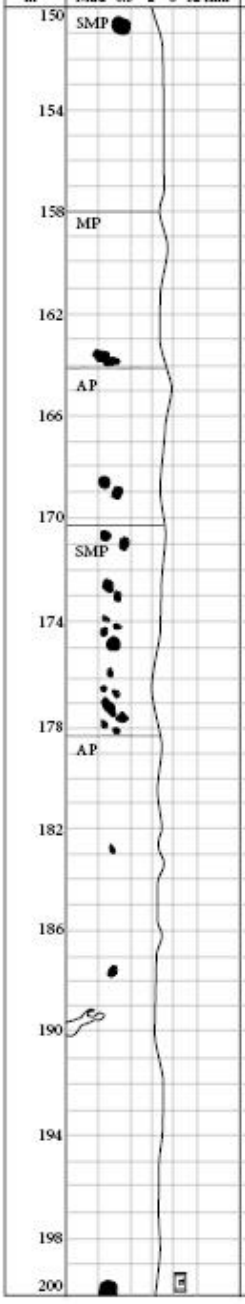

Description
Clast at 150,83 - 150,79m with disseminated pyrite + pyrrhotite (more magnetic than surrounding massive pyrite). Pyrite has banded structure (microfractures?). Otherwise unaltered.
In SMP: Lots of sulfosalts. Pyrite at ~70%.
At 163,33-163.73m is a strangely biotite altered clast, which later deformes around massive pyrite.
At 163,8m: Similiar rock as above.
At 168,7 - 168,9m: Clast with strong biotite alteration. Biotite layers wrap around surrounding pyrite walls. Some disseminated pyrite (5%).
At 189,36m: Similiar clast as above. These biotite altered clasts may be metapelites.
All of the clasts in SMP field are subjected to moderatio to strong greenscist facies metamorphism. The composition is same as described earlier.
At 182,87m: Strongly biotite-altered clast. Deformed into very thin (1cm) objects.
At 187,65m: Strong biotite-altered rock, especially at contact with massive sulfide. Disseminated pyrite (7%).
At 199,67 - 200,17m: Unaltered clast. Disseminated fine-grained pyrrhotite along microfractures. Aphanitc rock. Intermediate?
Thin section JSH-17012 at 199,88m.

Graphic Core Log		Hole No. R-2623	Depth 223,25 m
Scale	1:100 cm	Project	JSH Pro Gradu
By	Jesse Hettula	Section	
Date	22.09.2017	Coordinates:	3452570,449 E 7062097,425 N -1156,454m depth
Page	6 of 6		155,35 Azimuth 9 Inclination

Depth m	Main Grainsize Mud 0.5 2 8 32 mm	Max clast ø & structure	Alt	%	Description
200	AP				At 203m: Unclear whether this section was a clast which acted as a precipitation point for sulfosalt carbonates and silica or not. Either way, sulfosalt and carbonate composition. Cph + pyrrhotite has large grain sizes (anhedral).
204	SMP				
208					At 212,40 - 121,69m: a set of 3 clasts that have jigsaw-fit texture with massive pyrite + cph infill. The bigger clast has nice carbonate precipitates at contact. Otherwise contact (edges of the clast) are clear. Disseminated pyrite (40 - 50%), very fine grained, pervasive.
212	BZ				
216					Contact between massive pyrite and hangin-wall is not a clean cut, pyrite grains have disseminated into the wall. Minute disseminate pyrite all the way to 216,85m mark. 215,93
220					Hydrothermal fluid channel at 217,13m
224					The host rock itself has metamorphosed just as strongly as at the other side of the massive sulfide. Structure and composition are similiar as well. - Similiar layers in similiar amounts. - Clasts visible at 217,68m - Garnget porphyroblasts. - Sulfides are more common at mafic sections. - Grain size equal to mud. - Mafic sections are metamorphose to dark mica. Thin sections JSH-17013 and JSH-17014 at 218,39m and 222,41m, respectively.

APPENDIX 1.g. R-2642 drillcore log.

Graphic Core Log		Hole No. R-2642	Depth 126,75m
Scale	1:300cm	Project	JSH Pro Gradu
By	Jesse Hettula	Section	
Date	21.07.2017	Coordinates: 3452569,17 E 7061903,89 N - 1125,384m depth	
Page	1 of 4	KKJ 164,544 Azimuth -25,234 Inclination	

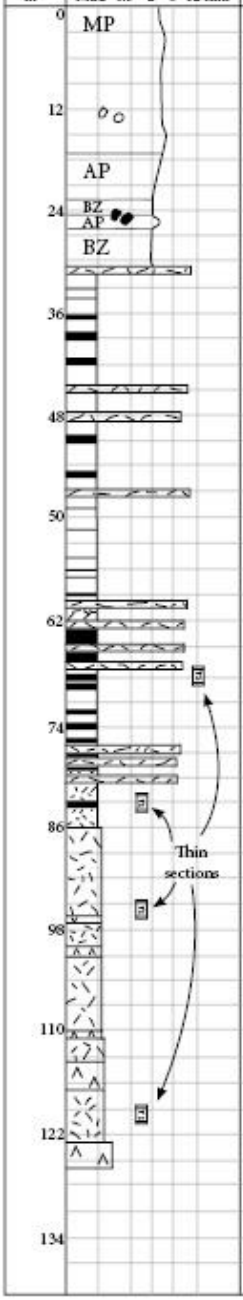

This drillcore starts from massive sulfide body and arrives to the hangin-wall at 29,95m, coming from BZ into granite pegmatite intrusion, after which comes the typical felsic/mafic lamillae that surround the deep massive sulfide body. Felsic sections are dominant.
With depth, textures within these units becomes more distinct.

What to note:
- α-angle change with depth.
- Textures of different units.
- Dacitic rocks metamorphosis grade changes with depth, but not in mafic/basaltic rocks. This could indicate that mafic rocks are intrusions.
However, felsic and mafic lamillae are both metamorphosed in similiar manner in the near vicinity of the massive sulfide body, meaning that the ore intruded along a fault line and metamorphosed the hanging-wall dacite, mafic rock units and hypotethical mafic intrusions. Granite pegmatite intruded to the site only after the "ore thrust."

Graphic Core Log		Hole No. R-2642	Depth 126,75m
Scale	1:300cm	Project	JSH Pro Gradu
By	Jesse Hettula	Section	
Date	21.07.2017	Coordinates: 3452569,17 E 7061903,89 N - 1125,384m depth	
Page	2 of 4	KKJ 164,544 Azimuth -25,234 Inclination	

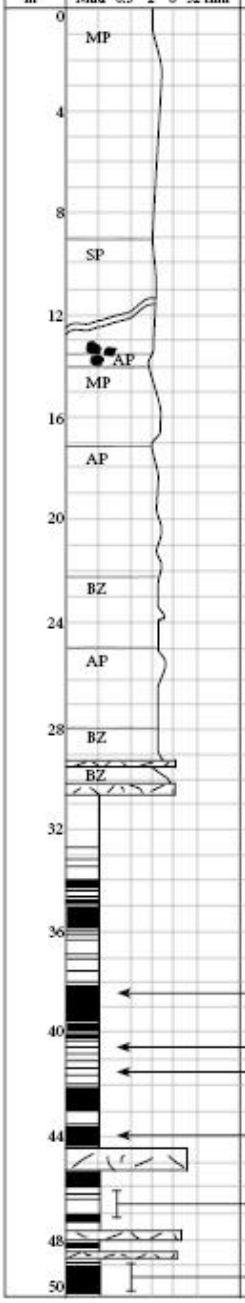

Description	
The massive sulfide lasts only until 29,96m, but it still exhibits the typical metal zonation pattern of VMS mineralizations. Massive pyrite is in the middle of the body, followed by Cu-rich zone and ending at Zn- rich zone.	
Nothingh abnormal in the massive sulfide.	
	12,22
	13,29
	13,35
	13,73
Granite pegmatite at the contact of massive sulfide body and the hangingwall. 3% py + cph in intrusions.	
After the pegmatite veins (30,37 - 32,72m), aphanitic felsic (colored white) rock with cleavage planes parallel to the massive sulfide contact. Aphanitic felsic rocks form several such layers. Matrix has magnetite porphyritic texture.	29,08 29,24 29,96 30,37
	32,74 32,85 33,07 33,19 33,36
Mafic units near the massive sulfide contact are mainly biotite schist (black color). After 36m, biotite schist has turned into aphanitic mafic rock with some mica, which is also alinged parallel to the massive sulfide body.	
	37,90
Mafic rocks have some disseminated pyrite (5%), whereas felsic units does not. Pyrite content degreases with depth.	38,37 39,68 40,03 40,45 40,93
Mafic units have from time to time epidote alterted.	
Felsic untis primarily show silicic alteration, if any.	
	44,33
	45,12
At 39,60m; pyrite lamillae in thin mafic lamillae.	
Carbonates are only found along fractures.	
	47,82 47,95 48,50

Graphic Core Log		Hole No. R-2642	Depth 126,75m
Scale	1:300cm	Project	JSH Pro Gradu
By	Jesse Hettula	Section	
Date	21.07.2017	Coordinates: 3452569,17 E 7061903,89 N - 1125,384m depth	
Page	3 of 4	KKJ 164,544 Azimuth -25,234 Inclination	

Depth m	Main Grainsize Mud 0.5 2 8 32 mm	Max clast ø & structure	Alt	%	Description	
50					Weak pervasive silicic alteration in rhyolitic/dacitic rock	
					A few patches of strong pervasive epidote + silicic hydrothermal alteration in mafic (basaltic) rock	50,83 52,10
54					Mostly dacitic unit with weak alteration and frequent patches of mafic intrusions / layers. Dacitic units are aphanitic, wheras mafic layers have slightly bigger grain size.	
58					Moderate alteration in dacite. Alt. intensifies with depth. It is unclear what kind of alteration, though (chl +qrtz + hematization?)	58,10
						60,03
					After granite pegmatite, strong alteration in (presumeably) dacitic unit.	60,20
62					Granite pegmatite.	62,05
					Dacite and basalt. Unaltered.	63,44
					Granite pegmatite.	64,05
66					Several patches of epidote alteration (moderate) in mafic / basaltic rock. There is also small clasts or pseudoclasts in the matrix.	65,74 67,08
					Granite pegmatite.	67,60
	JSH-17091 68,72m				Very granular texture. Strong silicic alteration + pyrite. The altered rock turns smoothly into basalt. Pyrite lamillae.	68,68
70					Dacite with moderate silicic alteration.	70,25
					Basalt with some patches of moderate alteration (epidote +qtz ± pyr).	72,07
74					Moderate - strong qtz + chl alteration	74,03 75,28
					Granite pegmatite.	75,62 77,28
78					Aphanitic andesite, which has been intruded by granite pegmatite in several different locations. The location of each intrusion has been measured and noted at right side of this page. After the intrusions, dacite has metamorphosed into phyllitic structure + garnet porphyry.	78,41 78,63 79,40 79,64 79,87 80,20
82					Porphyritic basalt with some dacite in between (?).	82,62
					Non-foliated porphyritic dacite. Thin section JSH-17093 at 83,57 - 83,77m.	83,42
					Porphyritic basalt.	85,20
86					Porphyritic dacite. Sometimes matrix is almost pure white with darker porphyry, and at times vice versa. Dominant minerals are quartz, mica and plagioclase.	85,50
90						
94						
					Aphanitic basalt. Deformed contacts with surrounding dacite. Thin section JSH-17096 at 96,72m.	95,71 97,18
98					Porphyritic dacite.	
					Rhyolite, quartzite.	98,90
					Porphyritic dacite.	99,50
100					Aphanitic basalt.	99,90

Graphic Core Log		Hole No. R-2642	Depth 126,75m
Scale	1:300cm	Project	JSH Pro Gradu
By	Jesse Hettula	Section	
Date	24.07.2017	Coordinates: 3452569,17 E 7061903,89 N - 1125,384m depth	
Page	4 of 4	KKJ 164,544 Azimuth -25,234 Inclination	

Depth m	Main Grainsize Mud 0.5 2 8 32 mm	Max clast ø & structure	Alt	%	Description	
100					Aphanitic basalt.	
						101,70
					Metamorphosed dacite.	
					Epidote alteration at around the following aphanitic basalt.	104,44
104						104,72
					70% of the dacite is healthy.	
					The rest is metamorphosed (grain size increaces with metamorphosis strenght).	
108						
						110,69
					Aphanitic basalt.	111,10
112					Dacite (?) which has been gone through hematization and metamorphsis (+ garnets).	
						112,80
					Relatively healthy dacite.	
					Aphanitic basalt with epidote alteration at around contacts.	114,50
					Rhyolite intrusion.	115,34
116					Aphanitic basalt.	115,64
					Aphanitic andesite contact metamorphosed with basalt.	116,72
					Strongly metamorphosed dacite.	117,21
					Aphanitic basalt + pyrite (2%).	117,92
						119,51
120					Strongly metamorphosed dacite.	
					Quartz + mica + plagioclase ± pyrite.	
					Thin section JSH-17100 at 120,05m.	
						123,70
124					Aphanitic homogenous basalt.	
					Some hydrothermal alteration at 120,2m - 120,66m, where mica has broken down to chlorite + quartz.	
					Also at 119,5 - 119,9m and 120,75 - 120,90m.	126,75
128						

1. **APPENDIX 2.** Selected 55 thin sections from JSH-17001 – JSH-17140 samples in numerological order:

Thin section №	**JSH-17001**
Sample information	R-2623, 1.52-1.72m: Mafic hanging-wall
Rock name	Amphibolite
Main minerals	Hornblende + quartz, felspar, plagioclase
Accessory minerals	Titanite, epidote, chlorite
Opaques	Sulfides
Texture	Foliated
Mineral alteration	Amphibolite facies
Hydrothermal alteration	Weak sericite alteration in plagioclase, apparent along fractures
Comments	Mostly homogenous amphibolite. There are several concentrations of white minerals where plgaioclase and quartz are the main minerals, where both have hornblende and titanite inclusions. The sample also has a few fractures that have served as fluid conduits. Along and near these fractures plagioclase minerals have slightly altered to what appears to be sericite. Sericite alteration can also be seen as plagioclase - selective weak alteration
Additional comments	

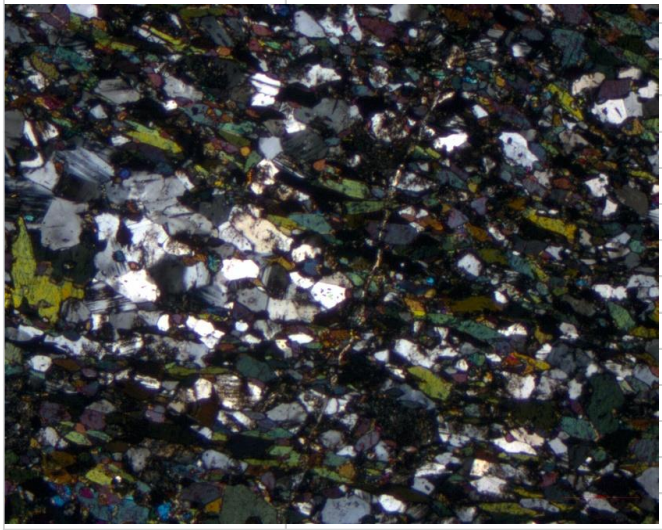

Thin section №	**JSH-17004**
Sample information	R-2623, 19.37-19.58m: Felsic hanging-wall
Rock name	Garnet - biotite felsic gneiss
Main minerals	Quartz + biotite, plagioclase
Accessory minerals	Muscovite, garnet, carbonates, diopside (?), andalusite (?), zircon
Opaques	Disseminated pyrrhotite + pyrite
Texture	Foliated
Mineral alteration	Most of accessory minerals listed are a result of metamoprhism
Hydrothermal alteration	-
Comments	Clearly foliated rock sample. There are several areas which are constructed of large quartz crystals. There is no clear indication how these quartz sections are constructed. However, it does seem like the biotite foliation has been disturbed around the quartz dominated sections, which would indicate that they were present during foliation event.
Additional comments	

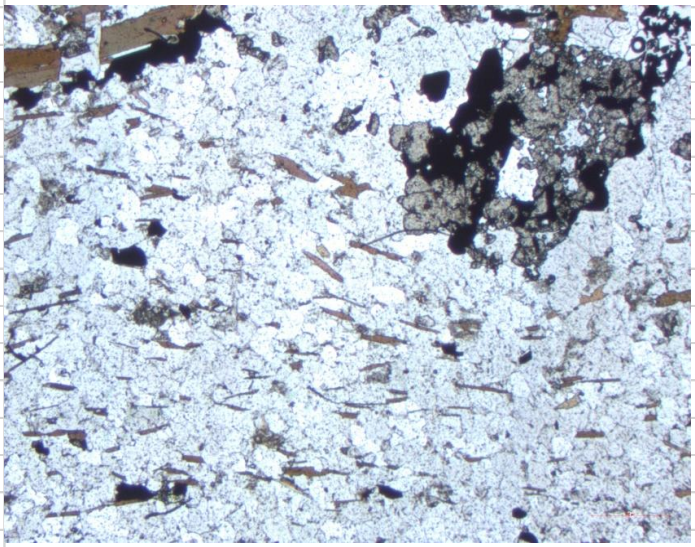

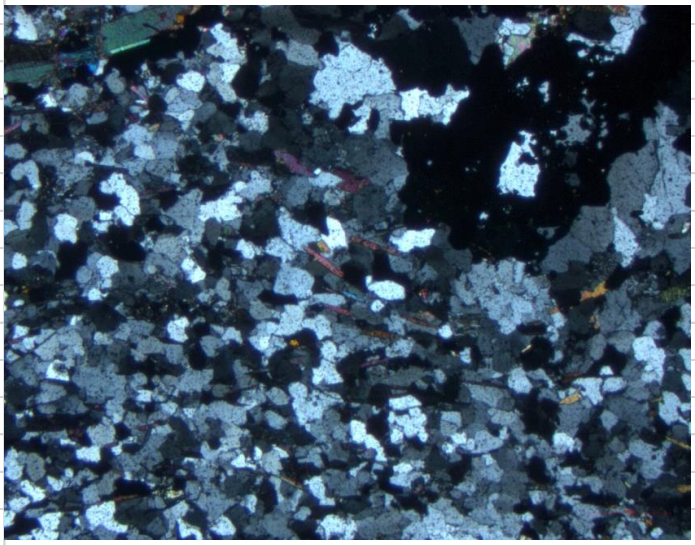

Thin section №	**JSH-17008**
Sample information	R-2623, 61.63-63.82m: Mafic clast from within massive sulfide
Rock name	Biotite amphibolite
Main minerals	Quartz + biotite, ferro-hornblende ± plagioclase
Accessory minerals	Carbonates, zircon, rutile
Opaques	Pyrrhotite + chalcopyrite
Texture	One primary foliation plane and the rest is random
Mineral alteration	Carbonates near sulfides
Hydrothermal alteration	-
Comments	According to Miettinen (2011), the mafic sections in massive pyrite are Mafic A-2 intrusions. In this thin section, there are around equal amounts of dark and white minerals with the addition of disseminated sulfides.
Additional comments	

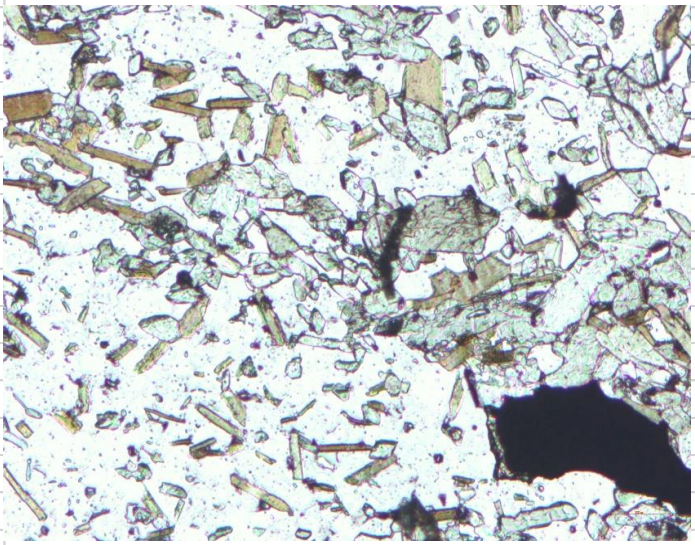

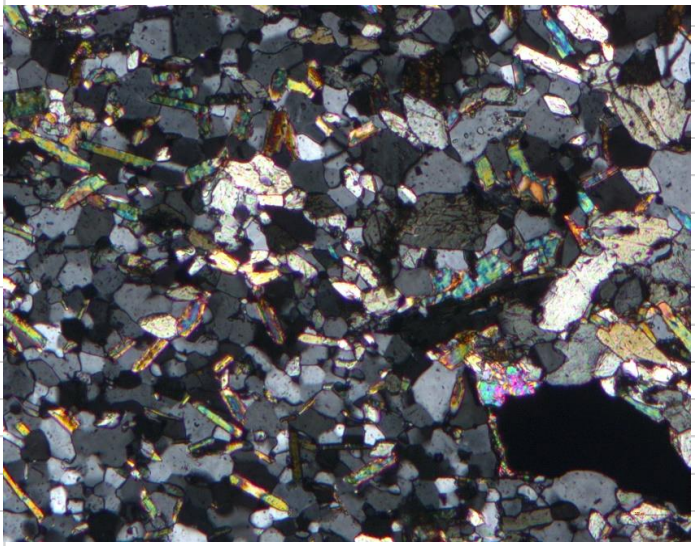

Thin section №	**JSH-17010**
Sample information	R-2623, 115.29-115.52: Silicic alteration and pyrite strings
Rock name	Stringer zone
Main minerals	Quartz ± muscovite, fibrous sillimanite
Accessory minerals	Carbonates, plagioclase
Opaques	Pyrite grains, chalcopyrite infill
Texture	Mostly crystallized veins, otherwise hydrothermal alteration
Mineral alteration	-
Hydrothermal alteration	Silisic alteration and some sericite alteration
Comments	Mostly composed of large quartz crystals. Sericite alteration is present in finer grained sections where plagioclase is also occasionally seen. Sericite has commonly metamorphosed into fibrous sillimanite. Sericite and sillimanite seems to overprint quartz. Miettinen (2011) also found that the massive sulfide hosts hydrothermally altered and unaltered Rhyolite B units.
Additional comments	This sample has the same TiO/Zr ratio as Rhyolite 2 in PYO-47

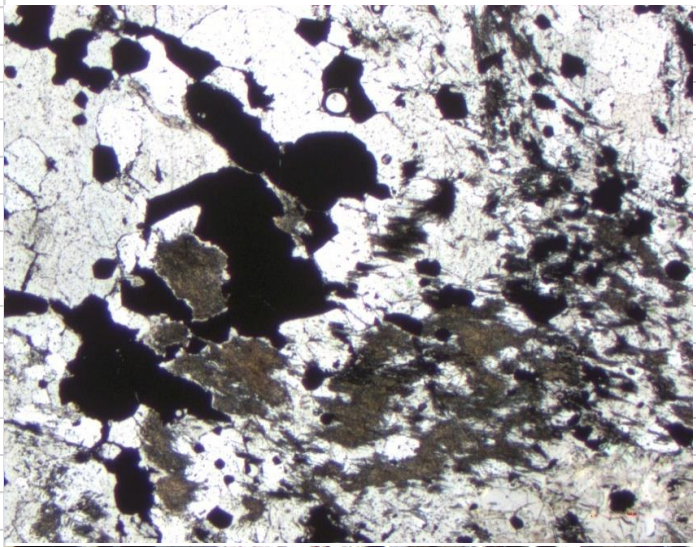

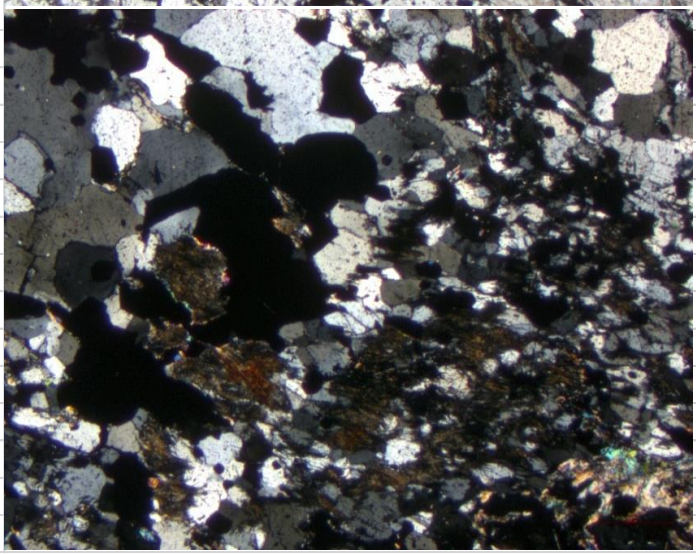

Thin section №	**JSH-17012**
Sample information	R-2623, 199.88-200.08m: Mafic clast with disseminated pyrite
Rock name	Biotite amphibolite
Main minerals	Quartz + biotite, hornblende
Accessory minerals	Titanite, chlorite, carbonates (?)
Opaques	Pyrrhotite + pyrite, chalcopyrite
Texture	Weakly foliated, larger mafic minerals are concentrated into small groups
Mineral alteration	Small hornblende minerals in matrix has altered into chlorite
Hydrothermal alteration	-
Comments	Similiar to JSH-17008. According to Miettinen (2011), the mafic sections in massive pyrite are Mafic A-2 intrusions. In this thin section, there are around equal amounts of dark and white minerals with the addition of disseminated sulfides. This sample is not homogenous in a sense that the vol-% of mafic minerals decreaces from one end of the thin section to the other side.
Additional comments	

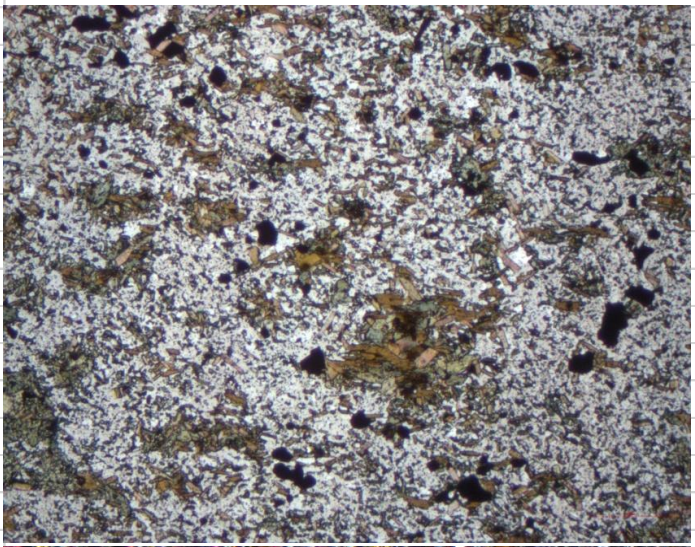

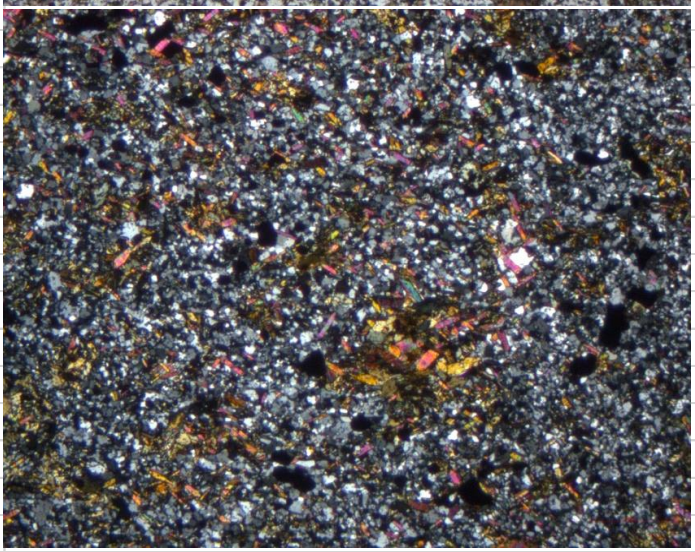

Thin section №	**JSH-17013**
Sample information	R-2623, 218.39-218.59m: Felsic hangin-wall
Rock name	Biotite rhyolite
Main minerals	Quartz + orthoclase, microcline, biotite ± plagioclase
Accessory minerals	Muscovite, epidote, zirkon, andalusite (?)
Opaques	Opaques
Texture	Foliated
Mineral alteration	-
Hydrothermal alteration	-
Comments	The main difference to JSH-17004 is that there is no major metamorphic index minerals such as garnet in this thin section. There is also less opaques.
Additional comments	

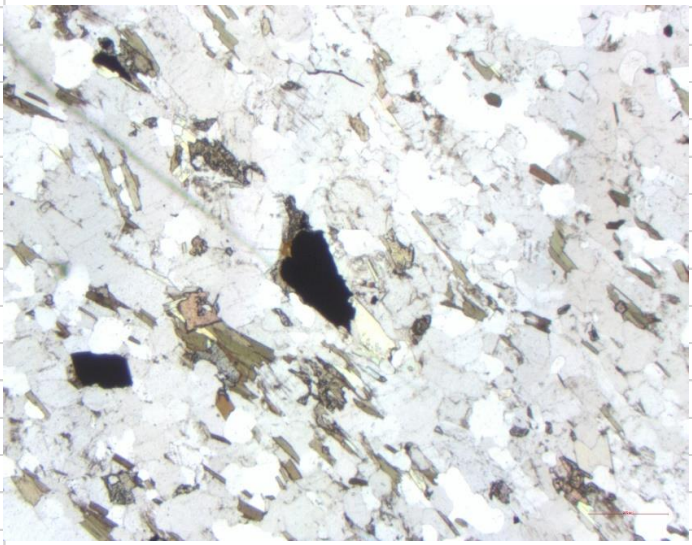

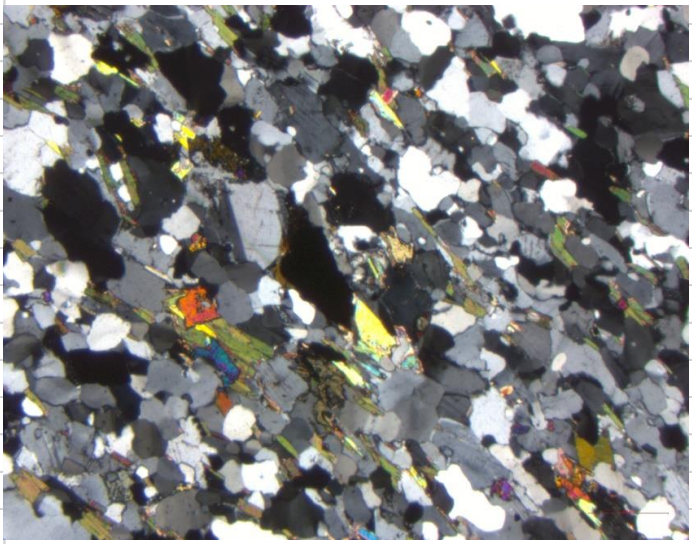

Thin section №	**JSH-17014**
Sample information	R-2623, 222.41-222.61m: Mafic hanginwall
Rock name	Felsic gneiss
Main minerals	Quartz + feldspars, biotite ± plagioclase
Accessory minerals	Muscovite, andalusite (?), carbonates
Opaques	Pyrite
Texture	Foliate, gneissic matrix
Mineral alteration	-
Hydrothermal alteration	Weak selective sericite alteration
Comments	Highly felsic rock with foliated biotite. Similiar to other felsic samples that are collected around the deep ore body.
Additional comments	It is unclear why hand sample information includes term "mafic."

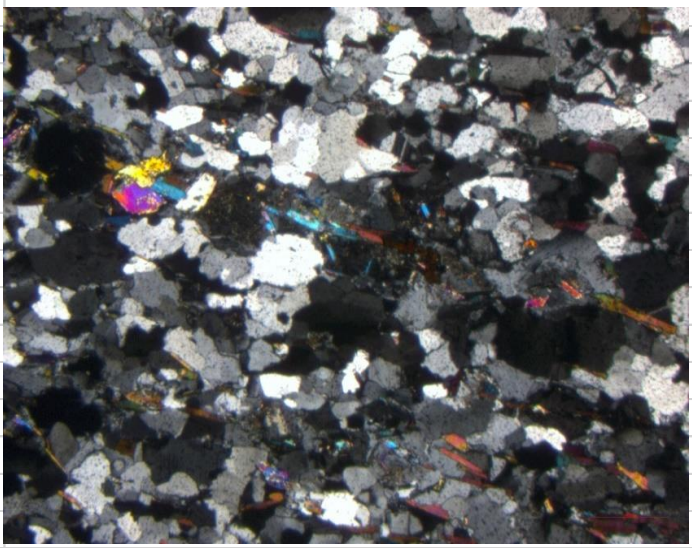

Thin section №	**JSH-17015**
Sample information	PYO-47, 9.97m: Footwall rhyolite
Rock name	Fine-grained rhyolite
Main minerals	Quartz + orthoclase ± biotite ± plagioclase
Accessory minerals	Chlorite and muscovite, rutile, zircon
Opaques	Pyrrhotite droplets, each has some chalcopyrite
Texture	Sligth gneissic texture in matrix
Mineral alteration	Biotite to other minor accessory micas
Hydrothermal alteration	-
Comments	Mostly fine-grained, there are a few areas where the white minerals are microcrystalline where alteration is apparently isochemical (the same minerals as elsewhere). Opaques are all sulfides, where chalcopyrite has mineralized in certain side of the droplet. I interpret that these sulfides have mineralized from monosulfide solutions.
Additional comments	Geochemical sample 8336883

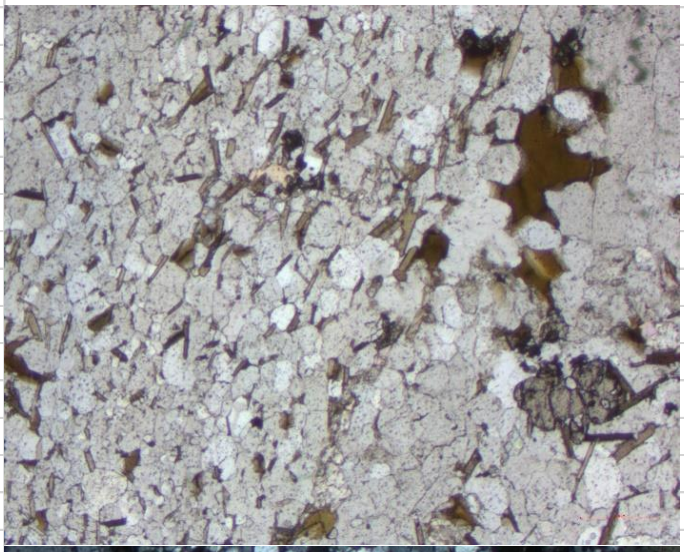

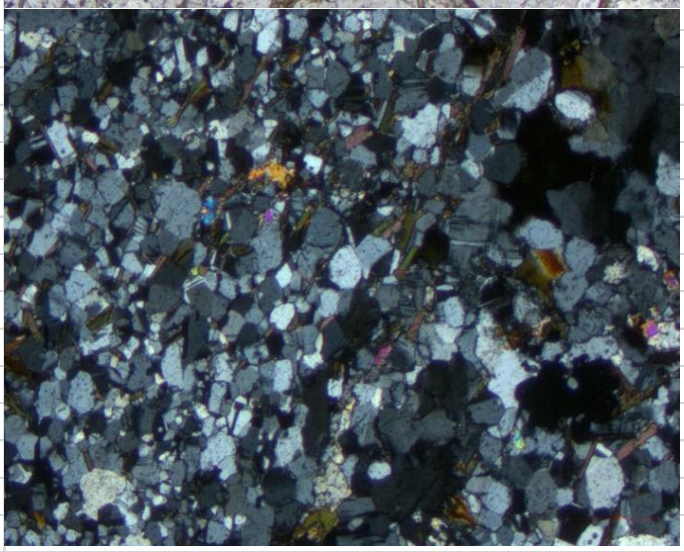

Thin section №	**JSH-17017**
Sample information	PYO-47, 29.29m: Footwall rhyolite
Rock name	Rhyolite
Main minerals	Quartz ± plagioclase, biotite
Accessory minerals	Epidote, zoisite (?), muscovite, rutile
Opaques	Pyrrhotite/pyrite droplets with chalcopyrite inclusions
Texture	Gneissic texture
Mineral alteration	Amphiboles as the result of metamorphism
Hydrothermal alteration	Weak sericite alteration in the matrix
Comments	No comments
Additional comments	Geochemical sample 8336890, AI and CCPI are both 55, so definetly hyd al

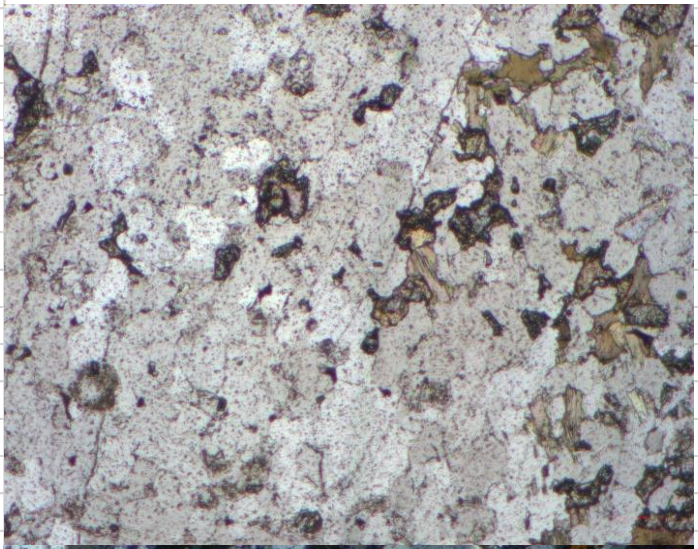

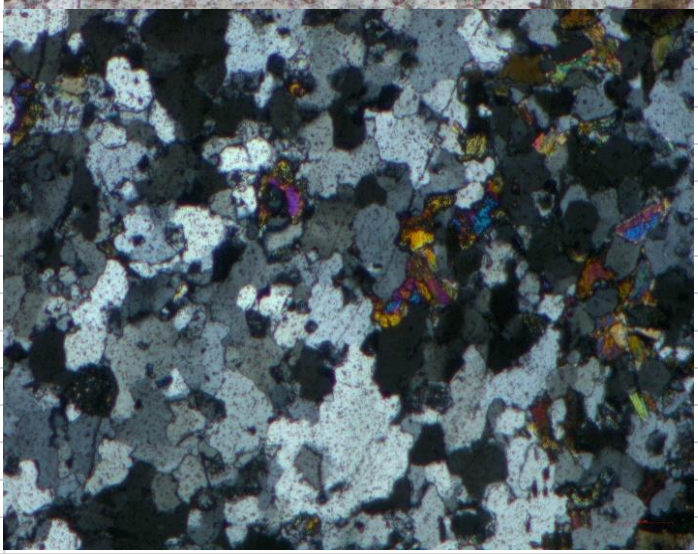

Thin section №	**JSH-17024**
Sample information	PYO-47, 132.2m: Footwall rhyolite.
Rock name	Rhyolite
Main minerals	Quartz ± orthoclase, plagioclase ± biotite
Accessory minerals	Epidote, biotite, zoisite (?), muscovite, rutile
Opaques	-
Texture	Fine-grained, gneissic texture
Mineral alteration	-
Hydrothermal alteration	Weak selective sericite alteration
Comments	Selective weak sericite alteration of plagioclase and feldspars, which is also accompanied with rutile, giving some minerals voggy outlook.
Additional comments	Geochemical sample ?

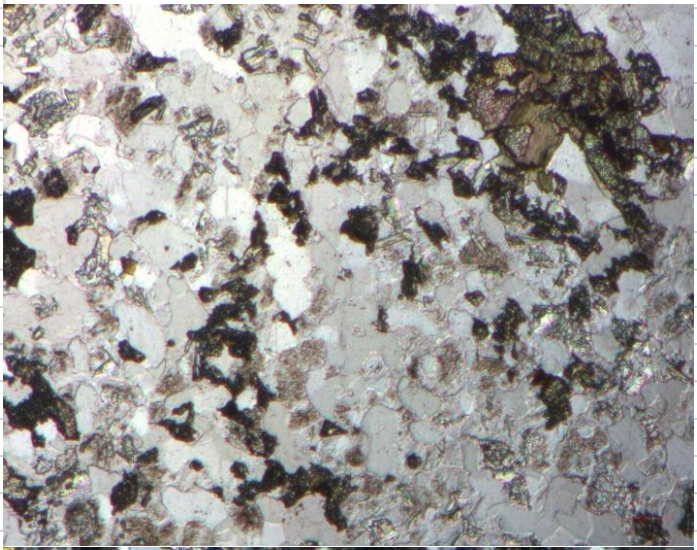

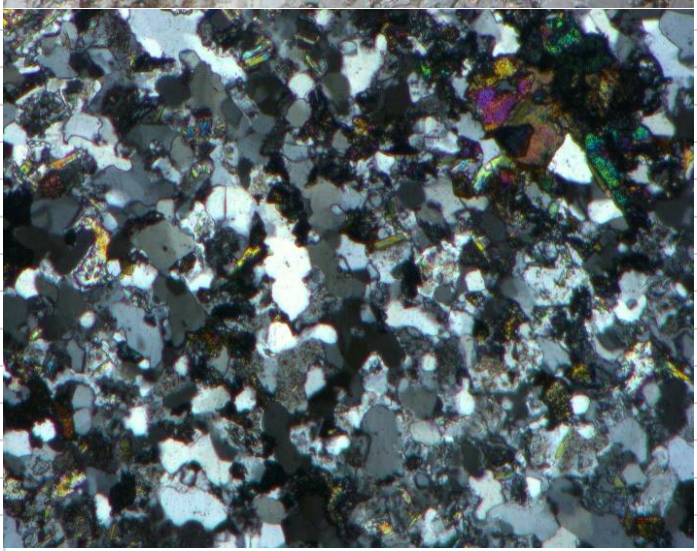

Thin section №	**JSH-17026**
Sample information	PYO-47, 166.9: Footwall basaltic andesite
Rock name	Biotite amphibolite
Main minerals	Hornblende (>35%) + biotite, quartz, plagioclase
Accessory minerals	Titanite, muscovite
Opaques	Accessory opaques
Texture	Matrix is fine-grained, hornblende and biotite are foliated
Mineral alteration	-
Hydrothermal alteration	-
Comments	Hornblende and biotite are 2-5 times larger than fine-grained matrix (quartz + plagioclase). The contrast between matrix and mafic mineral grain size and the lack of gneissic texture could indicate that this rock is an intrusion, which exhibits a flow direction or mineral setting plane in hornblende and biotite orientation. This thin section shows a contact between older (more andesitic) and younger (basaltic andesitic) intrusions, although there is no contact alteration. In drillcore, more mafic section is in the middle of the inrusion.
Additional comments	Geochemical sample ?

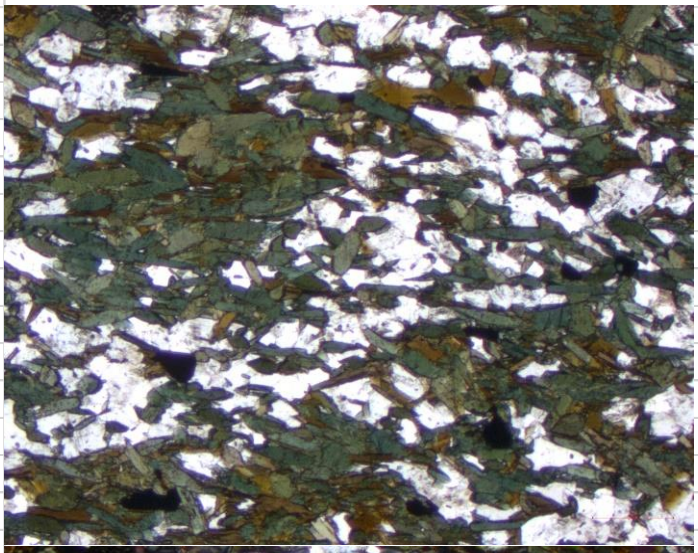

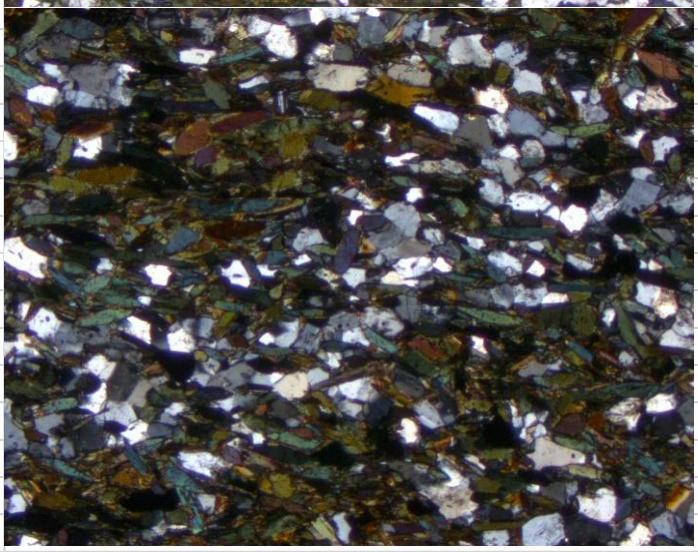

Thin section №	JSH-17029
Sample information	PYO-47, 213.5m: Footwall dacite intrusion
Rock name	Biotite schist
Main minerals	Biotite, quartz ± plagioclase
Accessory minerals	Chlorite, muscovite, titanite carbonates
Opaques	Sulfides
Texture	Schistous
Mineral alteration	-
Hydrothermal alteration	A single small hydrothermal vein, weak sericitic alteration
Comments	It is hard to say based on this this section whether or not this rock is intrusion, but since it is located right next to hydrothermal zone, this rock is likely a intrusion, based on the lack of hydrothermal alteration. There is also a section of quatzite in there, which could simply be a quartz vein (it has some biotite that has similiar lineation with host rock). Originally it was interpreted to be a xenolith. There is also hydrothermal vein where biotite has altered into chlorite and muscovite and carbonate has replaced host rock regularly.
Additional comments	Geochemical sample ?

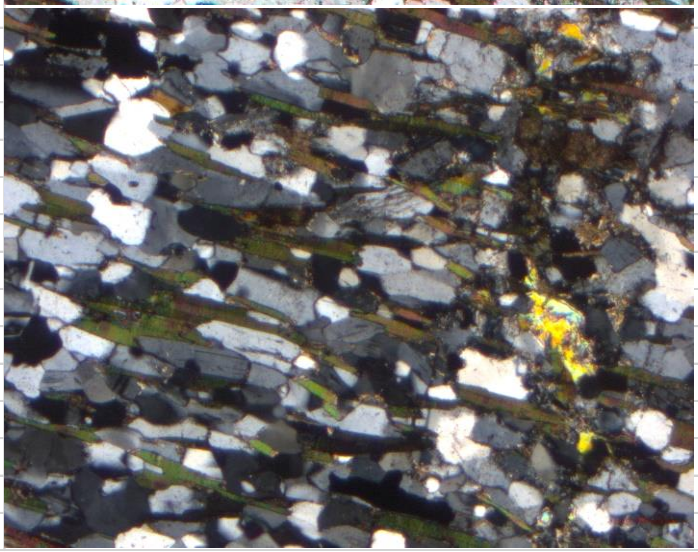

Thin section №	**JSH-17032**
Sample information	PYO-47, 234.52: Footwall rhyolite 2
Rock name	Porphyroblastic sericite schist
Main minerals	Quartz + muscovite (sericite), cordierite
Accessory minerals	Rutile, fibrolite sillimanite, garnet
Opaques	Sulfides
Texture	Cordierite porphyroblast growth in foliated sericite schist
Mineral alteration	Fibrolite sillimanite, cordierite, garnet
Hydrothermal alteration	Sericite alteration
Comments	Matrix is mostly fine-grained quartz that hosts yellowish cordierite porphyroblasts, irregular colorless and foliated muscovite. Muscovite has been at places metamorphosed into fibrolite sillimanite. There is some rare spots where it appears that cordierite has metamorphosed into subhedral garnet.
Additional comments	Geochemical sample ?

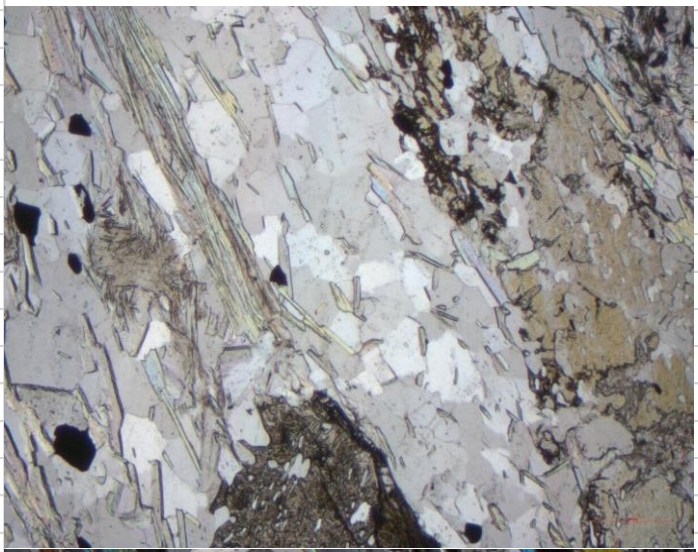

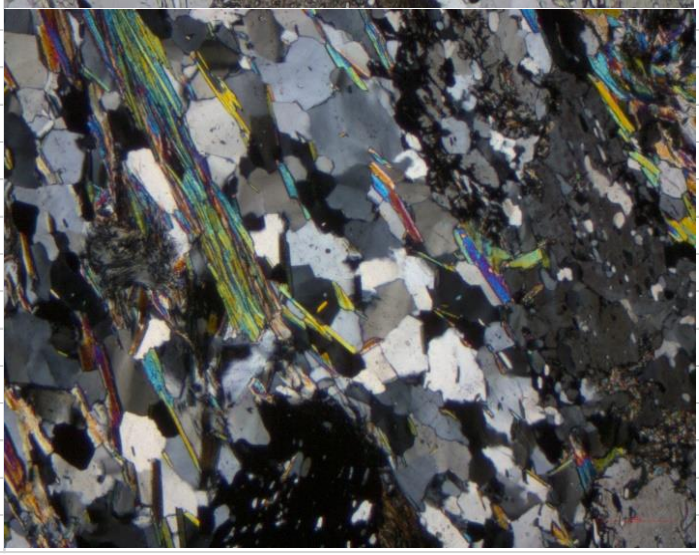

Thin section №	**JSH-17038**
Sample information	PYO-47, 317.86m: Footwall rhyolite 2
Rock name	Sericite schist
Main minerals	Quartz + muscovite ± andalusite
Accessory minerals	Biotite, rutile
Opaques	Pyrite ± chalcopyrite
Texture	Schistous, foliated
Mineral alteration	Propably hornfels - facies metamorphic grade, resulting andalusite and biotite
Hydrothermal alteration	Sericite is assumed to be a result of hydrothermal alteration
Comments	Most of the sample is composed of quartz, but it can be defined as sericite schist. It has been overprinted by andalusite and rare biotite alteration, possibly due to nearby intrusion?
Additional comments	Geochemical sample 8336949

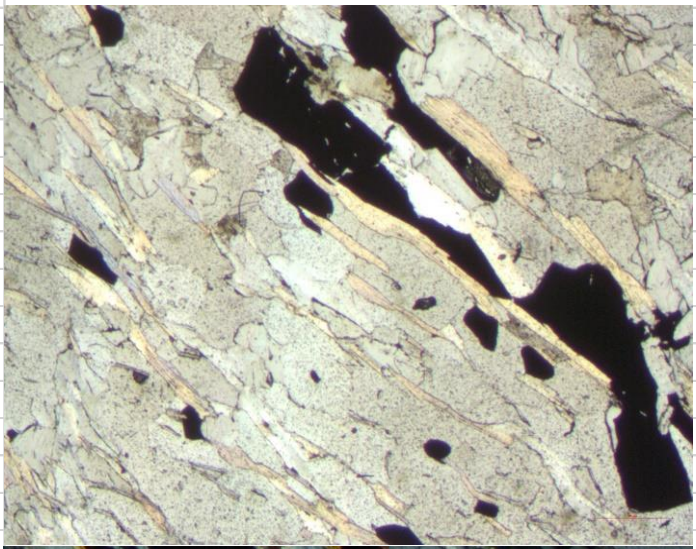

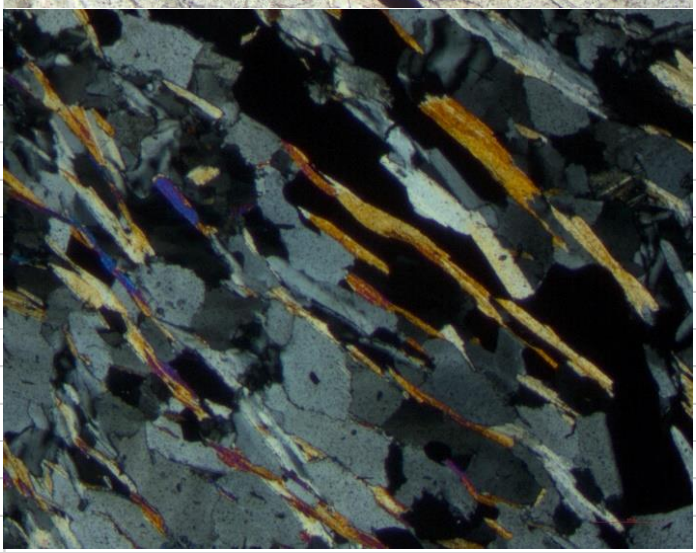

Thin section №	**JSH-17039**
Sample information	PYO-47, 331.21m: contact between sericite schist and mafic section
Rock name	Sericite - biotite - sillimanite schist
Main minerals	Quartz + biotite, muscovite, andalusite + plagioclase, feldspars (?)
Accessory minerals	Inclusions that are for the most part quartz and muscovite
Opaques	Pyrite ± chalcopyrite
Texture	Sericite and biotite-sillimanite schist veins, otherwise foliated, gneissic matrix
Mineral alteration	Micas -> sillimanite,
Hydrothermal alteration	Sericite alteration
Comments	In the middle of thin section, there is sericite and biotite-sillimanite veins, outside of which the matrix consists of quartz, andalusite + biotite + plagioclase, muscovite. In the matrix, there is this one common mineral that is colorless, pleochroic (white - yellowish), yellow interference color, positive uniaxial optical charecter and similiar relief to quartz. Assumption is made that this mineral is quartz with hightened maximum bireflectance. It seems that part of the thin section is not properly grinded to 30µm -> odd colors.
Additional comments	

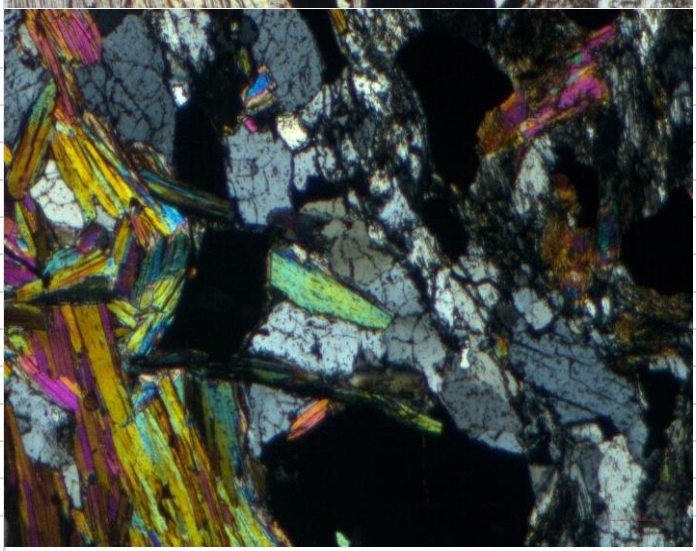

Thin section №	**JSH-17042**
Sample information	PYO-47, 358.47m: Massive sulfide
Rock name	Semimassive sulfide
Main minerals	Sulfides + kyanite, quartz, andalusite + carbonates
Accessory minerals	Rutile
Opaques	Pyrite ± chalcopyrite
Texture	Disseminated pyrite, weak foliation around opaques
Mineral alteration	Kyanite, andalusite
Hydrothermal alteration	Carbonates
Comments	Around 50% or more of the sample is sulfide, which is accompinied with rutile. The silicates and carbonates in between sulfide grains are fine-grained, where only kyanite is mostly subhedral and all the rest minerals are anhedral.
Additional comments	

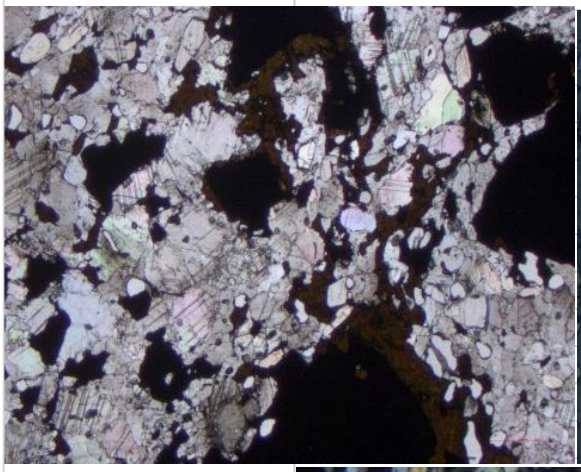

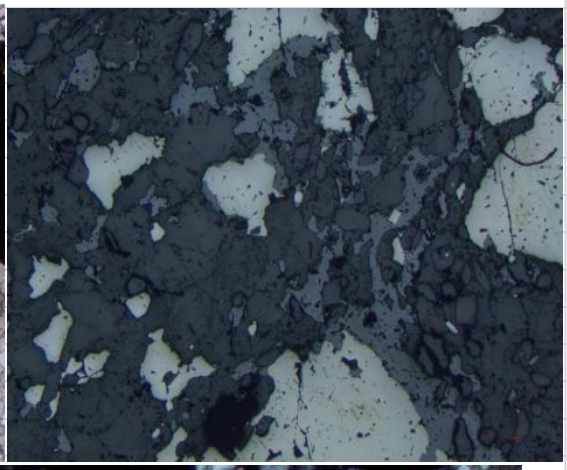

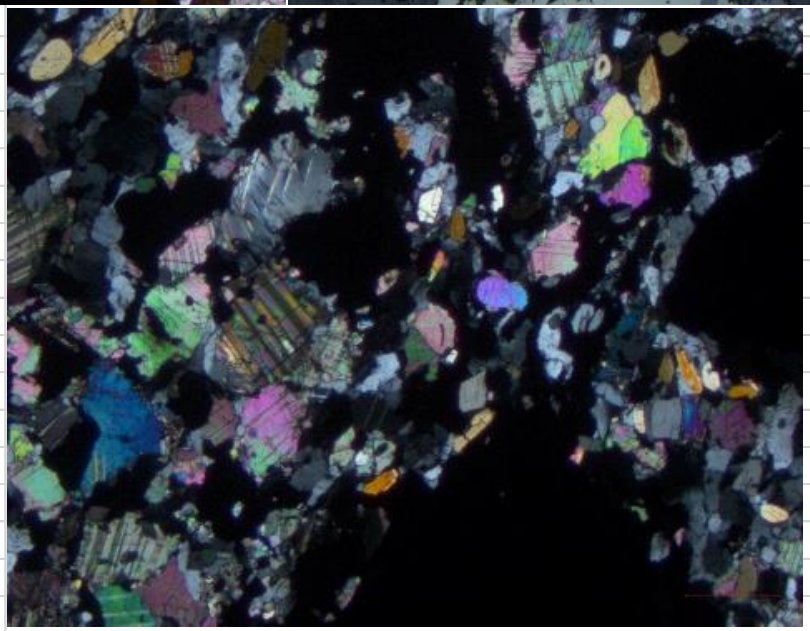

Thin section №	**JSH-17045**
Sample information	PYO-47, 405.08m: Biotite schist
Rock name	Cordierite-porphyroblastic biotite schist
Main minerals	Biotite, cordierite, quartz + clinochlore, andalusite, alkali feldspar ± plg
Accessory minerals	Sillimanite, granite, zircon, titanite
Opaques	Pyrite
Texture	Porphyroblastic schist, with some minor foliation
Mineral alteration	Cordierite, clinoclhore, andalusite, sillimanite
Hydrothermal alteration	Muscovite and chlorite alteration
Comments	According to drillcore logs and geochemical data, this sample should be a andesite intrusion that has not gone through hydrothermal alteration. However, it has been metamorphosed in greenschist facies, producing minerals such as cordierite, clinochlore, andalusite (?) and some sillimanite. It also has subjecte to weak chlorite alteration. Biotite is foliated around andalusite and metamorphosed into cordierite. Where biotite is not present, chlinochlore is. The sample also hosts some VMS related pyrite.
Additional comments	

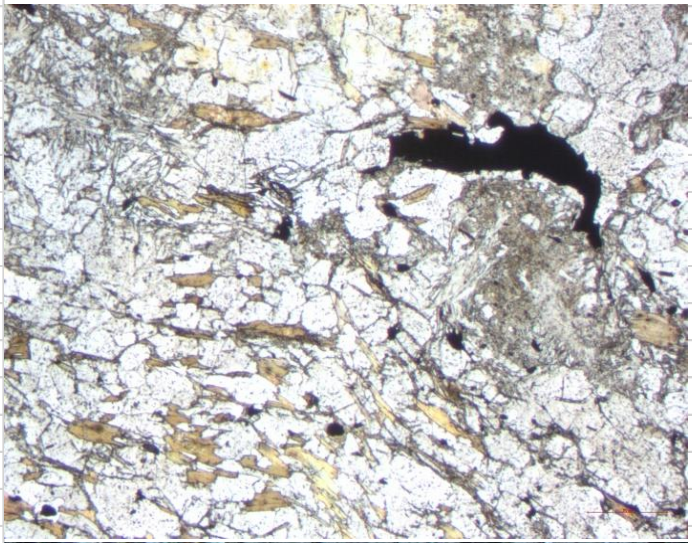

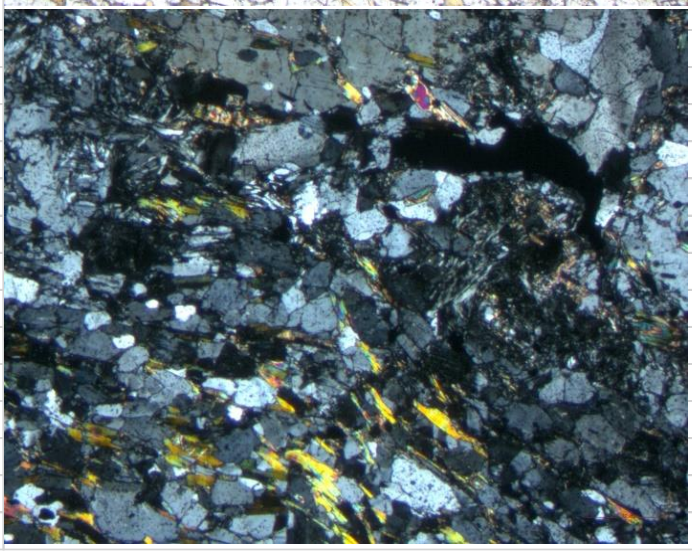

Thin section №	**JSH-17046**
Sample information	PYO-47, 418.13m: Sericite schist
Rock name	Sericite-biotite schist
Main minerals	Quartz + muscovite + biotite ± feldspars, plagioclase
Accessory minerals	Cordierite, apatite, rutile
Opaques	Pyrite
Texture	Foliated schist, porphyroblastic cordierite
Mineral alteration	Some cordierite crystallizations
Hydrothermal alteration	Moderate selective sericite alteration
Comments	Muscovite - biotite ratio is around 60:40. It is interesting how biotite appears everywhere with muscovite, which would indicate that sericite alteration was not complete and it was selective. There is more quartz than micas. Cordierite mineral are significantly larger than the rest, and they have all but mica minerals as inclusions. Mica minerals are foliated around them.
Additional comments	

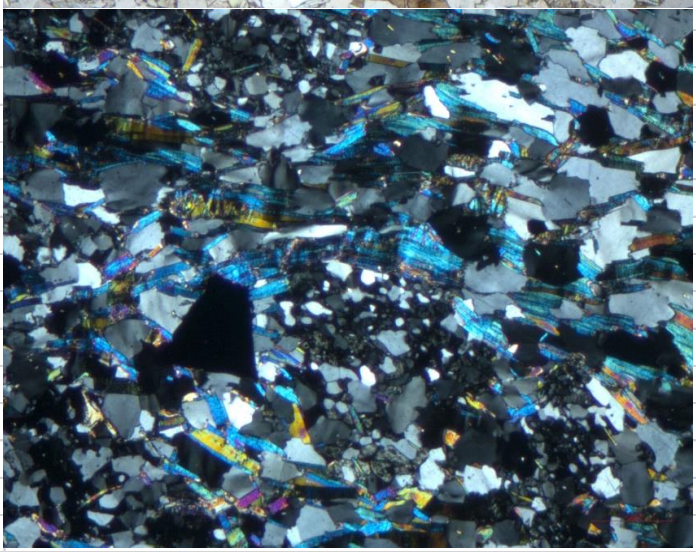

Thin section №	**JSH-17047**
Sample information	PYO-47, 411.33m: Rhyolite 2
Rock name	Amphibolite
Main minerals	Quartz + hornblende, biotite ± felspars, plagioclase
Accessory minerals	Muscovite, zoisite, garnet, titanite, gedrite
Opaques	A few %, probaply sulfides
Texture	Foliation
Mineral alteration	Possibly amphibolite facies
Hydrothermal alteration	All plagioclase and alkali feldspars are partially altered into muscovite, e.g. moderate selective sericite alteration
Comments	Selective weak sericite alteration. The sample is for the most part amphibolite (=30 vol% hornblende) and another small rock unit at bottom, which is biotite schist. Both has similiar lineation. Zoisite exhibits anomalous blue bireflectance and in one area where z axis is pointing up, gray bireflectance. The sample has several veins/fractures that has broken metamorphic zoisite, which have gray bireflectance color (z axis is pointing towards observer).
Additional comments	

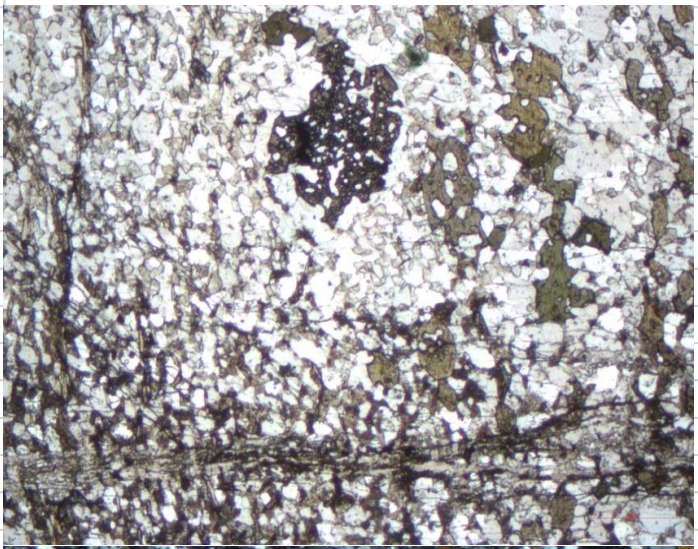

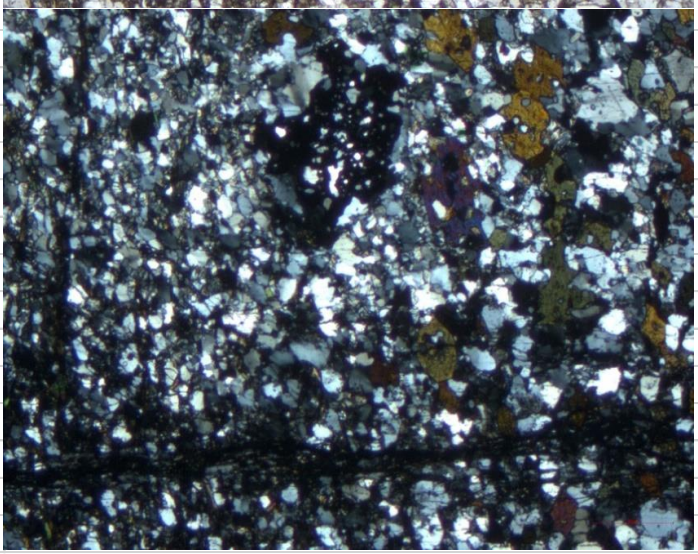

Thin section №	**JSH-17048**
Sample information	PYO-84, 99m: Rhyolite 1
Rock name	Rhyolite
Main minerals	Quartz + biotite ± feldspar
Accessory minerals	Muscovite, epidote (?)
Opaques	-
Texture	Foliated
Mineral alteration	Minor alteration from biotite to muscovite / epidote
Hydrothermal alteration	-
Comments	Foliated fine-grained rhyolite. There is some spots where quartz has formed bigger crystals than matrix, propably quartz veins. Biotite is the only euhedral mineral. Epidote might be something else, invidual mineral are too small to be sure.
Additional comments	

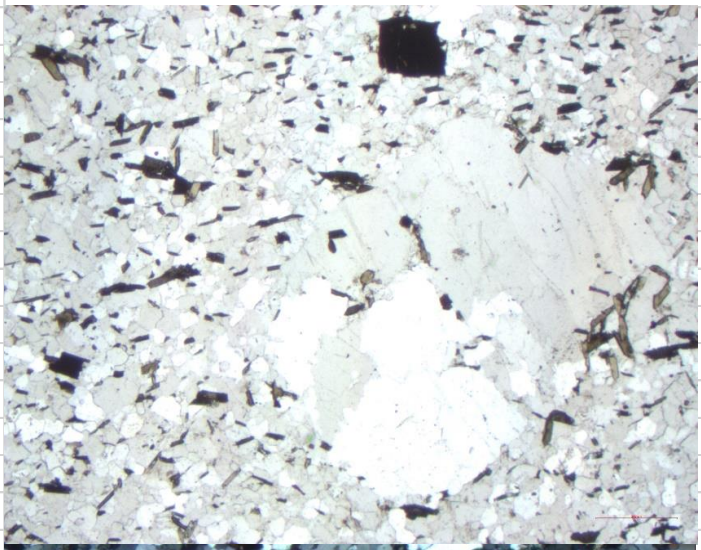

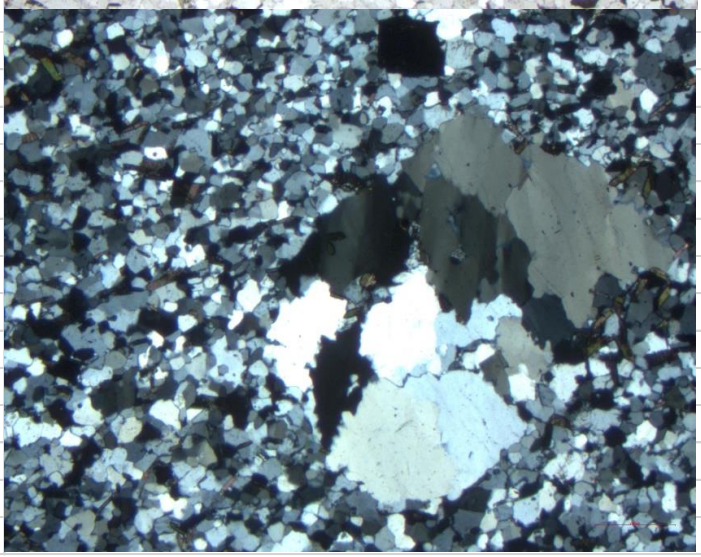

Thin section №	**JSH-17050**
Sample information	PYO-84, 146.17m: Rhyolite with red alteration
Rock name	Rhyolite
Main minerals	Quartz + microcline + hornblende ± plagioclase (Ab>90)
Accessory minerals	Titanite, rutile, biotite, epidote (?), vuggy quartz
Opaques	None
Texture	Fine-grained
Mineral alteration	Hornblende
Hydrothermal alteration	Some rare vuggy quartz, where presumeably alkali feldspar has altered to quartz which is vuggy due to rutile residue.
Comments	This sample has a more feldspars than JSH-17048, but can still be classified as rhyolite (even if it has been completely metamorphosed). Instead of biotite, this sample hosts hornblende, which is only rarely altered to epidote (?) and biotite. Hornblende also hosts quartz inclusions. This sample was originally selected because the hand sample had red tint in an area where hornblende grains are sparse. That area does not have anything anomalous, other that possibly marginally increased feldspar content.
Additional comments	

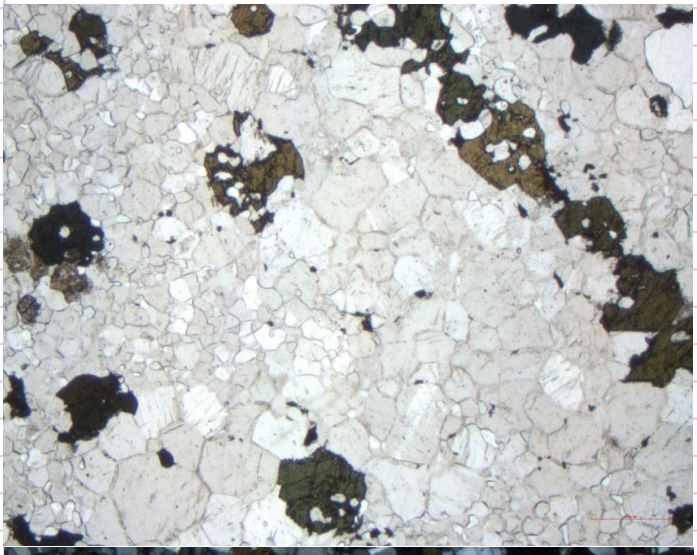

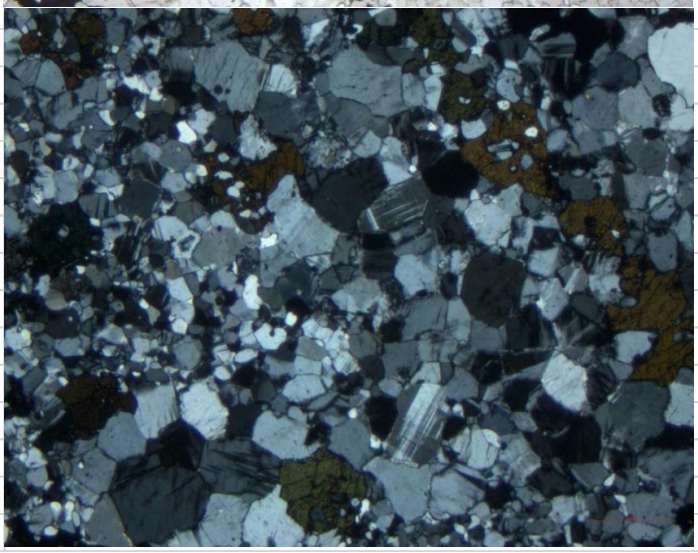

Thin section №	**JSH-17051**
Sample information	PYO-84, 187.09m: Basalt andesite
Rock name	Amphibolite
Main minerals	Quartz, hornblende + biotite ± feldspar, plagioclase
Accessory minerals	Epidote (?), muscovite
Opaques	Pyrite (referring to hand sample identification)
Texture	Foliation, fine-grained
Mineral alteration	Biotite has partly altered to fibrous sillimanite
Hydrothermal alteration	Selective minor alteration from alkali feldspars and plagioclase to muscovite
Comments	This sample was selected to see if there was any clues for protolith idenitification in the quartz nuclei. In thin section, the innermost part is large grained quartz (where one has pyrite as core), and then smaller grained anhedral quartz and some alkali feldspars and plagioclase. The nuclei has completely recrystallized, leaving no textures but only some zonation of elements.
Additional comments	

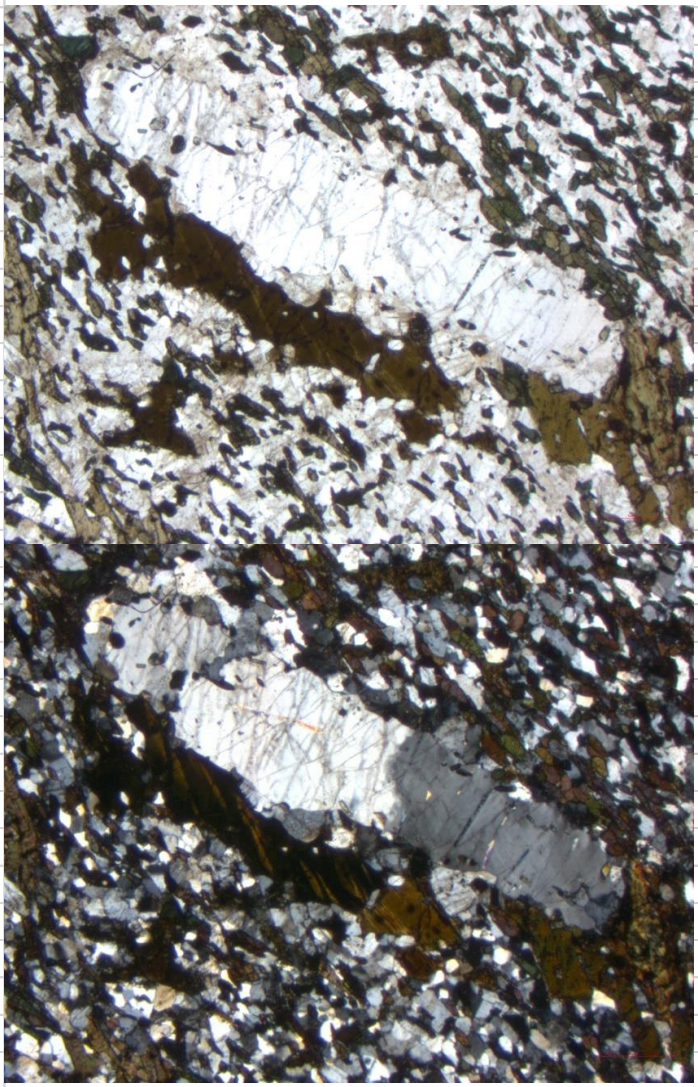

Thin section №	**JSH-17053 Amphibolite**
Sample information	PYO-84, 254.85m: Contact between mafic and felsic unit
Rock name	Amphibolite section
Main minerals	Hornblende + quartz + plagioclase, feldspar
Accessory minerals	Biotite, apatite
Opaques	Pyrite + chalcopyrite
Texture	Foliation
Mineral alteration	-
Hydrothermal alteration	Small vein, where hydrothermal alteration is apparent in small areas (sericite and others)
Comments	Hornblende appears to be euhedral and larger than other minerals. It has some small inclusions, which appear to be apatite in part. The contact between felsic rock unit is constructed of large felsic minerals and some hornblende.
Additional comments	

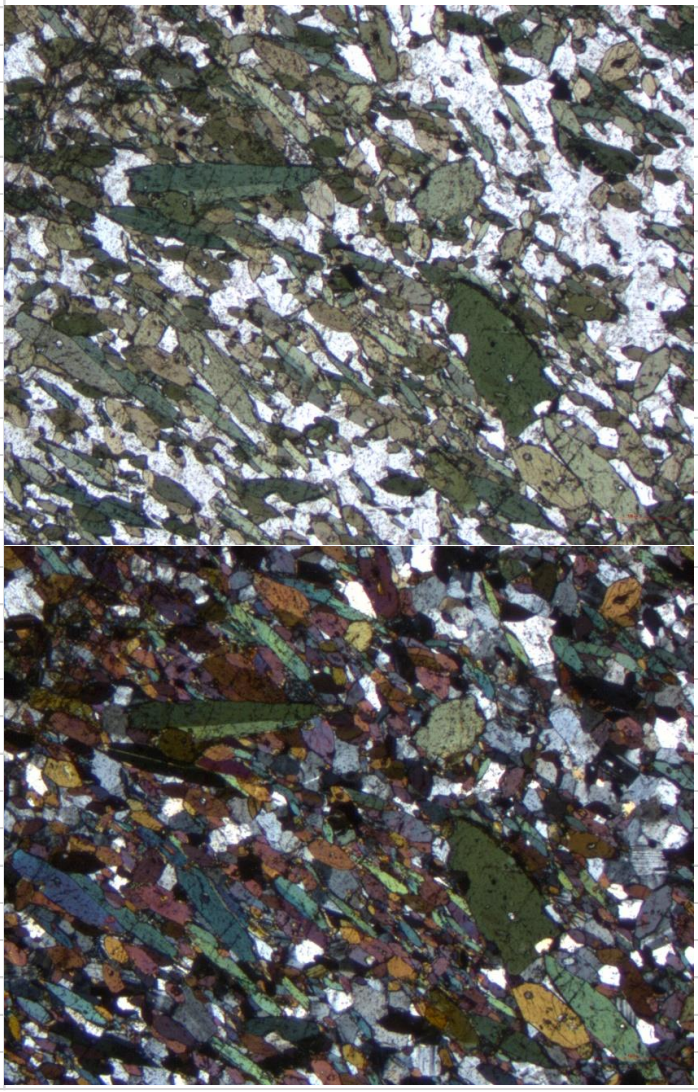

Thin section №	**JSH-17053 Rhyolite**
Sample information	PYO-84, 254.85m: Contact between mafic and felsic unit
Rock name	Rhyolite section
Main minerals	Quartz ± biotite, plagioclase, microcline (?)
Accessory minerals	Hornblende, rutile
Opaques	Pyrite + chalcopyrite
Texture	Fine-grained, gneissic texture
Mineral alteration	Quartz recrystallization
Hydrothermal alteration	-
Comments	The boundary between rhyolitic and ambibolitic hosts has the same mineral composition as the rest of rhyolite section with addition of some hornblende and opaques. The minerals in this boundary are large. Most of mineral in rhyolite section host small inclusions, most of which are too small for identification.
Additional comments	

Thin section №	**JSH-17054**
Sample information	PYO-84, 272.83m: Basaltic andesite
Rock name	Porphyroblastic hornblende - biotite schist
Main minerals	Hornblende, biotite + plagioclase, alkali feldspars ± quartz
Accessory minerals	Muscovite, chlorite, apatite, zircon
Opaques	Some opaques
Texture	Foliated with pressure shadows around porphyroblasts, sheared
Mineral alteration	-
Hydrothermal alteration	Some weak sericite alteration in white minerals, small fractures that have worked as fluid conduits.
Comments	Porphyroblasts are constructed of recrystrallized large felsic minerals: feldspars, plagioclase and some quartz. One of the largest porphyroblasts has linear small micas oriented along the porphyroblasts 100 and 010 surfaces. The crystal itself is oriented along the general foliation in longitudal axis. There are several explanations to how these porphyrobasts formed (vesicle infill, partial melting, xenocryst, etc.) but there is no obious clues to parent rock.
Additional comments	

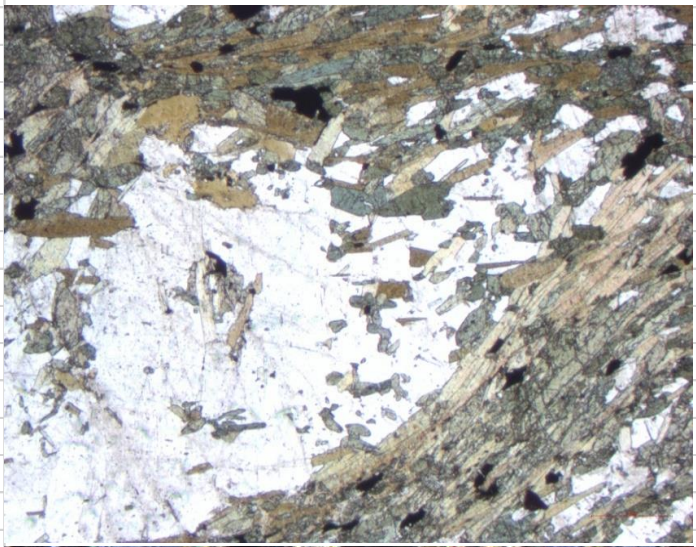

Thin section №	**JSH-17055**
Sample information	PYO-84, 319.5m: Rhyolite with weak sericite alteration
Rock name	Rhyolite
Main minerals	Quartz + microcline, plagioclase ± biotite
Accessory minerals	Muscovite, clinozoisite, garnet
Opaques	Sulfides
Texture	Micas have somewhat foliated, gneissic texture
Mineral alteration	Quartz recrystallized
Hydrothermal alteration	Weak sericite alteration in some locations
Comments	This is excatly what was presumed from hand-sample: rhyolite with wak sericite alteration. In addition to that, there has been some quartz recrystallization since there are some larger quartz grains that have smaller quartz and other minerals as inclusions.
Additional comments	

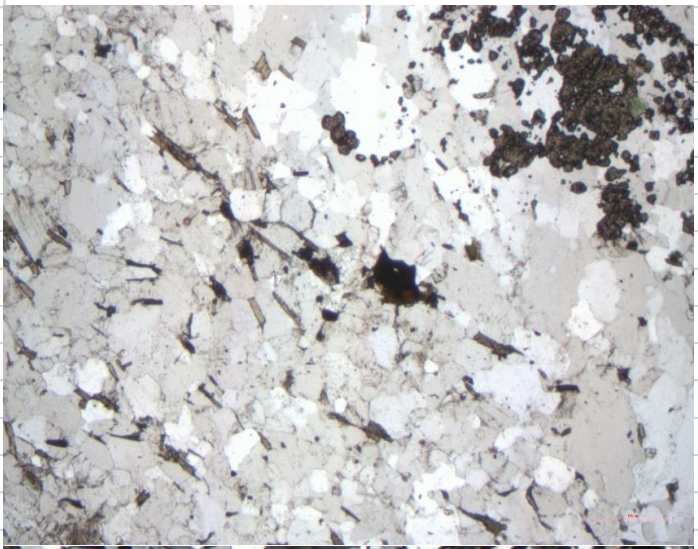

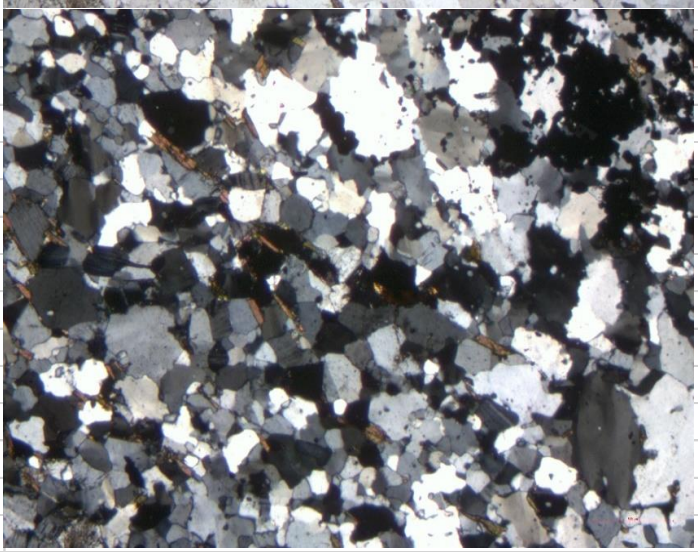

Thin section №	**JSH-17058**
Sample information	PYO-84, 380.14m: Rhyolite with clasts
Rock name	Rhyolite
Main minerals	Quartz + hornblende ± feldspar, plagioclase, biotite
Accessory minerals	Muscovite, rutile
Opaques	Pyrite + chalcopyrite
Texture	Fine-grained, weakly foliated hornblende
Mineral alteration	Some odd-looking hornblende crystallised due to metamorphism?
Hydrothermal alteration	Weak sericite alteration in felspars
Comments	There are some areas where hornblende is absent and quartz grains are larger. In between those areas hornblende has concentrated and foliated.
Additional comments	

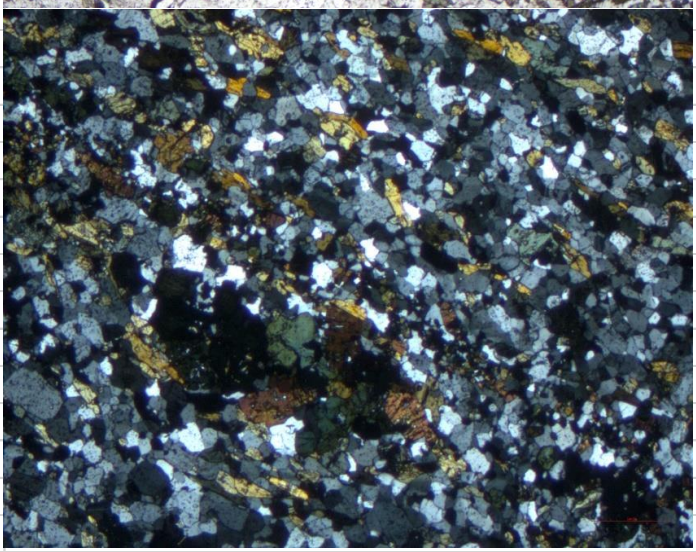

Thin section №	**JSH-17062**
Sample information	PYO-84, 423.82m: Sericite altered rhyolite
Rock name	Pyrite strings in rhyolite
Main minerals	Quartz + feldspar, plagioclase, biotite
Accessory minerals	Andalusite (?), zirkon, zoisite, rutile
Opaques	Pyrite + pyrrhotite, chalcopyrite
Texture	Strings of pyrite, foliated micas along the direction of pyrite veins.
Mineral alteration	Possibly some andalusite.
Hydrothermal alteration	Phyllic alteration which mainly produced quartz and pyrite
Comments	Quartz - pyrite veins are concordant with biotite orientation, e.g. concordant with lowest pressure axis.
Additional comments	

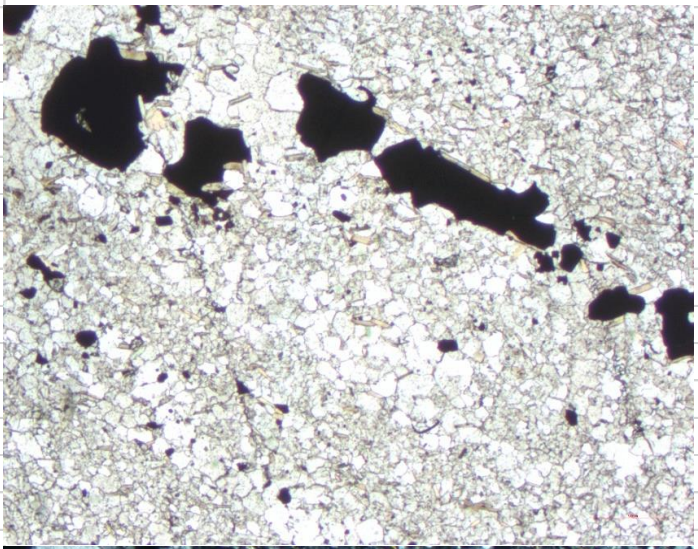

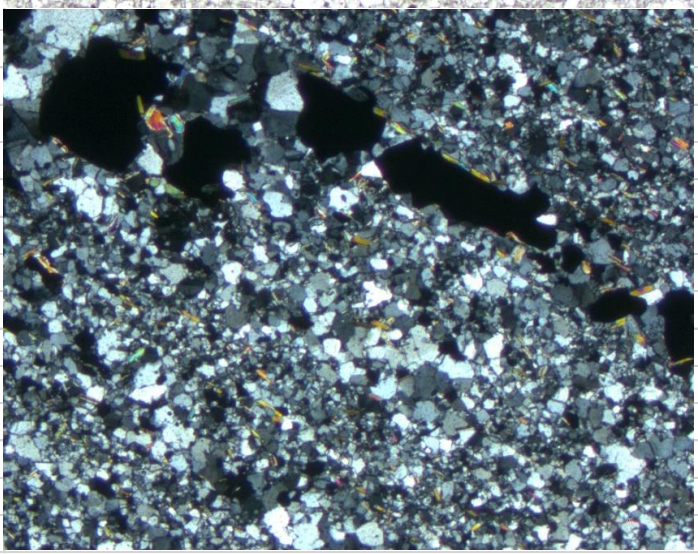

Thin section №	**JSH-17063**
Sample information	PYO-84, 424.28m: Sericite schist
Rock name	Sericite schist
Main minerals	Sericite + quartz ± biotite, feldspar, plagioclase
Accessory minerals	Nefeline (?), rutile
Opaques	Pyrite + pyrrhotite ± chalcopyrite
Texture	Strongly foliated
Mineral alteration	Nefeline (?)
Hydrothermal alteration	Moderate to strong sericite alteration + sulfides
Comments	Strongly foliated with sericite and some biotite. Matrix is composed by unaltered fine-grained white minerals. Quartz - sulfide veins appear concordant to general foliation. These veins also host most of the rutile present and a mineral that has similiar properties to nefeline (colorless, uniaxial, negative, max bireflectance is between 0.009-0.012, high relief). Opaque grains are either composed of pyrite or pyrrhotite that also hosts chalcopyrite.
Additional comments	

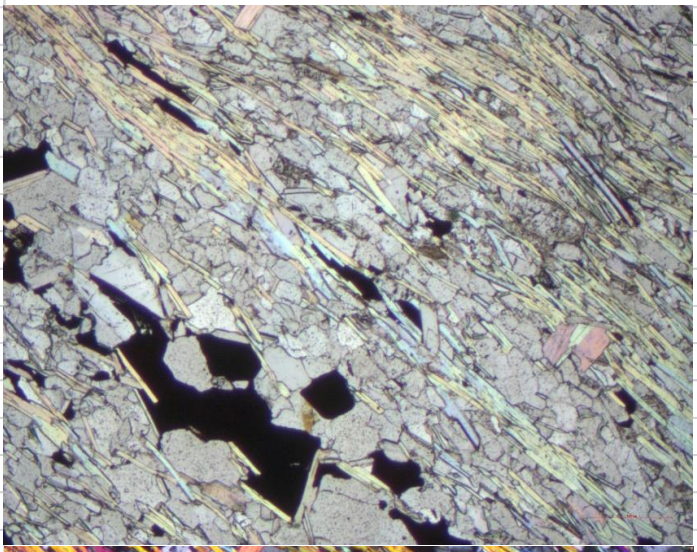

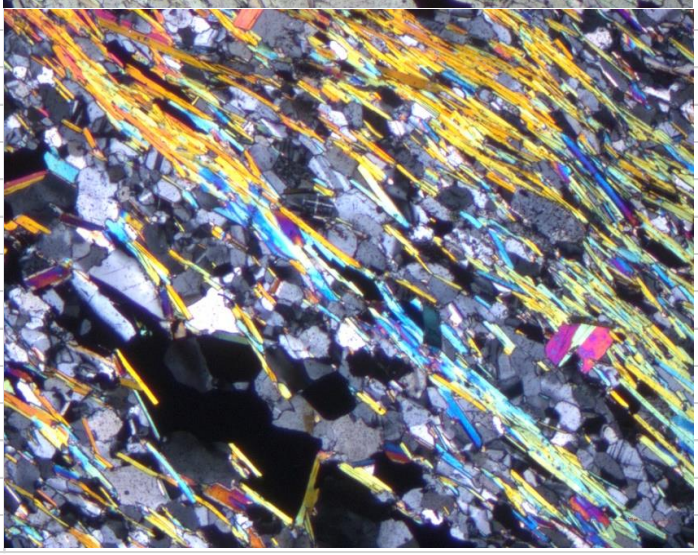

Thin section №	**JSH-17064**
Sample information	PYO-84, 440.6m: Matrix section
Rock name	Rhyolite
Main minerals	Quartz + feldspar group minerals ± biotite, plagioclase
Accessory minerals	Muscovite, rutile
Opaques	Pyrite
Texture	Moderately foliated, fine-grained, gneissic texture
Mineral alteration	-
Hydrothermal alteration	Weak sericite alteration
Comments	This sample has two different kinds of rock units in it: a section of quartz - pyrite vein and fine-grained matrix. The fine-grained matrix can be classified as rhyolite that hosts minor disseminated pyrite. Feldspars are somewhat abundat when compared to other sericite zone samples, and appear as orthoclase and microcline. None of them exhibit any obvious alteration.
Additional comments	

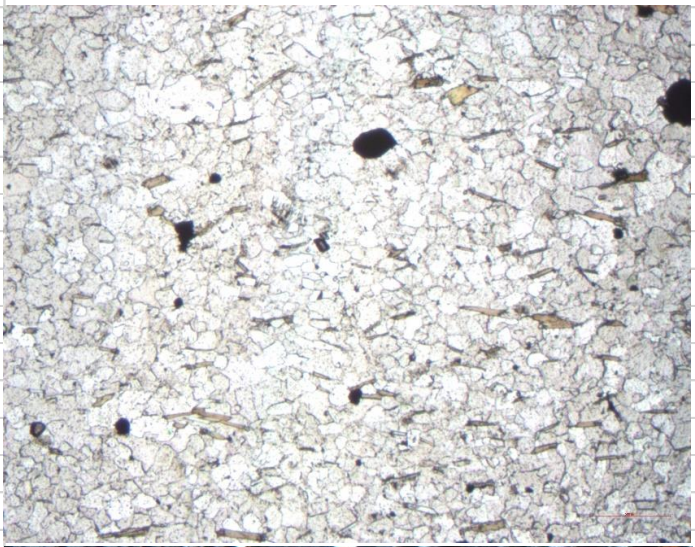

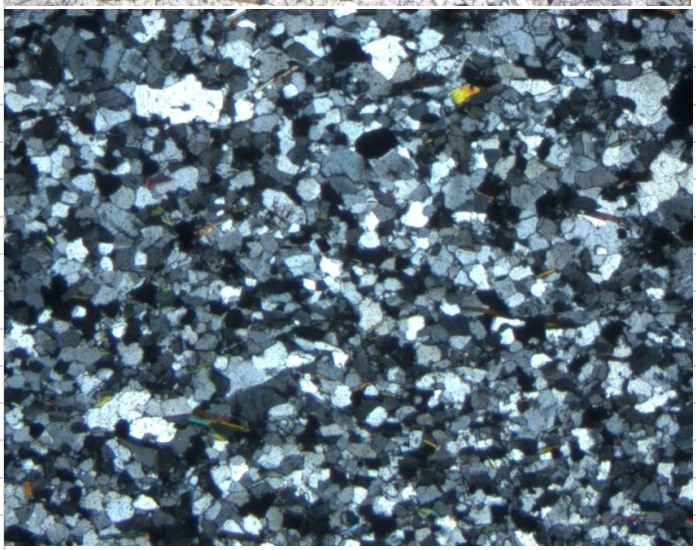

Thin section №	**JSH-17064**
Sample information	PYO-84, 440.6m: Pyrite vein
Rock name	Sericite schist + pyrite veins
Main minerals	Quartz + feldspar group minerals + muscovite, biotite
Accessory minerals	Rutile
Opaques	Pyrite
Texture	Moderate foliation, quartz - pyrite veins
Mineral alteration	-
Hydrothermal alteration	Moderate sericite alteration
Comments	This thin section has two different rock units: Pyrite vein and matrix. In comparison to matrix, pyrite vein section has larger grains in average and less plagioclase. Also, feldspar group minerals are weakly altered to sericite, whereas they were not in the matrix section. Plagioclase is absent. Micas are for the most part constructed of muscovite and some biotite. >15 vol% of the pyrite vein section is composed of pyrite. Pyrite stringers are concordant to general foliation.
Additional comments	

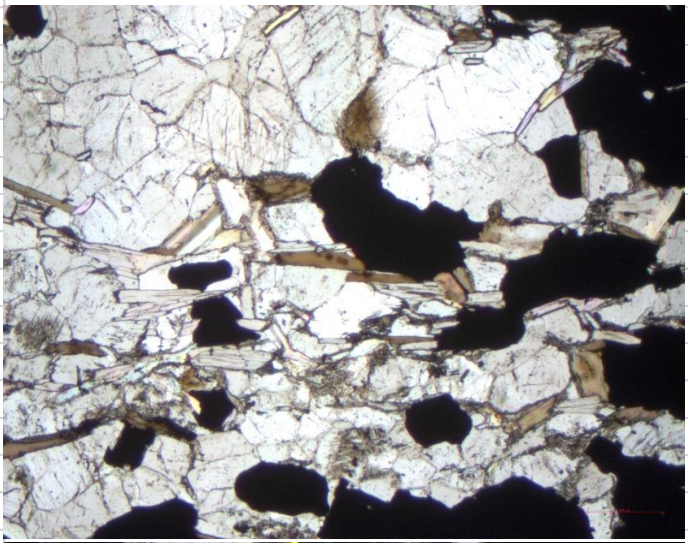

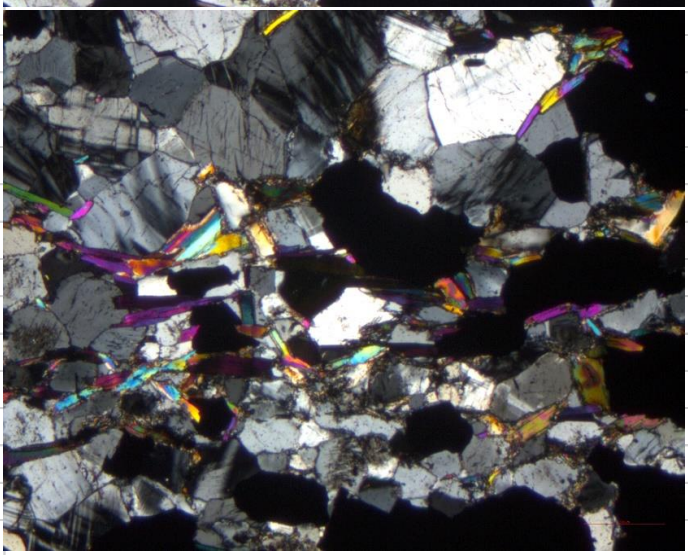

Thin section №	**JSH-17067**
Sample information	PYO-84, 481.55m: Mafic unit within sericite zone
Rock name	Biotite schist
Main minerals	Biotite ± quartz, plagioclase
Accessory minerals	Garnet, carbonates
Opaques	Pyrite, pyrrhotite ± chalcopyrite, rutile
Texture	Foliated and sheared
Mineral alteration	Garnet
Hydrothermal alteration	-
Comments	Biotite dominated sample. There are random quartz - pyrite veins that do not exhibit any alteration haloes. Granulite has clearly crystallized after foliation happened, since granulite grains do not appear to have any effect on foliation and they cut biotite grains. Granulite grains have biotite and pyrite as inclusion. Carbonates are rare, and one of them appear to be an inclusion in unidentified silicate which is cutting surrounfing biotite. The matrix is composed of quartz and plagioclase, where most of the plagioclase has been sligthly altered.
Additional comments	

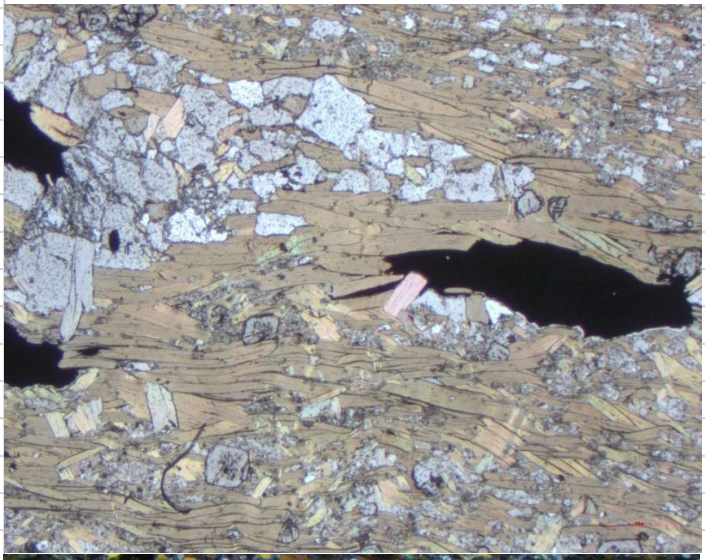

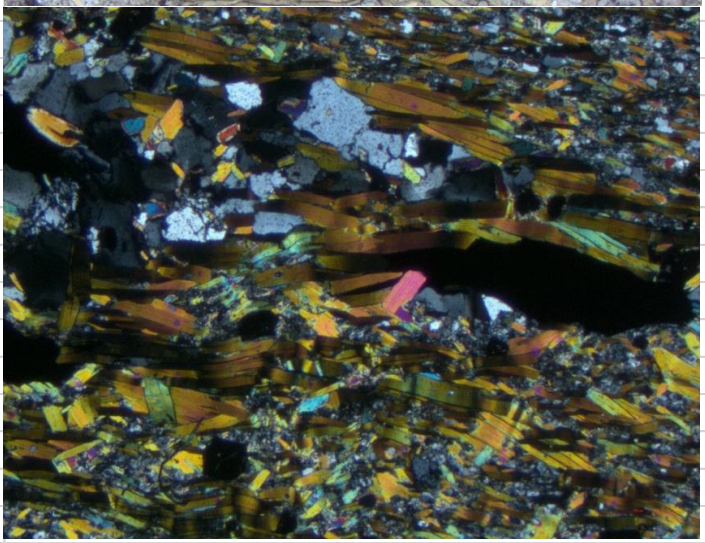

Thin section №	**JSH-17071**
Sample information	R-2394, 0.46-0.65m: Felsic hanging-wall
Rock name	Felsic gneiss
Main minerals	Quartz, feldspars ± chlorite, plagioclase, muscovite
Accessory minerals	Garnet, carbonate, epidote, rutile
Opaques	Opaques, not polished
Texture	Foliated, recrystallized, metamorphosed, grain size varies, gneissic
Mineral alteration	Chlorite and epidote appear near biotite
Hydrothermal alteration	-
Comments	Clearly foliated gneissic rock. There are several sections where the texture is fine-grained and apparently recrystallized due to increased pressure. There are pressure marks in quartz crystals. All primary textures are destroyed.
Additional comments	

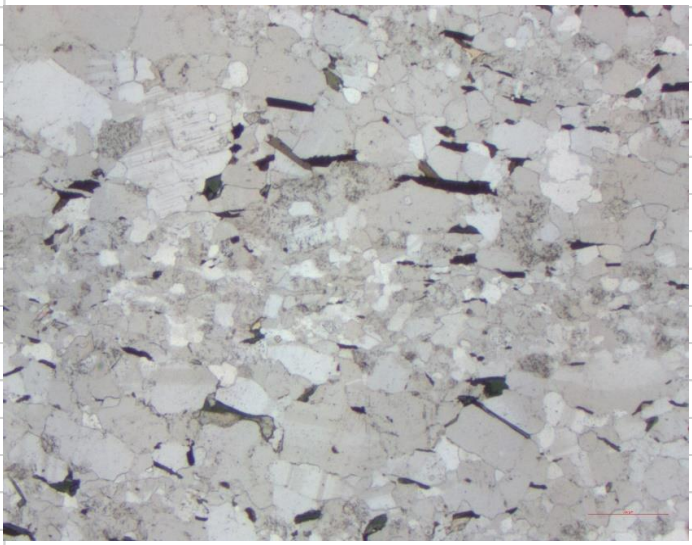

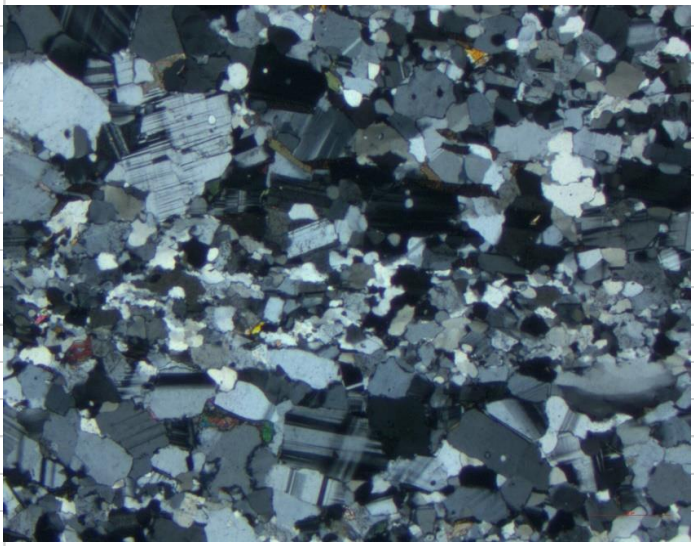

Thin section №	**JSH-17072**
Sample information	R-2394, 8.02-8.21: Mafic hanging-wall
Rock name	Ambhibolite
Main minerals	Hornblende + quartz, plagioclase ± biotite
Accessory minerals	Hastingsite, zirkon,
Opaques	Opaques, not polished
Texture	Foliated
Mineral alteration	Hastingsite, biotite
Hydrothermal alteration	-
Comments	Foliated, mostly euhedral hornblende. Hastingsite appears as zoned metamorphosed rock, dark brownish green color when compared to hornblende. It has quartz, hornblende and apatite (?) as inclusions, forming subhedral minerals.
Additional comments	

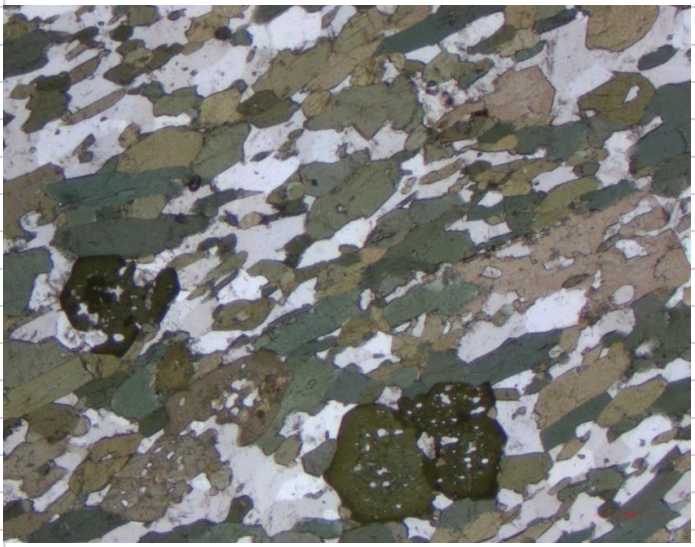

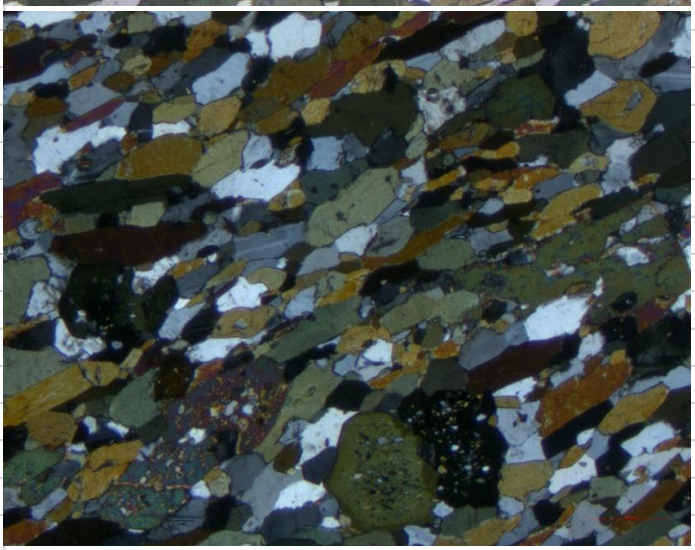

Thin section №	**JSH-17080**
Sample information	R-2394, 85-85.21m: Porphyroblastic mafic intrusion
Rock name	Metagabbro
Main minerals	Plagioclase, hornblende, biotite ± feldspars
Accessory minerals	Chlorite, muscovite
Opaques	Opaques, not polished
Texture	Conglomerates of anhedral dark minerals, large plg crystals in between.
Mineral alteration	Biotite to chlorite and muscovite, sligth breakdown of plagioclase
Hydrothermal alteration	-
Comments	According to hornblende zonation, the hornblende began to mineralize as ferro-hornblende and later as magnesio-hornblende. Plagioclase albite content is 15% or less. Porphyroblastic texture in hand sample is the result of a microscopic conglomeration of biotite and hornblende. These minerals appear as anhedral large crystal in the middle of conglomerates and as small euhedral crystals at the outer edge. Darker minerals also occur as small euhedral inclusons in large plagioclase crystals and other white minerals.
Additional comments	

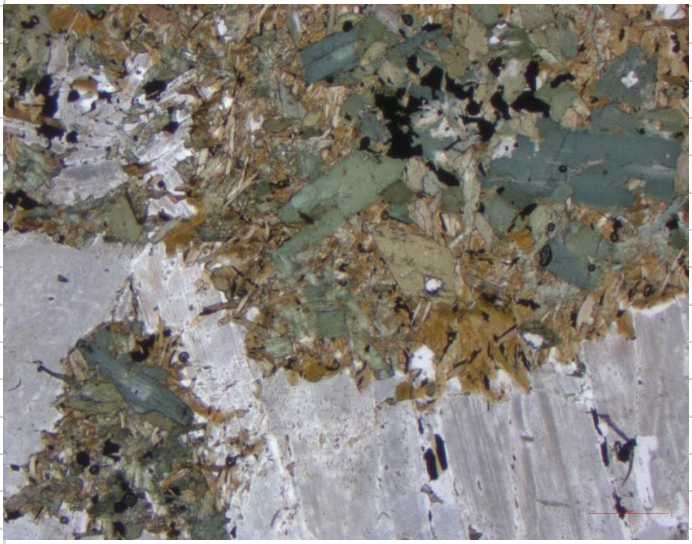

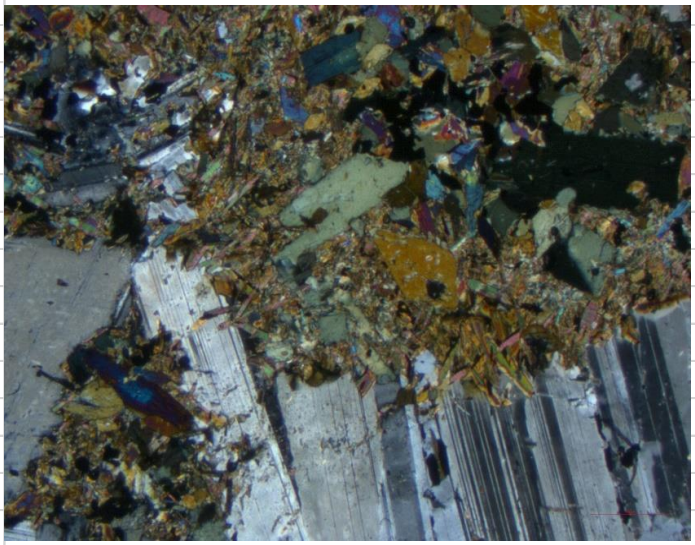

Thin section №	**JSH-17082**
Sample information	R-2394, 151.15-151.3m: Felsic intrusion into massive sulfide
Rock name	?
Main minerals	(?) , biotite
Accessory minerals	Rutile
Opaques	Pyrrhotite, chalcopyrite + pyrite
Texture	Fine-grained
Mineral alteration	?
Hydrothermal alteration	?
Comments	Subhedral biotite crystals are the larges minerals in thin sample. Most of the fine-grained subhedral matrix is unidentified. Colorless, no pleochroism, bireflectance = 0.039, 2V=90, optical nature = propably -. Sulfides are mostly disseminated auhedral pyrite, subhedral pyrrhotite and anhedral chalcopyrite. Based on the MgO content (21%), the matrix could be amphibole minerals.
Additional comments	Immobile element ratio indicates that this was originally rhyolite.

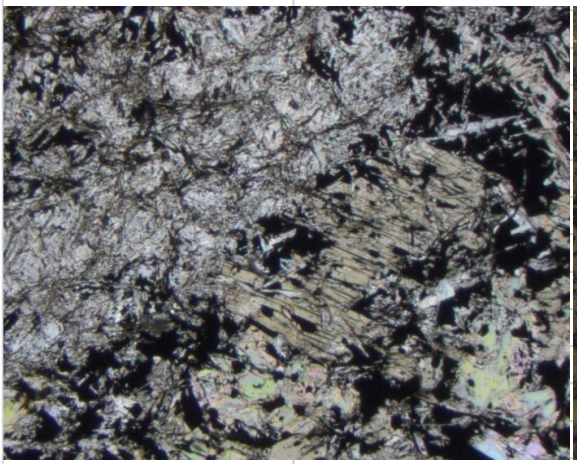

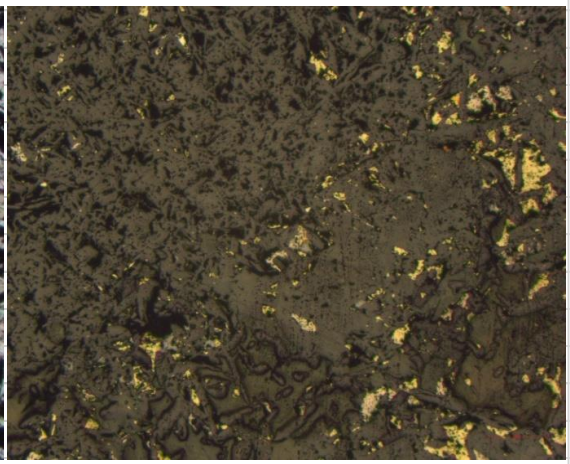

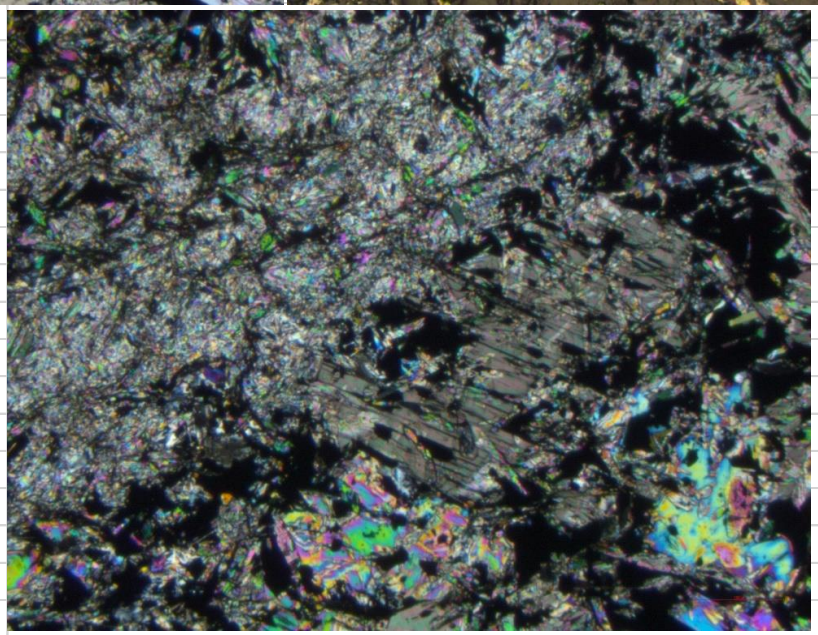

Thin section №	**JSH-17091**
Sample information	R-2394, 68.72-68.9m: Near pegmatite intrusion
Rock name	Foliated felsic gneiss
Main minerals	Quartz, feldspars + biotite, plagioclase, andalusite
Accessory minerals	Zircon
Opaques	Pyrite + pyrrhotite ± rutile
Texture	Moderately foliated
Mineral alteration	-
Hydrothermal alteration	-
Comments	Subhedral foliated bioite, where all the matrix is composed of white anhedral minerals. The amount of andalusite is hard to measure, since they are most reliably identified by optic axis figure.
Additional comments	

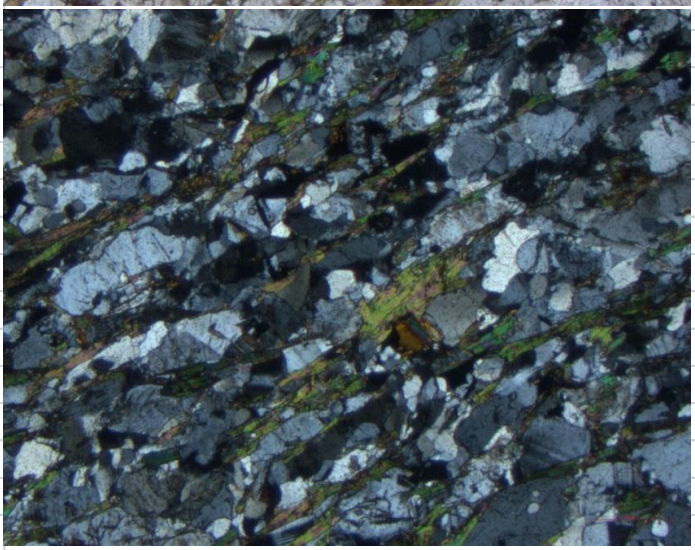

Thin section №	**JSH-17093 Amphibolite**
Sample information	R-2394, 83.57-83.77m: Mafic section
Rock name	Ambpibolite
Main minerals	Quartz, hornblende + plagioclasce, biotite ± unidentified amphibole
Accessory minerals	Titanite, andalusite, chlorite, muscovite
Opaques	-
Texture	Weakly foliated
Mineral alteration	Unidentified amphibolite from biotite
Hydrothermal alteration	Weak alteration of plagioclase to muscovite
Comments	This sample has two kinds of rock in it: amphibolite and felsic gneiss. Amphibolite is described for the most part above. The boundary in between amphibolite and felsic gneiss has a distinct increace of epidote and in general increace in white minerals grain size.
Additional comments	

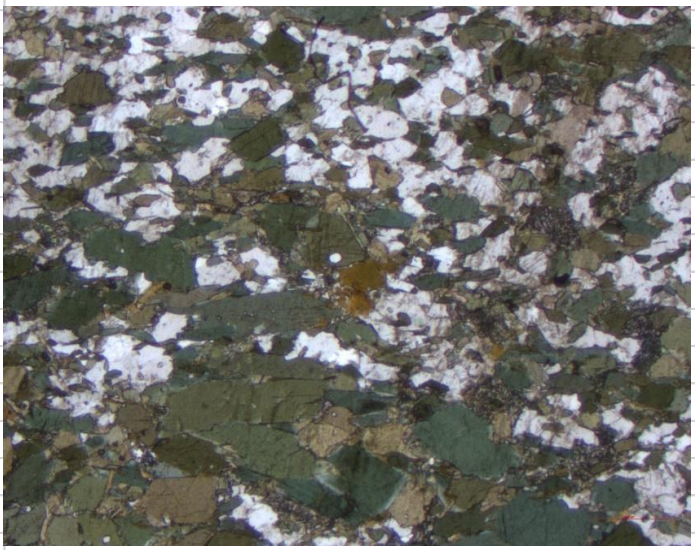

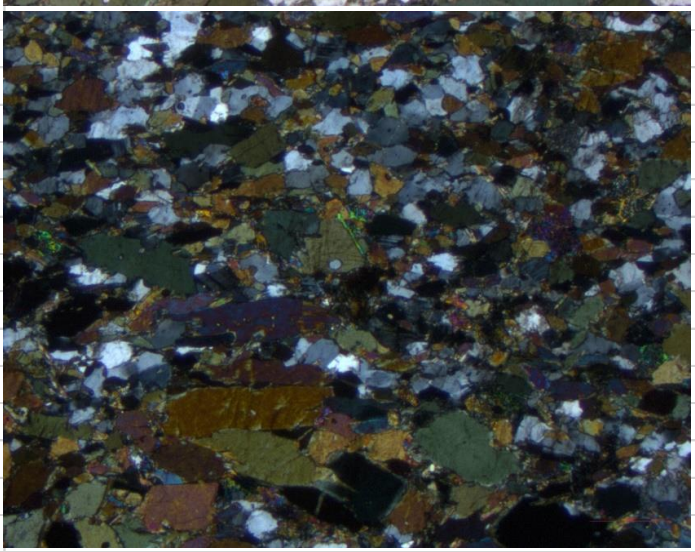

Thin section №	**JSH-17093 Felsic gneiss**
Sample information	R-2394, 83.57-83.77m: Metamorphosed felsic rock
Rock name	Felsic gneiss
Main minerals	Quartz + plagioclase, biotite ± unidentified amphibole
Accessory minerals	Carbonate, titanite
Opaques	-
Texture	Moderately foliated
Mineral alteration	Unidentified amphiboles as metamorphic minerals
Hydrothermal alteration	-
Comments	Moderately foliated felsic gneiss. Some of the biotite has metamorphosed into biaxial amphibolite (2V=90, bireflectance is around 0,023 and 0,028). All of the metamoprhic minerals are too small to reliable identification. Could be tremolite, cummingtonite and / or anthopyllite.
Additional comments	Geochemical analysis is made from this felsic section

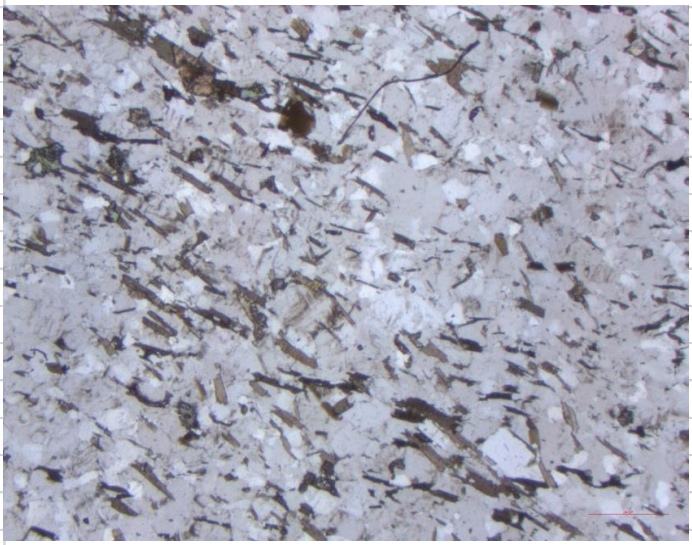

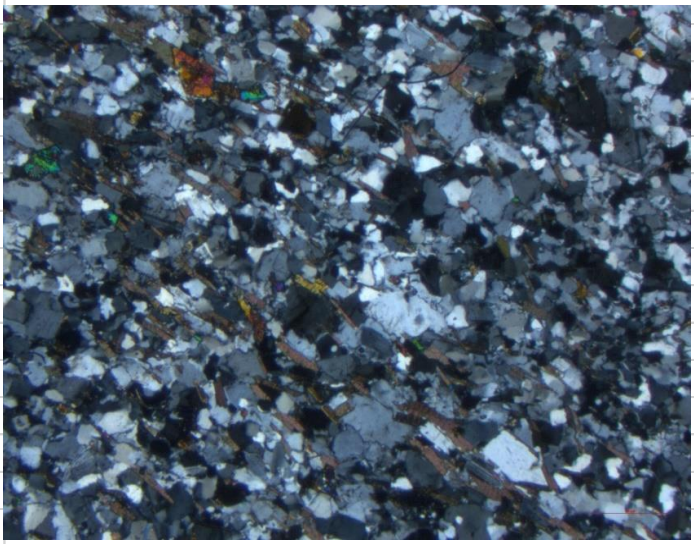

Thin section №	**JSH-17096**
Sample information	R-2394, 96.72-96.92m: Aphanitic mafic rock
Rock name	Biotite amphibolite
Main minerals	Hornblende, biotite + feldspar, andalusite ± plagioclase
Accessory minerals	Titanite, apatite, muscovite, unidentified amphibolite
Opaques	Opaques, not polished
Texture	Moderately foliated
Mineral alteration	Metamorphic unidentified amphibole, andalusite
Hydrothermal alteration	Some plagioclase has altered to muscovite along fluid veins. Biotite has also altered sparsely to muscovite.
Comments	Moderately foliated biotite amphibolite. Cutting across the foliation is a couple of fluid veins that are accompanied by weak sericite alteration. Most of the white minerals in matrix are biaxial, but only have rare or weak twinning texture that is associated plagioclase and feldspars, and so the identification methods are restricted to interpretation of optical nature and 2V. There may be some quartz in the sample, but none was found.
Additional comments	

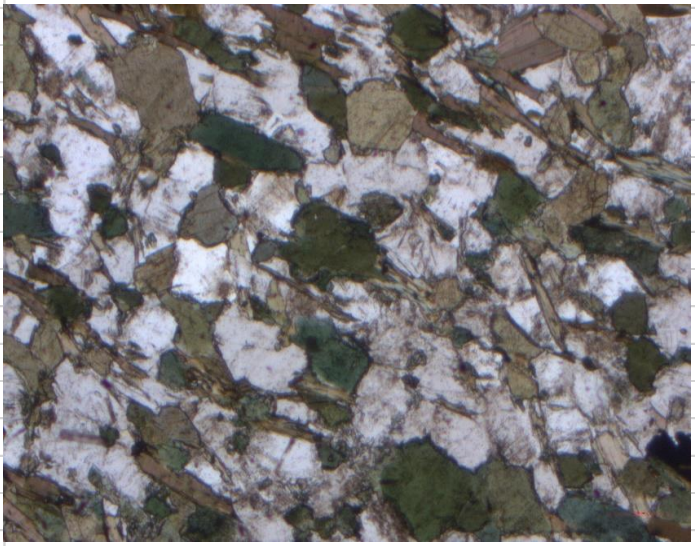

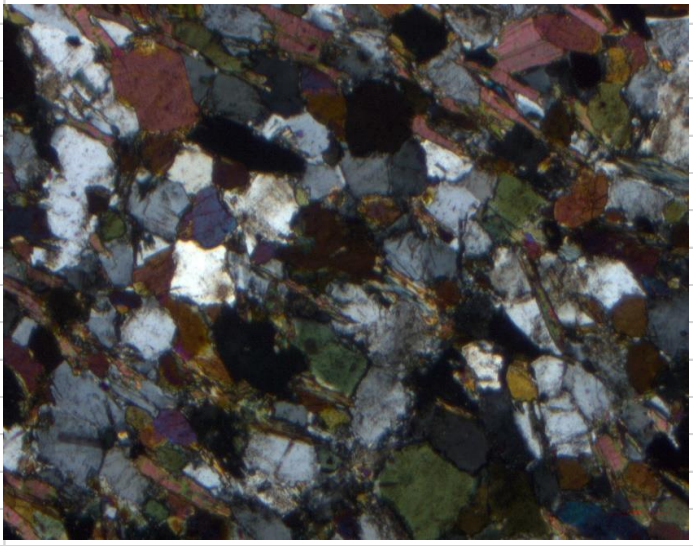

Thin section №	**JSH-17100**
Sample information	R-2394, 120.05-120.25m: Metamorphosed felsic rock
Rock name	Felsic gneiss
Main minerals	Quartz + feldspars, plagioclase ± biotite, epidote
Accessory minerals	Kyanite
Opaques	Opaques
Texture	Gneissic texture
Mineral alteration	Kyanite and epidote from biotite
Hydrothermal alteration	-
Comments	Epidote is only weakly greenish in color, and it is possible that some of those yellowish birefectance minerals that have similiar relief as epidote, is kyanite since there is some twinning observable.
Additional comments	

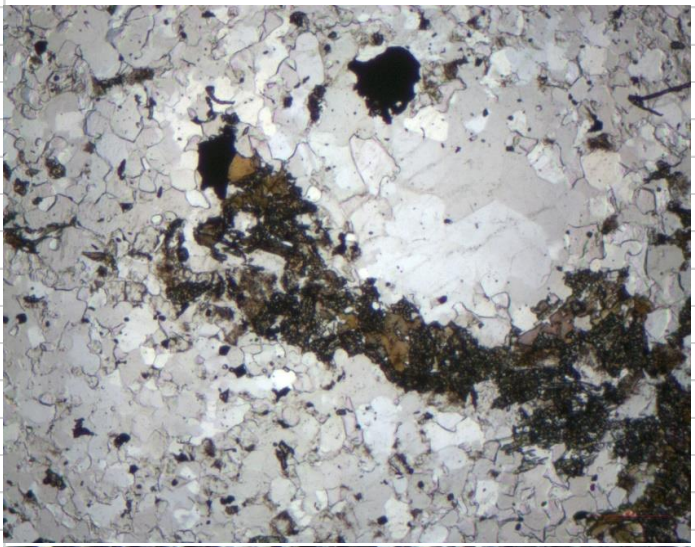

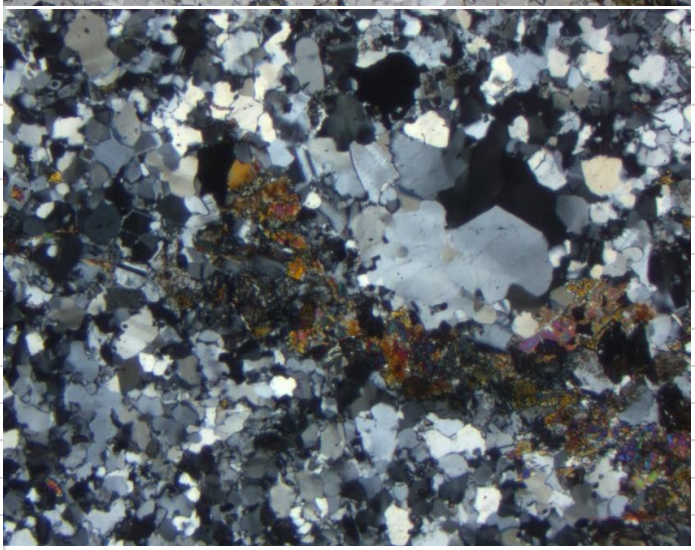

Thin section №	**JSH-17102**
Sample information	R-2242, 5.65-5.85m: Porphyroblastic basalt
Rock name	Hornblende - biotite schist
Main minerals	Quartz + plagioclase, hornblende, biotite
Accessory minerals	Muscovite, titanite, unidentified amphibole, zirkon
Opaques	-
Texture	Strongly foliated
Mineral alteration	Biotite to muscovite and occasional unidentified amphibole
Hydrothermal alteration	-
Comments	Strongly foliated, where all hornblende, biotite and even plagioclase has foliated to the same plane.
Additional comments	

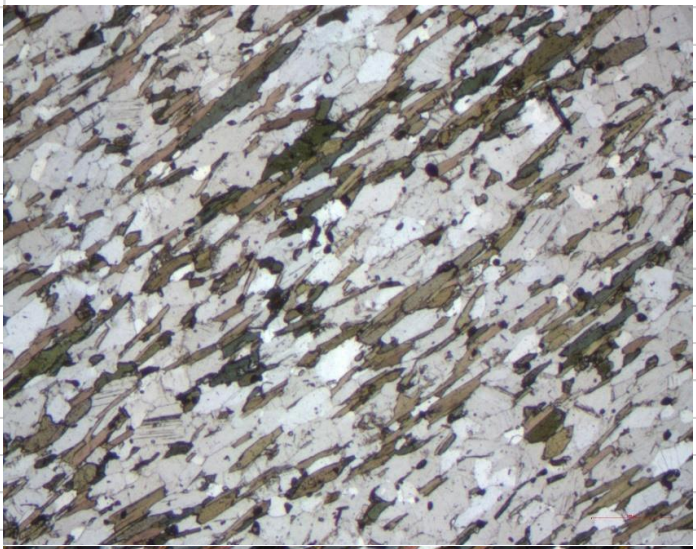

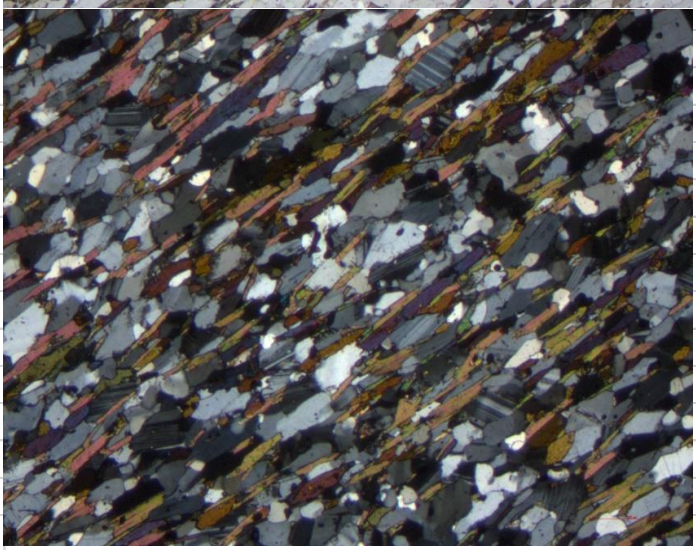

Thin section №	**JSH-17103**
Sample information	R-2242, 65-65.2m: Metamorphosed felsic rock, sericite alteration?
Rock name	Biotite gneiss
Main minerals	Quartz + plagioclase, biotite, feldspar ± muscovite
Accessory minerals	Kyanite, chlorite, carbonates, titanite, unidentified amphibolite, garnet
Opaques	Opaqes, not polished
Texture	Foliated gneissic texture
Mineral alteration	Kyanite
Hydrothermal alteration	Weak to moderate sericite alteration
Comments	The unidentified mineral has 6 sides that exhibits twinnding along 100, bireflectance is 0.02 along Z axis. Quartz grain size varies, and most of the mineral alteration has occured to feldspars and plagioclase (seritization), and biotite (metamorphosed to kyanite). It seems like carbonates are a byproduct of biotite metamorphosis, sice these two are often seen close together, but it is also present near opaques and garnets.
Additional comments	

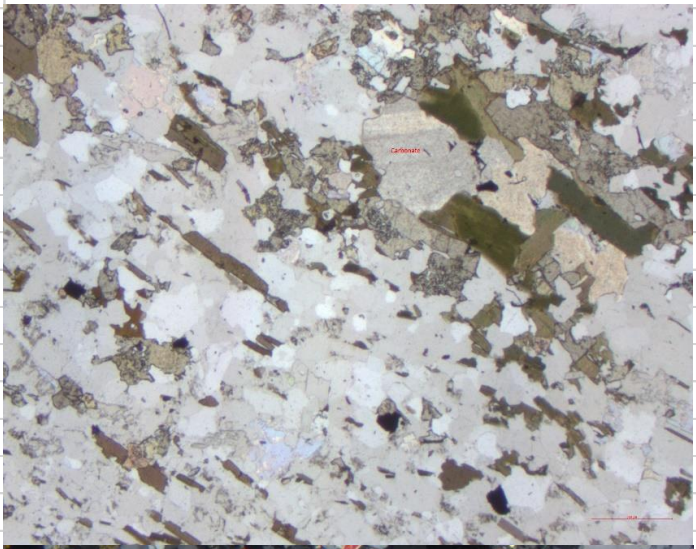

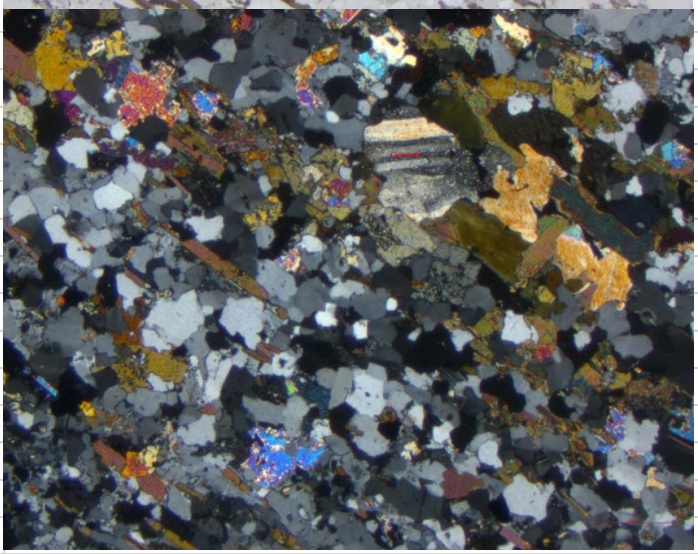

Thin section №	**JSH-17106 Amphibolite**
Sample information	R-2242, 122.04-122.24: Mafic intrusion with contact altertation in dacite?
Rock name	Foliated biotite amphibolite
Main minerals	Hornblende + biotite, plagioclase ± quartz, tremolite (?)
Accessory minerals	Muscovite, chlorite, rutile, titanite, carbonates, kyanite (?)
Opaques	None
Texture	Strongly foliated
Mineral alteration	Tremolite (and kyanite ?) from hornblende, chlorite from biotite
Hydrothermal alteration	All of the plagioclase has weakly to moderately altered into sericite
Comments	There is a hornblende rich layer along the felsic gneiss contact. Most of the hornblende appears as subherdal and at times euhedral. Sericite alteration in plagioclase crystals is hard to verify since it has not formed big enough crystals to be sure.
Additional comments	

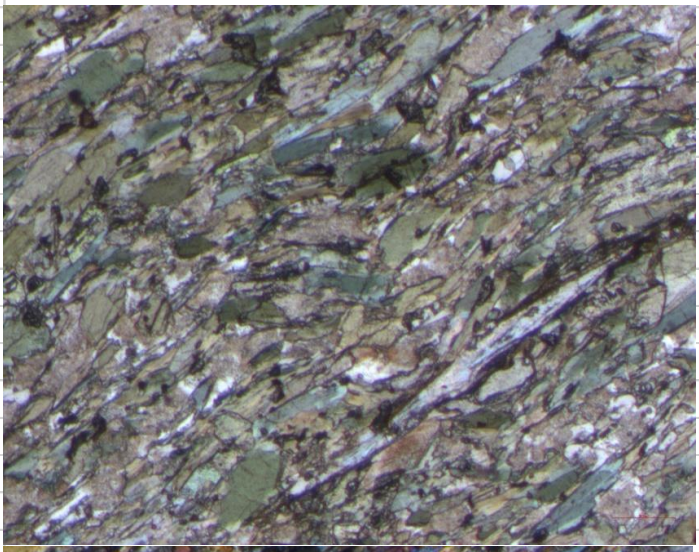

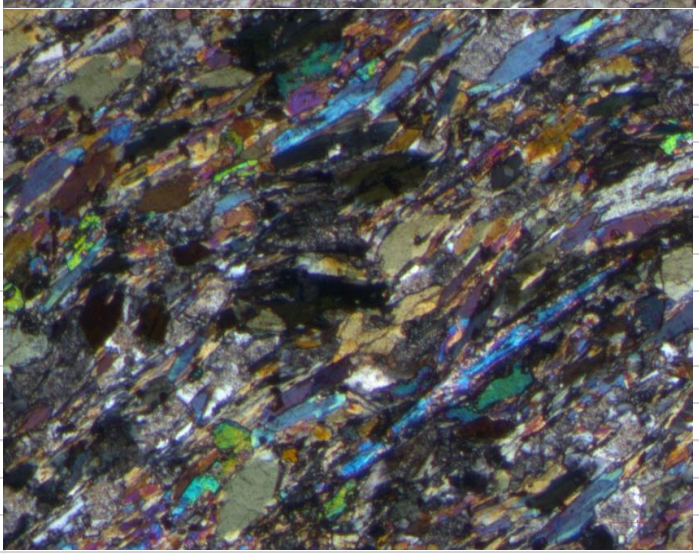

Thin section №	**JSH-17106 Felsic gneiss**
Sample information	R-2242, 122.04-122.24m: Dacite with mafic intrusion contact?
Rock name	Felsic gneiss
Main minerals	Quartz + plagioclase, andalusite, biotite
Accessory minerals	Carbonates, hornblende, unidentified amphibolite
Opaques	Rare opaques
Texture	Foliated with pressure shadows around quartz porphyroblasts
Mineral alteration	Biotite to amphibolite
Hydrothermal alteration	-
Comments	The white matrix is hard to determine, since there is no obvious twinning textures. Easiest ways to differentiate quartz from other biaxial white minerals is by looking at relief. The contact area between the ambhibolite and felsic gneiss rock units exhibits large grained vuggy quartz, weakly altered plagioclase, rutile, a few titanite minerals and a few hornblende minerals.
Additional comments	

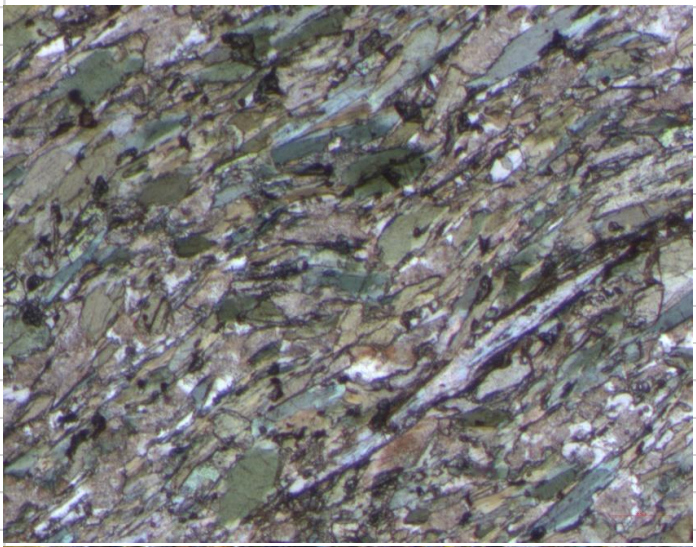

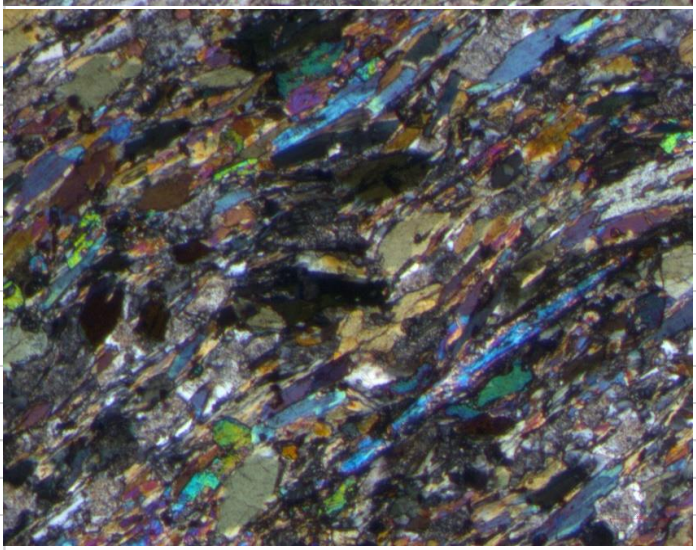

Thin section №	**JSH-17112**
Sample information	R-2242, 171.15-171.4m: Felsic unit near the deep ore body, disseminated pyrite
Rock name	Felsic gneiss
Main minerals	Quartz + microcline, plagioclase ± muscovite, kyanite
Accessory minerals	Titanite, carbonates, rutile, zoisite (?)
Opaques	Opaques
Texture	Weakly foliated, most obvious when observing hand sample, gneissic texture.
Mineral alteration	Titanite appears along kyanite, and kyanite appears along muscovite
Hydrothermal alteration	Some weak seritization in white minerals
Comments	Fine-grained matrix for the most part, but there are several layers of large-grained layers that are for the most part constructed of quartz and some plagioclase and host euhedral micas, anhedral carbonates and large opaques. These large-grained sections coul be quartz veins. In other parts the matrix has gneissic texture. There is no mafic minerals.
Additional comments	

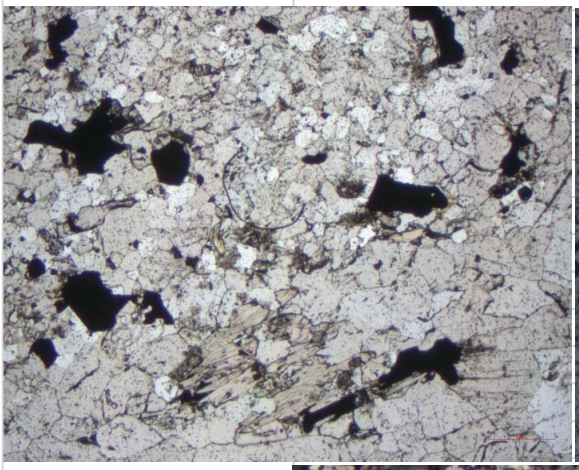

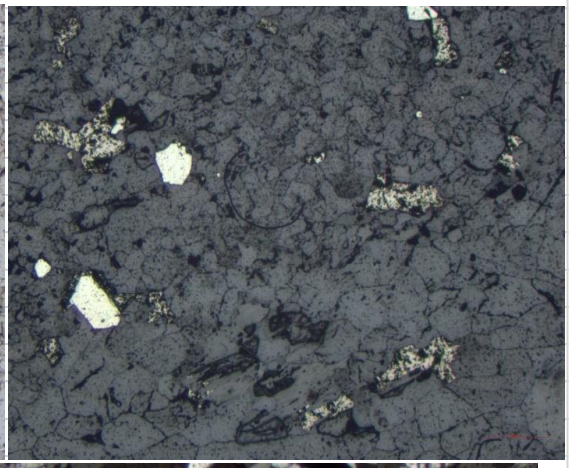

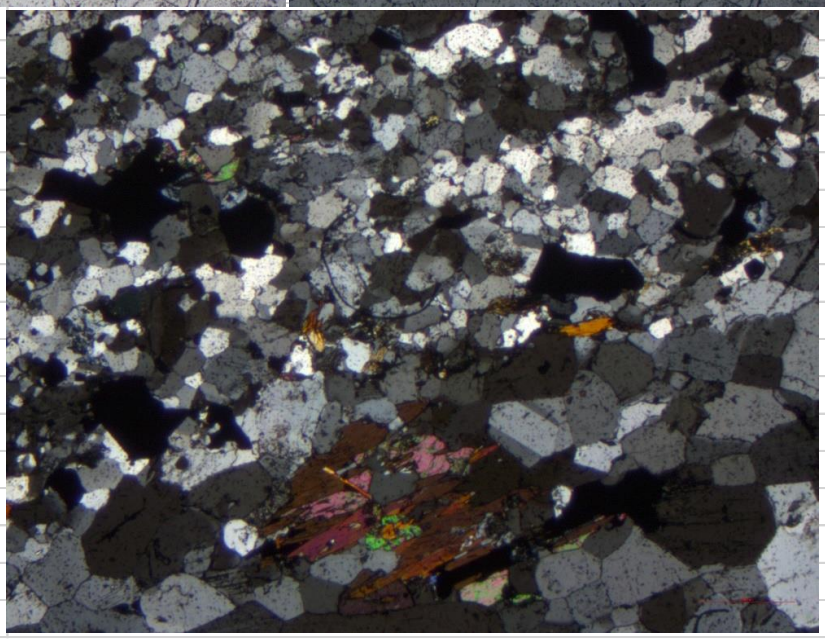

Thin section №	**JSH-17113**
Sample information	R-2242, 174.13-174.33m: Aphanitic mafic section near the deep ore body
Rock name	Amphibolite
Main minerals	Hornblende + quartz, plagioclase
Accessory minerals	Diopside-Hedenbergite, muscovite, rutile, titanite,
Opaques	Opaques
Texture	Foliated
Mineral alteration	Hornblende metamorphosed into diopside-Hedenbergite
Hydrothermal alteration	Sericite alteration in some plagioclase grains
Comments	Hornblende makes up almost 50 vol-% of this rock. Auhedral diopside-hedenbergite minerals have honrblende inclusions that are physically divided by diopside hedenbergite, but still have the excact same angle of extinction. Optical properties of observed diopside-hedenbergite: color is weakly green, weak phleocroism (light green - green), bireflectance is 0.03, optical nature is positive and 2V is around 60°. Diopside-hedebergite is surrounded by white minerals and hornblende is absent.
Additional comments	

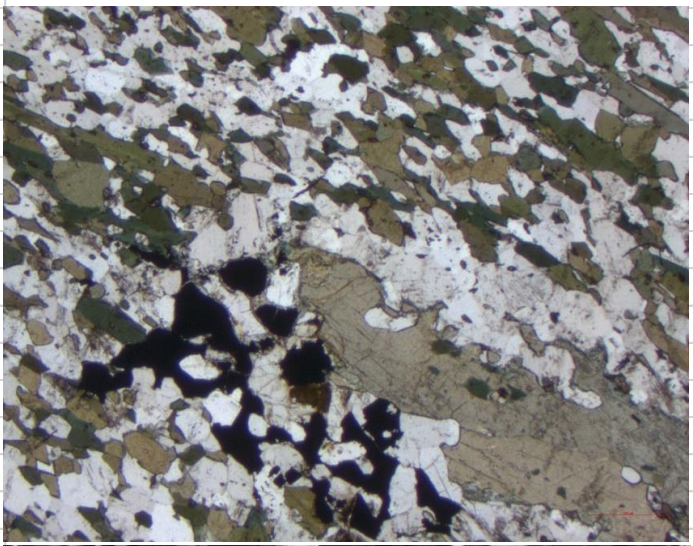

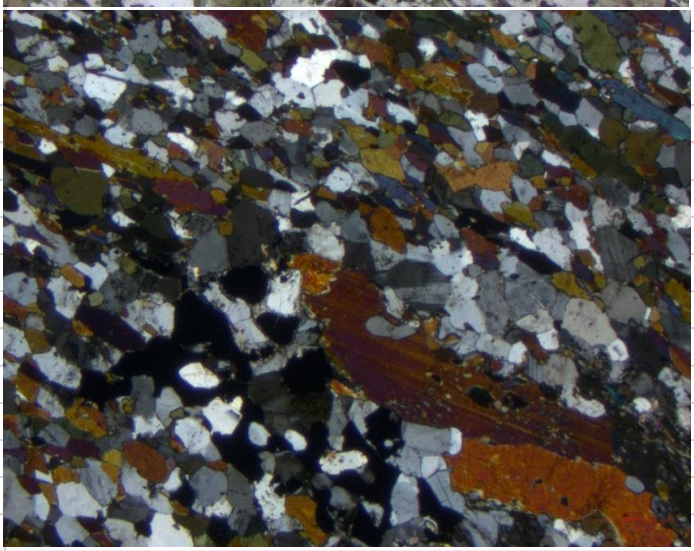

Thin section №	**JSH-17116**
Sample information	R-2242, 237.44-237.63m: "Odd rock unit, dacite?"
Rock name	Schistous felsic gneiss
Main minerals	Quartz + feldpars, plagioclase, biotite, muscovite
Accessory minerals	Rutile, andalusite (?)
Opaques	Opaques
Texture	Foliated gneissic texture
Mineral alteration	Andalusite
Hydrothermal alteration	Slight alteration in plagioclases
Comments	For the most part, white minerals are hard to differentiate from each other since only plagioclase exhibits easy to recognize twinning. The fastest way is to look at relief differences between grains, and after that the only way to identify them is by looking at the optical axis figure. Some of the white minerals are negative, other are positive and some have 2V value of 90°. Also, this sample could be called schist in general, where biotite schist and muscovite schist sections are separated.
Additional comments	

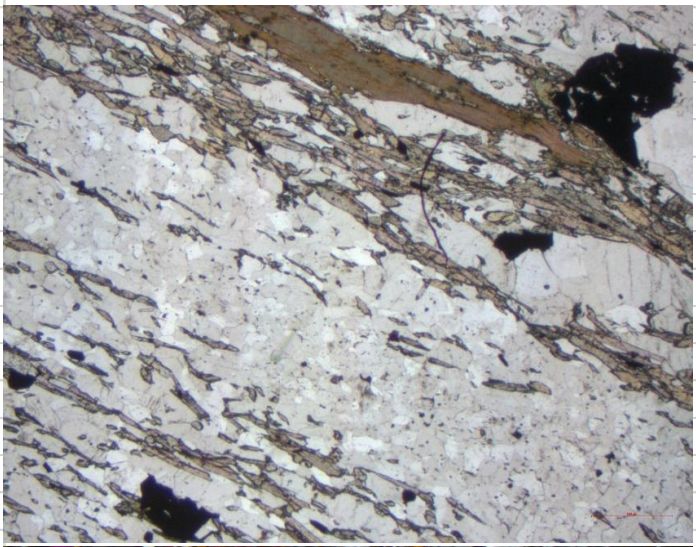

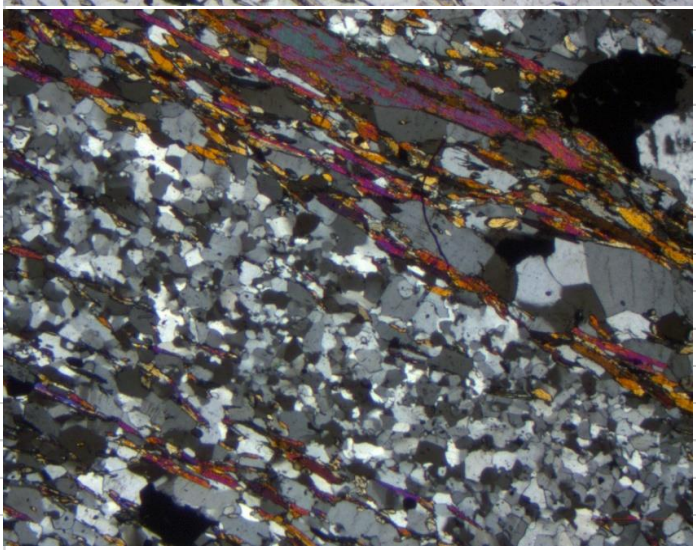

Thin section №	**JSH-17118**
Sample information	R-2242, 275.85-276m: Porphyroblastic basalt
Rock name	Amphibolite
Main minerals	Hornblende + plagioclase, andalusite (?), feldspars (?)
Accessory minerals	Apatite (?), muscovite
Opaques	Opaques
Texture	Porphyroblastic, no foliation
Mineral alteration	-
Hydrothermal alteration	Weak seritization in plagioclases
Comments	Porphyroblastic texture is due to large concentrations of plagioclase and other white minerals. In hand sample, this appears as porphyroblastic, since otherwise hornblende is dominant mineral (> 40 vol%). There seems to be some pressure shadows around these "white clasts" that is observeable when looking at hornblende pleochroism. Plagioclase crystals are the only white minerals with obvious twinning,. The other white minreals are alway biaxial, either positive or negative and with varying 2V angle. Some of the plagioclase minerals have been weakly seritized.
Additional comments	Amygdaloid texture?

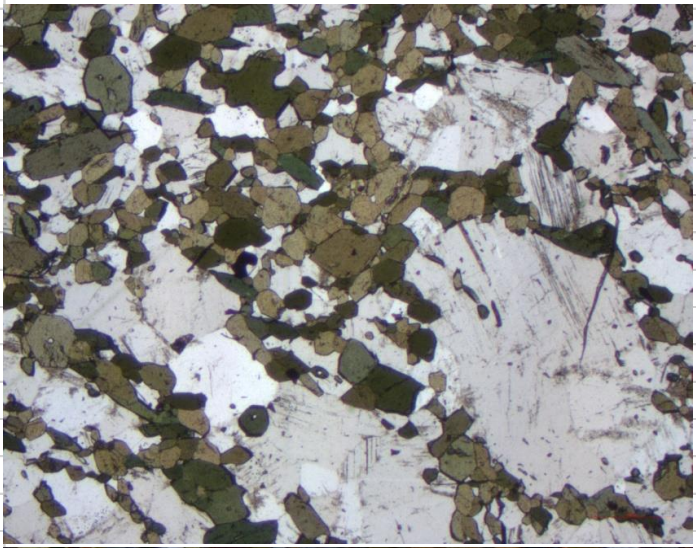

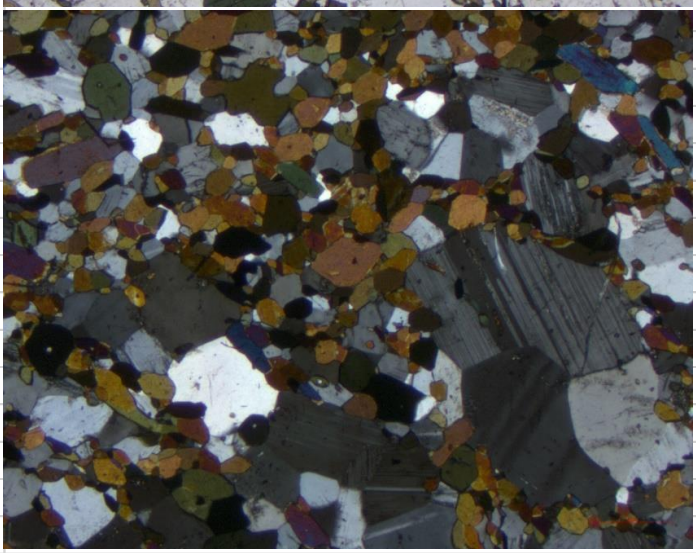

Thin section №	JSH-17121 Altered section
Sample information	R-2242, 324.58-324.78: Contact between to different mafic sections
Rock name	Sericite altered fine-grained amphibolite
Main minerals	Hornblende + plagioclase, andalusite (?), feldspars (?)
Accessory minerals	Biotite, chlorite, muscovite, carbonates
Opaques	Opaques
Texture	Weakly foliated host rock, selective and in part pervasive hydrothermal alt.
Mineral alteration	Quartz and andalusite recrystallization?
Hydrothermal alteration	Sericite + chlorite alteration with carbonate infill in largest hydrothermal veins.
Comments	The protolith resembles thin section JSH-17118, where the rock is mostly amphibolite with white mineral matrix which is hard to determine. The white minerals have been selectively, from weakly to strongly, sericitized. This sample has two different types of rock that are compositionally similiar; fine grained and larger grained amphibolite, where fine-grained section is more altered. The rock types are divided by hydrothermal veins which have carbonate infill. It seems like some quartz and andalusite has recrystallized after hydrotermal alteration, since there is no marks of alteration in them.
Additional comments	Compare immobile element ratio to sample JSH-17118

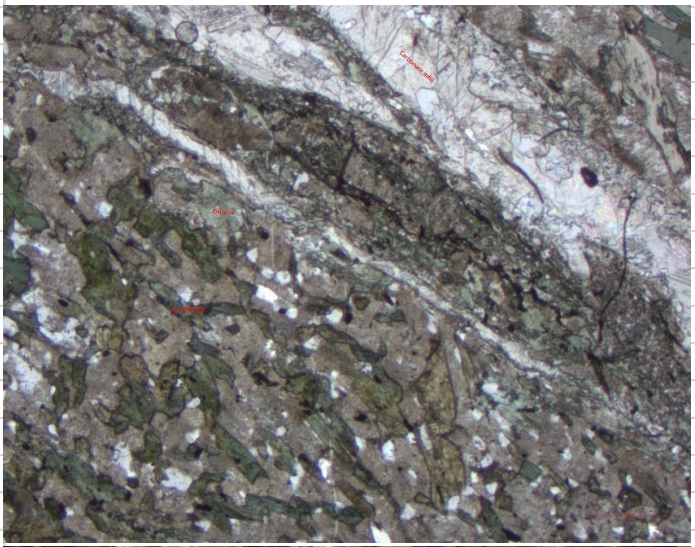

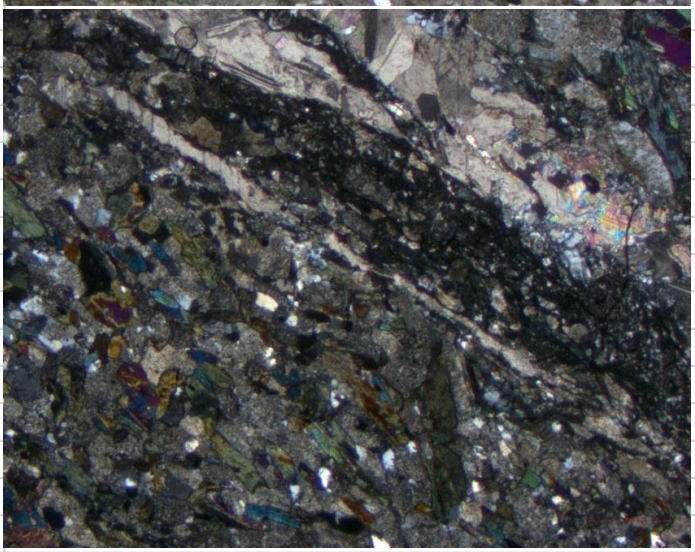

Thin section №	**JSH-17121 Unaltered section**
Sample information	R-2242, 324.58-324.78m: Contact between to different mafic sections
Rock name	Amphibolite
Main minerals	Hornblende + plagioclase, andalusite (?), felspars
Accessory minerals	Biotite, chlorite, muscovite, carbonates
Opaques	Opaques
Texture	Weakly foliated, moderate grain size
Mineral alteration	Hornblende to biotite
Hydrothermal alteration	Hornblende to chlorite, white minerals to sericite
Comments	Protolith grain size is moderate. The strength of hydrothermal alteration decreaces with increasing distance from the carbonate vein. Commonly white minerals are at least weakly seritized and hornblende has occasionaly chloritized. After choliritization ends, hornblende started to occassionaly turn into biotite.
Additional comments	

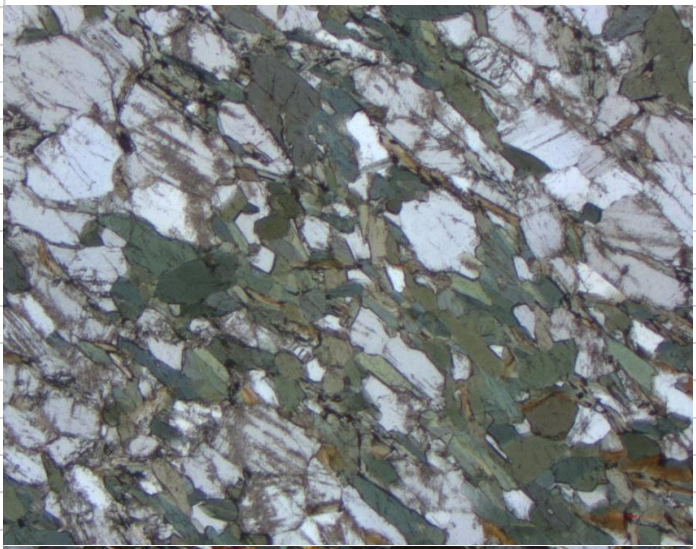

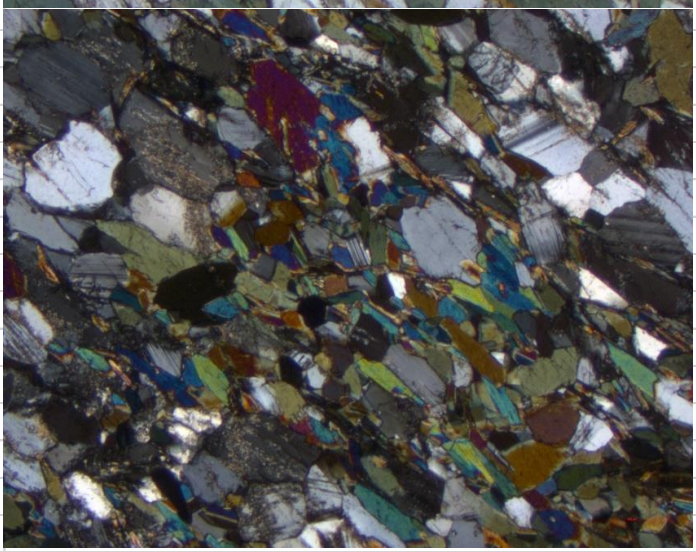

Thin section №	**JSH-17122**
Sample information	R-2252, 1-1.2m: Sericite (?) altererd felsic rock
Rock name	Felsic gneiss
Main minerals	Quartz + plagioclase, feldspars, andalusite (?)
Accessory minerals	Muscovite, biotite, carbonates, garnet, chlorite, kyanite, epidote (?)
Opaques	Opaques
Texture	Foliated gneissic texture
Mineral alteration	All high bireflectance minerals are the results of metamoprhism, up to garnet
Hydrothermal alteration	None, or overprinted by metamorphism
Comments	There is a great variety of accessory minerals. It seems like subhedral carbonates are the excess result of whatever metamorphosed into subhedral muscovite and kyanite, and sometimes into subhedral biotite and kyanite. When garnets with euhedral outlines are present, kyanite is comletely absent and garnet minerals have mica, quartz and carbonate inclusions. Some biotite crystals are partially altered into chlorite. Felsic matrix is for the most part fine-grained, but it also forms larger grained bands that are concordant to foliation.
Additional comments	

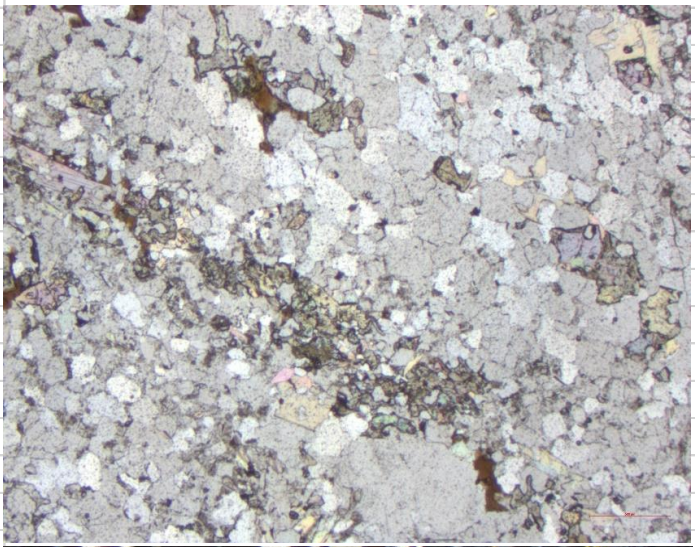

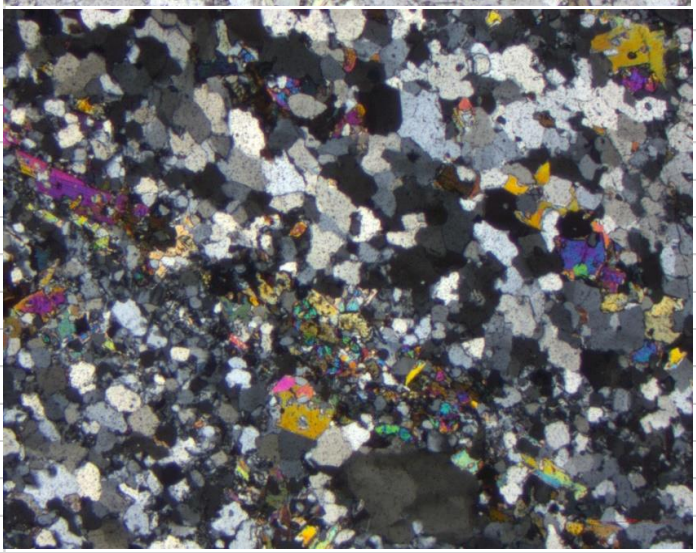

Thin section №	**JSH-17127**
Sample information	R-2252, 59.76-59.96m: Foliated felsic schist (?)
Rock name	Felsic biotite schist
Main minerals	Quartz + plagioclase, andalusite (?) ± biotite, feldspars
Accessory minerals	Garnet, carbonates, muscovite, chlorite, epidote (?)
Opaques	Rare opaques
Texture	Foliated gneissic texture
Mineral alteration	Biotite and parts of matrix have metamophosed into rare garnets
Hydrothermal alteration	-
Comments	Foliated biotite - felsic rock with gneissic texture. Biotite composes less than 10 vol% of the rock, but indicates clear foliation. Biotite color is greenish brown, and biotite minerals are occasionally weakly altered into chlorite, muscovite and something that is assumed to be epidote. Carbonates often offer in close proximity with biotites.
Additional comments	

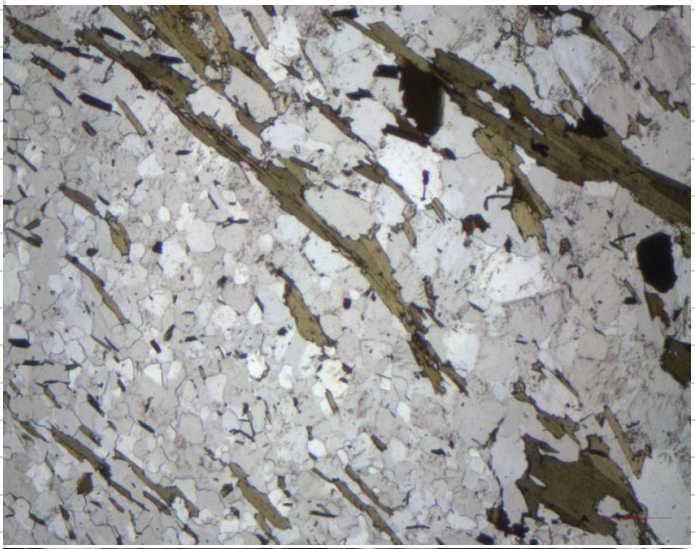

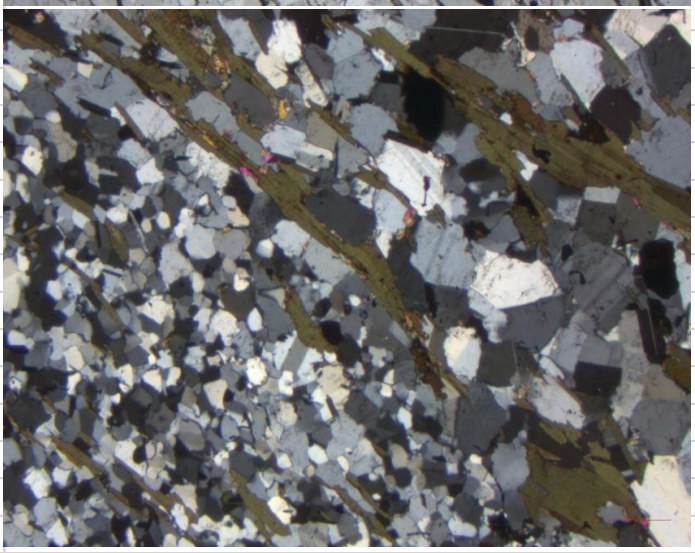

Thin section №	**JSH-17129**
Sample information	R-2252, 103.46-103.66m: Moderately altered felsic rock?
Rock name	Sericite altered, diopside felsic gneiss
Main minerals	Quartz + epidote, diopside, plagioclase, feldspars ± andalusite
Accessory minerals	Chlorite, muscovite, rutile, titanite, carbonates
Opaques	Pyrrhotite ± pyrite, chalcopyrite
Texture	Foliated gneissic texture
Mineral alteration	Amphibolites has turned at the edges into andalusite
Hydrothermal alteration	Restricted or overprinted weak sericite altertaion
Comments	It seems like amphiboles have altered into andalusite around the edges at sericite altered sections, whereas they do not exhibit this alteration metamorphosed areas. No interpretation is made of this thin section, since it is too complex.
Additional comments	

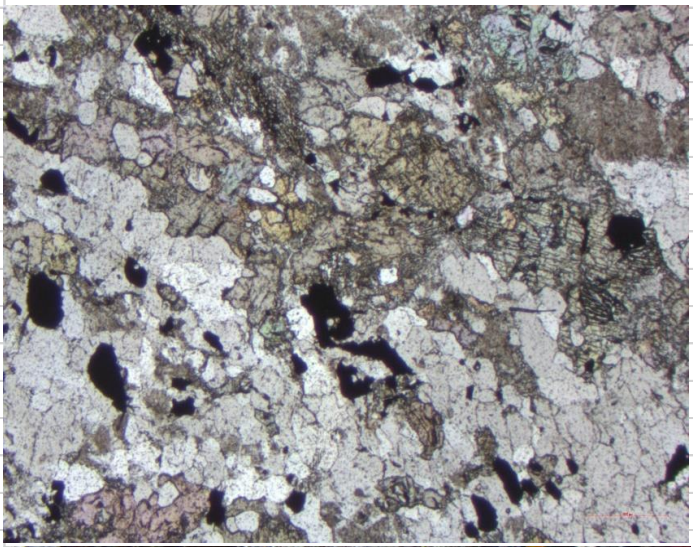

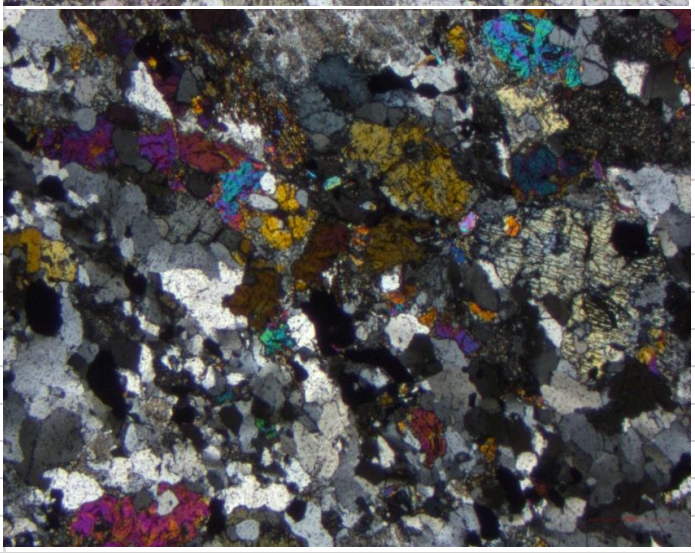

Thin section №	**JSH-17130**
Sample information	R-2252, 151.27-151.47m: Least altered section of mafic intrusion
Rock name	Hornblende monzogabbro
Main minerals	Hornblende + plagioclase, feldspars
Accessory minerals	Titanite, apatite (?)
Opaques	Sulfides
Texture	Moderately foliated hornblede minerals
Mineral alteration	-
Hydrothermal alteration	Random weak sericite (?) alteration
Comments	Igneous rock unit. Order of crystallization: sulfides that are surrounded by andhedal titanite, which appear as inclusions in hornblende. Hornblende appaears as euhedral and subhedral to each other. In between hornblende minerals appears small grains of anhedral plagioclase and feldspar. If there is quartz among the matrix, it is rare. The designated rock name is based on the interpretation that the sample is not metamorphosed.
Additional comments	

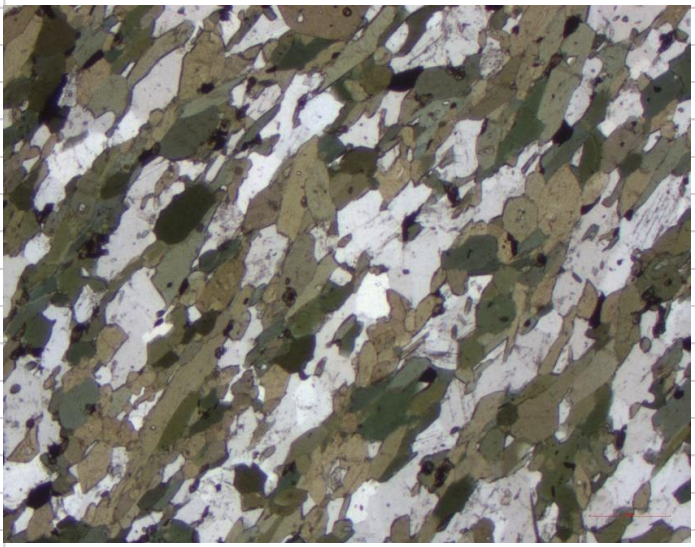

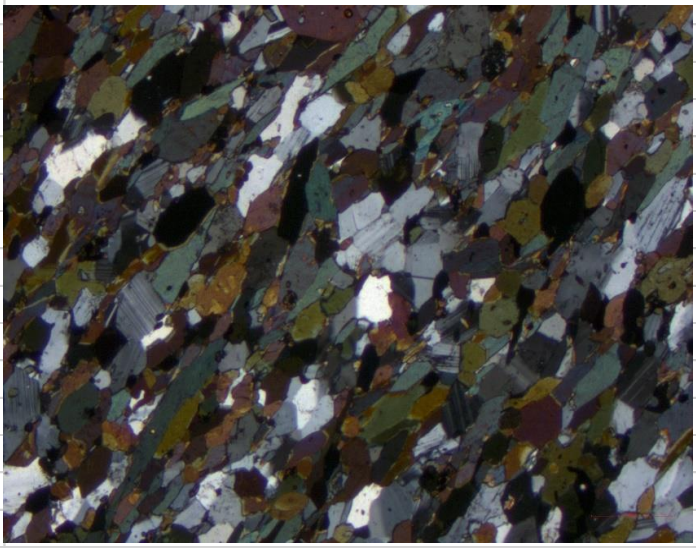

Thin section №	**JSH-17133**
Sample information	R-2252, 211.46-211.66m: Felsic rock with odd texture
Rock name	Biotite schist
Main minerals	Quartz, feldspars + biotite, plagioclase
Accessory minerals	Muscovite, chlorite, garnet, zirkon
Opaques	-
Texture	Foliated, matrix has gneissic texture
Mineral alteration	Muscovite and chlorite from biotite
Hydrothermal alteration	-
Comments	No additional comments
Additional comments	

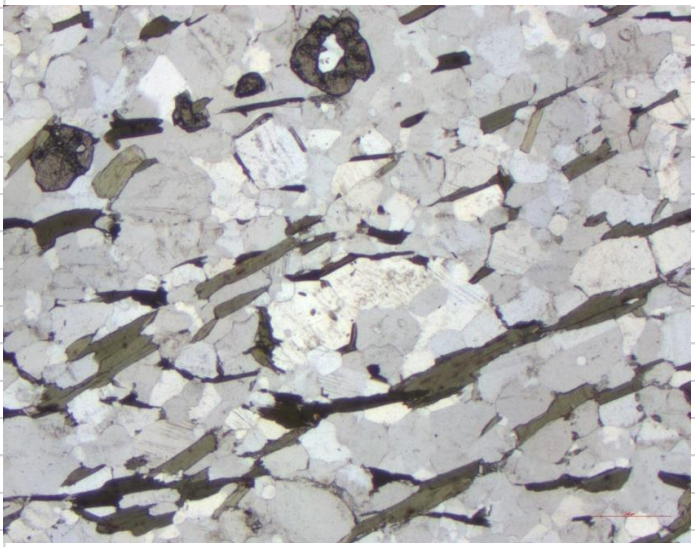

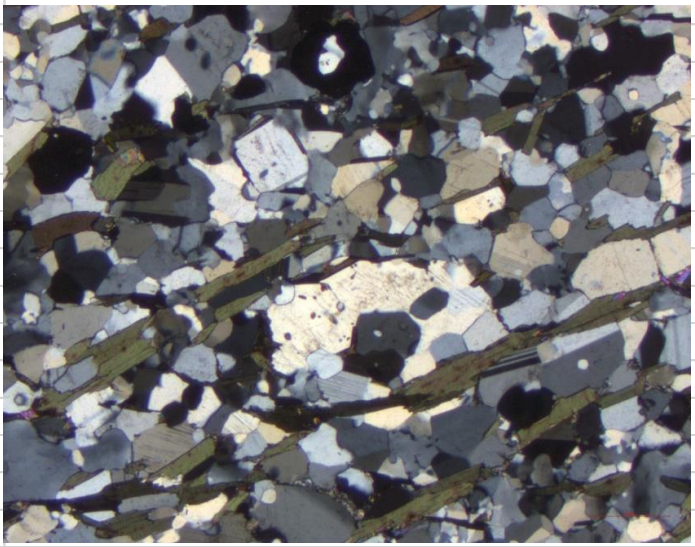

Thin section №	**JSH-17134**
Sample information	R-2252, 264.56-264.76m: Unaltered aphanitic massive rhyolite-dacite
Rock name	Biotitic rhyolite
Main minerals	Quartz + bioite, plagioclase, feldspars
Accessory minerals	Rutile, chlorite
Opaques	Opaques, sulfides
Texture	Recrystallized matrix and weakly foliated biotite
Mineral alteration	Chlorite from biotite
Hydrothermal alteration	-
Comments	No addicional comments
Additional comments	

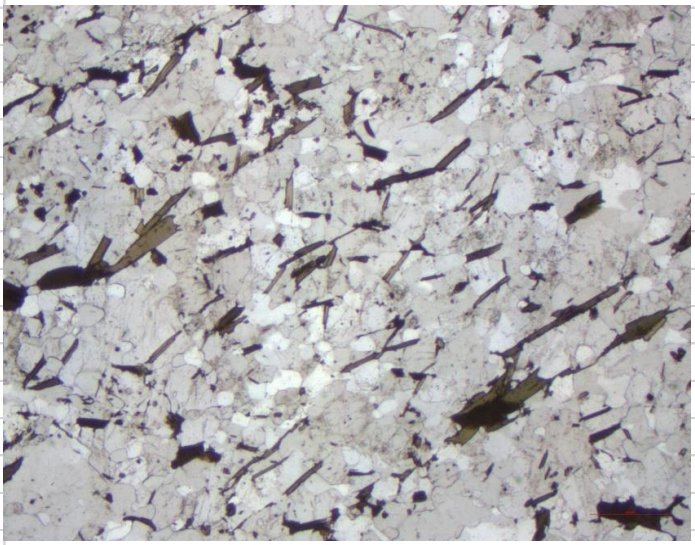

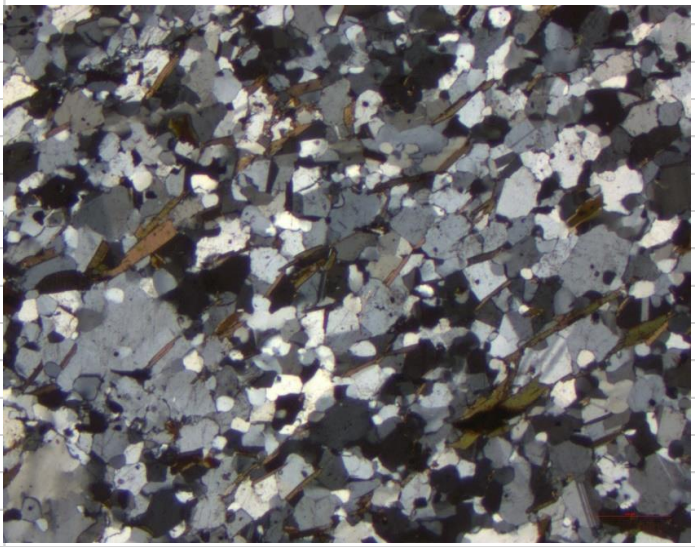

Thin section №	**JSH-17137**
Sample information	R-2252, 305.8-306m: Dacite with unclear texture
Rock name	Biotite schist
Main minerals	Quartz + feldspar, biotite, plagioclase
Accessory minerals	Zirkon
Opaques	-
Texture	Matrix has been recrystallized, otherwise foliated biotite
Mineral alteration	-
Hydrothermal alteration	-
Comments	Biotite has greenish color.
Additional comments	

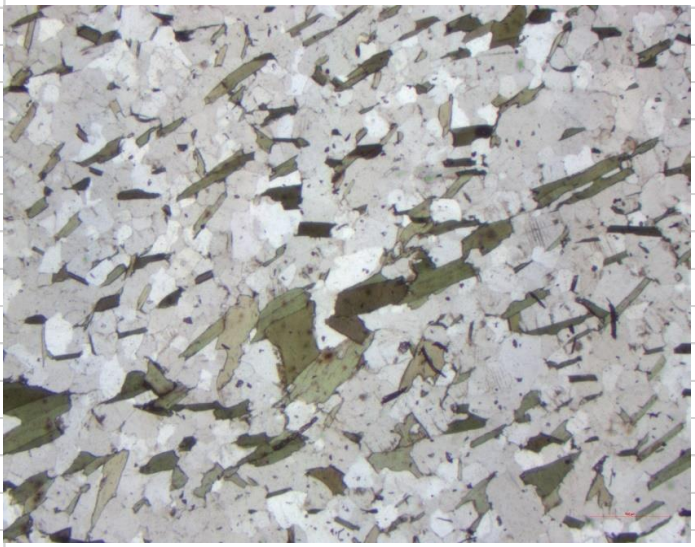

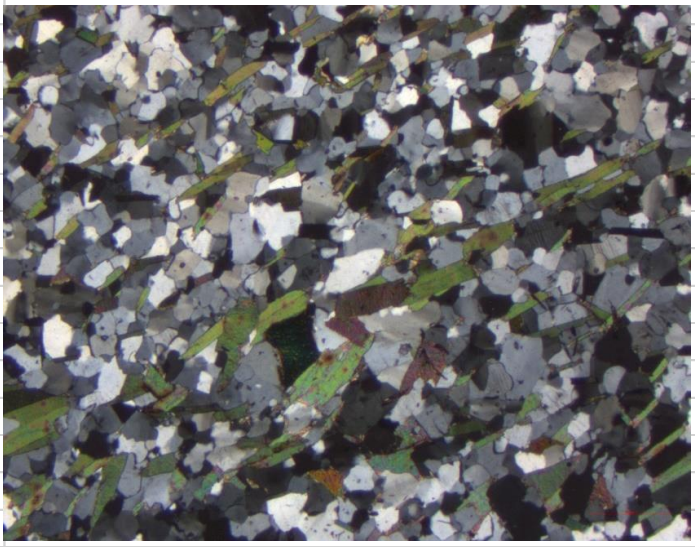

Thin section №	**JSH-17139**
Sample information	R-2252, 325.07-325.27m: Biotite schist
Rock name	Hornblende - biotite schist
Main minerals	Biotite, hornblende + feldspar, plagioclase, quartz
Accessory minerals	Chlorite, muscovite, rutile
Opaques	Opaques
Texture	Foliated
Mineral alteration	Chlorite and muscovite from biotite
Hydrothermal alteration	-
Comments	Thin section is cut along the biotite foliation plane. Almost all biotite minerals z axis is pointing upwards from the thin section.
Additional comments	

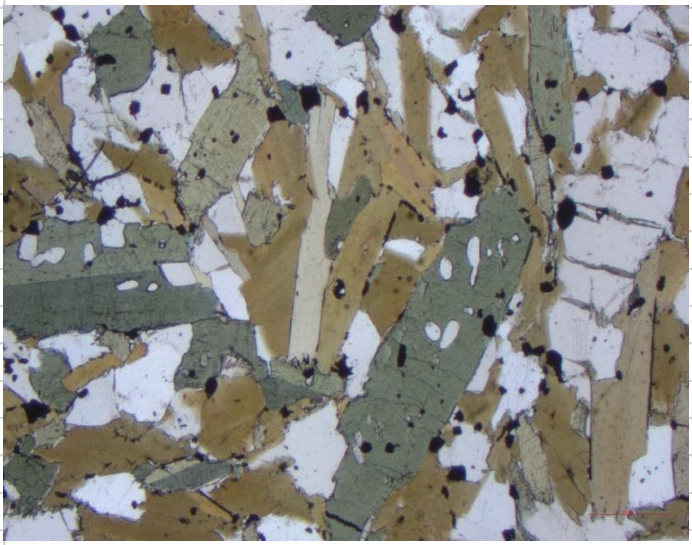

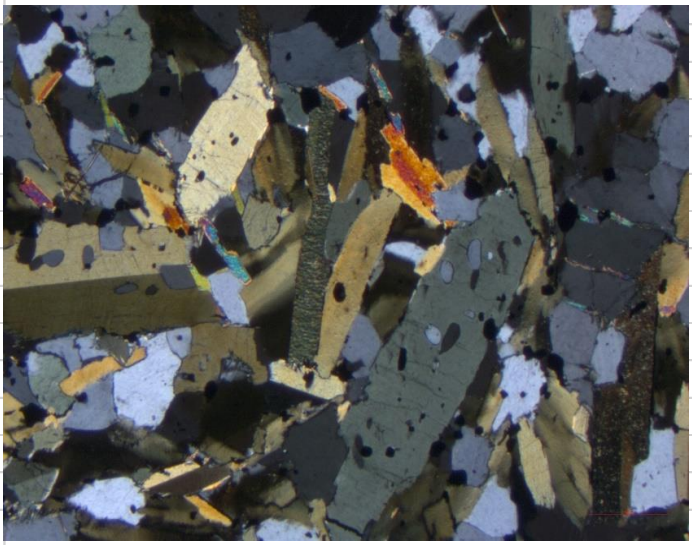

APPENDIX 3. Selected 31 samples from JSH-17001 – JSH-17140 XRF / ICP-MS geochemical data in numerological order.

BUREAU VERITAS MINERAL LABORATORIES Canada

www.bureauveritas.com/um

Bureau Veritas Commodities Canada Ltd.
9050 Shaughnessy St Vancouver British Columbia V6P 6E5 Canada
PHONE (604) 253-3158

Client: **Pyhasalmi Mine OY**
Box 51
Pyhasalmi FIN-86801 Finland

Submitted By: Kjell Kurten
Receiving Lab: Canada-Vancouver
Received: March 19, 2018
Report Date: May 09, 2018
Page: 1 of 3

CERTIFICATE OF ANALYSIS VAN18000623A.1

CLIENT JOB INFORMATION

Project: Pyhasalmi alteration
Shipment ID:
P.O. Number 20180209
Number of Samples: 33

SAMPLE DISPOSAL

IMM-PLP Return immediately after analysis
IMM-RJT Return immediately after analysis

SAMPLE PREPARATION AND ANALYTICAL PROCEDURES

Procedure Code	Number of Samples	Code Description	Test Wgt (g)	Report Status	Lab
PRP70-250	31	Crush, split and pulverize 250 g rock to 200 mesh			VAN
PULSW	31	Extra Wash with Silica between each sample			VAN
HANDX	1	Special Handling - see Job Notes			VAN
LF600	33	XRF Whole Rock & ICP-MS Trace Elements	0.66	Completed	VAN
SLBHP	2	Sort, label and box pulps			VAN

ADDITIONAL COMMENTS

Bureau Veritas does not accept responsibility for samples left at the laboratory after 90 days without prior written instructions for sample storage or return.

Invoice To: Pyhasalmi Mine OY
Box 51
Pyhasalmi FIN-86801
Finland

CC:

BRITISH COLUMBIA CERTIFIED ASSAYER
MARCUS LAU
Production Manager

This report supersedes all previous preliminary and final reports with this file number dated prior to the date on this certificate. Signature indicates final approval; preliminary reports are unsigned and should be used for reference only.
All results are considered the confidential property of the client. Bureau Veritas assumes the liabilities for actual cost of analysis only. Results apply to samples as submitted.
"**" asterisk indicates that an analytical result could not be provided due to unusually high levels of interference from other elements.

BUREAU VERITAS MINERAL LABORATORIES Canada

www.bureauveritas.com/um

Bureau Veritas Commodities Canada Ltd.

9050 Shaughnessy St Vancouver British Columbia V6P 6E5 Canada
PHONE (604) 253-3158

Client: **Pyhasalmi Mine OY**
Box 51
Pyhasalmi FIN-86801 Finland

Project: Pyhasalmi alteration
Report Date: May 09, 2018

CERTIFICATE OF ANALYSIS VAN18000623A.1

Method		WGHT	XF700	XF700	XF700	XF700	XF700	XF700	XF700	XF700	XF700	XF700	XF700	XF700	XF700	XF700	XF700	TC000	TC000	LF100	LF100
Analyte		Wgt	SiO2	Al2O3	Fe2O3	CaO	MgO	Na2O	K2O	MnO	TiO2	P2O5	Cr2O3	Ba	LOI	SO3	Sr	TOT/C	TOT/S	Ba	Be
Unit		kg	%	%	%	%	%	%	%	%	%	%	%	%	%	%	%	%	%	ppm	ppm
MDL		0.01	0.01	0.01	0.01	0.01	0.01	0.01	0.01	0.01	0.01	0.01	0.01	0.01	-5.11	0.002	0.002	0.02	0.02	1	1
JSH-17001	Drill Core	0.21	49.50	17.00	11.00	10.90	6.35	3.40	0.38	0.17	0.49	0.07	0.01	<0.01	0.38	0.065	0.024	0.07	0.02	110	<1
JSH-17004	Drill Core	0.19	71.70	12.40	4.68	3.27	1.15	2.15	2.97	0.12	0.24	0.05	<0.01	0.08	0.46	0.807	0.005	0.05	0.33	807	<1
JSH-17008	Drill Core	0.20	55.90	16.10	5.94	7.21	6.39	3.73	1.14	0.34	0.70	0.26	0.04	0.36	0.74	0.970	0.055	0.05	0.41	3492	<1
JSH-17010	Drill Core	0.26	74.40	6.29	10.50	0.22	0.35	0.39	1.28	0.01	0.12	<0.01	<0.01	0.13	5.61	>10	0.005	0.03	8.34	1211	<1
JSH-17012	Drill Core	0.23	54.90	14.70	9.61	8.17	5.05	3.01	0.95	0.19	1.54	0.83	0.02	0.10	0.59	1.220	0.080	0.03	0.50	953	1
JSH-17013	Drill Core	0.17	76.10	12.00	2.51	2.37	0.28	2.98	2.39	0.06	0.13	<0.01	<0.01	0.04	0.21	0.218	0.006	0.05	0.08	364	<1
JSH-17014	Drill Core	0.21	73.50	12.80	2.94	2.33	1.10	2.60	3.45	0.05	0.14	<0.01	<0.01	0.10	0.41	0.047	0.008	0.03	0.02	915	<1
JSH-17071	Drill Core	0.18	76.60	11.70	2.87	0.76	0.29	5.14	1.35	0.08	0.17	0.02	<0.01	0.06	0.24	0.497	0.004	0.06	0.21	495	<1
JSH-17072	Drill Core	0.22	52.00	16.60	9.40	8.34	6.58	5.18	0.36	0.15	0.50	0.06	0.03	<0.01	0.58	0.208	0.008	0.03	0.08	56	<1
JSH-17080	Drill Core	0.18	48.40	16.50	11.60	8.32	6.64	3.59	0.72	0.21	1.97	0.39	0.01	0.04	1.16	3.100	0.068	0.08	1.67	361	<1
JSH-17082	Drill Core	0.15	51.50	3.97	4.81	11.90	21.70	0.49	0.05	0.48	0.11	0.06	<0.01	0.04	3.21	4.040	<0.002	0.17	2.04	487	<1
JSH-17091	Drill Core	0.17	68.40	13.80	4.00	0.63	1.82	2.34	7.22	0.05	0.29	0.04	<0.01	0.23	0.49	1.340	0.003	0.03	0.59	2204	<1
JSH-17093	Drill Core	0.20	71.70	13.70	4.16	3.03	0.65	4.43	1.32	0.08	0.34	0.09	<0.01	0.07	0.34	0.332	0.015	0.05	0.15	684	<1
JSH-17096	Drill Core	0.24	52.50	15.20	12.70	7.30	5.03	4.89	1.12	0.20	0.64	0.09	<0.01	0.02	0.49	0.620	0.020	0.02	0.31	197	<1
JSH-17100	Drill Core	0.18	72.10	12.80	3.08	2.94	0.73	1.94	5.15	0.07	0.18	0.02	<0.01	0.11	0.42	0.842	0.006	0.03	0.44	1007	<1
JSH-17102	Drill Core	0.23	60.70	16.70	5.91	6.14	3.38	4.12	1.31	0.09	0.64	0.25	0.02	0.04	0.37	0.039	0.057	0.02	<0.02	393	2
JSH-17103	Drill Core	0.17	73.40	12.40	4.11	3.01	0.70	2.46	2.67	0.11	0.26	0.05	<0.01	0.05	0.76	0.042	0.006	0.11	<0.02	428	<1
JSH-17106	Drill Core	0.17	75.50	11.50	3.80	1.43	0.64	4.91	0.73	0.06	0.17	0.02	<0.01	0.05	0.56	0.029	0.019	0.06	<0.02	447	<1
JSH-17112	Drill Core	0.20	71.40	11.70	5.83	2.76	0.64	2.84	3.07	0.04	0.17	0.02	<0.01	0.02	1.18	5.090	0.009	0.07	2.44	160	<1
JSH-17113	Drill Core	0.25	52.50	15.30	11.60	7.92	5.25	5.16	0.38	0.18	0.73	0.14	<0.01	<0.01	0.36	0.524	0.015	0.03	0.28	53	<1
PHYA_BCR-2	Pulp		54.10	13.40	13.90	7.16	3.66	3.24	1.78	0.20	2.27	0.36	<0.01	0.07		0.074	0.035			677	<1
PHYA_W2-A	Pulp		52.40	15.30	10.90	10.90	6.50	2.26	0.62	0.17	1.08	0.13	0.02	0.02		0.018	0.017			166	2
JSH-17116	Drill Core	0.21	71.20	12.30	6.07	1.42	1.52	4.86	1.00	0.08	0.49	0.15	<0.01	0.02	0.31	0.202	0.006	0.06	0.08	200	<1
JSH-17118	Drill Core	0.14	55.20	15.80	10.10	8.16	4.54	5.00	0.18	0.14	0.58	0.15	<0.01	<0.01	0.29	0.017	0.008	0.04	<0.02	37	<1
JSH-17121	Drill Core	0.21	51.70	17.60	10.80	8.27	3.47	4.18	1.08	0.16	1.11	0.35	<0.01	0.01	0.69	0.273	0.040	0.05	0.11	146	2
JSH-17122	Drill Core	0.21	74.20	12.40	2.72	3.76	0.42	1.45	3.42	0.07	0.14	<0.01	<0.01	0.05	1.02	0.023	0.003	0.12	<0.02	485	<1
JSH-17127	Drill Core	0.19	71.60	13.50	5.00	0.38	0.66	6.30	1.55	0.15	0.27	0.04	<0.01	0.03	0.16	0.038	0.004	0.04	<0.02	215	<1
JSH-17129	Drill Core	0.19	61.20	11.20	14.50	7.25	0.54	1.84	0.43	0.08	0.21	0.04	<0.01	0.03	2.56	>10	0.004	0.04	5.08	234	3
JSH-17130	Drill Core	0.23	47.90	15.00	14.50	10.30	6.34	3.25	0.36	0.20	1.46	0.12	0.03	<0.01	0.22	0.783	0.024	0.06	0.36	66	3
JSH-17133	Drill Core	0.18	75.10	12.10	3.85	0.66	0.79	4.89	1.52	0.09	0.21	0.03	<0.01	0.05	0.06	0.015	0.008	0.03	<0.02	461	<1

BUREAU VERITAS MINERAL LABORATORIES Canada

Bureau Veritas Commodities Canada Ltd.

9050 Shaughnessy St Vancouver British Columbia V6P 6E5 Canada
PHONE (604) 253-3158

www.bureauveritas.com/um

Client: **Pyhasalmi Mine OY**
Box 51
Pyhasalmi FIN-86801 Finland

Project: Pyhasalmi alteration
Report Date: May 09, 2018

CERTIFICATE OF ANALYSIS VAN18000623A.1

Method		LF100	LF100	LF100	LF100	LF100	LF100	LF100	LF100	LF100	LF100	LF100	LF100	LF100	LF100	LF100	LF100	LF100	LF100	LF100	LF100
Analyte		Co	Cs	Ga	Hf	Nb	Rb	Sn	Sr	Ta	Th	U	V	W	Zr	Y	La	Ce	Pr	Nd	Sm
Unit		ppm	ppm	ppm	ppm	ppm	ppm	ppm	ppm	ppm	ppm	ppm	ppm	ppm	ppm	ppm	ppm	ppm	ppm	ppm	ppm
MDL		0.2	0.1	0.5	0.1	0.1	0.1	1	0.5	0.1	0.2	0.1	8	0.5	0.1	0.1	0.1	0.1	0.02	0.3	0.05
JSH-17001	Drill Core	37.1	0.7	13.2	0.5	1.0	3.9	<1	267.0	<0.1	0.3	0.2	251	<0.5	17.4	8.7	2.9	6.2	0.78	3.7	1.02
JSH-17004	Drill Core	1.3	2.0	13.8	3.6	7.6	50.0	1	63.8	0.5	3.6	1.2	9	<0.5	134.5	29.5	18.8	36.7	4.46	17.8	4.12
JSH-17008	Drill Core	18.0	0.9	19.1	2.3	5.0	17.3	4	538.8	0.2	4.0	2.2	147	<0.5	91.6	13.6	23.4	43.6	5.28	21.9	3.72
JSH-17010	Drill Core	43.0	0.6	6.3	2.2	4.0	9.2	<1	30.1	0.3	2.3	6.5	<8	0.5	67.1	11.9	12.7	25.2	2.76	10.7	1.92
JSH-17012	Drill Core	26.6	0.5	19.1	4.1	15.4	15.4	2	731.3	0.8	4.0	1.9	152	0.9	171.1	17.8	50.3	107.9	13.51	55.5	9.26
JSH-17013	Drill Core	0.4	1.1	13.6	5.3	9.3	29.3	1	76.3	0.7	4.6	1.7	<8	<0.5	190.5	38.4	27.0	51.7	5.95	24.1	5.26
JSH-17014	Drill Core	1.3	1.9	14.3	5.8	10.2	47.3	1	82.6	0.8	5.0	1.8	<8	<0.5	204.8	39.5	26.4	52.7	6.18	24.1	5.06
JSH-17071	Drill Core	1.3	0.7	11.8	4.0	8.2	15.8	1	54.5	0.5	4.4	1.6	<8	<0.5	158.2	33.7	21.3	39.9	5.09	20.6	4.74
JSH-17072	Drill Core	37.0	0.8	13.3	0.6	1.0	3.7	<1	108.9	<0.1	0.4	0.7	232	<0.5	22.4	10.1	3.3	6.3	0.82	3.8	0.97
JSH-17080	Drill Core	38.4	0.4	20.3	3.1	4.7	7.7	1	658.0	0.3	0.8	0.3	224	<0.5	116.2	23.0	16.1	36.5	5.07	24.1	5.64
JSH-17082	Drill Core	0.7	0.1	9.2	1.4	1.6	0.4	2	28.9	0.2	0.5	1.2	28	<0.5	50.5	25.0	6.5	23.8	3.68	16.8	3.86
JSH-17091	Drill Core	4.3	11.5	15.7	5.5	8.2	202.6	1	33.4	0.5	4.1	1.5	19	<0.5	193.4	39.1	20.0	43.0	5.36	23.3	5.52
JSH-17093	Drill Core	7.1	2.4	12.9	3.1	5.9	26.1	<1	164.0	0.5	3.9	1.6	21	<0.5	114.0	23.8	16.8	32.2	3.70	14.8	3.16
JSH-17096	Drill Core	48.9	2.5	12.9	0.8	1.3	17.9	<1	192.4	<0.1	0.6	0.2	301	<0.5	29.3	12.8	4.1	9.2	1.19	5.3	1.45
JSH-17100	Drill Core	1.3	1.6	14.4	4.1	8.2	64.0	1	63.2	0.5	3.8	1.7	<8	<0.5	158.6	32.3	16.8	35.5	4.34	16.5	3.66
JSH-17102	Drill Core	17.2	3.2	17.8	3.1	6.8	28.6	<1	556.0	0.5	3.1	1.2	72	<0.5	117.0	10.7	20.1	40.5	4.85	19.9	3.91
JSH-17103	Drill Core	1.4	1.6	12.5	4.0	7.5	45.2	1	56.1	0.6	3.9	1.1	<8	0.8	144.3	29.1	20.9	43.1	4.99	20.8	3.96
JSH-17106	Drill Core	0.6	1.2	14.2	3.8	5.6	16.8	<1	193.6	0.4	2.4	1.0	<8	<0.5	125.6	38.2	15.4	32.9	4.05	17.2	4.56
JSH-17112	Drill Core	2.9	0.4	10.9	3.8	5.0	38.1	1	75.4	0.5	2.6	1.2	<8	<0.5	136.5	26.2	14.3	31.2	3.82	17.3	3.35
JSH-17113	Drill Core	41.9	0.8	13.7	0.9	1.4	4.5	<1	162.4	<0.1	0.5	1.2	293	<0.5	33.6	14.3	4.9	10.1	1.39	6.0	1.73
PHYA_BCR-2	Pulp	36.4	1.2	20.0	4.5	11.0	44.3	2	341.2	0.8	6.2	1.8	369	<0.5	177.9	33.4	27.2	52.8	6.70	28.0	6.40
PHYA_W2-A	Pulp	42.2	0.8	16.3	2.3	6.5	19.4	2	196.1	0.5	2.2	0.5	237	<0.5	89.4	19.9	10.7	22.4	2.91	12.1	3.18
JSH-17116	Drill Core	8.6	1.2	14.2	3.0	4.5	12.6	1	72.0	0.3	2.3	1.5	44	<0.5	106.0	29.0	13.5	27.7	3.71	15.7	3.68
JSH-17118	Drill Core	34.1	0.4	14.2	0.8	1.2	3.1	<1	100.7	<0.1	0.6	2.2	303	<0.5	24.1	13.4	5.3	10.0	1.28	6.0	1.45
JSH-17121	Drill Core	23.9	1.4	17.2	1.6	4.1	31.8	<1	407.9	0.2	1.6	0.9	146	<0.5	54.0	10.6	11.7	28.2	3.74	17.0	3.96
JSH-17122	Drill Core	0.3	0.9	14.6	6.0	10.7	57.5	1	52.9	0.6	5.1	1.6	<8	<0.5	207.5	41.2	30.1	58.0	6.72	27.5	5.42
JSH-17127	Drill Core	1.4	5.9	15.8	4.6	8.4	41.4	1	45.2	0.7	4.5	1.3	<8	<0.5	159.2	33.7	23.2	46.8	5.34	20.4	4.82
JSH-17129	Drill Core	7.9	1.0	18.0	3.2	7.5	12.8	35	37.7	0.4	3.0	1.7	17	<0.5	121.5	24.1	18.7	36.7	4.22	16.7	3.67
JSH-17130	Drill Core	46.1	<0.1	17.4	1.7	3.8	2.4	<1	242.9	0.2	0.9	0.3	239	0.8	57.7	19.0	8.3	18.1	2.51	12.6	3.41
JSH-17133	Drill Core	1.2	3.0	12.9	3.8	6.4	54.3	1	74.1	0.3	3.8	1.1	<8	<0.5	144.1	32.0	14.9	31.5	3.91	15.9	3.87

This report supersedes all previous preliminary and final reports with this file number dated prior to the date on this certificate. Signature indicates final approval; preliminary reports are unsigned and should be used for reference only.

BUREAU VERITAS MINERAL LABORATORIES Canada

www.bureauveritas.com/um

Bureau Veritas Commodities Canada Ltd.
9050 Shaughnessy St Vancouver British Columbia V6P 6E5 Canada
PHONE (604) 253-3158

Client: **Pyhasalmi Mine OY**
Box 51
Pyhasalmi FIN-86801 Finland

Project: Pyhasalmi alteration
Report Date: May 09, 2018

CERTIFICATE OF ANALYSIS VAN18000623A.1

Method		LF100	LF100	LF100	LF100	LF100	LF100	LF100	LF100	LF100	AQ200	AQ200	AQ200	AQ200	AQ200	AQ200	AQ200	AQ200	AQ200	AQ200	AQ200
Analyte		Eu	Gd	Tb	Dy	Ho	Er	Tm	Yb	Lu	Mo	Cu	Pb	Zn	Ni	As	Cd	Sb	Bi	Ag	Au
Unit		ppm	ppm	ppm	ppm	ppm	ppm	ppm	ppm	ppm	ppm	ppm	ppm	ppm	ppm	ppm	ppm	ppm	ppm	ppm	ppb
MDL		0.02	0.05	0.01	0.05	0.02	0.03	0.01	0.05	0.01	0.1	0.1	0.1	1	0.1	0.5	0.1	0.1	0.1	0.1	0.5
JSH-17001	Drill Core	0.40	1.27	0.23	1.35	0.36	1.04	0.18	1.15	0.19	0.3	107.5	2.9	53	13.2	0.8	<0.1	<0.1	<0.1	0.2	9.6
JSH-17004	Drill Core	0.90	4.23	0.74	4.79	1.11	3.67	0.56	3.81	0.60	3.1	10.0	2.3	114	2.9	1.0	<0.1	<0.1	<0.1	<0.1	1.5
JSH-17008	Drill Core	1.10	3.33	0.45	2.42	0.49	1.37	0.22	1.50	0.23	0.5	375.9	543.5	732	95.9	68.3	1.9	1.4	25.6	4.0	464.5
JSH-17010	Drill Core	0.36	1.73	0.29	1.96	0.45	1.51	0.23	1.60	0.24	9.7	542.8	316.5	85	1.7	141.5	0.5	3.8	40.8	5.2	205.3
JSH-17012	Drill Core	2.54	6.89	0.84	4.07	0.65	1.69	0.22	1.40	0.20	0.5	251.8	7.2	131	46.5	40.6	<0.1	0.2	2.0	0.2	43.9
JSH-17013	Drill Core	0.95	5.41	0.97	6.27	1.39	4.60	0.69	4.96	0.77	0.2	20.5	2.8	69	1.3	39.8	<0.1	0.3	0.2	<0.1	4.5
JSH-17014	Drill Core	0.93	5.48	0.93	6.29	1.37	4.43	0.69	4.51	0.73	1.0	6.0	2.0	76	3.1	2.1	<0.1	<0.1	<0.1	<0.1	3.1
JSH-17071	Drill Core	0.92	4.62	0.86	5.35	1.26	4.00	0.58	4.02	0.61	0.5	21.6	5.0	125	1.7	2.5	0.2	0.3	<0.1	0.3	3.9
JSH-17072	Drill Core	0.44	1.31	0.22	1.42	0.35	1.12	0.18	1.21	0.18	0.2	39.3	3.4	48	32.0	1.6	<0.1	0.1	<0.1	0.1	3.5
JSH-17080	Drill Core	1.84	5.23	0.76	4.52	0.89	2.56	0.34	2.22	0.29	0.4	830.8	159.4	178	51.5	74.9	0.3	2.2	13.6	1.4	245.0
JSH-17082	Drill Core	0.96	3.75	0.64	4.01	0.85	2.66	0.41	2.72	0.47	0.2	>10000	79.8	1283	1.1	126.4	7.5	1.5	9.8	40.6	65545.2
JSH-17091	Drill Core	0.95	6.02	1.07	6.84	1.58	4.99	0.76	4.97	0.77	1.0	43.0	21.7	467	3.2	1.5	1.8	<0.1	0.2	0.7	73.3
JSH-17093	Drill Core	0.73	3.49	0.60	3.59	0.82	2.76	0.43	3.08	0.48	0.4	78.2	2.7	69	4.3	1.8	<0.1	<0.1	<0.1	0.1	18.0
JSH-17096	Drill Core	0.57	1.92	0.31	2.15	0.52	1.54	0.24	1.68	0.26	0.1	194.8	1.2	50	22.2	<0.5	0.1	<0.1	<0.1	0.2	3.3
JSH-17100	Drill Core	0.84	4.43	0.82	5.26	1.17	4.11	0.60	3.83	0.64	2.2	13.6	2.9	93	2.3	1.6	0.2	0.1	<0.1	0.1	5.6
JSH-17102	Drill Core	1.10	3.11	0.43	2.39	0.40	1.12	0.16	1.05	0.13	0.2	14.2	8.2	56	34.6	1.9	<0.1	0.5	<0.1	<0.1	1.5
JSH-17103	Drill Core	0.88	4.17	0.69	4.59	1.01	3.52	0.55	3.82	0.62	0.2	8.4	1.7	49	1.3	3.2	<0.1	0.2	<0.1	<0.1	3.0
JSH-17106	Drill Core	1.23	5.29	0.93	6.58	1.36	4.47	0.69	4.63	0.74	0.5	5.7	1.1	62	0.7	0.7	<0.1	<0.1	<0.1	<0.1	1.5
JSH-17112	Drill Core	0.81	3.78	0.66	4.31	0.96	3.03	0.45	3.06	0.50	2.2	29.6	2.3	227	89.1	6.8	0.6	0.3	<0.1	0.4	3.6
JSH-17113	Drill Core	0.71	2.10	0.36	2.58	0.55	1.69	0.25	1.77	0.27	0.3	98.5	1.1	30	10.0	<0.5	<0.1	<0.1	<0.1	<0.1	2.2
PHYA_BCR-2	Pulp	1.90	6.59	1.06	6.28	1.34	3.72	0.53	3.31	0.50											
PHYA_W2-A	Pulp	1.07	3.65	0.63	3.73	0.84	2.27	0.32	2.05	0.30											
JSH-17116	Drill Core	0.95	4.22	0.72	4.77	1.17	3.57	0.56	3.64	0.58	0.5	39.6	7.3	164	2.2	0.6	0.2	<0.1	<0.1	0.1	9.5
JSH-17118	Drill Core	0.56	1.80	0.29	2.07	0.49	1.60	0.22	1.60	0.25	0.4	7.4	1.5	34	11.0	0.6	<0.1	<0.1	<0.1	<0.1	0.5
JSH-17121	Drill Core	1.45	3.90	0.54	2.64	0.45	1.22	0.14	0.95	0.14	0.7	131.1	3.9	65	2.6	0.5	0.1	<0.1	<0.1	0.1	3.1
JSH-17122	Drill Core	1.10	5.95	1.05	6.74	1.48	5.06	0.75	5.01	0.82	0.2	3.6	1.8	84	0.7	2.1	<0.1	<0.1	<0.1	<0.1	0.6
JSH-17127	Drill Core	1.10	4.71	0.86	5.72	1.32	4.25	0.62	4.13	0.67	0.2	3.3	1.1	112	0.9	0.7	<0.1	<0.1	<0.1	<0.1	<0.5
JSH-17129	Drill Core	0.96	3.93	0.64	3.98	0.88	2.84	0.41	3.00	0.46	1.1	85.1	11.5	551	334.1	4.8	4.3	0.2	1.3	1.3	4.3
JSH-17130	Drill Core	1.24	4.15	0.63	3.82	0.82	2.14	0.29	1.92	0.28	0.4	164.9	1.7	49	59.6	0.5	<0.1	<0.1	<0.1	0.1	2.3
JSH-17133	Drill Core	0.98	4.53	0.81	5.24	1.32	4.21	0.63	4.45	0.68	0.1	2.5	0.8	73	1.1	<0.5	<0.1	<0.1	<0.1	<0.1	0.7

BUREAU VERITAS MINERAL LABORATORIES Canada

www.bureauveritas.com/um

Bureau Veritas Commodities Canada Ltd.
9050 Shaughnessy St Vancouver British Columbia V6P 6E5 Canada
PHONE (604) 253-3158

Client: **Pyhasalmi Mine OY**
Box 51
Pyhasalmi FIN-86801 Finland

Project: Pyhasalmi alteration
Report Date: May 09, 2018

CERTIFICATE OF ANALYSIS VAN18000623A.1

		Method	AQ200	AQ200	AQ200
		Analyte	Hg	Tl	Se
		Unit	ppm	ppm	ppm
		MDL	0.01	0.1	0.5
JSH-17001	Drill Core		0.02	<0.1	<0.5
JSH-17004	Drill Core		<0.01	0.4	<0.5
JSH-17008	Drill Core		0.09	82.1	1.8
JSH-17010	Drill Core		1.25	0.5	11.1
JSH-17012	Drill Core		0.09	3.5	2.3
JSH-17013	Drill Core		0.01	0.2	<0.5
JSH-17014	Drill Core		<0.01	0.3	<0.5
JSH-17071	Drill Core		0.02	0.2	<0.5
JSH-17072	Drill Core		0.01	<0.1	<0.5
JSH-17080	Drill Core		0.07	20.6	11.4
JSH-17082	Drill Core		6.03	1.6	8.2
JSH-17091	Drill Core		0.04	1.1	<0.5
JSH-17093	Drill Core		0.01	0.2	<0.5
JSH-17096	Drill Core		<0.01	0.2	<0.5
JSH-17100	Drill Core		0.01	0.1	<0.5
JSH-17102	Drill Core		<0.01	0.3	<0.5
JSH-17103	Drill Core		<0.01	0.2	<0.5
JSH-17106	Drill Core		<0.01	0.1	<0.5
JSH-17112	Drill Core		0.01	<0.1	1.5
JSH-17113	Drill Core		<0.01	0.1	0.6
PHYA_BCR-2	Pulp				
PHYA_W2-A	Pulp				
JSH-17116	Drill Core		0.04	0.1	<0.5
JSH-17118	Drill Core		<0.01	<0.1	<0.5
JSH-17121	Drill Core		0.02	<0.1	<0.5
JSH-17122	Drill Core		<0.01	<0.1	<0.5
JSH-17127	Drill Core		<0.01	0.3	<0.5
JSH-17129	Drill Core		0.01	<0.1	2.9
JSH-17130	Drill Core		<0.01	<0.1	<0.5
JSH-17133	Drill Core		<0.01	0.4	<0.5

BUREAU VERITAS MINERAL LABORATORIES Canada

www.bureauveritas.com/um

Bureau Veritas Commodities Canada Ltd.
9050 Shaughnessy St Vancouver British Columbia V6P 6E5 Canada
PHONE (604) 253-3158

Client: **Pyhasalmi Mine OY**
Box 51
Pyhasalmi FIN-86801 Finland

Project: Pyhasalmi alteration
Report Date: May 09, 2018

CERTIFICATE OF ANALYSIS VAN18000623A.1

	Method	WGHT	XF700	XF700	XF700	XF700	XF700	XF700	XF700	XF700	XF700	XF700	XF700	XF700	XF700	XF700	XF700	TC000	TC000	LF100	LF100
	Analyte	Wgt	SiO2	Al2O3	Fe2O3	CaO	MgO	Na2O	K2O	MnO	TiO2	P2O5	Cr2O3	Ba	LOI	SO3	Sr	TOT/C	TOT/S	Ba	Be
	Unit	kg	%	%	%	%	%	%	%	%	%	%	%	%	%	%	%	%	%	ppm	ppm
	MDL	0.01	0.01	0.01	0.01	0.01	0.01	0.01	0.01	0.01	0.01	0.01	0.01	0.01	-5.11	0.002	0.002	0.02	0.02	1	1
JSH-17134	Drill Core	0.21	77.10	11.60	3.40	0.52	0.41	5.52	0.99	0.07	0.19	0.03	<0.01	0.02	0.03	0.031	0.006	0.02	<0.02	152	3
JSH-17137	Drill Core	0.17	73.20	12.70	4.39	1.58	1.12	4.38	1.45	0.13	0.22	0.04	<0.01	0.02	0.31	0.014	0.005	0.03	<0.02	125	2
JSH-17139	Drill Core	0.22	45.80	16.10	18.30	4.47	6.32	4.00	2.66	0.15	1.02	0.12	<0.01	0.03	0.54	0.912	0.009	0.03	0.37	287	<1

BUREAU VERITAS MINERAL LABORATORIES Canada

www.bureauveritas.com/um

Bureau Veritas Commodities Canada Ltd.
9050 Shaughnessy St Vancouver British Columbia V6P 6E5 Canada
PHONE (604) 253-3158

Client: **Pyhasalmi Mine OY**
Box 51
Pyhasalmi FIN-86801 Finland

Project: Pyhasalmi alteration
Report Date: May 09, 2018

CERTIFICATE OF ANALYSIS VAN18000623A.1

	Method	LF100	LF100	LF100	LF100	LF100	LF100	LF100	LF100	LF100	LF100	LF100	LF100	LF100	LF100	LF100	LF100	LF100	LF100	LF100	LF100
	Analyte	Co	Cs	Ga	Hf	Nb	Rb	Sn	Sr	Ta	Th	U	V	W	Zr	Y	La	Ce	Pr	Nd	Sm
	Unit	ppm	ppm	ppm	ppm	ppm	ppm	ppm	ppm	ppm	ppm	ppm	ppm	ppm	ppm	ppm	ppm	ppm	ppm	ppm	ppm
	MDL	0.2	0.1	0.5	0.1	0.1	0.1	1	0.5	0.1	0.2	0.1	8	0.5	0.1	0.1	0.1	0.1	0.02	0.3	0.05
JSH-17134	Drill Core	0.8	2.2	11.0	4.0	5.6	36.9	1	59.7	0.4	3.4	1.5	<8	<0.5	134.5	33.7	16.1	33.9	3.91	15.7	3.78
JSH-17137	Drill Core	2.1	7.2	11.8	4.5	6.7	112.8	9	52.1	0.5	3.5	1.5	<8	0.5	144.5	35.9	18.2	39.0	4.79	18.9	4.56
JSH-17139	Drill Core	50.0	8.1	16.7	1.5	2.2	45.5	<1	79.4	<0.1	0.8	0.3	358	<0.5	48.2	20.8	6.4	14.4	1.98	9.6	2.45

BUREAU VERITAS MINERAL LABORATORIES Canada

Bureau Veritas Commodities Canada Ltd.
9050 Shaughnessy St Vancouver British Columbia V6P 6E5 Canada
PHONE (604) 253-3158

www.bureauveritas.com/um

Client: **Pyhasalmi Mine OY**
Box 51
Pyhasalmi FIN-86801 Finland

Project: Pyhasalmi alteration
Report Date: May 09, 2018

CERTIFICATE OF ANALYSIS VAN18000623A.1

	Method	LF100	LF100	LF100	LF100	LF100	LF100	LF100	LF100	LF100	AQ200	AQ200	AQ200	AQ200	AQ200	AQ200	AQ200	AQ200	AQ200	AQ200	AQ200
	Analyte	Eu	Gd	Tb	Dy	Ho	Er	Tm	Yb	Lu	Mo	Cu	Pb	Zn	Ni	As	Cd	Sb	Bi	Ag	Au
	Unit	ppm	ppm	ppm	ppm	ppm	ppm	ppm	ppm	ppm	ppm	ppm	ppm	ppm	ppm	ppm	ppm	ppm	ppm	ppm	ppb
	MDL	0.02	0.05	0.01	0.05	0.02	0.03	0.01	0.05	0.01	0.1	0.1	0.1	1	0.1	0.5	0.1	0.1	0.1	0.1	0.5
JSH-17134	Drill Core	0.83	4.62	0.84	5.95	1.39	4.35	0.66	4.27	0.76	0.2	3.2	1.1	47	1.0	<0.5	<0.1	<0.1	<0.1	<0.1	0.7
JSH-17137	Drill Core	0.88	5.13	0.90	5.76	1.33	4.38	0.65	4.80	0.73	<0.1	2.0	1.7	110	5.1	<0.5	<0.1	<0.1	<0.1	<0.1	1.4
JSH-17139	Drill Core	0.72	3.06	0.55	3.62	0.90	2.65	0.40	2.70	0.43	0.3	97.3	0.9	99	4.4	<0.5	<0.1	<0.1	<0.1	0.1	3.2

BUREAU VERITAS MINERAL LABORATORIES Canada

www.bureauveritas.com/um

Bureau Veritas Commodities Canada Ltd.

9050 Shaughnessy St Vancouver British Columbia V6P 6E5 Canada

PHONE (604) 253-3158

Client: **Pyhasalmi Mine OY**
Box 51
Pyhasalmi FIN-86801 Finland

Project: Pyhasalmi alteration
Report Date: May 09, 2018

CERTIFICATE OF ANALYSIS VAN18000623A.1

		Method	AQ200	AQ200	AQ200
		Analyte	Hg	Tl	Se
		Unit	ppm	ppm	ppm
		MDL	0.01	0.1	0.5
JSH-17134	Drill Core		<0.01	0.3	<0.5
JSH-17137	Drill Core		<0.01	0.8	<0.5
JSH-17139	Drill Core		<0.01	0.7	0.6

BUREAU VERITAS MINERAL LABORATORIES Canada

www.bureauveritas.com/um

Bureau Veritas Commodities Canada Ltd.
9050 Shaughnessy St Vancouver British Columbia V6P 6E5 Canada
PHONE (604) 253-3158

Client: **Pyhasalmi Mine OY**
Box 51
Pyhasalmi FIN-86801 Finland

Project: Pyhasalmi alteration
Report Date: May 09, 2018

QUALITY CONTROL REPORT VAN18000623A.1

	Method	WGHT	XF700	XF700	XF700	XF700	XF700	XF700	XF700	XF700	XF700	XF700	XF700	XF700	XF700	XF700	XF700	TC000	TC000	LF100	LF100
	Analyte	Wgt	SiO2	Al2O3	Fe2O3	CaO	MgO	Na2O	K2O	MnO	TiO2	P2O5	Cr2O3	Ba	LOI	SO3	Sr	TOT/C	TOT/S	Ba	Be
	Unit	kg	%	%	%	%	%	%	%	%	%	%	%	%	%	%	%	%	%	ppm	ppm
	MDL	0.01	0.01	0.01	0.01	0.01	0.01	0.01	0.01	0.01	0.01	0.01	0.01	0.01	-5.11	0.002	0.002	0.02	0.02	1	1
JSH-17091	Drill Core	0.17	68.40	13.80	4.00	0.63	1.82	2.34	7.22	0.05	0.29	0.04	<0.01	0.23	0.49	1.340	0.003	0.03	0.59	2204	<1
Pulp Duplicates																					
JSH-17012	Drill Core	0.23	54.90	14.70	9.61	8.17	5.05	3.01	0.95	0.19	1.54	0.83	0.02	0.10	0.59	1.220	0.080	0.03	0.50	953	1
REP JSH-17012	QC																				
JSH-17080	Drill Core	0.18	48.40	16.50	11.60	8.32	6.64	3.59	0.72	0.21	1.97	0.39	0.01	0.04	1.16	3.100	0.068	0.08	1.67	361	<1
REP JSH-17080	QC																				
JSH-17082	Drill Core	0.15	51.50	3.97	4.81	11.90	21.70	0.49	0.05	0.48	0.11	0.06	<0.01	0.04	3.21	4.040	<0.002	0.17	2.04	487	<1
REP JSH-17082	QC																			479	1
JSH-17093	Drill Core	0.20	71.70	13.70	4.16	3.03	0.65	4.43	1.32	0.08	0.34	0.09	<0.01	0.07	0.34	0.332	0.015	0.05	0.15	684	<1
REP JSH-17093	QC		71.60	13.70	4.17	3.02	0.65	4.45	1.34	0.08	0.35	0.09	<0.01	0.07	0.34	0.374	0.017				
JSH-17113	Drill Core	0.25	52.50	15.30	11.60	7.92	5.25	5.16	0.38	0.18	0.73	0.14	<0.01	<0.01	0.36	0.524	0.015	0.03	0.28	53	<1
REP JSH-17113	QC																				
JSH-17137	Drill Core	0.17	73.20	12.70	4.39	1.58	1.12	4.38	1.45	0.13	0.22	0.04	<0.01	0.02	0.31	0.014	0.005	0.03	<0.02	125	2
REP JSH-17137	QC																	0.03	<0.02		
Reference Materials																					
STD DS11	Standard																				
STD DS11	Standard																				
STD DS11	Standard																				
STD GS311-1	Standard																	0.99	2.26		
STD GS910-4	Standard																	2.71	8.33		
STD OREAS184	Standard		41.90	4.60	39.20	0.22	3.08	<0.01	<0.01	0.67	0.06	0.02	1.71	0.02	6.24	0.002	<0.002				
STD OREAS45EA	Standard																				
STD OREAS45EA	Standard																				
STD OREAS45EA	Standard																				
STD SO-19	Standard																			463	22
STD SO-19	Standard																			466	14
STD SY-4(D)	Standard		49.90	20.80	6.18	8.02	0.53	7.26	1.66	0.11	0.30	0.16	<0.01	0.03	4.56	0.084	0.124				
STD GS311-1 Expected																		1.02	2.35		
STD GS910-4 Expected																		2.65	8.27		

BUREAU VERITAS MINERAL LABORATORIES Canada

www.bureauveritas.com/um

Bureau Veritas Commodities Canada Ltd.
9050 Shaughnessy St Vancouver British Columbia V6P 6E5 Canada
PHONE (604) 253-3158

Client: **Pyhasalmi Mine OY**
Box 51
Pyhasalmi FIN-86801 Finland

Project: Pyhasalmi alteration
Report Date: May 09, 2018

QUALITY CONTROL REPORT VAN18000623A.1

	Method	LF100	LF100	LF100	LF100	LF100	LF100	LF100	LF100	LF100	LF100	LF100	LF100	LF100	LF100	LF100	LF100	LF100	LF100	LF100	LF100
	Analyte	Co	Cs	Ga	Hf	Nb	Rb	Sn	Sr	Ta	Th	U	V	W	Zr	Y	La	Ce	Pr	Nd	Sm
	Unit	ppm	ppm	ppm	ppm	ppm	ppm	ppm	ppm	ppm	ppm	ppm	ppm	ppm	ppm	ppm	ppm	ppm	ppm	ppm	ppm
	MDL	0.2	0.1	0.5	0.1	0.1	0.1	1	0.5	0.1	0.2	0.1	8	0.5	0.1	0.1	0.1	0.1	0.02	0.3	0.05
JSH-17091	Drill Core	4.3	11.5	15.7	5.5	8.2	202.6	1	33.4	0.5	4.1	1.5	19	<0.5	193.4	39.1	20.0	43.0	5.36	23.3	5.52
Pulp Duplicates																					
JSH-17012	Drill Core	26.6	0.5	19.1	4.1	15.4	15.4	2	731.3	0.8	4.0	1.9	152	0.9	171.1	17.8	50.3	107.9	13.51	55.5	9.26
REP JSH-17012	QC																				
JSH-17080	Drill Core	38.4	0.4	20.3	3.1	4.7	7.7	1	658.0	0.3	0.8	0.3	224	<0.5	116.2	23.0	16.1	36.5	5.07	24.1	5.64
REP JSH-17080	QC																				
JSH-17082	Drill Core	0.7	0.1	9.2	1.4	1.6	0.4	2	28.9	0.2	0.5	1.2	28	<0.5	50.5	25.0	6.5	23.8	3.68	16.8	3.86
REP JSH-17082	QC	0.6	<0.1	10.1	1.6	1.7	0.4	2	29.0	0.2	0.5	0.9	27	<0.5	53.8	26.1	7.4	24.9	3.89	17.0	3.86
JSH-17093	Drill Core	7.1	2.4	12.9	3.1	5.9	26.1	<1	164.0	0.5	3.9	1.6	21	<0.5	114.0	23.8	16.8	32.2	3.70	14.8	3.16
REP JSH-17093	QC																				
JSH-17113	Drill Core	41.9	0.8	13.7	0.9	1.4	4.5	<1	162.4	<0.1	0.5	1.2	293	<0.5	33.6	14.3	4.9	10.1	1.39	6.0	1.73
REP JSH-17113	QC																				
JSH-17137	Drill Core	2.1	7.2	11.8	4.5	6.7	112.8	9	52.1	0.5	3.5	1.5	<8	0.5	144.5	35.9	18.2	39.0	4.79	18.9	4.56
REP JSH-17137	QC																				
Reference Materials																					
STD DS11	Standard																				
STD DS11	Standard																				
STD DS11	Standard																				
STD GS311-1	Standard																				
STD GS910-4	Standard																				
STD OREAS184	Standard																				
STD OREAS45EA	Standard																				
STD OREAS45EA	Standard																				
STD OREAS45EA	Standard																				
STD SO-19	Standard	21.2	4.5	15.3	3.1	64.7	18.6	17	310.8	4.7	12.3	18.5	164	8.6	106.6	34.9	68.8	150.6	18.14	72.6	12.61
STD SO-19	Standard	22.7	4.1	15.1	3.2	64.6	18.8	18	314.5	4.7	13.1	19.9	155	10.2	106.9	34.1	68.6	155.1	18.80	72.9	13.36
STD SY-4(D)	Standard																				
STD GS311-1 Expected																					
STD GS910-4 Expected																					

BUREAU VERITAS MINERAL LABORATORIES Canada

www.bureauveritas.com/um

Bureau Veritas Commodities Canada Ltd.
9050 Shaughnessy St Vancouver British Columbia V6P 6E5 Canada
PHONE (604) 253-3158

Client: **Pyhasalmi Mine OY**
Box 51
Pyhasalmi FIN-86801 Finland

Project: Pyhasalmi alteration
Report Date: May 09, 2018

QUALITY CONTROL REPORT VAN18000623A.1

	Method	LF100	LF100	LF100	LF100	LF100	LF100	LF100	LF100	LF100	AQ200	AQ200	AQ200	AQ200	AQ200	AQ200	AQ200	AQ200	AQ200	AQ200	AQ200
	Analyte	Eu	Gd	Tb	Dy	Ho	Er	Tm	Yb	Lu	Mo	Cu	Pb	Zn	Ni	As	Cd	Sb	Bi	Ag	Au
	Unit	ppm	ppm	ppm	ppm	ppm	ppm	ppm	ppm	ppm	ppm	ppm	ppm	ppm	ppm	ppm	ppm	ppm	ppm	ppm	ppb
	MDL	0.02	0.05	0.01	0.05	0.02	0.03	0.01	0.05	0.01	0.1	0.1	0.1	1	0.1	0.5	0.1	0.1	0.1	0.1	0.5
JSH-17091	Drill Core	0.95	6.02	1.07	6.84	1.58	4.99	0.76	4.97	0.77	1.0	43.0	21.7	467	3.2	1.5	1.8	<0.1	0.2	0.7	73.3
Pulp Duplicates																					
JSH-17012	Drill Core	2.54	6.89	0.84	4.07	0.65	1.69	0.22	1.40	0.20	0.5	251.8	7.2	131	46.5	40.6	<0.1	0.2	2.0	0.2	43.9
REP JSH-17012	QC										0.9	254.3	7.7	135	47.4	41.4	<0.1	0.2	2.3	0.2	46.6
JSH-17080	Drill Core	1.84	5.23	0.76	4.52	0.89	2.56	0.34	2.22	0.29	0.4	830.8	159.4	178	51.5	74.9	0.3	2.2	13.6	1.4	245.0
REP JSH-17080	QC										0.5	834.2	157.6	178	52.0	75.3	0.3	2.3	13.8	1.5	235.9
JSH-17082	Drill Core	0.96	3.75	0.64	4.01	0.85	2.66	0.41	2.72	0.47	0.2	>10000	79.8	1283	1.1	126.4	7.5	1.5	9.8	40.6	65545.2
REP JSH-17082	QC	1.01	3.66	0.63	3.86	0.88	2.81	0.42	2.80	0.46											
JSH-17093	Drill Core	0.73	3.49	0.60	3.59	0.82	2.76	0.43	3.08	0.48	0.4	78.2	2.7	69	4.3	1.8	<0.1	<0.1	<0.1	0.1	18.0
REP JSH-17093	QC																				
JSH-17113	Drill Core	0.71	2.10	0.36	2.58	0.55	1.69	0.25	1.77	0.27	0.3	98.5	1.1	30	10.0	<0.5	<0.1	<0.1	<0.1	<0.1	2.2
REP JSH-17113	QC										0.3	95.1	1.1	29	9.5	0.5	<0.1	<0.1	<0.1	<0.1	2.4
JSH-17137	Drill Core	0.88	5.13	0.90	5.76	1.33	4.38	0.65	4.80	0.73	<0.1	2.0	1.7	110	5.1	<0.5	<0.1	<0.1	<0.1	<0.1	1.4
REP JSH-17137	QC																				
Reference Materials																					
STD DS11	Standard										13.5	149.5	135.7	356	79.8	42.0	2.4	7.1	11.8	2.0	80.4
STD DS11	Standard										13.3	149.4	130.8	341	77.5	42.6	2.2	7.1	10.9	1.6	75.7
STD DS11	Standard										13.7	148.7	131.7	352	77.8	41.7	2.4	6.9	11.5	1.7	61.1
STD GS311-1	Standard																				
STD GS910-4	Standard																				
STD OREAS184	Standard																				
STD OREAS45EA	Standard										1.4	723.2	13.4	31	418.6	12.7	<0.1	0.3	0.3	0.3	58.5
STD OREAS45EA	Standard										1.7	686.7	13.2	31	393.8	12.3	<0.1	0.3	0.2	0.3	62.1
STD OREAS45EA	Standard										1.7	703.3	13.6	33	402.9	12.9	<0.1	0.3	0.3	0.3	61.4
STD SO-19	Standard	3.45	10.09	1.31	7.36	1.30	3.67	0.52	3.27	0.48											
STD SO-19	Standard	3.44	9.94	1.34	7.10	1.31	3.88	0.52	3.30	0.49											
STD SY-4(D)	Standard																				
STD GS311-1 Expected																					
STD GS910-4 Expected																					

BUREAU VERITAS MINERAL LABORATORIES Canada

www.bureauveritas.com/um

Bureau Veritas Commodities Canada Ltd.
9050 Shaughnessy St Vancouver British Columbia V6P 6E5 Canada
PHONE (604) 253-3158

Client: **Pyhasalmi Mine OY**
Box 51
Pyhasalmi FIN-86801 Finland

Project: Pyhasalmi alteration
Report Date: May 09, 2018

QUALITY CONTROL REPORT VAN18000623A.1

		Method	AQ200	AQ200	AQ200
		Analyte	Hg	Tl	Se
		Unit	ppm	ppm	ppm
		MDL	0.01	0.1	0.5
JSH-17091	Drill Core		0.04	1.1	<0.5
Pulp Duplicates					
JSH-17012	Drill Core		0.09	3.5	2.3
REP JSH-17012	QC		0.08	3.6	2.0
JSH-17080	Drill Core		0.07	20.6	11.4
REP JSH-17080	QC		0.08	20.4	11.6
JSH-17082	Drill Core		6.03	1.6	8.2
REP JSH-17082	QC				
JSH-17093	Drill Core		0.01	0.2	<0.5
REP JSH-17093	QC				
JSH-17113	Drill Core		<0.01	0.1	0.6
REP JSH-17113	QC		<0.01	<0.1	0.6
JSH-17137	Drill Core		<0.01	0.8	<0.5
REP JSH-17137	QC				
Reference Materials					
STD DS11	Standard		0.31	5.0	2.1
STD DS11	Standard		0.25	4.8	2.3
STD DS11	Standard		0.26	5.4	2.2
STD GS311-1	Standard				
STD GS910-4	Standard				
STD OREAS184	Standard				
STD OREAS45EA	Standard		<0.01	<0.1	1.3
STD OREAS45EA	Standard		<0.01	<0.1	1.8
STD OREAS45EA	Standard		0.01	0.3	1.4
STD SO-19	Standard				
STD SO-19	Standard				
STD SY-4(D)	Standard				
STD GS311-1 Expected					
STD GS910-4 Expected					

BUREAU VERITAS MINERAL LABORATORIES Canada

www.bureauveritas.com/um

Bureau Veritas Commodities Canada Ltd.
9050 Shaughnessy St Vancouver British Columbia V6P 6E5 Canada
PHONE (604) 253-3158

Client: **Pyhasalmi Mine OY**
Box 51
Pyhasalmi FIN-86801 Finland

Project: Pyhasalmi alteration
Report Date: May 09, 2018

QUALITY CONTROL REPORT VAN18000623A.1

		WGHT Wgt kg 0.01	XF700 SiO2 % 0.01	XF700 Al2O3 % 0.01	XF700 Fe2O3 % 0.01	XF700 CaO % 0.01	XF700 MgO % 0.01	XF700 Na2O % 0.01	XF700 K2O % 0.01	XF700 MnO % 0.01	XF700 TiO2 % 0.01	XF700 P2O5 % 0.01	XF700 Cr2O3 % 0.01	XF700 Ba % 0.01	XF700 LOI % -5.11	XF700 SO3 % 0.002	XF700 Sr % 0.002	TC000 TOT/C % 0.02	TC000 TOT/S % 0.02	LF100 Ba ppm 1	LF100 Be ppm 1
STD SO-19 Expected																				486	20
STD OREAS45EA Expected																					
STD DS11 Expected																					
STD OREAS184 Expected			42.25	4.62	39.3	0.216	3.05			0.676	0.06	0.017	1.75		6.24						
STD SY-4(D) Expected			49.8	20.69	6.18		0.54	7.1	1.66	0.108	0.287	0.131		0.034	4.56		0.1203				
BLK	Blank																	<0.02	<0.02		
BLK	Blank																			<1	<1
BLK	Blank																				
BLK	Blank																				
SI BLK	Blank		98.10	0.33	0.03	0.01	0.02	0.01	0.01	<0.01	0.02	<0.01	<0.01	<0.01	0.00	<0.002	<0.002				
Prep Wash																					
ROCK-VAN	Prep Blank		70.80	13.90	2.94	2.08	0.95	4.72	2.08	0.09	0.35	0.09	<0.01	0.09	0.98	0.105	0.019	0.07	0.03	830	3
ROCK-VAN	Prep Blank		71.10	14.00	2.89	2.11	0.95	4.76	2.08	0.09	0.35	0.10	<0.01	0.09	0.96	0.107	0.019	0.07	0.03	836	1

BUREAU VERITAS MINERAL LABORATORIES Canada

www.bureauveritas.com/um

Bureau Veritas Commodities Canada Ltd.
9050 Shaughnessy St Vancouver British Columbia V6P 6E5 Canada
PHONE (604) 253-3158

Client: **Pyhasalmi Mine OY**
Box 51
Pyhasalmi FIN-86801 Finland

Project: Pyhasalmi alteration
Report Date: May 09, 2018

QUALITY CONTROL REPORT VAN18000623A.1

		LF100 Co ppm 0.2	LF100 Cs ppm 0.1	LF100 Ga ppm 0.5	LF100 Hf ppm 0.1	LF100 Nb ppm 0.1	LF100 Rb ppm 0.1	LF100 Sn ppm 1	LF100 Sr ppm 0.5	LF100 Ta ppm 0.1	LF100 Th ppm 0.2	LF100 U ppm 0.1	LF100 V ppm 8	LF100 W ppm 0.5	LF100 Zr ppm 0.1	LF100 Y ppm 0.1	LF100 La ppm 0.1	LF100 Ce ppm 0.1	LF100 Pr ppm 0.02	LF100 Nd ppm 0.3	LF100 Sm ppm 0.05
STD SO-19 Expected		24	4.5	17.5	3.1	68.5	19.5	19	317.1	4.9	13	19.4	165	9.8	112	35.5	71.3	161	19.4	75.7	13.7
STD OREAS45EA Expected																					
STD DS11 Expected																					
STD OREAS184 Expected																					
STD SY-4(D) Expected																					
BLK	Blank																				
BLK	Blank	<0.2	<0.1	<0.5	<0.1	0.1	<0.1	<1	<0.5	<0.1	<0.2	<0.1	<8	<0.5	<0.1	<0.1	<0.1	<0.1	0.05	<0.3	<0.05
BLK	Blank																				
BLK	Blank																				
SI BLK	Blank																				
Prep Wash																					
ROCK-VAN	Prep Blank	4.1	0.5	12.5	3.6	6.6	32.4	<1	188.8	0.4	2.8	1.5	48	<0.5	135.4	15.6	13.6	23.8	2.92	11.8	2.67
ROCK-VAN	Prep Blank	3.5	0.4	12.1	2.9	6.5	31.9	<1	185.4	0.4	3.0	1.3	40	<0.5	122.8	16.7	14.5	25.0	2.90	11.8	2.46

BUREAU VERITAS MINERAL LABORATORIES Canada

www.bureauveritas.com/um

Bureau Veritas Commodities Canada Ltd.
9050 Shaughnessy St Vancouver British Columbia V6P 6E5 Canada
PHONE (604) 253-3158

Client: **Pyhasalmi Mine OY**
Box 51
Pyhasalmi FIN-86801 Finland

Project: Pyhasalmi alteration
Report Date: May 09, 2018

QUALITY CONTROL REPORT VAN18000623A.1

		LF100 Eu ppm 0.02	LF100 Gd ppm 0.05	LF100 Tb ppm 0.01	LF100 Dy ppm 0.05	LF100 Ho ppm 0.02	LF100 Er ppm 0.03	LF100 Tm ppm 0.01	LF100 Yb ppm 0.05	LF100 Lu ppm 0.01	AQ200 Mo ppm 0.1	AQ200 Cu ppm 0.1	AQ200 Pb ppm 0.1	AQ200 Zn ppm 1	AQ200 Ni ppm 0.1	AQ200 As ppm 0.5	AQ200 Cd ppm 0.1	AQ200 Sb ppm 0.1	AQ200 Bi ppm 0.1	AQ200 Ag ppm 0.1	AQ200 Au ppb 0.5
STD SO-19 Expected		3.81	10.53	1.41	7.5	1.39	3.78	0.55	3.55	0.53											
STD OREAS45EA Expected											1.6	709	14.3	31.4	381	10.3	0.03	0.32	0.26	0.26	53
STD DS11 Expected											13.9	149	138	345	77.7	42.8	2.37	7.2	12.2	1.71	79
STD OREAS184 Expected																					
STD SY-4(D) Expected																					
BLK	Blank																				
BLK	Blank	<0.02	<0.05	<0.01	<0.05	<0.02	<0.03	<0.01	<0.05	<0.01											
BLK	Blank										<0.1	<0.1	<0.1	<1	<0.1	<0.5	<0.1	<0.1	<0.1	<0.1	<0.5
BLK	Blank										<0.1	<0.1	<0.1	<1	<0.1	<0.5	<0.1	<0.1	<0.1	<0.1	<0.5
SI BLK	Blank																				
Prep Wash																					
ROCK-VAN	Prep Blank	0.71	2.67	0.43	2.67	0.58	1.98	0.29	2.05	0.35	1.5	7.6	1.6	36	1.6	1.5	<0.1	<0.1	<0.1	<0.1	2.7
ROCK-VAN	Prep Blank	0.72	2.57	0.42	2.70	0.58	1.92	0.30	2.14	0.36	1.2	8.4	1.4	37	0.7	<0.5	<0.1	<0.1	<0.1	<0.1	2.9

BUREAU VERITAS MINERAL LABORATORIES Canada

www.bureauveritas.com/um

Bureau Veritas Commodities Canada Ltd.
9050 Shaughnessy St Vancouver British Columbia V6P 6E5 Canada
PHONE (604) 253-3158

Client: **Pyhasalmi Mine OY**
Box 51
Pyhasalmi FIN-86801 Finland

Project: Pyhasalmi alteration
Report Date: May 09, 2018

QUALITY CONTROL REPORT VAN18000623A.1

		AQ200 Hg ppm 0.01	AQ200 Tl ppm 0.1	AQ200 Se ppm 0.5
STD SO-19 Expected				
STD OREAS45EA Expected			0.072	0.78
STD DS11 Expected		0.26	4.9	2.2
STD OREAS184 Expected				
STD SY-4(D) Expected				
BLK	Blank			
BLK	Blank			
BLK	Blank	<0.01	<0.1	<0.5
BLK	Blank	<0.01	<0.1	<0.5
SI BLK	Blank			
Prep Wash				
ROCK-VAN	Prep Blank	<0.01	<0.1	<0.5
ROCK-VAN	Prep Blank	<0.01	<0.1	<0.5

Appendix 4.a. PYO-47 XRF/AAS whole-rock geochemical data, by the courtesy of Pyhäsalmi Mine Oy:

HOLEID$	FROM	TO	X COORD	Y COORD	Z COORD	YEAR	SAMPLENO	SIO2_O %	TIO2_O %	AL2O3_O %	FE2O3_O %	MNO_O %	MGO_O %	CAO_O %	NA2O_O %	K2O_O %	P2O5_O %
PYO47	1.65	2.45	7062228	3453140.5	150.52	1983	8336879	69.9	0.131	11.6	2.545536	0.051	1.01	1.78	1.78	3.98	0.007
PYO47	2.45	3.27	7062228	3453140.25	149.74	1983	8336880	50.1	0.366	13.9	10.6379	0.332	6.14	11.2	1.12	1.48	0.032
PYO47	3.27	5.47	7062228	3453140	148.28	1983	8336881	72.7	0.135	11.6	2.145365	0.052	0.71	3.19	0.87	3.48	0.003
PYO47	5.47	6.68	7062228.5	3453139.5	146.63	1983	8336882	48.1	0.51	13.4	11.44936	0.28	6.81	9.85	1.32	1.22	0.167
PYO47	7.89	11	7062228.5	3453138.5	143.38	1983	8336883	71.2	0.134	13.4	2.634464	0.069	0.51	2.7	1.08	4.92	0.003
PYO47	11	14.06	7062228.5	3453137.75	140.4	1983	8336884	75.8	0.12	11.4	2.601116	0.09	0.23	3.62	1.14	2.16	0.003
PYO47	15	17.94	7062228.5	3453136.75	136.59	1983	8336885	73.9	0.139	11.1	2.701159	0.092	0.36	2.54	1.84	2.56	0.01
PYO47	17.94	20.66	7062229	3453136	133.86	1983	8336886	70.7	0.136	11.6	2.634464	0.054	0.29	2.71	1.64	2.95	0.006
PYO47	20.66	22.45	7062229	3453135.5	131.68	1983	8336887	72.1	0.131	11.9	3.034635	0.066	0.47	2.73	1.83	2.73	0.003
PYO47	23.77	26.4	7062229	3453134.5	128.27	1983	8336888	68.7	0.15	12.9	3.790515	0.086	0.51	3.16	2.56	2.2	0.009
PYO47	27.7	29.67	7062229.5	3453133.75	124.79	1983	8336889	73.3	0.105	10.7	2.623348	0.037	0.11	1.75	2.13	2.72	0.007
PYO47	29.67	30.48	7062229.5	3453133.25	123.45	1983	8336890	66.7	0.104	9.94	8.425837	0.077	0.74	1.82	1.47	3.43	0.003
PYO47	30.48	32.34	7062229.5	3453133	122.16	1983	8336891	77	0.117	9.83	5.535708	0.109	0.44	3.92	1.62	1.63	0.003

PYO47	32.34	36.64	7062229.5	3453132.25	119.19	1983	8336892	71.3	0.14	12.4	2.756738	0.045	0.3	2.04	2.33	3.43	0.022
PYO47	36.64	38.5	7062229.5	3453131.5	116.21	1983	8336893	70.6	0.144	12.7	2.979056	0.059	0.47	2.31	2.63	2.55	0.007
PYO47	41.8	42.57	7062230	3453130.25	111.75	1983	8336894	77.5	0.108	11.3	2.167597	0.064	0.44	3.74	2.53	0.56	0.013
PYO47	42.57	42.9	7062230	3453130	111.22	1983	8336895	51.7	0.976	19.3	10.72682	0.15	1.49	4.45	4.11	3.62	0.137
PYO47	42.9	44.05	7062230	3453130	110.51	1983	8336896	67.4	0.3	14.5	5.057725	0.089	0.64	2.26	2.92	4.1	0.073
PYO47	44.05	47.43	7062230	3453129.25	108.32	1983	8336897	73	0.123	12	1.911931	0.039	0.13	1.98	2.99	2.46	0.007
PYO47	47.43	48.5	7062230	3453128.75	106.17	1983	8336898	49.6	0.415	14.6	11.67167	0.379	5.67	12.2	3.04	0.61	0.056
PYO47	48.5	50.65	7062230	3453128.25	104.61	1983	8336899	73.7	0.119	11.3	2.445494	0.044	0.32	2.31	3.37	1.18	0.011
PYO47	69.8	73.8	7062231	3453122.75	83.15	1983	8336900	60.4	0.712	13.5	10.20438	0.185	1.92	5	4.27	0.69	0.261
PYO47	73.8	78.11	7062231.5	3453121.5	79.14	1983	8336901	54	0.458	13.9	8.859356	0.168	3.96	6.22	4.69	0.68	0.04
PYO47	78.11	79.81	7062231.5	3453120.75	76.24	1983	8336902	57.6	0.759	12.9	11.22704	0.17	2.99	4.85	3.75	1.31	0.217
PYO47	79.81	82.28	7062231.5	3453120.25	74.24	1983	8336903	51.8	0.526	12.8	11.67167	0.223	3.62	10.6	2.81	0.41	0.091
PYO47	82.28	84	7062232	3453119.75	72.22	1983	8336904	50.9	0.699	13.7	13.11674	0.18	3.56	7.95	4.36	0.45	0.109
PYO47	84	86.9	7062232	3453119	70	1983	8336905	53.3	0.558	13.9	10.39335	0.195	3.61	9.28	3.79	0.36	0.11
PYO47	87.82	89.88	7062232	3453118.25	66.73	1983	8336906	50.2	0.784	13.5	14.00601	0.202	4.26	6.12	2.87	1.42	0.145
PYO47	89.88	91.75	7062232	3453117.5	64.85	1983	8336907	56.9	0.464	16.2	7.303133	0.159	1.91	6.69	4.28	0.55	0.26

PYO47	93	96.8	7062232.5	3453116.5	60.93	1983	8336908	54.6	0.523	15.2	7.77	0.134	2.16	5.37	3.87	1.27	0.302
PYO47	105.72	110.72	7062233	3453112.5	48.22	1983	8336909	51.1	0.459	13.6	10.05987	0.187	4.5	6.35	5.23	0.31	0.077
PYO47	110.72	115.72	7062233.5	3453111	43.48	1983	8336910	50	0.558	13.8	10.5712	0.202	5.34	5.17	4.74	1.31	0.053
PYO47	115.72	120.55	7062233.5	3453109.5	38.83	1983	8336911	51.8	0.489	14.7	9.615236	0.173	4.48	5.54	4.84	1.26	0.08
PYO47	120.55	122.4	7062234	3453108.25	35.69	1983	8336912	55.5	1.08	13	11.44936	0.196	2.9	4.51	2.35	2.51	0.559
PYO47	122.4	126.48	7062234	3453107.25	32.91	1983	8336913	70.3	0.217	12	4.279614	0.065	0.41	1.7	3.5	2.29	0.02
PYO47	126.48	129.86	7062234	3453106	29.41	1983	8336914	48.1	0.575	12.5	11.78283	0.22	6.02	9.04	3.35	0.86	0.157
PYO47	129.86	135.5	7062234.5	3453104.5	25.2	1983	8336915	75.6	0.128	11.1	2.756738	0.046	0.3	1.7	3.08	2.76	0.009
PYO47	135.5	140	7062235	3453102.75	20.47	1983	8336916	56.2	0.706	13	12.00515	0.258	3.05	7.92	3.09	1.48	0.139
PYO47	140	141.9	7062235	3453101.5	17.49	1983	8336917	80.1	0.101	10.2	2.334335	0.03	0.2	1.65	2.19	2.9	0.003
PYO47	141.9	146.45	7062235	3453100.25	14.49	1983	8336918	53.5	0.747	14	13.89485	0.229	3.11	8.39	3.69	0.59	0.157
PYO47	146.45	146.8	7062235.5	3453099.5	12.21	1983	8336919	76.2	0.106	9.06	2.690043	0.045	0.38	2.68	2.6	0.6	0.006
PYO47	146.8	151	7062235.5	3453098.75	10.1	1983	8336920	50.4	0.844	13.7	14.00601	0.238	3.74	7.51	2.98	1.57	0.185
PYO47	151	153.95	7062235.5	3453097.25	6.78	1983	8336921	74.7	0.118	10.5	2.945708	0.049	0.24	2.23	2.6	1.9	0.003
PYO47	157.14	161.88	7062236	3453094.75	0.25	1983	8336922	73.3	0.121	10.6	1.945279	0.043	0.27	2.81	3.17	0.83	0.003
PYO47	161.88	165.35	7062236.5	3453093.25	-3.54	1983	8336923	73.4	0.104	10.4	3.657124	0.026	0.31	1.49	3.53	1.5	0.003

PYO47	165.35	170.35	7062236.5	3453091.5	-7.41	1983	8336924	46.2	0.521	14.2	11.11588	0.242	6.04	7.73	3.38	1.6	0.092
PYO47	170.35	172.43	7062237	3453090	-10.62	1983	8336925	47.9	0.511	13.5	12.00515	0.26	7.59	10.1	2.54	1.05	0.048
PYO47	172.43	173.75	7062237	3453089.25	-12.14	1983	8336926	79	0.099	9.51	1.478412	0.026	0.17	1.85	3.17	0.78	0.003
PYO47	173.75	175.2	7062237	3453088.75	-13.38	1983	8336927	56.6	0.729	14.6	9.948712	0.168	2.32	5.08	4.14	1.39	0.153
PYO47	175.2	177.2	7062237.5	3453088	-14.92	1983	8336928	74.1	0.094	9.49	3.379227	0.059	0.43	2.87	3.3	0.29	0.006
PYO47	177.2	177.94	7062237.5	3453087.5	-16.14	1983	8336929	48.8	0.775	16.6	12.44979	0.199	3.51	3.64	4.11	2.88	0.124
PYO47	177.94	179.73	7062237.5	3453086.75	-17.26	1983	8336930	80.8	0.108	9.52	3.179142	0.042	0.24	2.26	2.37	0.83	0.003
PYO47	179.73	181.17	7062237.5	3453086	-18.68	1983	8336931	52.3	0.821	13.1	14.45064	0.258	3.89	5.71	2.26	1.98	0.132
PYO47	181.17	181.89	7062238	3453085.5	-19.63	1983	8336932	73.9	0.13	13.1	3.123562	0.121	0.63	3.21	3.54	0.9	0.003
PYO47	181.89	183.69	7062238	3453085	-20.73	1983	8336933	76.5	0.139	12.5	2.134249	0.051	0.46	2.05	2.95	2.49	0.009
PYO47	183.69	187.44	7062238	3453083.75	-23.15	1983	8336934	70.7	0.141	12	2.434378	0.089	0.45	2.08	2.68	2.46	0.014
PYO47	193.5	196.08	7062239	3453079	-31.06	1983	8336935	76.3	0.136	10.9	2.523305	0.152	0.4	2.37	2.28	1.94	0.007
PYO47	196.08	197.05	7062239	3453078	-32.57	1983	8336936	56	0.499	16.1	7.447639	0.186	1.94	6.76	2	1.52	0.281
PYO47	206.42	211.42	7062240.5	3453071.5	-42.9	1983	8336937	57.2	0.511	16.4	7.080815	0.14	2.34	5.87	2.83	1.36	0.267
PYO47	211.42	213.97	7062240.5	3453069.25	-46.01	1983	8336938	59.9	0.504	17.1	6.947425	0.123	2.13	6	2.51	1.49	0.281
PYO47	213.97	214.84	7062241	3453068.25	-47.41	1983	8336939	59.6	0.489	16.5	6.713991	0.107	2.47	4.87	2.11	1.93	0.27

PYO47	214.84	215.66	7062241	3453067.75	-48.11	1983	8336940	73.8	0.184	11	6.113734	0.013	1.16	0.24	0.88	2.4	0.003
PYO47	215.66	217.33	7062241	3453067.25	-49.12	1983	8336941	69.5	0.217	13	7.636609	0.002	0.64	0.002	0.4	3.04	0.048
PYO47	217.33	219.45	7062241	3453066	-50.66	1983	8336942	60.3	0.409	12.5	7.147511	0.123	7.69	0.61	0.96	2.89	0.064
PYO47	219.45	221.85	7062241.5	3453064.75	-52.49	1983	8336943	64.9	0.221	13.6	9.404034	0.072	4.9	1	1.33	1.78	0.021
PYO47	221.85	223.2	7062241.5	3453063.75	-54	1983	8336944	49.6	0.898	14.7	7.603262	0.163	7.54	5.2	0.35	2.89	0.61
PYO47	223.2	228.2	7062242	3453061.75	-56.55	1983	8336945	70.9	0.225	12.1	4.123991	0.081	4.96	0.31	0.42	2.34	0.074
PYO47	228.2	233.2	7062242.5	3453058.75	-60.54	1983	8336946	68.5	0.247	14	4.457468	0.118	4.58	0.3	0.46	2.06	0.025
PYO47	233.2	237.85	7062243	3453056	-64.35	1983	8336947	68.1	0.205	13.9	2.601116	0.198	6.85	0.82	0.37	1.8	0.033
PYO47	237.85	241.37	7062243.5	3453053.5	-67.56	1983	8336948	70.5	0.233	14.1	2.501073	0.189	3.46	0.06	0.38	1.77	0.06
PYO47	241.37	243.42	7062243.5	3453051.75	-69.72	1983	8336949	73.7	0.212	13.5	3.023519	0.168	4.45	0.01	0.44	2.82	0.032
PYO47	253.33	256.62	7062245	3453043.75	-79.37	1983	8336950	65	0.233	15	5.735794	0.119	4.85	0.07	0.67	3.41	0.012
PYO47	256.62	262.1	7062245.5	3453041	-82.66	1983	8336951	70.8	0.236	12.9	1.934163	0.144	6.69	1.29	0.38	2.5	0.051
PYO47	262.1	264.95	7062246	3453038.25	-85.74	1983	8336952	71.2	0.237	13.6	2.512189	0.084	4.56	0.51	0.32	3.22	0.041
PYO47	264.95	268.57	7062246.5	3453036	-88.1	1983	8336953	69.1	0.243	12.6	3.201373	0.107	5.24	1.95	1.13	2.22	0.056
PYO47	271.47	271.94	7062247	3453032.75	-91.66	1983	8336954	59.1	1.18	14	6.680644	0.176	5.29	5.85	0.94	2.22	0.922
PYO47	271.94	276.94	7062247.5	3453030.75	-93.6	1983	8336955	74.5	0.218	12	3.056867	0.086	3.73	2.35	0.59	2.37	0.042

PYO47	276.94	280	7062248	3453028	-96.44	1983	8336956	71.6	0.223	12.6	2.634464	0.156	6.27	1.28	0.31	2.55	0.056
PYO47	280	282.28	7062248.5	3453026	-98.29	1983	8336957	73.3	0.222	13	2.667811	0.128	2.97	0.79	0.63	3.06	0.04
PYO47	282.28	285.17	7062248.5	3453024.25	-100.07	1983	8336958	71	0.228	13.3	2.200944	0.131	2.64	0.93	1.29	2.86	0.039
PYO47	285.17	290.17	7062249	3453021.25	-102.75	1983	8336959	74	0.226	13	3.079099	0.101	2.4	0.77	0.69	2.9	0.053
PYO47	290.17	295.17	7062249.5	3453017.75	-106.09	1983	8336960	69.2	0.256	15.9	2.545536	0.07	2.15	0.36	0.48	3.88	0.044
PYO47	295.17	300.17	7062250.5	3453014	-109.37	1983	8336961	69	0.254	15.7	2.578884	0.07	2.25	0.2	0.46	3.7	0.042
PYO47	300.17	303.7	7062251	3453010.75	-112.11	1983	8336962	70.6	0.247	13.7	3.145794	0.141	2.49	2.96	0.99	2.22	0.053
PYO47	303.7	304.95	7062251.5	3453009	-113.62	1983	8336963	59.3	0.521	17	6.836266	0.196	2.03	5.94	1.8	1.9	0.306
PYO47	304.95	309.95	7062251.5	3453006.5	-115.58	1983	8336964	73.3	0.205	12.2	3.868326	0.083	1.47	0.73	0.77	2.66	0.035
PYO47	309.95	314.95	7062252.5	3453002.75	-118.66	1983	8336965	74	0.234	14	3.646009	0.03	0.76	0.02	0.43	3.55	0.035
PYO47	314.95	318.9	7062253	3452999.25	-121.36	1983	8336966	73.7	0.231	13.6	4.66867	0.014	0.48	0.12	0.52	3.41	0.003
PYO47	318.9	319.8	7062253.5	3452997.25	-122.81	1983	8336967	62.5	0.153	9.73	16.11803	0.015	0.31	2.38	1.84	0.64	0.017
PYO47	319.8	321.3	7062253.5	3452996.25	-123.52	1983	8336968	73.6	0.196	12.2	5.024378	0.005	0.16	0.002	0.73	2.87	0.003
PYO47	322	324.5	7062254	3452994.25	-125.11	1983	8336969	71.5	0.189	10.7	11.07142	0.003	0.21	0.06	0.47	2.38	0.003
PYO47	324.5	326.4	7062254	3452992.5	-126.39	1983	8336970	48.6	0.656	16.2	11.22704	0.241	5.6	10.9	1.15	0.47	0.104
PYO47	326.4	331.17	7062254.5	3452989.75	-128.3	1983	8336971	60.1	0.194	11.2	18.78584	0.009	0.23	0.25	0.62	2.31	0.011

PYO47	331.17	331.83	7062255	3452987.5	-129.85	1983	8336972	55.1	0.376	14.5	6.158197	0.193	10.8	2.05	1.29	3.49	0.088
PYO47	331.83	333.96	7062255.5	3452986.25	-130.63	1983	8336973	71.7	0.221	13.3	7.125279	0.004	0.39	0.002	0.37	2.77	0.003
PYO47	333.96	334.93	7062255.5	3452985	-131.5	1983	8336974	47.7	1.71	15.6	12.22747	0.233	5.69	7.83	1.95	1.2	0.441
PYO47	334.93	338.34	7062256	3452983.25	-132.72	1983	8336975	46.2	0.268	16.3	26.78927	0.001	0.31	0.002	0.37	3.23	0.006
PYO47	338.34	339.12	7062256	3452981.5	-133.87	1983	8336976	52.6	0.93	15	9.6597	0.176	5.28	9.82	0.93	0.92	0.72
PYO47	339.12	340.05	7062256	3452981	-134.34	1983	8336977	79.4	0.203	11.9	3.268069	0.001	0.03	0.002	0.3	2.8	0.003
PYO47	340.05	341.64	7062256.5	3452979.75	-135.02	1959	5920692										
PYO47	341.64	343.88	7062256.5	3452978.25	-136.06	1959	5920693										
PYO47	343.88	346.4	7062257	3452976.25	-137.35	1983	8336978	63.8	0.256	15.3	12.00515	0.001	0.41	0.002	0.34	3.24	0.003
PYO47	346.4	349.5	7062257.5	3452974	-138.86	1983	8336979	65.6	0.174	11.5	9.626352	0.063	3.71	0.25	0.6	1.1	0.014
PYO47	349.5	351.92	7062258	3452971.75	-140.34	1983	8336980	53.3	0.975	15.8	7.703305	0.191	5.03	8.21	1.34	1.52	0.718
PYO47	351.92	353.1	7062258	3452970.25	-141.3	1983	8336981	58.2	0.267	17	4.601974	0.107	5.05	0.45	0.61	2.25	0.024
PYO47	353.1	355.84	7062258.5	3452968.5	-142.34	1983	8336982	63.2	0.251	14.3	9.203948	0.027	1.75	0.25	0.71	2.89	0.019
PYO47	355.84	356.3	7062258.5	3452967.25	-143.19	1983	8336983	56.9	0.638	16.4	6.602833	0.239	5.52	8.45	0.69	1.54	0.309
PYO47	356.3	356.9	7062258.5	3452966.75	-143.47	1983	8336984	49.8	0.207	15	22.78755	0.005	1.09	0.03	0.39	2.58	0.007
PYO47	356.9	358.9	7062259	3452965.75	-144.15	1959	5920701										

PYO47	358.9	360.78	7062259	3452964	-145.17	1959	5920702									
PYO47	360.78	362.66	7062259.5	3452962.5	-146.16	1959	5920703									
PYO47	362.66	364.65	7062260	3452960.75	-147.17	1959	5920704									
PYO47	364.65	366.3	7062260	3452959.25	-148.12	1959	5920705									
PYO47	366.3	367.46	7062260	3452958.25	-148.85	1959	5920706									
PYO47	367.46	368.84	7062260.5	3452957	-149.5	1959	5920707									
PYO47	368.84	371.12	7062260.5	3452955.5	-150.45	1959	5920708									
PYO47	371.12	371.38	7062261	3452954.5	-151.1	1983	8336985	52.9	0.643	15.1	5.958112	0.154	6.05	7.02	3.13	1.01	0.267
PYO47	371.38	373.27	7062261	3452953.5	-151.66	1959	5920710									
PYO47	373.27	374.38	7062261.5	3452952.25	-152.43	1959	5920711									
PYO47	374.38	375.11	7062261.5	3452951.5	-152.91	1983	8336986	49.2	0.72	18.8	8.025665	0.089	8.46	7.16	0.64	2.7	0.119
PYO47	375.11	375.85	7062261.5	3452951	-153.29	1959	5920713									
PYO47	375.85	377.05	7062261.5	3452950	-153.8	1959	5920714									
PYO47	377.05	378.39	7062262	3452949	-154.46	1959	5920715									
PYO47	378.39	378.72	7062262	3452948.25	-154.9	1983	8337071	48.4	0.324	22.4	11.22704	0.028	2	0.97	0.81	4.59	0.003
PYO47	378.72	379.87	7062262	3452947.75	-155.29	1959	5920717									

PYO47	379.87	381.67	7062262.5	3452946.5	-156.06	1959	5920718										
PYO47	381.67	383.11	7062262.5	3452945	-156.91	1983	8337072	80.2	0.146	11.1	2.112017	0.081	4.28	0.2	0.29	0.94	0.011
PYO47	383.11	385.13	7062263	3452943.75	-157.83	1983	8337073	65.8	0.228	14	3.045751	0.147	8.92	0.28	0.26	2.2	0.026
PYO47	385.13	390.13	7062263.5	3452940.75	-159.69	1983	8337074	58.8	0.397	20.2	5.491245	0.099	3.83	0.41	0.46	4.14	0.033
PYO47	390.13	395.28	7062264	3452936.5	-162.41	1983	8337075	68.9	0.245	14.4	5.469013	0.007	0.39	0.56	0.46	3.17	0.022
PYO47	395.28	396.92	7062264.5	3452933.75	-164.24	1983	8337076	67.9	0.183	9.9	7.825579	0.072	4.1	2.31	0.39	1.58	0.011
PYO47	396.92	401.92	7062265	3452931	-166.04	1983	8337077	71.8	0.254	16.4	3.679356	0.001	0.52	0.002	0.3	4.28	0.013
PYO47	401.92	403.75	7062265.5	3452928	-167.89	1983	8337078	75.9	0.236	14.3	2.59	0.047	1.41	0.36	0.44	3.58	0.022
PYO47	403.75	404.64	7062265.5	3452927	-168.63	1983	8337079	46.6	0.54	15.8	10.5712	0.248	13	1.04	1.98	2.42	0.041
PYO47	404.64	405.28	7062266	3452926.25	-169.04	1983	8337080	58.3	0.621	14.7	5.813605	0.447	4.65	3	1.98	1.09	0.108
PYO47	405.28	407.63	7062266	3452925	-169.85	1983	8337081	46.1	0.523	14.8	11.56052	0.415	12.1	1.02	0.64	2.98	0.092
PYO47	407.63	409.85	7062266.5	3452923.25	-171.07	1983	8337082	75.2	0.185	11.8	4.090644	0.191	3.54	0.54	0.75	2.53	0.018
PYO47	409.85	411.52	7062266.5	3452921.5	-172.12	1983	8337083	71	0.265	12.9	3.47927	0.108	0.81	3.12	1.99	2.45	0.036
PYO47	412.12	415.2	7062267	3452919	-173.7	1983	8337084	71.8	0.207	11.6	3.646009	0.126	1.06	2.8	1.56	2.47	0.024
PYO47	415.2	416.38	7062267.5	3452917.25	-174.83	1983	8337085	70.7	0.231	13.2	2.612232	0.069	0.54	3.69	1.15	4.61	0.037
PYO47	416.38	421.52	7062268	3452914.75	-176.5	1983	8337086	52.9	0.495	15	9.026094	0.154	4.32	8.22	3.92	0.86	0.141

PYO47	421.52	422.38	7062268.5	3452912.25	-178.07	1983	8337087	72.4	0.178	11.8	2.823433	0.064	0.23	2.61	2.04	2.54	0.021
PYO47	422.38	425.95	7062268.5	3452910.25	-179.23	1983	8337088	54.7	0.619	14.9	6.647296	0.115	4.23	7.17	3.34	1.27	0.279
PYO47	425.95	427.98	7062269	3452908	-180.68	1983	8337089	78.8	0.166	11.3	2.456609	0.06	0.32	3.02	0.61	3.35	0.013
PYO47	427.98	432.98	7062269.5	3452905	-182.49	1983	8337090	50.3	0.494	14.7	11.3382	0.19	4.77	10.4	2.14	1.65	0.095
PYO47	432.98	434.84	7062270	3452902	-184.26	1983	8337091	48.3	0.51	14.6	12.11631	0.216	5.27	9.53	3.61	0.5	0.092

HOLEID$	FROM	TO	SAMPLENO	ZR_O ppm	CR_O %	SR_O ppm	BA_O ppm	CU_O ppm	ZN_O ppm	PB_O ppm	NI_O ppm	CO_O ppm	FE_O %	S_O %	AG_O ppm	CU_XO ppm	ZN_XO ppm	PB_XO ppm	FE_XO ppm	S_XO %
PYO47	1.65	2.45	8336879	185	88.92	67.68	582.4	4	74	16	0.5	9	1.72	0.07	0.2	5	70	10	1.78	0.049
PYO47	2.45	3.27	8336880	51.8	314.64	152.28	1881.6	4	46	25	15	20	1.65	0.02	1.2	5	190	10	7.4388	0.041
PYO47	3.27	5.47	8336881	177.6	116.28	67.68	672	6	72	23	0.5	10	1.42	0.13	0.7	5	60	10	1.5002	0.059
PYO47	5.47	6.68	8336882	59.2	314.64	177.66	591.36	6	72	29	19	28	2.81	0.01	1.3	5	200	10	8.0062	0.058
PYO47	7.89	11	8336883	199.8	150.48	76.14	654.08	9	66	21	0.5	11	1.81	0.09	0.6	5	70	10	1.8422	0.147
PYO47	11	14.06	8336884	185	143.64	84.6	600.32	13	87	17	0.5	11	1.67	0.11	0.8	10	90	5	1.8189	0.193
PYO47	15	17.94	8336885	185	88.92	84.6	591.36	16	97	13	0.5	8	1.78	0.11	0.9	10	100	5	1.8888	0.172
PYO47	17.94	20.66	8336886	185	109.44	84.6	698.88	9	93	22	0.5	10	1.22	0.1	0.4	5	100	5	1.8422	0.19
PYO47	20.66	22.45	8336887	185	143.64	76.14	887.04	19	113	21	2	8	1.25	0.28	0.4	5	5	5		0.0005
PYO47	23.77	26.4	8336888	222	116.28	84.6	896	13	134	19	0.5	10	1.67	0.12	0.4	5	5	5		0.0005
PYO47	27.7	29.67	8336889	170.2	129.96	76.14	806.4	21	63	17	0.5	11	0.86	0.87	0.5	10	70	10	1.8344	0.946
PYO47	29.67	30.48	8336890	140.6	123.12	42.3	1164.8	204	113	21	22	15	5.4	5.79	1.9	5	5	5		0.0005
PYO47	30.48	32.34	8336891	162.8	143.64	67.68	824.32	57	117	20	20	3	2.82	1.75	1.6	5	5	5		0.0005
PYO47	32.34	36.64	8336892	199.8	95.76	76.14	1120	16	80	9	6	1	1.27	0.34	0.4	10	90	10	1.9277	0.481

PY047	36.64	38.5	8336893	207.2	109.44	76.14	1326.08	14	102	14	9	2	1.21	0.32	0.6	10	120	5	2.0832	0.381
PY047	41.8	42.57	8336894	177.6	150.48	84.6	618.24	15	25	11	3	1	0.58	0.09	0.4	10	40	5	1.5157	0.119
PY047	42.57	42.9	8336895	74	68.4	101.52	1326.08	28	307	14	20	31	6.62	0.18	1.1	10	320	20	7.5009	0.189
PY047	42.9	44.05	8336896	162.8	123.12	84.6	1209.6	7	157	18	8	9	3.14	0.04	0.6	5	5	5		0.0005
PY047	44.05	47.43	8336897	199.8	136.8	84.6	636.16	6	58	11	4	2	0.9	0.04	0.05	5	5	5		0.0005
PY047	47.43	48.5	8336898	44.4	403.56	186.12	582.4	0.5	90	17	25	16	2.24	0.01	0.4	5	300	10	8.1616	0.0005
PY047	48.5	50.65	8336899	185	136.8	101.52	636.16	26	70	10	7	2	1.29	0.46	0.3	30	80	10	1.7101	0.51
PY047	69.8	73.8	8336900	96.2	102.6	160.74	698.88	12	55	13	1	11	3.03	0.04	0.6	5	120	5	7.1356	0.078
PY047	73.8	78.11	8336901	88.8	95.76	143.82	546.56	35	30	7	14	15	1.46	0.18	0.5	20	100	5	6.1951	0.19
PY047	78.11	79.81	8336902	81.4	109.44	143.82	743.68	27	67	7	9	21	3.81	0.14	0.7	5	120	10	7.8507	0.155
PY047	79.81	82.28	8336903	59.2	307.8	169.2	555.52	2	15	9	10	3	0.47	0.01	0.05	5	130	5	8.1616	0.02
PY047	82.28	84	8336904	74	95.76	236.88	627.2	103	32	12	8	27	2.1	0.73	0.05	80	140	10	9.1721	0.682
PY047	84	86.9	8336905	74	150.48	236.88	492.8	95	31	11	9	17	1.72	0.41	0.3	5	5	5		0.0005
PY047	87.82	89.88	8336906	74	123.12	228.42	770.56	195	94	20	20	43	5.77	1.09	0.8	5	5	5		0.0005
PY047	89.88	91.75	8336907	155.4	88.92	532.98	600.32	25	38	17	2	12	1.81	0.12	0.4	10	90	5	5.1069	0.208
PY047	93	96.8	8336908	140.6	82.08	456.84	940.8	70	66	14	3	14	3	0.37	1	50	100	20	5.4333	0.405

PY047	105.72	110.72	8336909	66.6	116.28	101.52	430.08	78	25	14	18	22	1.7	0.23	0.4	5	5	5		0.0005
PY047	110.72	115.72	8336910	66.6	102.6	101.52	546.56	28	45	10	15	21	2.45	0.07	0.7	10	110	5	7.3921	0.122
PY047	115.72	120.55	8336911	66.6	102.6	118.44	537.6	58	48	13	15	21	2.46	0.16	0.9	40	100	5	6.7236	0.197
PY047	120.55	122.4	8336912	74	123.12	67.68	1729.28	35	215	18	57	24	6.12	0.78	1.3	5	5	5		0.0005
PY047	122.4	126.48	8336913	192.4	157.32	135.36	1245.44	38	359	11	81	9	2.55	1.09	0.5	5	5	5		0.0005
PY047	126.48	129.86	8336914	66.6	294.12	236.88	609.28	0.5	31	14	11	12	1.4	0.03	0.6	5	5	5		0.0005
PY047	129.86	135.5	8336915	162.8	171	152.28	922.88	35	198	14	37	4	1.22	0.69	0.6	40	240	10	1.9277	0.758
PY047	135.5	140	8336916	74	157.32	211.5	707.84	37	95	22	24	35	3.42	0.39	3.2	5	210	5	8.3948	0.49
PY047	140	141.9	8336917	162.8	198.36	118.44	1191.68	31	93	32	12	10	1.72	0.47	2	5	5	5		0.0005
PY047	141.9	146.45	8336918	74	143.64	245.34	672	64	40	23	6	34	3.84	0.48	1.6	5	5	5		0.0005
PY047	146.45	146.8	8336919	162.8	232.56	194.58	833.28	63	18	19	6	10	1.71	0.46	0.7	50	30	10	1.8811	0.527
PY047	146.8	151	8336920	74	109.44	228.42	1057.28	53	76	10	3	36	4.1	0.35	1.1	20	160	5	9.794	0.304
PY047	151	153.95	8336921	170.2	191.52	101.52	1030.4	27	161	18	15	9	2.07	0.65	1.1	20	180	20	2.0598	0.749
PY047	157.14	161.88	8336922	192.4	150.48	169.2	716.8	24	44	13	0.5	6	1.3	0.49	0.8	20	50	5	1.3603	0.466
PY047	161.88	165.35	8336923	170.2	157.32	126.9	788.48	169	76	15	3	10	3.38	2.13	0.9	5	5	5		0.0005
PY047	165.35	170.35	8336924	59.2	239.4	245.34	716.8	30	82	20	20	28	3.62	0.08	1.1	5	5	5		0.0005

PY047	170.35	172.43	8336925	51.8	471.96	203.04	779.52	2	69	21	34	24	2.79	0.06	1.5	5	5	5		0.0005
PY047	172.43	173.75	8336926	155.4	246.24	126.9	663.04	19	38	15	0.5	5	1.02	0.17	0.7	5	5	5		0.0005
PY047	173.75	175.2	8336927	96.2	157.32	219.96	940.8	37	110	21	0.5	30	4.4	0.42	1.1	20	170	10	6.9568	0.439
PY047	175.2	177.2	8336928	155.4	218.88	169.2	636.16	31	55	6	6	10	1.84	1.02	0.5	30	70	10	2.363	1.768
PY047	177.2	177.94	8336929	59.2	157.32	160.74	1137.92	165	283	18	18	48	8.91	2.18	2.4	130	320	10	8.7058	1.842
PY047	177.94	179.73	8336930	170.2	184.68	135.36	1120	42	36	14	1	6	2.29	1.26	0.6	40	40	20	2.2231	1.16
PY047	179.73	181.17	8336931	66.6	102.6	152.28	1379.84	48	233	21	11	44	6.96	0.89	0.9	20	340	5	10.1049	0.806
PY047	181.17	181.89	8336932	207.2	164.16	143.82	564.48	9	248	6	0.5	6	2.29	0.14	0.9	5	290	10	2.1842	0.183
PY047	181.89	183.69	8336933	199.8	136.8	152.28	1442.56	14	126	13	0.5	5	1.59	0.19	0.8	20	150	30	1.4924	0.36
PY047	183.69	187.44	8336934	199.8	136.8	135.36	1164.8	32	324	12	0.5	7	1.95	0.28	0.8	20	370	30	1.7023	0.287
PY047	193.5	196.08	8336935	185	109.44	126.9	1102.08	21	257	7	0.5	6	1.9	0.45	0.3	20	290	10	1.7645	0.504
PY047	196.08	197.05	8336936	125.8	82.08	380.7	931.84	24	109	26	17	23	4.32	0.17	2.3	5	120	10	5.2079	0.209
PY047	206.42	211.42	8336937	148	82.08	516.06	752.64	58	103	22	8	24	4.36	0.23	0.8	5	5	5		0.0005
PY047	211.42	213.97	8336938	148	102.6	490.68	878.08	21	120	22	7	20	4.81	0.13	0.7	5	5	5		0.0005
PY047	213.97	214.84	8336939	133.2	116.28	380.7	985.6	190	237	32	11	23	4.78	0.51	1.2	5	5	5		0.0005
PY047	214.84	215.66	8336940	103.6	191.52	59.22	1388.8	30	63	20	3	10	5.65	5.68	0.6	5	5	5		0.0005

PY047	215.66	217.33	8336941	103.6	280.44	16.92	1576.96	10	26	15	12	13	7.69	8.45	0.4	5	60	10	5.3401	5.982
PY047	217.33	219.45	8336942	103.6	232.56	59.22	1039.36	207	297	32	22	20	5.68	2.53	1.8	200	360	30	4.998	2.174
PY047	219.45	221.85	8336943	140.6	280.44	118.44	1621.76	134	148	16	15	22	7.86	7.14	1.7	5	5	5		0.0005
PY047	221.85	223.2	8336944	140.6	506.16	321.48	2132.48	229	232	60	104	44	6.16	2.96	3.6	5	5	5		0.0005
PY047	223.2	228.2	8336945	125.8	266.76	42.3	1648.64	114	3020	23	12	7	3.88	3.7	1.1	5	5	5		0.0005
PY047	228.2	233.2	8336946	148	225.72	50.76	2042.88	88	317	24	26	10	4.79	4.77	0.8	5	5	5		0.0005
PY047	233.2	237.85	8336947	155.4	232.56	59.22	1496.32	159	1660	29	13	13	2.27	1.47	1.5	160	1850	10	1.8189	1.185
PY047	237.85	241.37	8336948	148	184.68	33.84	2607.36	59	2230	7	9	5	2.7	2.63	0.3	5	5	5		0.0005
PY047	241.37	243.42	8336949	140.6	225.72	25.38	1890.56	15	1040	14	10	6	2.76	1.88	0.5	5	5	5		0.0005
PY047	253.33	256.62	8336950	118.4	205.2	16.92	3682.56	459	23800	62	25	9	6.3	7.26	2.7	5	5	5		0.0005
PY047	256.62	262.1	8336951	140.6	266.76	50.76	1765.12	26	1580	43	12	8	1.84	1.35	0.7	20	1740	40	1.3525	1.027
PY047	262.1	264.95	8336952	140.6	259.92	50.76	2419.2	38	1020	21	17	5	2.38	1.59	0.8	5	5	5		0.0005
PY047	264.95	268.57	8336953	133.2	150.48	84.6	1971.2	114	3200	19	13	7	3.11	2.4	0.9	5	5	5		0.0005
PY047	271.47	271.94	8336954	177.6	287.28	296.1	1137.92	346	501	80	68	34	5.56	3.02	3.6	340	540	40	4.6716	2.734
PY047	271.94	276.94	8336955	133.2	136.8	67.68	1254.4	178	1650	105	10	8	3.03	2.38	1.2	180	1810	120	2.1376	1.897
PY047	276.94	280	8336956	133.2	143.64	42.3	1514.24	103	2700	1244	11	6	2.51	1.92	2.6	100	3100	1260	1.8422	1.554

PY047	280	282.28	8336957	125.8	157.32	33.84	1872.64	155	5700	63	10	7	2.67	2.65	1.2	160	6580	90	1.8655	2.086
PY047	282.28	285.17	8336958	133.2	143.64	50.76	2374.4	119	2640	232	16	8	2.39	2.3	1.2	110	2960	240	1.5391	1.682
PY047	285.17	290.17	8336959	125.8	157.32	33.84	1863.68	861	7100	90	10	7	2.85	2.99	2.2	950	7960	110	2.1531	2.577
PY047	290.17	295.17	8336960	125.8	82.08	42.3	3673.6	69	4630	44	6	9	2.99	3.41	1	5	5	5		0.0005
PY047	295.17	300.17	8336961	148	177.84	50.76	7651.84	52	2830	331	2	8	3.03	3.16	3.1	5	5	5		0.0005
PY047	300.17	303.7	8336962	162.8	157.32	186.12	4139.52	57	1380	252	9	11	3.32	2.99	2.6	5	5	5		0.0005
PY047	303.7	304.95	8336963	148	150.48	456.84	2096.64	129	345	166	10	24	4.96	1.09	3.5	5	5	5		0.0005
PY047	304.95	309.95	8336964	118.4	198.36	42.3	3745.28	61	8200	81	1	11	4.1	4.48	1.9	5	5	5		0.0005
PY047	309.95	314.95	8336965	118.4	225.72	16.92	1962.24	117	4760	70	2	7	4.1	4.48	2.1	5	5	5		0.0005
PY047	314.95	318.9	8336966	118.4	212.04	25.38	1720.32	644	3470	23	0.5	14	5.18	5.62	2.6	5	5	5		0.0005
PY047	318.9	319.8	8336967	96.2	321.48	50.76	1585.92	2226	1070	67	13	59	13.12	11.5	10.8	2560	1270	140	11.2709	12.28
PY047	319.8	321.3	8336968	111	232.56	33.84	2087.68	4040	60	22	0.5	21	4.64	4.09	4.6	5	5	5		0.0005
PY047	322	324.5	8336969	96.2	184.68	25.38	1603.84	475	145	26	1	29	9.61	9.38	3.2	530	170	20	7.7419	9.234
PY047	324.5	326.4	8336970	74	136.8	321.48	528.64	1136	88	95	23	34	3.15	0.89	7.5	1180	310	80	7.8507	1.131
PY047	326.4	331.17	8336971	96.2	184.68	42.3	1657.6	2338	2510	41	8	46	15.11	16.5	6.9	2780	3110	100	13.1364	16.45
PY047	331.17	331.83	8336972	155.4	417.24	160.74	1200.64	237	585	118	66	29	4.67	1.22	3.2	250	710	190	4.3062	1.455

PY047	331.83	333.96	8336973	111	184.68	42.3	1326.08	14	105	16	0.5	27	6.67	6.97	0.8	5	5	5		0.0005
PY047	333.96	334.93	8336974	185	157.32	634.5	761.6	169	173	156	61	36	4.57		2.4	5	5	5		0.0005
PY047	334.93	338.34	8336975	111	177.84	33.84	2078.72	47	191	296	8	98	21.48	25.8	4.3	10	240	320	18.7329	22.97
PY047	338.34	339.12	8336976	192.4	437.76	769.86	474.88	22	96	237	80	36	2.83	0.21	2.2	5	230	230	6.7547	0.479
PY047	339.12	340.05	8336977	103.6	239.4	33.84	1245.44	79	15	66	0.5	18	3.44	3.36	1	5	5	5		0.0005
PY047	340.05	341.64	5920692				501.76	700	200	50			39.8	47.1		5	5	5		0.0005
PY047	341.64	343.88	5920693				501.76	1900	200	30			41.2	48.8		5	5	5		0.0005
PY047	343.88	346.4	8336978	118.4	184.68	42.3	2768.64	697	445	45	2	29	10.68	12.8	3.4	780	540	90	8.3948	10.12
PY047	346.4	349.5	8336979	111	191.52	67.68	3288.32	57	9100	227	2	18	8.56	8.75	3.8	50	10330	310	6.7314	7.892
PY047	349.5	351.92	8336980	185	410.4	626.04	1352.96	537	303	210	45	27	3.13	0.38	2.8	570	570	280	5.3867	0.944
PY047	351.92	353.1	8336981	155.4	75.24	84.6	6881.28	144	4320	169	21	12	5.27	5.37	3.6	5	5	5		0.0005
PY047	353.1	355.84	8336982	125.8	259.92	67.68	7239.68	284	366	241	16	11	9.01	9.39	3.4	5	5	5		0.0005
PY047	355.84	356.3	8336983	155.4	458.28	541.44	761.6	366	273	222	108	33	3.29	0.49	3	360	460	240	4.6172	0.857
PY047	356.3	356.9	8336984	96.2	232.56	42.3	7866.88	344	592	3461	27	23	19.86	24.5	27.1	380	740	3760	15.9347	19.57
PY047	356.9	358.9	5920701				34012.16	1100	88000	1000			23.9	32.7		5	5	5		0.0005
PY047	358.9	360.78	5920702					1000	85000	50			26.9	35.2		5	5	5		0.0005

PY047	360.78	362.66	5920703					3000	46500	50			30.5	37.1		5	5	5		0.0005
PY047	362.66	364.65	5920704					2000	42000	50			33.9	40.3		5	5	5		0.0005
PY047	364.65	366.3	5920705					500	7400	20			34.1	41.2		5	5	5		0.0005
PY047	366.3	367.46	5920706					2400	62500	30			29.2	37.3		5	5	5		0.0005
PY047	367.46	368.84	5920707					5300	76500	50			24.5	32.8		5	5	5		0.0005
PY047	368.84	371.12	5920708					3000	7900	70			41.4	48.2		5	5	5		0.0005
PY047	371.12	371.38	8336985	177.6	458.28	600.66	4919.04	11500	2320	402	66	21	3.37	1.58	24.4	11170	2690	530	4.1663	2.687
PY047	371.38	373.27	5920710					12500	17300	100			37.9	45.3		5	5	5		0.0005
PY047	373.27	374.38	5920711					14500	25700	100			37.9	44.7		5	5	5		0.0005
PY047	374.38	375.11	8336986	81.4	102.6	228.42	5653.76	10830	1010	481	36	24	6.09	4	28.3	5	5	5		0.0005
PY047	375.11	375.85	5920713					17000	55600	300			22.8	30.1		5	5	5		0.0005
PY047	375.85	377.05	5920714					8000	12900	70			42.4	50.1		5	5	5		0.0005
PY047	377.05	378.39	5920715					3500	24600	10			40.5	48.6		5	5	5		0.0005
PY047	378.39	378.72	8337071	288.6	109.44	152.28	24371.2	1327	142	92	13	9	12.16	14.8	6.4	1360	180	170	7.8507	9.799
PY047	378.72	379.87	5920717				98.56	4000	61000	134000			33.2	41.4		5	5	5		0.0005
PY047	379.87	381.67	5920718					3000	17300	800			36	42.4		5	5	5		0.0005

PY047	381.67	383.11	8337072	148	191.52	50.76	1729.28	28	145	47	5	6	1.67	0.89	1.1	5	5	5		0.0005
PY047	383.11	385.13	8337073	148	177.84	50.76	1729.28	118	1820	76	10	7	2.57	1.73	2.2	110	1940	70	2.1298	1.274
PY047	385.13	390.13	8337074	170.2	171	42.3	4363.52	283	3110	37	7	9	5.19	5.15	2.3	300	3640	90	3.8399	3.281
PY047	390.13	395.28	8337075	125.8	164.16	42.3	1666.56	282	780	20	4	7	5.21	5.34	1.6	280	840	40	3.8243	3.993
PY047	395.28	396.92	8337076	111	143.64	67.68	2464	199	109	35	10	47	7.19	5.82	4.1	5	5	5		0.0005
PY047	396.92	401.92	8337077	140.6	191.52	25.38	1335.04	61	36	19	2	6	3.9	4.33	1	5	5	5		0.0005
PY047	401.92	403.75	8337078	140.6	129.96	33.84	1460.48	33	2810	15	2	3	2.5	2.6	0.9	5	5	5		0.0005
PY047	403.75	404.64	8337079	29.6	177.84	42.3	824.32	140	154	80	39	59	7.49	2.31	3.4	120	190	70	7.3921	1.709
PY047	404.64	405.28	8337080	111	150.48	101.52	1308.16	29	79	27	10	26	5.29	4.26	1.6	5	5	5		0.0005
PY047	405.28	407.63	8337081	37	143.64	101.52	824.32	310	910	45	37	46	8	2.06	3	5	5	5		0.0005
PY047	407.63	409.85	8337082	148	259.92	42.3	1093.12	87	400	17	4	6	2.67	0.73	1.5	5	5	5		0.0005
PY047	409.85	411.52	8337083	162.8	116.28	109.98	1003.52	70	145	65	0.5	6	2.38	0.17	1.4	5	5	5		0.0005
PY047	412.12	415.2	8337084	148	225.72	93.06	734.72	30	138	16	2	9	2.41	0.46	1	5	5	5		0.0005
PY047	415.2	416.38	8337085	162.8	171	93.06	931.84	13	70	9	1	8	1.43	0.17	1.2	5	5	5		0.0005
PY047	416.38	421.52	8337086	74	184.68	253.8	528.64	46	37	7	27	28	2.15	0.18	1.3	5	5	5		0.0005
PY047	421.52	422.38	8337087	148	205.2	109.98	680.96	9	71	8	0.5	4	1.83	0.04	0.9	5	70	10	1.9743	0.059

PY047	422.38	425.95	8337088	162.8	239.4	651.42	672	10	47	9	31	16	2.03	0.01	1.3	5	100	5	4.6483	0.074
PY047	425.95	427.98	8337089	148	157.32	101.52	940.8	18	68	11	0.5	7	1.31	0.09	1.2	5	5	5		0.0005
PY047	427.98	432.98	8337090	44.4	136.8	160.74	994.56	75	25	9	10	16	1.25	0.13	1.3	5	5	5		0.0005
PY047	432.98	434.84	8337091	51.8	164.16	236.88	734.72	27	59	7	10	10	1.16	0.07	1	5	5	5		0.0005

APPENDIX 4.b. PYO-84 XRF/AAS whole-rock geochemical data, by courtesy of Pyhäsalmi Mine Oy:

HOLEID $	FROM	TO	XCOORD	YCOORD	ZCOORD	YEAR	SAMPLENO	SIO2_O %	TIO2_O %	AL2O3_O %	FE2O3_O %	MNO_O %	MGO_O %	CAO_O %	NA2O_O %	K2O_O %	P2O5_O %
PYO84	16.6	20.3	7062322	3453502	136.29	1983	8336291	75.4	0.144	11.8	2.879013	0.066	0.82	1.49	4.77	0.98	0.015
PYO84	20.3	22.4	7062322	3453501	133.66	1983	8336292	75.8	0.132	11.8	3.245837	0.099	0.56	2.93	4.03	1.17	0.014
PYO84	22.4	22.77	7062322	3453501	132.55	1983	8336293	54.8	0.517	15.1	7.514335	0.205	4.65	7.35	4.91	0.81	0.279
PYO84	22.77	23.27	7062322	3453501	132.15	1983	8336294	75.6	0.135	11.4	2.912361	0.068	0.55	2.15	4.36	0.76	0.015
PYO84	23.27	23.67	7062322	3453500	131.75	1983	8336295	47.5	0.661	12.3	14.33948	0.225	5.33	6.7	3.16	1.72	0.106
PYO84	23.67	25.9	7062322	3453500	130.56	1983	8336296	76.4	0.119	12	3.079099	0.129	0.26	2.18	4.79	1.23	0.017
PYO84	25.9	26.95	7062322	3453499	129.08	1983	8336297	75.5	0.123	12	2.623348	0.065	0.27	1.03	4.91	1.75	0.011
PYO84	27.15	28.54	7062322	3453498	127.79	1983	8336298	75.3	0.128	11.8	2.956824	0.078	0.25	1.34	4.28	1.6	0.008
PYO84	28.54	29.15	7062322	3453498	126.89	1983	8336299	50.4	0.791	12.4	11.44936	0.245	6.71	8.77	3.95	0.76	0.162
PYO84	29.15	29.8	7062322	3453498	126.32	1983	8336300	75.2	0.14	11.3	2.945708	0.068	0.43	1.52	4.67	0.78	0.011
PYO84	29.8	30.88	7062322	3453497	125.54	1983	8336301	49.8	0.718	12.7	14.22833	0.191	4.16	6.78	3.36	1.39	0.125
PYO84	37.08	38.2	7062323	3453494	118.96	1983	8336302	75.3	0.127	12.1	2.879013	0.075	0.24	0.86	4.8	1.8	0.01
PYO84	38.2	38.8	7062323	3453494	118.18	1983	8336303	52.9	0.522	13.9	8.159056	0.17	5.76	6.03	3.71	1.83	0.27
PYO84	38.8	39.8	7062323	3453494	117.46	1983	8336304	74.3	0.143	12.1	3.201373	0.057	0.39	0.79	4.73	1.6	0.021
PYO84	42	42.44	7062323	3453492	114.83	1983	8336305	77.3	0.128	11.7	3.067983	0.096	0.16	1.64	4.91	1.18	0.015
PYO84	49.82	51.23	7062324	3453489	107.36	1983	8336306	75.9	0.099	12.1	3.334764	0.064	0.47	3.11	4.09	0.7	0.003
PYO84	51.23	52.73	7062324	3453488	106.06	1983	8336307	51.7	0.76	13.5	11.89399	0.19	3.86	5.25	3.3	1.99	0.249
PYO84	53.15	53.8	7062324	3453488	104.71	1983	8336308	48.8	0.739	14.6	13.00558	0.259	4.6	6.42	3.35	1.85	0.181
PYO84	53.8	54.45	7062324	3453487	104.13	1983	8336309	75.7	0.096	11.6	2.145365	0.027	0.43	1.16	5.17	0.74	0.003
PYO84	54.45	55.05	7062324	3453487	103.57	1983	8336310	42.6	0.768	12.2	15.33991	0.156	8.29	2.5	1.01	2.4	0.094
PYO84	58.22	58.75	7062325	3453485	100.21	1983	8336311	49.6	0.545	12.8	13.56137	0.246	6.23	7.42	2.46	1.79	0.083
PYO84	62.16	63.03	7062325	3453484	96.51	1983	8336312	77.7	0.001	13.1	0.633605	0.197	0.01	0.3	4.68	2.69	0.085
PYO84	63.03	63.7	7062325	3453483	95.82	1983	8336313	76.5	0.125	11.9	2.923476	0.049	0.38	1.01	4.24	2.07	0.011
PYO84	73.9	74.5	7062326	3453479	86.08	1983	8336314	47.7	0.43	14	11.78283	0.197	7.44	8.94	2.97	1.23	0.083
PYO84	74.5	76.1	7062326	3453478	85.1	1983	8336315	74.9	0.135	12.1	2.612232	0.048	0.25	0.79	5.24	1.43	0.013

PY084	79.1	84.81	7062326	3453475	79.11	1983	8336316	75.3	0.128	12	2.312103	0.076	0.07	1.31	5.31	1.34	0.037
PY084	85.74	86.46	7062327	3453473	75.39	1983	8336317	53.1	0.71	13.2	13.45021	0.262	3.38	6.42	3.71	1.5	0.2
PY084	88.5	89.8	7062327	3453472	72.65	1983	8336318	76.6	0.124	12.3	2.289871	0.055	0.13	0.96	4.86	1.78	0.013
PY084	89.8	91.58	7062327	3453471	71.26	1983	8336319	75.3	0.118	12.1	3.179142	0.072	0.55	1.2	3.85	2.58	0.009
PY084	91.78	96.78	7062327	3453470	68.04	1983	8336320	76.7	0.091	12.4	2.189828	0.073	0.2	1.65	4.66	1.81	0.031
PY084	96.78	98.74	7062328	3453468	64.91	1983	8336321	76.6	0.082	12.2	2.823433	0.065	0.33	1.3	5.27	1.11	0.007
PY084	98.74	99.74	7062328	3453468	63.58	1983	8336322	54.1	0.643	12.9	13.45021	0.261	3.3	6.52	4.2	1.27	0.208
PY084	99.74	105.44	7062328	3453466	60.57	1983	8336323	74.6	0.097	13.3	2.734506	0.073	0.2	1.62	3.91	3.41	0.008
PY084	105.44	111.1	7062328	3453464	55.47	1983	8336324	74.2	0.132	12.7	2.567768	0.056	0.77	0.86	2.97	4.17	0.012
PY084	111.1	111.45	7062329	3453463	52.77	1983	8336325	51.3	0.563	14.6	12.78326	0.293	6.29	8.47	3.39	1.42	0.08
PY084	112	112.9	7062329	3453462	51.72	1983	8336326	78.4	0.113	11.8	2.034206	0.03	0.46	0.78	3.39	3	0.003
PY084	113.2	114.2	7062329	3453461	50.6	1983	8336327	76.3	0.125	13.1	2.156481	0.044	0.21	0.87	3.07	4.14	0.003
PY084	114.2	115.84	7062329	3453461	49.41	1983	8336328	55.1	0.623	15.6	8.170172	0.186	5.56	7.68	4.37	1.12	0.268
PY084	115.84	117.13	7062329	3453460	48.1	1983	8336329	76.7	0.135	11.6	2.000858	0.043	0.32	1.02	4.29	1.57	0.013
PY084	117.13	118.63	7062329	3453460	46.85	1983	8336330	54.8	0.679	15.6	8.370258	0.198	5.39	7.39	4.41	1.46	0.296
PY084	118.63	120.09	7062329	3453459	45.52	1983	8336331	75.8	0.134	12.2	1.856352	0.025	0.2	1.15	3.55	2.91	0.011
PY084	120.09	120.92	7062329	3453459	44.5	1983	8336332	50.9	0.637	12.6	10.71571	0.214	9.26	10.1	2.46	1.22	0.246
PY084	120.92	125.92	7062330	3453457	41.89	1983	8336333	77.9	0.129	12.7	1.667382	0.026	0.02	0.69	4.77	2.12	0.003
PY084	125.92	131.8	7062330	3453455	37.02	1983	8336334	78.4	0.127	12.7	1.578455	0.026	0.01	0.68	5.69	0.86	0.006
PY084	131.8	134.36	7062330	3453453	33.25	1983	8336335	64.2	0.718	13.7	11.00472	0.212	1.19	4.46	4.1	0.98	0.349
PY084	134.36	136.5	7062331	3453452	31.15	1983	8336336	78.3	0.142	12.5	1.756309	0.024	0.01	0.76	4.69	1.83	0.021
PY084	136.5	140.13	7062331	3453451	28.57	1983	8336337	77.3	0.128	12.6	2.123133	0.032	0.16	0.87	4.32	2.51	0.003
PY084	142.4	144.68	7062331	3453448	23.91	1983	8336338	79.2	0.125	12	1.811888	0.022	0.13	1.12	4.02	1.69	0.003
PY084	144.68	145.97	7062331	3453448	22.32	1983	8336339	58.4	0.663	14.2	11.00472	0.207	3.06	3.62	4.04	1.84	0.28
PY084	145.97	147.3	7062331	3453447	21.15	1983	8336340	75.8	0.118	13.3	2.323219	0.039	0.28	1.08	3.84	3.27	0.009
PY084	147.3	147.7	7062331	3453447	20.38	1983	8336341	51.2	0.906	14.5	15.22876	0.277	3.97	7.22	4.23	1	0.154
PY084	147.7	150	7062332	3453446	19.17	1983	8336342	78.5	0.127	12.4	1.83412	0.027	0.16	1.4	4.74	0.86	0.01
PY084	150	150.28	7062332	3453445	18.03	1983	8336343	53.9	0.797	13.8	14.67296	0.253	3.36	7.69	3.9	0.92	0.139

PY084	150.28	151.9	7062332	3453445	17.18	1983	8336344	78.1	0.132	12.2	1.911931	0.024	0.25	0.93	5.04	0.99	0.003
PY084	151.9	157.13	7062332	3453443	14.13	1983	8336345	74.1	0.128	11.2	2.378798	0.058	0.38	1.51	4.2	1.2	0.008
PY084	157.13	158.8	7062332	3453442	11.05	1983	8336346	53.6	0.705	12.6	13.78369	0.217	5.06	7.85	2.83	0.8	0.102
PY084	158.8	160.35	7062332	3453441	9.62	1983	8336347	72.5	0.013	13.8	0.344592	0.082	0.01	0.73	6.73	1.03	0.057
PY084	160.35	161.2	7062333	3453441	8.55	1983	8336348	50.4	0.36	11.4	10.31554	0.241	9.61	10.1	2.62	0.59	0.067
PY084	161.2	161.8	7062333	3453440	7.9	1983	8336349	64.2	0.677	12.3	9.948712	0.186	1.58	6.24	2.96	0.95	0.376
PY084	161.8	163.8	7062333	3453440	6.75	1983	8336350	78.6	0.123	11.1	2.623348	0.046	0.4	1.87	3.89	0.79	0.008
PY084	163.8	164.9	7062333	3453439	5.36	1983	8336351	49.9	0.492	14.9	11.3382	0.203	5.93	8.82	3.88	1.03	0.077
PY084	164.9	167	7062333	3453438	3.94	1983	8336352	77.2	0.108	11	2.578884	0.034	0.46	0.98	2.61	3.62	0.003
PY084	167	167.4	7062333	3453438	2.82	1983	8336353	48.2	0.458	13.5	12.00515	0.236	6.06	9.02	2.78	1.11	0.07
PY084	167.4	168.56	7062333	3453437	2.13	1983	8336354	77.2	0.125	11.9	2.723391	0.064	0.38	1.5	2.74	3.48	0.003
PY084	168.56	171.8	7062333	3453436	0.17	1983	8336355	75.3	0.199	11.7	3.712704	0.055	0.41	1.49	4.77	1.04	0.031
PY084	171.8	173.75	7062333	3453435	-2.14	1983	8336356	50.4	0.651	11	13.00558	0.185	7.4	7.56	1.92	1.27	0.153
PY084	173.75	175.55	7062334	3453434	-3.81	1983	8336357	79.6	0.106	10.5	2.200944	0.042	0.15	1.26	3.83	1.2	0.003
PY084	175.55	176.13	7062334	3453434	-4.87	1983	8336358	60.2	0.835	13.4	11.78283	0.23	2.12	5.45	3.48	1.08	0.377
PY084	176.13	178.76	7062334	3453433	-6.3	1983	8336359	77.7	0.142	10.5	2.990172	0.061	0.4	2.08	3.74	0.76	0.003
PY084	178.76	179.6	7062334	3453432	-7.85	1983	8336360	61.1	0.924	12.9	10.72682	0.217	2.02	4.49	3.45	1.48	0.399
PY084	179.6	183.85	7062334	3453431	-10.12	1983	8336361	76.3	0.136	11.4	2.756738	0.053	0.35	1.55	4.28	1.21	0.003
PY084	183.85	185.8	7062334	3453430	-12.88	1983	8336362	48.9	0.421	12.9	10.10433	0.16	8.21	8.3	2.78	1.4	0.08
PY084	185.8	187.52	7062335	3453429	-14.51	1983	8336363	75.9	0.116	11.6	2.156481	0.031	0.28	1.51	2.59	3.33	0.003
PY084	187.52	188.8	7062335	3453428	-15.85	1983	8336364	52.6	0.774	12.7	14.33948	0.205	3.28	7.37	2.55	1.46	0.138
PY084	188.8	192.3	7062335	3453427	-17.98	1983	8336365	76.9	0.116	12.1	2.034206	0.05	0.07	1.66	4.54	1.45	0.003
PY084	192.3	194	7062335	3453426	-20.3	1983	8336366	49.7	0.517	10.8	11.78283	0.212	9.13	9.05	1.83	1.42	0.093
PY084	194	198.15	7062335	3453425	-22.9	1983	8336367	74	0.139	13.1	3.056867	0.058	0.32	2.56	3.14	2.73	0.003
PY084	198.15	199.15	7062335	3453424	-25.2	1983	8336368	50.3	0.407	15	10.70459	0.199	5.57	10	1.85	2.81	0.064
PY084	199.15	200.1	7062336	3453423	-26.07	1983	8336369	77.8	0.116	11.2	2.323219	0.055	0.18	2.39	2.44	2.73	0.003
PY084	200.1	201.9	7062336	3453423	-27.29	1983	8336370	67.3	0.151	16	2.612232	0.049	0.09	1.07	5.14	4.46	0.003
PY084	201.9	203.6	7062336	3453422	-28.85	1983	8336371	76.9	0.123	11.6	2.300987	0.055	0.31	2.34	3.57	1.56	0.003

PY084	203.6	208.95	7062336	3453420	-31.98	1983	8336372	76.2	0.123	12.3	2.645579	0.058	0.16	2.71	2.61	3.03	0.003
PY084	208.95	209.75	7062336	3453419	-34.72	1983	8336373	47.9	0.495	13.7	12.22747	0.172	6.32	11	2.35	0.63	0.081
PY084	209.75	211.1	7062336	3453418	-35.67	1983	8336374	75.9	0.129	11.2	2.790086	0.038	0.6	2.12	3.71	0.9	0.003
PY084	211.1	214.95	7062337	3453417	-37.98	1983	8336375	47	0.655	15	12.6721	0.207	5.51	9.79	2.49	0.9	0.148
PY084	215.5	217.67	7062337	3453416	-41.13	1983	8336376	47	0.635	14.6	12.56094	0.197	5.35	9.76	2.31	0.69	0.135
PY084	218.5	221.45	7062337	3453414	-44.13	1983	8336377	48.4	0.606	14.7	12.44979	0.195	5.57	9.19	2.54	0.74	0.131
PY084	221.98	224.1	7062337	3453413	-46.84	1983	8336378	47.8	0.628	14.6	12.44979	0.209	5.44	8.56	2.63	0.96	0.175
PY084	224.1	225.2	7062338	3453412	-48.26	1983	8336379	42.5	0.647	12.3	13.78369	0.203	6.72	7.8	1.82	1.91	0.11
PY084	225.2	230.2	7062338	3453410	-50.96	1983	8336380	47.3	0.67	14.3	13.11674	0.218	5.53	9.19	2.7	0.77	0.137
PY084	230.2	233.3	7062338	3453409	-54.52	1983	8336381	46.7	0.647	14.6	12.56094	0.195	5.74	7.53	2.73	1.49	0.136
PY084	233.3	235.55	7062338	3453407	-56.88	1983	8336382	70.6	0.299	12.7	4.357425	0.08	0.73	4.04	3.09	0.9	0.085
PY084	235.55	240.55	7062339	3453406	-60.07	1983	8336383	47.7	0.636	15.4	12.56094	0.188	4.81	9.7	2.33	0.95	0.148
PY084	240.55	245.55	7062339	3453403	-64.45	1983	8336384	48.1	0.62	15.3	12.44979	0.191	5.21	10	2.31	0.59	0.123
PY084	245.55	250.55	7062340	3453401	-68.83	1983	8336385	46.9	0.57	15.3	12.56094	0.19	5.42	9.62	2.29	0.7	0.121
PY084	250.55	253.35	7062340	3453399	-72.24	1983	8336386	53.3	0.582	13.9	11.89399	0.158	3.92	6.62	2.8	1.08	0.176
PY084	253.35	254.35	7062340	3453398	-73.9	1983	8336387	57.7	0.67	12.8	10.61567	0.114	2.84	3.39	3.08	1.65	0.252
PY084	254.35	254.78	7062340	3453398	-74.52	1983	8336388	73.8	0.106	11.4	3.090215	0.038	0.73	1.88	3.93	0.68	0.003
PY084	254.78	255.35	7062340	3453398	-74.96	1983	8336389	46.4	0.477	13.9	12.00515	0.191	7	8.31	2.74	1.22	0.08
PY084	255.35	257.45	7062340	3453397	-76.12	1983	8336390	72.1	0.104	11.3	2.445494	0.033	0.38	1.8	3.56	1.31	0.003
PY084	258.72	260.17	7062340	3453395	-78.76	1983	8336391	74.6	0.1	11.8	2.356567	0.036	0.23	1	3.03	3.31	0.003
PY084	260.17	265.6	7062341	3453394	-81.73	1983	8336392	47.5	0.641	13.5	12.89442	0.194	5.23	7.94	2.25	1.31	0.125
PY084	265.6	266.1	7062341	3453392	-84.29	1983	8336393	75.2	0.1	12	2.40103	0.033	0.14	0.96	3.92	2.46	0.003
PY084	266.1	266.7	7062341	3453392	-84.76	1983	8336394	48.1	0.438	14.3	10.19326	0.168	5.63	6.48	2.6	2.02	0.081
PY084	266.7	269.4	7062341	3453391	-86.18	1983	8336395	76.1	0.093	11.8	2.445494	0.041	0.25	1.09	2.78	3.71	0.003
PY084	269.4	272.4	7062341	3453390	-88.62	1983	8336396	72.6	0.119	12.3	2.790086	0.07	0.53	2.82	2.09	3.14	0.003
PY084	272.4	274.9	7062342	3453388	-90.97	1983	8336397	45.5	0.918	12.6	13.56137	0.194	5.07	7.68	2.67	0.94	0.23
PY084	274.9	278.09	7062342	3453387	-93.39	1983	8336398	72	0.142	12.3	2.478841	0.048	0.77	1.63	3.85	2.39	0.016
PY084	278.09	278.55	7062342	3453386	-94.94	1983	8336399	49	0.716	13	14.45064	0.19	4.5	7.07	3.05	1.38	0.106

PY084	278.55	280.75	7062342	3453385	-96.07	1983	8336400	74.2	0.199	12.4	1.600687	0.016	0.01	0.47	5.66	1.69	0.016
PY084	280.75	282.47	7062342	3453384	-97.73	1983	8336401	51.1	0.497	12.4	10.22661	0.172	6.33	8.54	3.12	0.67	0.062
PY084	282.47	282.97	7062343	3453384	-98.67	1983	8336402	69.1	0.112	12.4	3.601545	0.055	0.83	2.35	3.18	2.05	0.003
PY084	282.97	283.54	7062343	3453383	-99.12	1983	8336403	47.4	0.491	12	9.859785	0.186	7.04	8.85	2.77	0.93	0.158
PY084	283.54	287.7	7062343	3453382	-101.12	1983	8336404	68.4	0.242	12.7	3.490386	0.055	1.02	3.15	4.03	1.25	0.05
PY084	287.7	289	7062343	3453381	-103.41	1983	8336405	51	0.659	13	12.00515	0.202	4.95	6.94	2.62	1.87	0.151
PY084	289	290.1	7062343	3453380	-104.42	1983	8336406	75.4	0.116	10.1	2.256524	0.033	0.37	1.39	3.06	1.91	0.003
PY084	290.1	292.2	7062343	3453379	-105.76	1983	8336407	46.3	0.399	14.1	11.67167	0.18	6.12	9.61	2.63	0.98	0.058
PY084	292.2	293.1	7062343	3453378	-107.01	1983	8336408	73.6	0.105	12.4	2.656695	0.05	0.21	1.91	3.06	2.57	0.003
PY084	293.1	298.53	7062344	3453377	-109.65	1983	8336409	72.8	0.112	11.5	1.878584	0.022	0.01	0.83	3.9	2.46	0.003
PY084	299.43	300.65	7062344	3453374	-113.17	1983	8336410	73.4	0.103	11.1	2.323219	0.047	0.44	1.61	3.04	2.01	0.003
PY084	300.65	312.48	7062345	3453371	-118.57	1983	8336411	72.8	0.001	13.6	0.678069	0.099	0.01	0.36	4.48	2.96	0.051
PY084	312.48	314.37	7062346	3453367	-124.24	1983	8336412	67.6	0.293	13.4	4.035064	0.079	0.54	2.87	2.59	2.81	0.091
PY084	314.37	315.19	7062346	3453366	-125.36	1983	8336413	49.5	0.342	16.4	9.593004	0.125	3.98	3.05	3.31	3.27	0.038
PY084	315.19	320.52	7062346	3453364	-127.9	1983	8336414	71.9	0.108	12.6	2.712275	0.06	0.16	2.81	1.96	2.71	0.003
PY084	320.52	324	7062346	3453362	-131.54	1983	8336415	73	0.101	11.5	2.790086	0.071	0.6	1.59	1.25	2.74	0.003
PY084	324	324.8	7062347	3453361	-133.3	1983	8336416	67.1	0.005	17.3	1.45618	0.022	0.01	0.35	3.54	3.14	0.028
PY084	324.8	326.8	7062347	3453360	-134.46	1983	8336417	72	0.109	12.3	4.257382	0.135	0.66	1.31	2.36	2.9	0.027
PY084	326.8	327.9	7062347	3453359	-135.73	1983	8336418	71.6	0.121	10.9	5.480129	0.149	0.34	2.02	1.28	3.66	0.012
PY084	327.9	328.43	7062347	3453359	-136.4	1983	8336419	73.6	0.001	14	0.833691	0.291	0.01	0.26	3.4	4.46	0.093
PY084	328.43	330.91	7062347	3453358	-137.64	1983	8336420	60.4	0.813	13.8	10.58232	0.406	1.51	3.5	1.29	3.49	0.418
PY084	330.91	334.55	7062347	3453356	-140.16	1983	8336421	64.2	0.316	12.5	7.703305	0.123	1.33	3.85	1.12	3.81	0.122
PY084	334.55	337.75	7062348	3453354	-142.97	1983	8336422	77	0.09	13	1.767425	0.062	0.01	2.97	1.47	3.66	0.003
PY084	338.21	341.8	7062348	3453352	-146.14	1983	8336423	77	0.097	11.6	1.578455	0.046	0.05	1.24	2.25	3.16	0.003
PY084	341.8	346.38	7062349	3453350	-149.49	1983	8336424	72.8	0.098	12.4	2.300987	0.1	0.43	1.56	1.94	3.15	0.003
PY084	349.4	351.77	7062349	3453346	-154.82	1983	8336425	73.8	0.102	12.8	2.223176	0.065	0.36	1.67	1.73	2.95	0.003
PY084	351.77	352.37	7062349	3453345	-156.03	1983	8336426	79.7	0.076	10.1	3.112446	0.075	0.63	2.1	2.24	1.14	0.036
PY084	353.13	355.65	7062350	3453344	-157.92	1983	8336427	74	0.091	11.8	2.056438	0.066	0.49	2.01	2.04	2.55	0.003

PY084	355.65	356.3	7062350	3453343	-159.22	1983	8336428	59.5	0.541	13.2	10.12657	0.112	1.67	3.43	2.89	1.29	0.149
PY084	356.3	360.7	7062350	3453342	-161.27	1983	8336429	54.3	0.404	14.3	9.748627	0.223	2.74	9.53	3.4	0.7	0.146
PY084	360.7	364.47	7062350	3453339	-164.58	1983	8336430	50.6	0.428	15.8	9.292876	0.155	4.01	8.07	5.02	0.39	0.237
PY084	364.47	368.2	7062351	3453337	-167.61	1983	8336431	49.3	0.429	15.3	9.181717	0.149	4.17	7.11	4.94	0.29	0.099
PY084	368.2	373.2	7062351	3453334	-171.11	1983	8336432	47.3	0.447	15	11.22704	0.201	5.13	8.26	3.87	0.52	0.092
PY084	373.2	375.4	7062352	3453332	-173.99	1983	8336433	46.4	0.494	13.7	12.6721	0.212	5.25	9.42	3.37	0.46	0.104
PY084	375.4	376.85	7062352	3453331	-175.45	1983	8336434	46.8	0.394	14.9	10.18215	0.217	4.26	16	2.06	0.32	0.1
PY084	376.85	378.5	7062352	3453330	-176.69	1983	8336435	47.7	0.407	14.9	10.58232	0.204	4.67	10.9	3.17	0.68	0.081
PY084	378.5	380.47	7062352	3453329	-178.12	1983	8336436	65.9	0.299	12.7	4.80206	0.078	1.27	3.29	4.54	0.39	0.069
PY084	380.47	381.15	7062352	3453328	-179.18	1983	8336437	50.1	0.41	14.5	9.815322	0.169	3.93	6.77	4.04	0.54	0.089
PY084	381.15	381.65	7062352	3453328	-179.64	1983	8336438	70	0.239	11.5	4.190687	0.057	0.97	5.08	2.85	0.34	0.069
PY084	381.65	383.9	7062352	3453327	-180.73	1983	8336439	46	0.42	15	10.91579	0.225	4.89	13.1	2.3	0.34	0.117
PY084	383.9	385.15	7062353	3453326	-182.12	1983	8336440	46.4	0.426	14.6	11.22704	0.189	7.37	5.92	3.42	1.74	0.078
PY084	385.15	385.97	7062353	3453326	-182.93	1983	8336441	45.7	0.42	14.2	11.11588	0.198	5.84	12	2.5	0.26	0.118
PY084	385.97	386.41	7062353	3453325	-183.43	1983	8336442	46.1	0.467	14.6	11.67167	0.186	7.43	6.44	3.5	1.79	0.085
PY084	386.41	391.78	7062353	3453323	-185.72	1983	8336443	45.9	0.421	13.5	11.01584	0.23	5.53	11.6	3.17	0.33	0.091
PY084	391.78	392.33	7062353	3453322	-188.04	1983	8336444	60.4	0.404	12.8	6.814034	0.127	2.68	5.29	4.41	0.09	0.152
PY084	392.33	396.66	7062354	3453320	-189.95	1983	8336445	49.2	0.431	15.1	10.69348	0.214	7.06	6.27	2.66	1.95	0.061
PY084	396.66	402.05	7062354	3453317	-193.74	1983	8336446	76.4	0.114	12.4	1.622918	0.04	0.33	1.49	4.5	1.74	0.014
PY084	402.25	403.1	7062355	3453315	-196.32	1983	8336447	75.6	0.108	12.1	1.711845	0.015	0.01	0.96	4.26	2.38	0.01
PY084	403.1	403.8	7062355	3453315	-196.92	1983	8336448	54.5	0.484	14.5	7.036352	0.148	4.87	6.65	3.47	1.24	0.245
PY084	403.8	404.37	7062355	3453314	-197.41	1983	8336449	71.2	0.141	12.3	2.623348	0.03	0.83	1.59	3.65	2.8	0.024
PY084	404.37	405.15	7062355	3453314	-197.94	1983	8336450	57.2	0.436	16.1	7.25867	0.177	2.09	6.18	3.9	1.11	0.283
PY084	405.15	407.5	7062355	3453313	-199.15	1983	8336451	68.5	0.218	11.9	4.546395	0.085	2.26	3.52	3.36	1.9	0.051
PY084	407.5	410.7	7062355	3453311	-201.29	1983	8336452	46.8	0.427	14.7	9.203948	0.196	6	10.4	3.29	0.69	0.404
PY084	410.7	413.7	7062356	3453309	-203.68	1983	8336453	45.8	0.463	14.1	11.67167	0.205	7.58	8.55	2.82	1.58	0.094
PY084	413.7	417.95	7062356	3453307	-206.46	1983	8336454	70.2	0.163	14.1	1.811888	0.016	0.51	1.14	4.78	3.27	0.025
PY084	417.95	421.3	7062357	3453304	-209.36	1983	8336455	69.5	0.171	14.1	2.634464	0.048	1.18	2.34	2.92	4.05	0.03

PY084	421.3	422.3	7062357	3453303	-211.02	1983	8336456	56.3	0.14	11.4	8.203519	0.36	2.37	8.38	1.25	3.17	0.041
PY084	422.3	423.5	7062357	3453302	-211.86	1983	8336457	69.4	0.17	13.2	1.578455	0.116	1.08	2.8	2.23	3.56	0.025
PY084	423.5	424.9	7062357	3453302	-212.85	1983	8336458	60.4	0.214	14.9	7.514335	0.149	1.47	4.49	1.55	2.87	0.057
PY084	424.9	427.65	7062357	3453300	-214.43	1983	8336459	69.6	0.183	14.9	2.367682	0.083	0.85	1.61	1.71	5.36	0.03
PY084	427.65	430.2	7062358	3453299	-216.44	1983	8336460	71.8	0.188	12.1	2.956824	0.19	1.61	2.68	1.59	3.34	0.029
PY084	430.2	433	7062358	3453297	-218.46	1983	8336461	74.6	0.156	11.6	2.867897	0.201	1.15	1.99	1.84	2.8	0.023
PY084	433	433.45	7062358	3453296	-219.69	1983	8336462	52.5	0.749	15.5	7.892275	0.134	5.41	7.45	1.25	2.66	0.425
PY084	433.45	437.3	7062358	3453294	-221.31	1983	8336463	75.8	0.146	10.8	3.368112	0.2	1.17	1.82	2	2.02	0.022
PY084	437.3	441.55	7062359	3453292	-224.35	1983	8336464	74.1	0.136	11.4	2.289871	0.132	0.77	1.14	2.03	3.35	0.018
PY084	441.55	444.85	7062359	3453289	-227.18	1983	8336465	50.1	0.359	14.1	9.615236	0.591	8.26	10.5	1.69	0.87	0.092
PY084	444.85	445.95	7062359	3453288	-228.83	1983	8336466	77.8	0.104	10.8	3.501502	0.102	0.55	2.02	1.94	2.94	0.006
PY084	445.95	447.74	7062360	3453287	-229.9	1983	8336467	52.8	0.627	14.5	12.22747	0.36	4.33	8.47	1.07	1.58	0.096
PY084	447.74	449.08	7062360	3453286	-231.07	1983	8336468	54.4	0.434	14.2	9.526309	0.549	4.25	5.18	3.46	1.71	0.097
PY084	450.85	454.65	7062360	3453283	-234.29	1983	8336469	75.2	0.126	11.4	2.334335	0.094	0.75	2.03	3.97	1.72	0.028
PY084	454.65	456.75	7062361	3453281	-236.48	1983	8336470	52.7	0.532	13.8	6.82515	0.145	5.78	7.5	4.03	1.06	0.28
PY084	456.75	457.5	7062361	3453280	-237.53	1983	8336471	70.5	0.13	11.1	3.634893	0.07	1.63	2.25	4.34	0.61	0.025
PY084	457.5	461.5	7062361	3453279	-239.28	1983	8336472	50	0.643	14	11.3382	0.25	5.01	8.67	3.04	0.84	0.202
PY084	461.5	462.15	7062361	3453277	-241	1983	8336473	54.1	0.48	12.9	10.99361	0.387	4.12	4.56	2.61	1.99	0.082
PY084	462.15	463.9	7062362	3453276	-241.88	1983	8336474	62.7	0.362	16.1	5.291159	0.125	1.38	5.13	3.13	1.54	0.248
PY084	463.9	467.05	7062362	3453275	-243.68	1983	8336475	60.5	0.35	15.8	6.50279	0.518	2.86	2.88	1.26	5.6	0.109
PY084	467.05	467.5	7062362	3453273	-245	1983	8336476	44.5	0.497	16.9	9.003863	0.801	10.9	2.57	2.48	5.18	0.111
PY084	467.5	469.35	7062362	3453273	-245.84	1983	8336477	62.4	0.304	15.9	5.580172	0.287	1.55	2.31	1.44	5.53	0.061
PY084	469.35	471	7062362	3453271	-247.12	1983	8336478	74.2	0.109	12.3	2.278755	0.192	1.14	1.69	1.77	3.54	0.008
PY084	471	471.65	7062362	3453271	-247.97	1983	8336479	55.1	0.705	14.1	7.436524	0.118	6.63	6.54	1.36	2.85	0.287
PY084	471.65	473.24	7062363	3453270	-248.78	1983	8336480	73.5	0.105	12.7	2.067554	0.102	0.68	1.28	2.02	4.92	0.003
PY084	473.24	476.55	7062363	3453268	-250.58	1983	8336481	73.5	0.132	12.9	2.21206	0.069	0.62	2.26	1.88	3.33	0.003
PY084	476.55	478.6	7062363	3453266	-252.54	1983	8336482	76.5	0.113	11.8	2.145365	0.054	0.44	1.82	1.45	3.29	0.003
PY084	479.05	481.8	7062364	3453264	-254.62	1983	8336483	72.8	0.123	12.9	2.367682	0.057	0.34	2.14	2.43	3.33	0.003

PY084	481.8	482.3	7062364	3453263	-255.81	1983	8336484	77.7	0.089	10.7	2.423262	0.092	0.41	3.77	1.63	1.77	0.013
PY084	482.3	483.3	7062364	3453263	-256.36	1983	8336485	56.4	0.762	14.2	7.781116	0.154	3.68	6.47	2.48	1.81	0.662

HOLEID$	FROM	TO	SAMPLENO	ZR_O ppm	CR_O %	SR_O ppm	BA_O ppm	CU_O ppm	ZN_O ppm	PB_O ppm	NI_O ppm	CO_O ppm	FE_O %	S_O %	AG_O ppm	CU_XO ppm	ZN_XO ppm	PB_XO ppm	FE_XO ppm	S_XO %
PYO84	16.6	20.3	8336291	170.2	88.92	160.74	582.4	35	74	50	42	22	1.97	0.27	1	20	80	40	2.0132	0.332
PYO84	20.3	22.4	8336292	177.6	95.76	219.96	645.12	15	62	30	28	28	1.44	0.07	1	5	80	30	2.2697	0.061
PYO84	22.4	22.77	8336293	148	300.96	482.22	573.44	7	63	34	38	26	1.77	0.005	1.1	5	170	40	5.2545	0.0005
PYO84	22.77	23.27	8336294	177.6	88.92	219.96	492.8	30	56	18	1	12	1.64	0.05	0.7	5	5	5		0.0005
PYO84	23.27	23.67	8336295	51.8	82.08	152.28	680.96	22	67	27	12	32	3.22	0.03	1.1	5	5	5		0.0005
PYO84	23.67	25.9	8336296	170.2	102.6	143.82	573.44	12	51	17	2	13	1.28	0.01	0.4	5	5	5		0.0005
PYO84	25.9	26.95	8336297	170.2	129.96	135.36	680.96	11	50	12	3	10	1.26	0.01	0.8	5	5	5		0.0005
PYO84	27.15	28.54	8336298	170.2	143.64	126.9	672	13	61	16	3	11	1.52	0.04	0.7	5	70	30	2.0676	0.027
PYO84	28.54	29.15	8336299	96.2	396.72	287.64	528.64	20	46	12	11	22	2.01	0.005	0.9	5	180	40	8.0062	0.0005
PYO84	29.15	29.8	8336300	177.6	171	143.82	600.32	25	56	14	3	13	1.7	0.08	0.8	10	60	30	2.0598	0.066
PYO84	29.8	30.88	8336301	66.6	88.92	194.58	376.32	48	44	17	7	32	3.11	0.26	1	5	5	5		0.0005
PYO84	37.08	38.2	8336302	162.8	136.8	135.36	358.4	15	56	5	4	11	1.78	0.04	0.7	5	5	5		0.0005
PYO84	38.2	38.8	8336303	140.6	396.72	465.3	725.76	12	61	13	48	22	2.02	0.02	0.7	5	5	5		0.0005
PYO84	38.8	39.8	8336304	162.8	136.8	118.44	654.08	19	48	18	6	12	1.53	0.01	0.8	5	5	5		0.0005

PYO84	42	42.44	8336305	155.4	109.44	118.44	528.64	14	34	9	0.5	12	1.4	0.06	0.9	5	40	30	2.1453	0.022
PYO84	49.82	51.23	8336306	207.2	102.6	194.58	492.8	15	55	12	3	13	1.62	0.04	0.7	5	5	5		0.0005
PYO84	51.23	52.73	8336307	81.4	82.08	228.42	591.36	44	69	13	8	29	4.03	0.18	1.2	5	5	5		0.0005
PYO84	53.15	53.8	8336308	74	88.92	262.26	600.32	42	67	18	10	35	3.99	0.04	1.4	5	5	5		0.0005
PYO84	53.8	54.45	8336309	199.8	95.76	160.74	716.8	53	38	13	0.5	14	1.48	0.29	1.1	5	5	5		0.0005
PYO84	54.45	55.05	8336310	66.6	75.24	135.36	654.08	426	146	24	13	43	7	0.005	1.4	5	5	5		0.0005
PYO84	58.22	58.75	8336311	44.4	123.12	135.36	689.92	13	69	33	19	35	3.59	0.01	1.3	5	140	40	9.4831	0.0005
PYO84	62.16	63.03	8336312	37	102.6	16.92	322.56	10	41	21	4	12	0.23	0.02	0.3	5	70	40	0.4407	0.003
PYO84	63.03	63.7	8336313	155.4	102.6	76.14	627.2	15	53	30	10	8	1.85	0.19	0.2	5	5	5		0.0005
PYO84	73.9	74.5	8336314	51.8	109.44	194.58	582.4	5	45	14	24	29	2.83	0.005	0.5	5	110	40	8.2394	0.0005
PYO84	74.5	76.1	8336315	170.2	164.16	93.06	564.48	13	47	11	4	8	1.47	0.02	0.4	5	50	40	1.8267	0.004
PYO84	79.1	84.81	8336316	170.2	109.44	109.98	609.28	12	44	5	4	7	1.09	0.1	0.2	5	50	30	1.6168	0.045
PYO84	85.74	86.46	8336317	74	95.76	177.66	555.52	45	64	11	7	26	3.31	0.11	0.6	5	5	5		0.0005
PYO84	88.5	89.8	8336318	185	102.6	118.44	618.24	23	53	8	1	8	1.33	0.1	0.3	5	5	5		0.0005
PYO84	89.8	91.58	8336319	192.4	102.6	194.58	752.64	23	66	10	5	9	1.86	0.05	0.6	5	5	5		0.0005
PYO84	91.78	96.78	8336320	177.6	95.76	135.36	609.28	8	50	8	3	7	1.29	0.01	0.2	5	5	5		0.0005

PYO84	96.78	98.74	8336321	177.6	143.64	118.44	645.12	15	47	9	4	10	1.64	0.24	0.4	5	5	5		0.0005
PYO84	98.74	99.74	8336322	59.2	61.56	135.36	528.64	6	88	10	10	25	3.45	0.01	0.6	5	200	40	9.4053	0.01
PYO84	99.74	105.44	8336323	192.4	150.48	101.52	1164.8	17	54	7	6	9	1.35	0.1	0.6	5	5	5		0.0005
PYO84	105.44	111.1	8336324	199.8	54.72	101.52	1164.8	12	55	4	2	7	1.38	0.03	0.5	5	5	5		0.0005
PYO84	111.1	111.45	8336325	51.8	68.4	160.74	528.64	4	91	13	29	32	3.43	0.005	0.5	5	5	5		0.0005
PYO84	112	112.9	8336326	192.4	61.56	143.82	707.84	22	62	34	3	10	1.34	0.04	0.5	5	5	5		0.0005
PYO84	113.2	114.2	8336327	199.8	34.2	135.36	1200.64	25	55	8	6	8	1.33	0.03	0.5	5	60	10	1.508	0.029
PYO84	114.2	115.84	8336328	133.2	266.76	397.62	501.76	9	93	9	50	24	2.07		0.7	5	5	5		0.0005
PYO84	115.84	117.13	8336329	185	68.4	93.06	698.88	27	58	4	3	10	1.19	0.05	0.5	5	5	5		0.0005
PYO84	117.13	118.63	8336330	133.2	287.28	372.24	501.76	9	108	7	48	24	2.08	0.005	0.5	5	5	5		0.0005
PYO84	118.63	120.09	8336331	199.8	75.24	160.74	627.2	19	27	6	5	11	1.05	0.02	0.7	5	5	5		0.0005
PYO84	120.09	120.92	8336332	88.8	779.76	313.02	483.84	10	49	13	63	27	2.05	0.01	0.6	5	5	5		0.0005
PYO84	120.92	125.92	8336333	199.8	82.08	101.52	743.68	14	42	2	5	11	0.98	0.005	0.5	5	5	5		0.0005
PYO84	125.92	131.8	8336334	192.4	82.08	84.6	421.12	19	43	2	9	11	0.9	0.03	0.5	5	40	5	1.1038	0.0005
PYO84	131.8	134.36	8336335	88.8	68.4	177.66	483.84	19	88	12	6	18	3.57	0.03	0.8	5	140	5	7.6953	0.016
PYO84	134.36	136.5	8336336	177.6	68.4	93.06	546.56	12	41	5	2	13	0.93	0.01	0.4	5	40	5	1.2281	0.0005

PYO84	136.5	140.13	8336337	199.8	61.56	118.44	752.64	17	75	9	7	13	1.28	0.05	0.7	5	5	5		0.0005
PYO84	142.4	144.68	8336338	177.6	54.72	84.6	510.72	27	33	7	3	13	1.09	0.02	0.4	5	5	5		0.0005
PYO84	144.68	145.97	8336339	96.2	20.52	177.66	573.44	44	146	16	14	19	5.2	0.2	1.2	10	180	5	7.6953	0.192
PYO84	145.97	147.3	8336340	199.8	54.72	109.98	1048.32	10	82	13	1	5	1.25	0.03	0.7	5	90	5	1.6246	0.027
PYO84	147.3	147.7	8336341	51.8	10	152.28	474.88	27	53	13	2	27	3.75	0.08	0.7	5	140	5	10.649	0.077
PYO84	147.7	150	8336342	192.4	61.56	84.6	385.28	13	42	10	0.5	5	1.25	0.07	0.6	5	40	5	1.2825	0.058
PYO84	150	150.28	8336343	59.2	54.72	135.36	501.76	3	42	9	6	19	2.75	0.005	1	5	120	5	10.2604	0.0005
PYO84	150.28	151.9	8336344	199.8	41.04	109.98	465.92	13	52	8	0.5	6	1.2	0.04	0.7	5	5	5		0.0005
PYO84	151.9	157.13	8336345	199.8	150.48	126.9	645.12	13	75	12	0.5	7	1.38	0.13	0.8	5	5	5		0.0005
PYO84	157.13	158.8	8336346	66.6	280.44	228.42	501.76	138	49	19	24	28	3.33	0.04	1	110	110	5	9.6385	0.159
PYO84	158.8	160.35	8336347	37	129.96	16.92	313.6	4	7	5	0.5	4	0.21	0.03	0.6	5	10	20	0.2448	0.0005
PYO84	160.35	161.2	8336348	37	663.48	169.2	456.96	2	31	12	19	16	1.37	0.01	0.7	5	130	10	7.2133	0.0005
PYO84	161.2	161.8	8336349	88.8	143.64	219.96	430.08	6	72	15	0.5	11	3.07	0.01	0.6	5	90	5	6.9568	0.0005
PYO84	161.8	163.8	8336350	192.4	171	126.9	546.56	18	41	11	1	7	1.62	0.07	0.8	10	40	10	1.8344	0.069
PYO84	163.8	164.9	8336351	66.6	150.48	279.18	546.56	3	36	9	17	22	2.33	0.01	0.7	5	5	5		0.0005
PYO84	164.9	167	8336352	177.6	205.2	160.74	483.84	50	66	9	0.5	7	1.75	0.15	0.6	5	5	5		0.0005

PY084	167	167.4	8336353	51.8	75.24	186.12	456.96	9	47	14	11	26	2.74	0.005	1.1	5	5	5		0.0005
PY084	167.4	168.56	8336354	185	102.6	135.36	555.52	16	77	8	0.5	8	1.59	0.12	0.8	5	5	5		0.0005
PY084	168.56	171.8	8336355	155.4	171	126.9	546.56	22	59	3	0.5	10	2.08	0.05	0.6	5	60	5	2.5962	0.023
PY084	171.8	173.75	8336356	66.6	649.8	169.2	537.6	3	45	16	39	25	2.84	0.01	0.9	5	100	5	9.0944	0.0005
PY084	173.75	175.55	8336357	162.8	164.16	135.36	842.24	27	67	9	0.5	7	1.3	0.05	0.8	20	70	5	1.5391	0.047
PY084	175.55	176.13	8336358	81.4	123.12	203.04	564.48	10	68	15	3	23	4.42	0.08	0.9	5	5	5		0.0005
PY084	176.13	178.76	8336359	214.6	191.52	118.44	573.44	5	51	15	4	4	1.5	0.02	0.4	5	5	5		0.0005
PY084	178.76	179.6	8336360	81.4	88.92	143.82	573.44	4	85	15	5	16	3.71	0.005	0.4	5	5	5		0.0005
PY084	179.6	183.85	8336361	199.8	177.84	118.44	591.36	34	62	9	2	4	1.57	0.07	0.3	20	60	5	1.9277	0.05
PY084	183.85	185.8	8336362	66.6	663.48	236.88	546.56	2	41	18	45	22	2.24	0.005	0.2	5	90	5	7.0657	0.0005
PY084	185.8	187.52	8336363	177.6	177.84	126.9	654.08	40	44	7	1	4	1.14	0.07	0.05	30	40	20	1.508	0.064
PY084	187.52	188.8	8336364	59.2	129.96	160.74	627.2	17	67	11	2	25	3.46	0.02	0.1	5	130	5	10.0272	0.014
PY084	188.8	192.3	8336365	185	150.48	126.9	600.32	7	36	9	0.5	4	0.79	0.005	0.1	5	40	10	1.4225	0.001
PY084	192.3	194	8336366	66.6	1046.52	177.66	537.6	3	48	12	87	24	2.46	0.005	0.05	5	130	5	8.2394	0.0005
PY084	194	198.15	8336367	207.2	212.04	135.36	627.2	10	55	10	4	3	1.42	0.02	0.05	5	5	5		0.0005
PY084	198.15	199.15	8336368	59.2	218.88	211.5	734.72	5	35	15	17	16	1.6	0.005	0.3	5	5	5		0.0005

PY084	199.15	200.1	8336369	177.6	136.8	118.44	725.76	17	65	9	4	5	1.08	0.04	0.05	5	5	5		0.0005
PY084	200.1	201.9	8336370	229.4	171	93.06	824.32	5	59	15	2	5	1.49	0.03	0.05	5	5	5		0.0005
PY084	201.9	203.6	8336371	177.6	171	101.52	663.04	8	48	4	4	5	0.98	0.02	0.05	5	5	5		0.0005
PY084	203.6	208.95	8336372	185	136.8	118.44	689.92	15	62	14	0.5	5	1.12	0.04	0.05	5	70	5	1.85	0.049
PY084	208.95	209.75	8336373	59.2	136.8	228.42	483.84	3	20	5	6	12	1.16	0.005	0.05	5	5	5		0.0005
PY084	209.75	211.1	8336374	177.6	171	152.28	483.84	70	56	8	5	8	1.7	0.12	0.05	5	5	5		0.0005
PY084	211.1	214.95	8336375	74	129.96	262.26	528.64	119	48	12	11	21	2.04	0.16	0.2	5	5	5		0.0005
PY084	215.5	217.67	8336376	74	109.44	287.64	474.88	7	24	9	5	16	1.69	0.005	0.05	5	5	5		0.0005
PY084	218.5	221.45	8336377	74	95.76	279.18	510.72	4	30	9	8	18	1.97	0.005	0.1	5	100	10	8.7058	0.0005
PY084	221.98	224.1	8336378	74	95.76	270.72	501.76	50	44	15	7	23	2.61	0.005	0.2	5	5	5		0.0005
PY084	224.1	225.2	8336379	51.8	102.6	177.66	510.72	86	3440	27	26	55	6.85	2.01	0.5	5	5	5		0.0005
PY084	225.2	230.2	8336380	66.6	102.6	270.72	483.84	114	48	12	10	21	2.28	0.08	0.1	5	5	5		0.0005
PY084	230.2	233.3	8336381	74	88.92	262.26	546.56	28	116	14	13	25	3.31	0.01	0.2	5	5	5		0.0005
PY084	233.3	235.55	8336382	155.4	116.28	143.82	537.6	26	51	13	4	12	2	0.05	0.05	5	5	5		0.0005
PY084	235.55	240.55	8336383	74	116.28	262.26	528.64	172	28	10	6	21	1.82	0.17	0.3	5	5	5		0.0005
PY084	240.55	245.55	8336384	74	102.6	287.64	492.8	14	28	7	6	17	1.83	0.01	0.05	5	5	5		0.0005

PYO84	245.55	250.55	8336385	74	95.76	262.26	537.6	27	32	9	11	21	2.03	0.005	0.05	5	5	5		0.0005
PYO84	250.55	253.35	8336386	81.4	136.8	228.42	448	37	54	11	5	20	3.25	0.14	0.2	5	5	5		0.0005
PYO84	253.35	254.35	8336387	96.2	123.12	211.5	474.88	11	99	16	13	18	4.57	0.01	1.1	5	5	5		0.0005
PYO84	254.35	254.78	8336388	185	177.84	135.36	573.44	29	44	9	4	6	1.94	0.03	0.6	5	5	5		0.0005
PYO84	254.78	255.35	8336389	44.4	253.08	177.66	430.08	4	55	12	31	24	2.65	0.01	0.8	5	5	5		0.0005
PYO84	255.35	257.45	8336390	192.4	102.6	152.28	931.84	50	33	2	3	7	1.42	0.15	0.6	5	5	5		0.0005
PYO84	258.72	260.17	8336391	192.4	88.92	143.82	860.16	21	58	5	4	5	1.43	0.04	0.9	10	70	30	1.6479	0.046
PYO84	260.17	265.6	8336392	74	95.76	253.8	528.64	15	39	10	11	21	2.39	0.005	0.6	5	5	5		0.0005
PYO84	265.6	266.1	8336393	192.4	157.32	135.36	797.44	18	50	3	4	6	1.47	0.04	2.2	5	5	5		0.0005
PYO84	266.1	266.7	8336394	66.6	116.28	228.42	636.16	14	62	16	24	32	3.05	0.01	0.7	5	110	50	7.1278	0.014
PYO84	266.7	269.4	8336395	185	198.36	160.74	779.52	21	65	5	0.5	6	1.41	0.04	0.4	10	70	30	1.7101	0.004
PYO84	269.4	272.4	8336396	192.4	164.16	160.74	680.96	12	60	10	4	7	1.21	0.01	0.6	5	70	40	1.951	0.0005
PYO84	272.4	274.9	8336397	111	95.76	355.32	537.6	79	64	18	27	41	4.27	0.35	1.1	40	120	40	9.4831	0.327
PYO84	274.9	278.09	8336398	177.6	143.64	101.52	663.04	12	55	5	4	8	1.16	0.005	0.5	5	60	30	1.7334	0.02
PYO84	278.09	278.55	8336399	59.2	129.96	169.2	672	18	46	12	10	29	3.31	0.01	1.2	5	5	5		0.0005
PYO84	278.55	280.75	8336400	155.4	75.24	76.14	654.08	15	35	8	0.5	8	0.82	0.04	0.7	5	5	5		0.0005

PY084	280.75	282.47	8336401	88.8	417.24	253.8	456.96	10	24	2	30	17	1.25	0.01	0.8	5	100	50	7.1512	0.0005
PY084	282.47	282.97	8336402	214.6	157.32	203.04	1111.04	41	48	13	1	11	1.93	0.06	1.3	20	50	40	2.5185	0.058
PY084	282.97	283.54	8336403	96.2	649.8	313.02	663.04	11	36	12	33	21	1.34	0.005	1	5	130	40	6.8947	0.0005
PY084	283.54	287.7	8336404	140.6	102.6	143.82	591.36	29	31	9	2	16	1.31	0.05	0.9	10	40	30	2.4407	0.034
PY084	287.7	289	8336405	66.6	68.4	211.5	645.12	24	61	12	12	28	3.44	0.01	1.3	5	120	40	8.3948	0.018
PY084	289	290.1	8336406	162.8	150.48	84.6	474.88	24	54	12	2	14	1.36	0.06	0.8	5	50	20	1.5779	0.061
PY084	290.1	292.2	8336407	59.2	157.32	236.88	564.48	6	44	11	21	18	2.22	0.005	0.7	5	5	5		0.0005
PY084	292.2	293.1	8336408	199.8	184.68	118.44	949.76	7	80	10	5	5	1.46	0.02	0.2	5	5	5		0.0005
PY084	293.1	298.53	8336409	199.8	129.96	118.44	1191.68	18	45	7	3	6	1.16	0.15	0.05	10	40	20	1.3136	0.153
PY084	299.43	300.65	8336410	207.2	205.2	160.74	1003.52	8	67	9	4	6	1.3	0.06	0.3	5	70	20	1.6246	0.068
PY084	300.65	312.48	8336411	22.2	143.64	25.38	295.68	2	27	9	1	4	0.21	0.01	0.05	5	40	50	0.4757	0.025
PY084	312.48	314.37	8336412	177.6	177.84	160.74	913.92	21	84	11	9	10	2.38	0.4	0.1	10	100	40	2.8216	0.489
PY084	314.37	315.19	8336413	66.6	212.04	109.98	1137.92	133	1010	32	55	43	6.78	1.73	1	110	1020	70	6.7081	1.853
PY084	315.19	320.52	8336414	207.2	143.64	109.98	851.2	19	80	14	6	7	1.64	0.34	0.1	10	90	50	1.8966	0.377
PY084	320.52	324	8336415	185	129.96	76.14	896	19	102	8	17	7	1.45	0.28	0.05	10	130	40	1.951	0.37
PY084	324	324.8	8336416	22.2	116.28	16.92	286.72	6	41	11	3	5	0.41	0.1	0.2	5	60	40	1.0183	0.171

PYO84	324.8	326.8	8336417	185	136.8	59.22	734.72	34	300	15	100	11	2.78	1.11	0.7	20	340	60	2.9771	1.294
PYO84	326.8	327.9	8336418	148	171	67.68	833.28	60	309	38	141	14	4.38	2.9	0.9	40	320	110	3.8321	2.953
PYO84	327.9	328.43	8336419	37	164.16	8.46	286.72	4	165	23	5	7	0.2	0.05	0.2	5	5	5		0.0005
PYO84	328.43	330.91	8336420	103.6	198.36	67.68	913.92	45	423	42	95	28	6.83	2.47	1.1	5	5	5		0.0005
PYO84	330.91	334.55	8336421	103.6	143.64	93.06	931.84	141	652	24	115	29	4.97	2.76	0.8	130	730	70	5.3867	3.129
PYO84	334.55	337.75	8336422	192.4	143.64	84.6	770.56	14	156	23	10	11	1.22	0.56	0.3	5	180	60	1.2359	0.71
PYO84	338.21	341.8	8336423	192.4	171	101.52	680.96	8	52	9	3	8	0.82	0.33	0.05	5	5	5		0.0005
PYO84	341.8	346.38	8336424	192.4	123.12	93.06	752.64	6	157	12	7	10	1.38	0.62	0.1	5	180	50	1.609	0.647
PYO84	349.4	351.77	8336425	192.4	171	76.14	672	13	150	23	9	10	1.36	0.62	0.2	5	160	60	1.5546	0.738
PYO84	351.77	352.37	8336426	155.4	184.68	67.68	492.8	32	525	38	9	10	1.92	0.7	0.3	20	620	70	2.1764	0.851
PYO84	353.13	355.65	8336427	177.6	102.6	67.68	815.36	19	384	37	10	9	1.52	0.81	0.2	10	420	90	1.438	0.909
PYO84	355.65	356.3	8336428	88.8	171	93.06	752.64	213	306	34	137	41	7.74	5.24	1.9	200	340	90	7.0812	5.213
PYO84	356.3	360.7	8336429	59.2	136.8	135.36	860.16	180	132	22	99	39	4.4	2.88	0.8	160	390	70	6.8169	3.579
PYO84	360.7	364.47	8336430	44.4	150.48	160.74	528.64	114	22	14	35	45	2.31	1.07	0.5	100	120	50	6.4982	1.339
PYO84	364.47	368.2	8336431	44.4	157.32	160.74	412.16	116	14	17	37	47	2.48	1.12	0.5	5	5	5		0.0005
PYO84	368.2	373.2	8336432	59.2	171	219.96	985.6	97	23	15	26	34	2.14	0.48	0.5	5	5	5		0.0005

PYO84	373.2	375.4	8336433	51.8	171	211.5	582.4	99	14	12	16	23	1.18	0.2	0.5	70	110	40	8.8612	0.218
PYO84	375.4	376.85	8336434	51.8	164.16	194.58	555.52	181	13	19	25	27	1.12	0.53	0.6	150	110	40	7.1201	0.623
PYO84	376.85	378.5	8336435	66.6	164.16	270.72	2553.6	75	17	9	18	16	1.22	0.18	0.9	40	90	40	7.3999	0.239
PYO84	378.5	380.47	8336436	140.6	171	211.5	412.16	48	51	8	24	15	1.93	0.71	0.3	40	120	30	3.3579	0.898
PYO84	380.47	381.15	8336437	111	164.16	236.88	591.36	124	64	12	37	29	2.97	1	0.6	100	180	40	6.8636	1.106
PYO84	381.15	381.65	8336438	148	198.36	321.48	403.2	58	33	10	17	13	1.55	0.85	0.2	50	150	30	2.9304	1.042
PYO84	381.65	383.9	8336439	51.8	150.48	219.96	663.04	87	7	14	10	10	0.53	0.16	0.7	50	100	40	7.6331	0.212
PYO84	383.9	385.15	8336440	66.6	143.64	321.48	1370.88	143	55	19	27	34	3.84	0.16	0.8	120	90	40	7.8507	0.232
PYO84	385.15	385.97	8336441	59.2	136.8	279.18	537.6	44	7	13	5	7	0.43	0.01	0.1	10	90	40	7.773	0.046
PYO84	385.97	386.41	8336442	74	157.32	304.56	1854.72	238	60	22	30	36	3.77	0.38	0.6	230	100	40	8.1616	0.45
PYO84	386.41	391.78	8336443	59.2	143.64	245.34	734.72	92	9	10	7	12	0.79	0.21	0.4	60	90	50	7.703	0.256
PYO84	391.78	392.33	8336444	148	150.48	304.56	403.2	189	13	8	77	27	1.85	1.1	0.2	5	5	5		0.0005
PYO84	392.33	396.66	8336445	74	143.64	152.28	931.84	112	57	20	21	28	2.64	0.26	0.4	5	5	5		0.0005
PYO84	396.66	402.05	8336446	155.4	102.6	118.44	672	9	56	15	0.5	4	1.38	1.2	0.2	5	5	5		0.0005
PYO84	402.25	403.1	8336447	170.2	150.48	177.66	770.56	11	38	22	0.5	5	1.37	1.18	0.2	5	40	40	1.197	0.997
PYO84	403.1	403.8	8336448	148	396.72	490.68	528.64	11	74	18	61	20	2.17	0.04	0.4	5	5	5		0.0005

PY084	403.8	404.37	8336449	148	123.12	160.74	689.92	23	39	17	2	8	1.95	1.52	0.3	5	5	5		0.0005
PY084	404.37	405.15	8336450	148	88.92	490.68	761.6	18	69	17	0.5	15	2.51	0.34	0.3	5	5	5		0.0005
PY084	405.15	407.5	8336451	118.4	116.28	160.74	752.64	43	59	16	12	17	2.33	1.08	0.5	5	5	5		0.0005
PY084	407.5	410.7	8336452	51.8	143.64	228.42	672	115	28	19	36	25	1.87	0.2	0.8	5	5	5		0.0005
PY084	410.7	413.7	8336453	51.8	150.48	186.12	1075.2	136	71	23	37	40	3.74	0.85	0.6	5	5	5		0.0005
PY084	413.7	417.95	8336454	162.8	88.92	135.36	1854.72	12	64	23	0.5	4	1.88	1.79	0.5	5	70	40	1.267	1.174
PY084	417.95	421.3	8336455	162.8	88.92	126.9	2007.04	7	113	21	5	5	2.16	2.12	0.5	5	130	60	1.8422	1.536
PY084	421.3	422.3	8336456	162.8	164.16	177.66	9766.4	13	593	288	12	12	7.06	8.76	3.5	5	5	5		0.0005
PY084	422.3	423.5	8336457	140.6	143.64	76.14	1872.64	120	2300	1089	5	5	1.78	1.69	3	5	5	5		0.0005
PY084	423.5	424.9	8336458	125.8	164.16	59.22	1514.24	316	11500	3618	13	14	7.52	10.1	10.5	300	11400	3240	5.2545	7.011
PY084	424.9	427.65	8336459	162.8	164.16	76.14	1881.6	39	1220	220	1	3	2.23	2.33	0.2	5	5	5		0.0005
PY084	427.65	430.2	8336460	133.2	136.8	67.68	878.08	15	101	30	8	8	2.1	0.69	0.4	5	5	5		0.0005
PY084	430.2	433	8336461	133.2	123.12	76.14	725.76	6	82	13	1	4	1.92	0.73	0.3	5	90	70	2.0054	0.83
PY084	433	433.45	8336462	170.2	383.04	642.96	887.04	27	135	58	53	42	3.97	0.57	1.2	5	5	5		0.0005
PY084	433.45	437.3	8336463	133.2	205.2	109.98	779.52	14	860	67	6	5	2.44	1.65	0.2	5	5	5		0.0005
PY084	437.3	441.55	8336464	140.6	171	84.6	1120	7	199	43	6	4	1.9	1.52	0.3	5	5	5		0.0005

PYO84	441.55	444.85	8336465	59.2	150.48	143.82	1075.2	94	113	81	51	42	4.45	2.87	1.5	5	5	5		0.0005
PYO84	444.85	445.95	8336466	148	157.32	42.3	967.68	41	600	180	62	8	2.74	2.26	0.7	5	5	5		0.0005
PYO84	445.95	447.74	8336467	66.6	116.28	152.28	1792	45	85	36	28	46	5.78	2.22	1.6	5	5	5		0.0005
PYO84	447.74	449.08	8336468	88.8	164.16	219.96	2114.56	116	124	30	35	36	5.44	2.38	0.9	100	190	70	6.6615	2.843
PYO84	450.85	454.65	8336469	148	102.6	109.98	1308.16	29	730	95	2	5	1.57	0.94	0.3	5	5	5		0.0005
PYO84	454.65	456.75	8336470	155.4	376.2	499.14	815.36	5	85	12	63	17	1.83	0.03	0.4	5	5	5		0.0005
PYO84	456.75	457.5	8336471	162.8	150.48	203.04	591.36	93	155	19	6	14	2.18	1.16	0.5	5	5	5		0.0005
PYO84	457.5	461.5	8336472	103.6	205.2	355.32	1039.36	67	50	17	25	20	2	0.39	0.1	5	5	5		0.0005
PYO84	461.5	462.15	8336473	74	123.12	169.2	1729.28	79	179	20	23	39	4.91	1.05	1	5	5	5		0.0005
PYO84	462.15	463.9	8336474	170.2	164.16	575.28	1048.32	11	124	27	7	15	3.25	0.23	0.6	5	120	70	3.6999	0.267
PYO84	463.9	467.05	8336475	59.2	157.32	84.6	4426.24	137	780	408	46	48	5.87	6.12	1.6	130	850	510	4.5472	4.259
PYO84	467.05	467.5	8336476	37	143.64	76.14	1514.24	121	630	118	65	52	6.07	2.31	2.5	5	5	5		0.0005
PYO84	467.5	469.35	8336477	103.6	157.32	126.9	5608.96	33	1420	376	70	36	5	5	1	5	5	5		0.0005
PYO84	469.35	471	8336478	185	171	143.82	1935.36	27	213	142	4	5	1.53	0.83	0.3	20	250	240	1.5935	0.855
PYO84	471	471.65	8336479	192.4	437.76	752.94	860.16	56	74	27	44	32	2.86	0.51	0.8	40	130	60	5.2001	0.577
PYO84	471.65	473.24	8336480	192.4	171	143.82	1344	18	75	24	3	3	1.31	0.5	0.5	10	100	90	1.4458	0.569

PY084	473.24	476.55	8336481	214.6	164.16	169.2	2132.48	18	64	16	2	4	1.13	0.2	0.2	5	5	5	0.0005
PY084	476.55	478.6	8336482	192.4	177.84	101.52	707.84	9	53	11	4	2	1.01	0.05	0.4	5	5	5	0.0005
PY084	479.05	481.8	8336483	199.8	109.44	109.98	913.92	7	90	7	6	4	1.23	0.02	0.7	5	5	5	0.0005
PY084	481.8	482.3	8336484	162.8	171	118.44	582.4	10	39	18	4	7	1.1	0.04	0.5	10	50	40	1.6945	0.084
PY084	482.3	483.3	8336485	222	212.04	693.72	842.24	29	114	16	51	23	3.2	0.19	0.8	5	5	5	0.0005

APPENDIX 4.c. R-2394 AAS geochemical data, by courtesy of Pyhäsalmi Mine Oy:

HOLE_ID	*SAMPLE_ID*	*DEPTH_FROM*	*DEPTH_TO*	*Y_COORD*	*X_COORD*	*Z_COORD*	*CU%*	*ZN%*	*S%*	*AU ppm*	*AG ppm*	*FE%*	*PB%*	*BA%*
R-2394	44155	17.82	18.52	2281.461	8423.83	-1253.87	0.07	0.01	0.3	1.3	32.6	-1	0.23	-1
R-2394	44156	18.52	19.47	2280.646	8423.344	-1253.83	0.02	0.01	0.1	0.1	2.9	-1	0.02	-1
R-2394	44157	27.16	28.74	2272.699	8418.603	-1253.28	0.05	0.01	0.3	11	77.5	-1	0.21	-1
R-2394	44158	28.74	30	2271.619	8417.959	-1253.2	0.01	0.02	0.1	0.3	1.6	-1	0.02	-1
R-2394	44159	30	32	2269.906	8416.937	-1253.06	0.01	0.01	0.1	0.1	0.6	-1	0.01	-1
R-2394	44160	32	32.62	2269.375	8416.62	-1253.01	0.1	0.02	0.4	1.7	28.6	-1	0.38	-1
R-2394	44161	40.89	41.45	2261.81	8412.107	-1252.4	0.14	0.02	0.7	2.6	52.5	-1	0.52	-1
R-2394	44162	41.45	43.66	2259.917	8410.978	-1252.24	0.62	6.46	40.4	-1	-1	-1	-1	-1
R-2394	44163	43.66	45.35	2258.469	8410.114	-1252.12	0.78	4.72	43.5	-1	-1	-1	-1	-1
R-2394	44164	45.35	46.71	2257.304	8409.419	-1252.02	1.61	1.2	44.6	-1	-1	-1	-1	-1
R-2394	44165	46.71	47.63	2256.516	8408.949	-1251.96	1.21	0.92	20.1	0.7	35.7	-1	-1	-1
R-2394	44166	47.63	50.83	2253.775	8407.314	-1251.72	1.37	0.49	47.9	-1	-1	-1	-1	-1
R-2394	44167	50.83	52.63	2252.234	8406.394	-1251.59	1.48	0.29	47.7	-1	-1	-1	-1	-1

R-2394	44168	52.63	55.37	2249.887	8404.994	-1251.39	2.03	1.23	47.3	-1	-1	-1	-1	-1
R-2394	44169	55.37	56.94	2248.543	8404.192	-1251.27	2.2	0.42	44.3	-1	-1	-1	-1	-1
R-2394	44170	56.94	59.29	2246.531	8402.992	-1251.09	1.31	0.31	48.7	-1	-1	-1	-1	-1
R-2394	44171	59.29	62.1	2244.125	8401.556	-1250.87	2.02	0.56	49.6	-1	-1	-1	-1	-1
R-2394	44172	62.1	63.72	2242.738	8400.729	-1250.75	2.51	0.51	50.3	-1	-1	-1	-1	-1
R-2394	44173	63.72	65.5	2241.214	8399.819	-1250.61	2.4	1.29	48.9	-1	-1	-1	-1	-1
R-2394	44174	65.5	69.45	2237.832	8397.802	-1250.29	1.55	0.24	49	-1	-1	-1	-1	-1
R-2394	44175	69.45	71.57	2236.017	8396.719	-1250.12	2.8	0.44	47.3	-1	-1	-1	-1	-1
R-2394	44176	71.57	74.31	2233.672	8395.32	-1249.9	2.52	0.29	48.7	-1	-1	-1	-1	-1
R-2394	44177	74.31	76.49	2231.806	8394.207	-1249.72	1.85	0.08	45.7	-1	-1	-1	-1	-1
R-2394	44178	76.49	78.95	2229.701	8392.951	-1249.52	1.36	0.06	49.4	-1	-1	-1	-1	-1
R-2394	44179	78.95	79.67	2229.085	8392.583	-1249.46	1.59	0.08	22.1	1.5	22	-1	-1	-1
R-2394	44180	79.67	81.24	2227.741	8391.782	-1249.33	1.17	0.07	49.9	-1	-1	-1	-1	-1
R-2394	44181	81.24	84.07	2225.32	8390.337	-1249.09	1.36	0.12	49.9	-1	-1	-1	-1	-1
R-2394	44182	84.07	85.58	2224.028	8389.566	-1248.96	1.38	0.14	4.8	21.5	19.3	-1	-1	-1
R-2394	44183	85.58	88.46	2221.564	8388.096	-1248.71	1.39	0.08	49.6	-1	-1	-1	-1	-1

R-2394	44184	88.46	89.27	2220.871	8387.683	-1248.64	0.74	0.07	45.4	-1	-1	-1	-1	-1
R-2394	44185	89.27	92.32	2218.261	8386.126	-1248.37	0.66	0.07	51.2	-1	-1	-1	-1	-1
R-2394	44186	92.32	95.25	2215.755	8384.631	-1248.11	0.27	0.04	51.6	-1	-1	-1	-1	-1
R-2394	44187	95.25	97.71	2213.651	8383.376	-1247.89	0.52	0.06	50.8	-1	-1	-1	-1	-1
R-2394	44188	97.71	98.33	2213.121	8383.059	-1247.84	0.99	0.09	18.9	1.6	22	-1	-1	-1
R-2394	44189	98.33	103.25	2208.913	8380.549	-1247.39	0.89	0.1	50.2	-1	-1	-1	-1	-1
R-2394	44190	103.25	104	2208.271	8380.166	-1247.32	0.15	0.03	2.5	0.4	3.2	-1	-1	-1
R-2394	44191	104	106.18	2206.407	8379.054	-1247.12	0.82	0.1	43.9	0	15.1	-1	-1	-1
R-2394	44192	106.18	108.38	2204.526	8377.932	-1246.92	0.35	0.07	50.6	-1	-1	-1	-1	-1
R-2394	44193	108.38	110.62	2202.611	8376.789	-1246.71	0.25	0.07	44.8	-1	-1	-1	-1	-1
R-2394	44194	110.62	112.39	2201.098	8375.887	-1246.54	0.35	0.08	48.5	-1	-1	-1	-1	-1
R-2394	44195	112.39	114.31	2199.456	8374.907	-1246.36	0.37	0.07	44.5	-1	-1	-1	-1	-1
R-2394	44196	114.31	117.46	2196.764	8373.301	-1246.05	0.39	0.04	49.6	-1	-1	-1	-1	-1
R-2394	44197	117.46	120.1	2194.507	8371.955	-1245.8	0.66	0.08	42.1	-1	-1	-1	-1	-1
R-2394	44198	120.1	122	2192.884	8370.986	-1245.61	0.53	0.07	50.5	-1	-1	-1	-1	-1
R-2394	44199	122	125.5	2189.893	8369.202	-1245.26	0.36	0.08	44.5	-1	-1	-1	-1	-1

R-2394	44200	125.5	129.5	2186.475	8367.163	-1244.86	0.4	0.07	51.5	-1	-1	-1	-1	-1
R-2394	44201	129.5	133.5	2183.057	8365.124	-1244.46	0.48	0.05	51.5	-1	-1	-1	-1	-1
R-2394	44202	133.5	137.41	2179.717	8363.131	-1244.05	0.84	0.09	51	-1	-1	-1	-1	-1
R-2394	44203	137.41	141.47	2176.25	8361.062	-1243.63	1.07	0.23	49.1	-1	-1	-1	-1	-1
R-2394	44204	141.47	143.64	2174.397	8359.957	-1243.4	1.24	0.29	49.5	-1	-1	-1	-1	-1
R-2394	44205	143.64	146	2172.381	8358.755	-1243.15	1.21	0.15	48.9	-1	-1	-1	-1	-1
R-2394	44206	146	148.71	2170.067	8357.374	-1242.86	1.03	0.08	50.4	-1	-1	-1	-1	-1
R-2394	44207	148.71	149.84	2169.103	8356.799	-1242.74	2.1	0.16	42.4	0.3	24.1	-1	-1	-1
R-2394	44208	149.84	151.05	2168.07	8356.182	-1242.61	1.48	0.18	48.7	0.01	18	-1	-1	-1
R-2394	44209	151.05	153.35	2166.106	8355.011	-1242.36	2	0.17	35.4	2.2	25	-1	-1	-1
R-2394	44210	153.35	155.19	2164.535	8354.074	-1242.16	1.55	0.11	44.6	-1	-1	-1	-1	-1
R-2394	44211	155.19	159.3	2161.027	8351.981	-1241.7	1.26	0.08	49.8	-1	-1	-1	-1	-1
R-2394	44212	159.3	163.39	2157.537	8349.899	-1241.25	0.97	0.04	49.9	-1	-1	-1	-1	-1
R-2394	44213	163.39	167.15	2154.329	8347.985	-1240.82	0.66	0.04	49	-1	-1	-1	-1	-1
R-2394	44214	167.15	169.75	2152.111	8346.661	-1240.52	0.49	0.04	51.2	-1	-1	-1	-1	-1
R-2394	44215	169.75	172.61	2149.671	8345.206	-1240.19	0.66	0.05	51.4	-1	-1	-1	-1	-1

R-2394	44216	172.61	175.92	2146.848	8343.521	-1239.81	0.99	0.05	47.7	-1	-1	-1	-1	-1
R-2394	44217	175.92	176.71	2146.174	8343.119	-1239.71	1.83	0.23	44.6	-1	-1	-1	-1	-1
R-2394	44218	176.71	179.14	2144.102	8341.883	-1239.43	0.91	0.09	44.9	-1	-1	-1	-1	-1
R-2394	44219	179.14	182.25	2141.45	8340.301	-1239.06	1.03	0.08	49.1	-1	-1	-1	-1	-1
R-2394	44220	182.25	183.17	2140.665	8339.833	-1238.95	1.8	0.27	43.7	-1	-1	-1	-1	-1
R-2394	44221	183.17	185.69	2138.517	8338.551	-1238.65	1.07	0.07	46.9	0.03	15	-1	-1	-1
R-2394	44222	185.69	187.44	2137.025	8337.661	-1238.44	1.39	0.1	35.7	0.2	20.9	-1	-1	-1
R-2394	44223	187.44	189.91	2134.919	8336.405	-1238.14	0.93	0.16	50.7	-1	-1	-1	-1	-1
R-2394	44224	189.91	190.71	2134.238	8335.998	-1238.04	0.07	4.82	46.2	-1	-1	-1	-1	-1
R-2394	44225	190.71	193.59	2131.783	8334.534	-1237.69	0.08	13.58	41.8	-1	-1	-1	-1	-1
R-2394	44226	193.59	196.56	2129.252	8333.024	-1237.32	0.47	4.15	48.2	-1	-1	-1	-1	-1
R-2394	44227	196.56	197.12	2128.775	8332.739	-1237.25	0.46	0.14	3.2	-1	-1	-1	-1	-1

APPENDIXC 4.d. R-2623 AAS geochemical data, by courtesy of Pyhäsalmi Mine Oy:

HOLE_ID	*SAMPLE_ID*	*DEPTH_FROM*	*DEPTH_TO*	*Y_COORD*	*Z_COORD*	*Z_COORD*	*CU%*	*ZN%*	*S%*	*AU ppm*	*AG ppm*	*FE%*	*PB%*
R-2623	54695	40.28	42.66				0.84	4.62	45.2	-1	-1	-1	-1
R-2623	54696	42.66	44.67				0.88	3.65	47.2	-1	-1	-1	-1
R-2623	54697	44.67	46.67				0.93	3.12	48.2	-1	-1	-1	-1
R-2623	54698	46.67	48.48				0.68	1.77	47.7	-1	-1	-1	-1
R-2623	54699	48.48	50.12				0.87	1.19	21.4	-1	-1	-1	-1
R-2623	54700	50.12	52				0.76	1.55	47.1	-1	-1	-1	-1
R-2623	54701	52	53.6				1.1	1.49	46.3	-1	-1	-1	-1
R-2623	54702	53.6	56.13				2.22	1.1	48.7	-1	-1	-1	-1
R-2623	54703	56.13	59.35				0.26	6.36	41.4	-1	-1	-1	-1
R-2623	54704	59.35	61.56				0.16	4.06	44	-1	-1	-1	-1
R-2623	54705	61.56	63.56				0.89	2.69	42.5	-1	-1	-1	-1
R-2623	54706	63.56	66.07				1.78	1.46	44	-1	-1	-1	-1
R-2623	54707	66.07	68.15				1.74	1.47	46.2	-1	-1	-1	-1
R-2623	54708	68.15	68.86				0.54	0.48	15.5	0	9	-1	-1
R-2623	54709	68.86	71.2				1.8	0.6	48.3	-1	-1	-1	-1
R-2623	54710	71.2	72.97				0.94	0.13	49.1	-1	-1	-1	-1
R-2623	54711	72.97	74.85				0.88	0.05	48.9	-1	-1	-1	-1
R-2623	54712	74.85	76.81				1.39	0.41	39.7	-1	-1	-1	-1
R-2623	54713	76.81	78.97				1.18	0.72	49.3	-1	-1	-1	-1
R-2623	54714	78.97	81				0.92	1.3	50.2	-1	-1	-1	-1
R-2623	54715	81	83				1.16	0.93	50.3	-1	-1	-1	-1
R-2623	54716	83	84.96				1.29	0.58	49.2	-1	-1	-1	-1
R-2623	54717	84.96	86.84				1.05	0.96	44	-1	-1	-1	-1
R-2623	54718	86.84	88.78				1.36	0.42	46.5	-1	-1	-1	-1
R-2623	54719	88.78	91.02				1.14	0.15	48.4	-1	-1	-1	-1

R-2623	54720	91.02	93.46	0.84	0.16	50.2	-1	-1	-1	-1
R-2623	54721	93.46	95	0.29	4.96	41.2	-1	-1	-1	-1
R-2623	54722	95	96.71	0.78	2.38	48.7	-1	-1	-1	-1
R-2623	54723	96.71	98.8	1.26	0.68	43.8	-1	-1	-1	-1
R-2623	54724	98.8	100.96	1.62	0.11	42.4	-1	-1	-1	-1
R-2623	54725	100.96	103.03	1.8	0.08	48.9	-1	-1	-1	-1
R-2623	54726	103.03	104.96	1.18	0.06	49.1	-1	-1	-1	-1
R-2623	54727	104.96	107.02	1.11	0.08	49	-1	-1	-1	-1
R-2623	54728	107.02	109.14	0.82	0.13	50.3	-1	-1	-1	-1
R-2623	54729	109.14	111.1	0.68	0.34	48	-1	-1	-1	-1
R-2623	54730	111.1	113.27	1.3	0.82	48	-1	-1	-1	-1
R-2623	54731	113.27	114.27	1.54	0.14	45.7	-1	-1	-1	-1
R-2623	54732	114.27	115.73	0.24	0.05	31.9	-1	-1	-1	-1
R-2623	54733	115.73	117.24	1.7	0.36	34.9	-1	-1	-1	-1
R-2623	54734	117.24	119	1.95	0.47	48.2	-1	-1	-1	-1
R-2623	54735	119	120.95	1.61	0.41	44.2	-1	-1	-1	-1
R-2623	54736	120.95	123	1.42	0.29	39.9	-1	-1	-1	-1
R-2623	54737	123	125	1.08	0.39	47.2	-1	-1	-1	-1
R-2623	54738	125	127.48	0.27	0.03	49	-1	-1	-1	-1
R-2623	54739	127.48	129.47	0.03	0.01	52	-1	-1	-1	-1
R-2623	54740	129.47	131.36	0.02	0.01	51.9	-1	-1	-1	-1
R-2623	54741	131.36	133.33	0.01	0.01	52.1	-1	-1	-1	-1
R-2623	54742	133.33	135.17	0.01	0.01	51.5	-1	-1	-1	-1
R-2623	54743	135.17	137	0.02	0.01	52.2	-1	-1	-1	-1
R-2623	54744	137	138.96	0.01	0.01	51.7	-1	-1	-1	-1
R-2623	54745	138.96	140.48	0.04	0.01	51.2	-1	-1	-1	-1
R-2623	54746	140.48	142.1	0.15	0.02	50.4	-1	-1	-1	-1
R-2623	54747	142.1	144.28	0.22	0.03	51.4	-1	-1	-1	-1

R-2623	54748	144.28	146.1	0.17	0.02	50.9	-1	-1	-1	-1
R-2623	54749	146.1	148.17	0.14	0.02	50.3	-1	-1	-1	-1
R-2623	54750	148.17	150.38	0.11	0.02	49.8	-1	-1	-1	-1
R-2623	54751	150.38	152.11	0.17	0.02	43.6	-1	-1	-1	-1
R-2623	54752	152.11	154.2	0.51	0.05	50.5	-1	-1	-1	-1
R-2623	54753	154.2	156.07	0.52	0.06	50.1	-1	-1	-1	-1
R-2623	54754	156.07	158.15	0.61	0.07	51.2	-1	-1	-1	-1
R-2623	54755	158.15	160	0.28	0.06	52.2	-1	-1	-1	-1
R-2623	54756	160	162	0.37	0.04	51	-1	-1	-1	-1
R-2623	54757	162	164.16	0.55	0.09	50	-1	-1	-1	-1
R-2623	54758	164.16	166.08	0.85	0.19	52.1	-1	-1	-1	-1
R-2623	54759	166.08	168	0.78	0.17	52	-1	-1	-1	-1
R-2623	54760	168	170.15	0.56	0.19	48.5	-1	-1	-1	-1
R-2623	54761	170.15	172.73	0.67	0.13	46.7	-1	-1	-1	-1
R-2623	54762	172.73	174.89	0.41	0.1	37.1	-1	-1	-1	-1
R-2623	54763	174.89	176.98	0.74	0.12	47.4	-1	-1	-1	-1
R-2623	54764	176.98	178.2	0.51	0.67	26.8	-1	-1	-1	-1
R-2623	54765	178.2	180.23	0.53	0.19	51.5	-1	-1	-1	-1
R-2623	54766	180.23	181.7	0.53	0.16	52.7	-1	-1	-1	-1
R-2623	54767	181.7	184.02	0.42	0.19	52.1	-1	-1	-1	-1
R-2623	54768	184.02	186	0.21	0.21	51.9	-1	-1	-1	-1
R-2623	54769	186	187.46	0.29	0.16	52.3	-1	-1	-1	-1
R-2623	54770	187.46	189.31	0.36	0.27	51	-1	-1	-1	-1
R-2623	54771	189.31	190.45	0.33	0.25	51.9	-1	-1	-1	-1
R-2623	54772	190.45	192.15	0.66	0.28	51.3	-1	-1	-1	-1
R-2623	54773	192.15	194.03	0.75	0.17	50.7	-1	-1	-1	-1
R-2623	54774	194.03	196.1	1.17	0.13	51.1	-1	-1	-1	-1
R-2623	54775	196.1	198.41	0.92	0.15	51.1	-1	-1	-1	-1

R-2623	54776	198.41	200.38	0.36	0.07	43.5	-1	-1	-1	-1
R-2623	54777	200.38	202.6	0.09	0.01	49.3	-1	-1	-1	-1
R-2623	54778	202.6	204.56	0.28	0.03	50	-1	-1	-1	-1
R-2623	54779	204.56	206.41	0.2	0.01	46.1	-1	-1	-1	-1
R-2623	54780	206.41	208.53	0.16	0.02	50.1	-1	-1	-1	-1
R-2623	54781	208.53	210.32	1.27	0.09	46.8	-1	-1	-1	-1
R-2623	54782	210.32	212.2	1.28	0.15	47.6	-1	-1	-1	-1
R-2623	54783	212.2	213.79	1.08	0.11	47	-1	-1	-1	-1
R-2623	54784	213.79	214.96	0.32	4.26	38.9	-1	-1	-1	-1
R-2623	54785	214.96	215.9	0.41	9.22	37.5	-1	-1	-1	-1
R-2623	54786	215.9	218.26	0.16	0.03	2	4.8	52	-1	-1

APPENDIX 4.e. R-2642 AAS geochemical data, by courtesy of Pyhäsalmi Mine Oy:

HOLE_ID	*SAMPLE_ID*	*DEPTH_FROM*	*DEPTH_TO*	*Y_COORD*	*X_COORD*	*Z_COORD*	*CU%*	*ZN%*	*S%*	*AU ppm*	*AG ppm*	*FE%*	*PB%*
R-2642	56426	0	2				0.17	0.14	52.5	-1	-1	-1	-1
R-2642	56427	2	4				0.21	0.14	52.6	-1	-1	-1	-1
R-2642	56428	4	6				0.14	0.11	52.6	-1	-1	-1	-1
R-2642	56429	6	8				0.13	0.15	52.8	-1	-1	-1	-1
R-2642	56430	8	9.3				0.08	0.14	51.6	-1	-1	-1	-1
R-2642	56432	9.3	11.3				0.18	0.12	49	-1	-1	-1	-1
R-2642	56433	11.3	12				0.28	0.29	52.1	-1	-1	-1	-1
R-2642	56434	12	13.44				0.08	0.02	44.7	-1	-1	-1	-1
R-2642	56435	13.44	15.44				0.41	0.25	51.2	-1	-1	-1	-1
R-2642	56436	15.44	17.73				0.38	0.05	50.5	-1	-1	-1	-1
R-2642	56437	17.73	20.25				1.15	0.09	45.6	-1	-1	-1	-1
R-2642	56438	20.25	22.08				1.23	0.25	46.4	-1	-1	-1	-1
R-2642	56440	22.08	25.08				0.49	11.41	39.7	-1	-1	-1	-1
R-2642	56441	25.08	27.77				0.84	3.58	45.6	-1	-1	-1	-1
R-2642	56442	27.77	29.81				0.55	7.6	39.5	-1	-1	-1	-1
R-2642	56443	29.81	30.37				0.88	0.12	4	0	76	-1	-1
R-2642	56444	30.37	32.28				0	0.01	0.3	3.3	1	-1	-1

APPENDIX 5.a. PYO-47 geophysical properties:

Drillcore	*Sample ID*	*Sample beginning*	*Sample end*	*RQD*	*Susceptibility SI-units*	*Conductivity Ωm*	*Specific gravity (kg/dm³)*
PYO-47	8336879	1.65	2.45		0.11	1000000.00	2.65
PYO-47	8336880	2.45	3.27		0.40	1000000.00	2.98
PYO-47	8336881	3.27	5.47		0.13	1000000.00	2.66
PYO-47	8336882	5.47	6.68		0.33	1000000.00	2.96
PYO-47	8336883	7.89	11		0.13	1000000.00	2.7
PYO-47	8336884	11	14.06		0.50	1000000.00	2.71
PYO-47	8336885	15	17.94		0.32	1000000.00	2.69
PYO-47	8336886	17.94	20.66		1.44	1000000.00	2.7
PYO-47	8336887	20.66	22.45		0.50	1000000.00	2.72
PYO-47	8336888	23.77	26.4		0.17	1000000.00	2.69
PYO-47	8336889	27.7	29.67		0.30	1000000.00	2.66
PYO-47	8336890	29.67	30.48		3.00	800000.00	2.78

PYO-47	8336891	30.48	32.34	0.73	1000000.00	2.8
PYO-47	8336892	32.34	36.64	0.35	1000000.00	2.7
PYO-47	8336893	36.64	38.5	0.40	1000000.00	2.68
PYO-47	8336894	41.8	42.57	1.10	1000000.00	2.71
PYO-47	8336895	42.57	42.9	20.13	1000000.00	2.74
PYO-47	8336896	42.9	44.05	25.00	1000000.00	2.76
PYO-47	8336897	44.05	47.43	1.50	1000000.00	2.69
PYO-47	8336898	47.43	48.5	0.35	1000000.00	2.99
PYO-47	8336899	48.5	50.65	1.10	1000000.00	2.67
PYO-47	8336900	69.8	73.8	3.06	1000000.00	2.84
PYO-47	8336901	73.8	78.11	9.50	1000000.00	2.89
PYO-47	8336902	78.11	79.81	0.33	1000000.00	2.91
PYO-47	8336903	79.81	82.28	14.00	1000000.00	2.89
PYO-47	8336904	82.28	84	7.00	1000000.00	2.98
PYO-47	8336905	84	86.9	1.20	1000000.00	2.91
PYO-47	8336906	87.82	89.88	2.50	1000000.00	2.96

PYO-47	8336907	89.88	91.75	0.30	1000000.00	2.81
PYO-47	8336908	93	96.8	0.23	1000000.00	2.81
PYO-47	8336909	105.72	110.72	0.25	1000000.00	2.9
PYO-47	8336910	110.72	115.72	12.20	1000000.00	2.84
PYO-47	8336911	115.72	120.55	0.45	1000000.00	2.86
PYO-47	8336912	120.55	122.4	3.55	1000000.00	2.91
PYO-47	8336913	122.4	126.48	0.21	1000000.00	2.71
PYO-47	8336914	126.48	129.86	0.50	1000000.00	2.97
PYO-47	8336915	129.86	135.5	0.23	1000000.00	2.7
PYO-47	8336916	135.5	140	0.45	1000000.00	3.09
PYO-47	8336917	140	141.9	0.11	1000000.00	2.71
PYO-47	8336918	141.9	146.45	19.00	1000000.00	2.98
PYO-47	8336919	146.45	146.8	0.60	1000000.00	2.69
PYO-47	8336920	146.8	151	0.36	1000000.00	2.97
PYO-47	8336921	151	153.95	0.90	1000000.00	2.75
PYO-47	8336922	157.14	161.88	0.25	1000000.00	2.67

PYO-47	8336923	161.88	165.35	0.26	1000000.00	2.71
PYO-47	8336924	165.35	170.35	0.32	1000000.00	2.94
PYO-47	8336925	170.35	172.43	0.32	1000000.00	2.99
PYO-47	8336926	172.43	173.75	0.60	1000000.00	2.67
PYO-47	8336927	173.75	175.2	24.60	1000000.00	2.92
PYO-47	8336928	175.2	177.2	2.20	1000000.00	2.69
PYO-47	8336929	177.2	177.94	5.20	1000000.00	2.89
PYO-47	8336930	177.94	179.73	0.50	1000000.00	2.74
PYO-47	8336931	179.73	181.17	7.00	1000000.00	2.93
PYO-47	8336932	181.17	181.89	0.60	1000000.00	2.7
PYO-47	8336933	181.89	183.69	0.20	1000000.00	2.67
PYO-47	8336934	183.69	187.44	0.21	1000000.00	2.68
PYO-47	8336935	193.5	196.08	0.60	1000000.00	2.7
PYO-47	8336936	196.08	197.05	4.50	1000000.00	2.81
PYO-47	8336937	206.42	211.42	6.00	1000000.00	2.79
PYO-47	8336938	211.42	213.97	26.90	1000000.00	2.79

PYO-47	8336939	213.97	214.84	24.90	1000000.00	2.79
PYO-47	8336940	214.84	215.66	0.80	1000000.00	2.86
PYO-47	8336941	215.66	217.33	0.05	1000000.00	2.93
PYO-47	8336942	217.33	219.45	0.08	600000.00	2.84
PYO-47	8336943	219.45	221.85	2.50	1000000.00	2.82
PYO-47	8336944	221.85	223.2	0.20	400000.00	2.83
PYO-47	8336945	223.2	228.2	0.05	1000000.00	2.72
PYO-47	8336946	228.2	233.2	0.04	1000000.00	2.72
PYO-47	8336947	233.2	237.85	0.07	1000000.00	2.69
PYO-47	8336948	237.85	241.37	0.05	1000000.00	2.72
PYO-47	8336949	241.37	243.42	0.09	1000000.00	2.79
PYO-47	8336950	253.33	256.62	0.05	600000.00	2.84
PYO-47	8336951	256.62	262.1	0.04	800000.00	2.79
PYO-47	8336952	262.1	264.95	0.08	1000000.00	2.71
PYO-47	8336953	264.95	268.57	0.07	400000.00	2.76
PYO-47	8336954	271.47	271.94	2.20	400000.00	2.82

PYO-47	8336955	271.94	276.94	0.24	1000000.00	2.81
PYO-47	8336956	276.94	280	0.08	400000.00	2.74
PYO-47	8336957	280	282.28	0.07	300000.00	2.75
PYO-47	8336958	282.28	285.17	0.06	600000.00	2.76
PYO-47	8336959	285.17	290.17	0.06	1000000.00	2.76
PYO-47	8336960	290.17	295.17	0.05	700000.00	2.8
PYO-47	8336961	295.17	300.17	0.05	600000.00	2.86
PYO-47	8336962	300.17	303.7	0.06	1000000.00	2.82
PYO-47	8336963	303.7	304.95	4.50	1000000.00	2.8
PYO-47	8336964	304.95	309.95	0.05	1000000.00	2.77
PYO-47	8336965	309.95	314.95	0.06		2.77
PYO-47	8336966	314.95	318.9	0.06		2.89
PYO-47	8336967	318.9	319.8	0.72		2.85
PYO-47	8336968	319.8	321.3	0.08		2.85
PYO-47	8336969	322	324.5	0.04		2.84
PYO-47	8336970	324.5	326.4	2.00		2.97

PYO-47	8336971	326.4	331.17	0.40	2.78
PYO-47	8336972	331.17	331.83	0.30	2.84
PYO-47	8336973	331.83	333.96	0.06	2.84
PYO-47	8336974	333.96	334.93	1.10	2.93
PYO-47	8336975	334.93	338.34	0.01	2.89
PYO-47	8336976	338.34	339.12	6.00	2.9
PYO-47	8336977	339.12	340.05	0.03	2.81
PYO-47	5920692	340.05	341.64	0.07	4.32
PYO-47	5920693	341.64	343.88	0.11	4.61
PYO-47	8336978	343.88	346.4	0.05	3.3
PYO-47	8336979	346.4	349.5	0.07	2.76
PYO-47	8336980	349.5	351.92	5.75	2.9
PYO-47	8336981	351.92	353.1	0.08	2.97
PYO-47	8336982	353.1	355.84	0.07	2.87
PYO-47	8336983	355.84	356.3	1.60	2.8
PYO-47	8336984	356.3	356.9	0.06	2.92

PYO-47	5920701	356.9	358.9	5.80	4.38
PYO-47	5920702	358.9	360.78	17.50	4.44
PYO-47	5920703	360.78	362.66	5.40	4.32
PYO-47	5920704	362.66	364.65	5.30	4.44
PYO-47	5920705	364.65	366.3	1.80	4.34
PYO-47	5920706	366.3	367.46	6.16	4.15
PYO-47	5920707	367.46	368.84	4.46	3.96
PYO-47	5920708	368.84	371.12	3.33	4.8
PYO-47	8336985	371.12	371.38	0.26	2.92
PYO-47	5920710	371.38	373.27	0.10	4.74
PYO-47	5920711	373.27	374.38	6.60	4.71
PYO-47	8336986	374.38	375.11	1.50	2.87
PYO-47	5920713	375.11	375.85	1.40	4.6
PYO-47	5920714	375.85	377.05	0.80	4.86
PYO-47	5920715	377.05	378.39	0.08	4.82
PYO-47	8337071	378.39	378.72	0.33	3

PYO-47	5920717	378.72	379.87	0.12	4.16
PYO-47	5920718	379.87	381.67	0.97	4.74
PYO-47	8337072	381.67	383.11	0.06	2.7
PYO-47	8337073	383.11	385.13	0.08	2.74
PYO-47	8337074	385.13	390.13	0.10	2.78
PYO-47	8337075	390.13	395.28	0.12	2.79
PYO-47	8337076	395.28	396.92	0.77	2.77
PYO-47	8337077	396.92	401.92	0.06	2.83
PYO-47	8337078	401.92	403.75	0.03	2.78
PYO-47	8337079	403.75	404.64	0.15	2.68
PYO-47	8337080	404.64	405.28	0.20	2.82
PYO-47	8337081	405.28	407.63	2.70	2.74
PYO-47	8337082	407.63	409.85	0.99	2.69
PYO-47	8337083	409.85	411.52	0.20	2.71
PYO-47	8337084	412.12	415.2	2.13	2.75

APPENDIX 5.b. PYO-84 geophysical properties.

Drillcore	*Sample*	*Sample beginning*	*Sample end*	*RQD*	*Susceptibility SI-units*	*Conductivity Ωm*	*Specific gravity (kg/dm³)*
PYO-84	8336291	16.6	20.3		2.60		2.68
PYO-84	8336292	20.3	22.4		1.70		2.68
PYO-84	8336293	22.4	22.77		0.20		2.84
PYO-84	8336294	22.77	23.27		4.00		2.7
PYO-84	8336295	23.27	23.67		0.40		2.97
PYO-84	8336296	23.67	25.9		4.50		2.7
PYO-84	8336297	25.9	26.95		4.19		2.69
PYO-84	8336298	27.15	28.54		5.00		2.71
PYO-84	8336299	28.54	29.15		4.10		2.67
PYO-84	8336300	29.15	29.8		0.70		2.98
PYO-84	8336301	29.8	30.88		0.50		2.69
PYO-84	8336302	37.08	38.2		0.20		2.69
PYO-84	8336303	38.2	38.8		0.20		2.79
PYO-84	8336304	38.8	39.8		1.60		2.67
PYO-84	8336305	42	42.44		3.50		2.7
PYO-84	8336306	49.82	51.23		0.43		2.69
PYO-84	8336307	51.23	52.73		0.35		2.91
PYO-84	8336308	53.15	53.8		0.40		2.93
PYO-84	8336309	53.8	54.45		0.15		2.68
PYO-84	8336310	54.45	55.05		0.40		2.91
PYO-84	8336311	58.22	58.75		0.39		2.96

PYO-84	8336312	62.16	63.03	0.01	2.59
PYO-84	8336313	63.03	63.7	0.40	2.68
PYO-84	8336314	73.9	74.5	0.26	2.95
PYO-84	8336315	74.5	76.1	0.10	2.67
PYO-84	8336316	79.1	84.81	1.82	2.66
PYO-84	8336317	85.74	86.46	0.40	2.93
PYO-84	8336318	88.5	89.8	0.10	2.6
PYO-84	8336319	89.8	91.58	0.10	2.65
PYO-84	8336320	91.78	96.78	0.08	2.65
PYO-84	8336321	96.78	98.74	0.10	2.69
PYO-84	8336322	98.74	99.74	0.76	2.91
PYO-84	8336323	99.74	105.44	0.08	2.68
PYO-84	8336324	105.44	111.1	0.09	2.66
PYO-84	8336325	111.1	111.45	0.30	2.95
PYO-84	8336326	112	112.9	0.40	2.64
PYO-84	8336327	113.2	114.2	0.10	2.65
PYO-84	8336328	114.2	115.84	0.25	2.86
PYO-84	8336329	115.84	117.13	1.50	2.71
PYO-84	8336330	117.13	118.63	0.25	2.85
PYO-84	8336331	118.63	120.09	0.20	2.69
PYO-84	8336332	120.09	120.92	0.28	2.97
PYO-84	8336333	120.92	125.92	0.07	2.71
PYO-84	8336334	125.92	131.8	5.70	2.66
PYO-84	8336335	131.8	134.36	25.00	2.8
PYO-84	8336336	134.36	136.5	0.25	2.65
PYO-84	8336337	136.5	140.13	0.11	2.67
PYO-84	8336338	142.4	144.68	5.76	2.67
PYO-84	8336339	144.68	145.97	0.30	2.91

PYO-84	8336340	145.97	147.3	0.15	2.65
PYO-84	8336341	147.3	147.7	0.40	2.95
PYO-84	8336342	147.7	150	2.60	2.66
PYO-84	8336343	150	150.28	0.49	2.98
PYO-84	8336344	150.28	151.9	0.20	2.67
PYO-84	8336345	151.9	157.13	3.25	2.65
PYO-84	8336346	157.13	158.8	0.88	2.93
PYO-84	8336347	158.8	160.35	0.05	2.63
PYO-84	8336348	160.35	161.2	0.32	2.96
PYO-84	8336349	161.2	161.8	1.71	2.88
PYO-84	8336350	161.8	163.8	0.54	2.7
PYO-84	8336351	163.8	164.9	0.80	2.89
PYO-84	8336352	164.9	167	2.00	2.69
PYO-84	8336353	167	167.4	0.39	2.93
PYO-84	8336354	167.4	168.56	1.30	2.7
PYO-84	8336355	168.56	171.8	0.27	2.69
PYO-84	8336356	171.8	173.75	0.45	2.94
PYO-84	8336357	173.75	175.55	0.17	2.67
PYO-84	8336358	175.55	176.13	16.50	2.84
PYO-84	8336359	176.13	178.76	0.18	2.68
PYO-84	8336360	178.76	179.6	27.00	2.83
PYO-84	8336361	179.6	183.85	8.00	2.71
PYO-84	8336362	183.85	185.8	0.30	2.93
PYO-84	8336363	185.8	187.52	2.20	2.68
PYO-84	8336364	187.52	188.8	1.20	2.99
PYO-84	8336365	188.8	192.3	1.70	2.66
PYO-84	8336366	192.3	194	0.35	2.98
PYO-84	8336367	194	198.15	1.70	2.68

PYO-84	8336368	198.15	199.15	0.70	3.03
PYO-84	8336369	199.15	200.1	1.60	2.66
PYO-84	8336370	200.1	201.9	0.20	2.66
PYO-84	8336371	201.9	203.6	0.10	2.71
PYO-84	8336372	203.6	208.95	0.11	2.71
PYO-84	8336373	208.95	209.75	0.26	3.01
PYO-84	8336374	209.75	211.1	0.12	2.68
PYO-84	8336375	211.1	214.95	0.40	3
PYO-84	8336376	215.5	217.67	0.35	2.97
PYO-84	8336377	218.5	221.45	0.30	2.95
PYO-84	8336378	221.98	224.1	0.38	2.95
PYO-84	8336379	224.1	225.2	0.50	2.84
PYO-84	8336380	225.2	230.2	0.35	2.97
PYO-84	8336381	230.2	233.3	0.30	2.97
PYO-84	8336382	233.3	235.55	0.20	2.76
PYO-84	8336383	235.55	240.55	0.30	2.96
PYO-84	8336384	240.55	245.55	0.30	2.94
PYO-84	8336385	245.55	250.55	0.33	2.99
PYO-84	8336386	250.55	253.35	0.34	2.99
PYO-84	8336387	253.35	254.35	25.00	2.86
PYO-84	8336388	254.35	254.78	5.00	2.69
PYO-84	8336389	254.78	255.35	0.45	2.99
PYO-84	8336390	255.35	257.45	0.07	2.68
PYO-84	8336391	258.72	260.17	28.00	2.67
PYO-84	8336392	260.17	265.6	0.55	2.96
PYO-84	8336393	265.6	266.1	0.30	2.68
PYO-84	8336394	266.1	266.7	0.25	2.86
PYO-84	8336395	266.7	269.4	2.90	2.65

PYO-84	8336396	269.4	272.4	0.13	2.72
PYO-84	8336397	272.4	274.9	0.35	2.93
PYO-84	8336398	274.9	278.09	0.11	2.68
PYO-84	8336399	278.09	278.55	0.44	2.98
PYO-84	8336400	278.55	280.75	2.10	2.66
PYO-84	8336401	280.75	282.47	0.33	2.9
PYO-84	8336402	282.47	282.97	0.10	2.67
PYO-84	8336403	282.97	283.54	0.29	2.93
PYO-84	8336404	283.54	287.7	0.12	2.69
PYO-84	8336405	287.7	289	0.31	2.96
PYO-84	8336406	289	290.1	0.10	2.66
PYO-84	8336407	290.1	292.2	0.31	2.96
PYO-84	8336408	292.2	293.1	0.13	2.64
PYO-84	8336409	293.1	298.53	0.18	2.65
PYO-84	8336410	299.43	300.65	1.54	2.67
PYO-84	8336411	300.65	312.48	0.07	2.64
PYO-84	8336412	312.48	314.37	0.36	2.7
PYO-84	8336413	314.37	315.19	2.37	2.89
PYO-84	8336414	315.19	320.52	0.15	2.68
PYO-84	8336415	320.52	324	0.15	2.67
PYO-84	8336416	324	324.8	0.05	2.64
PYO-84	8336417	324.8	326.8	0.20	2.72
PYO-84	8336418	326.8	327.9	0.24	2.7
PYO-84	8336419	327.9	328.43	0.06	2.65
PYO-84	8336420	328.43	330.91	4.75	2.74
PYO-84	8336421	330.91	334.55	0.25	2.73
PYO-84	8336422	334.55	337.75	0.46	2.63
PYO-84	8336423	338.21	341.8	0.11	2.7

PYO-84	8336424	341.8	346.38	0.21	2.67
PYO-84	8336425	349.4	351.77	1.27	2.69
PYO-84	8336426	351.77	352.37	0.30	2.68
PYO-84	8336427	353.13	355.65	0.75	2.68
PYO-84	8336428	355.65	356.3	0.81	2.77
PYO-84	8336429	356.3	360.7	3.01	3.03
PYO-84	8336430	360.7	364.47	1.21	2.91
PYO-84	8336431	364.47	368.2	0.40	2.88
PYO-84	8336432	368.2	373.2	0.40	2.9
PYO-84	8336433	373.2	375.4	0.30	2.95
PYO-84	8336434	375.4	376.85	1.00	3.1
PYO-84	8336435	376.85	378.5	0.90	2.94
PYO-84	8336436	378.5	380.47	1.00	2.73
PYO-84	8336437	380.47	381.15	2.00	2.88
PYO-84	8336438	381.15	381.65	1.22	2.75
PYO-84	8336439	381.65	383.9	2.40	2.86
PYO-84	8336440	383.9	385.15	0.55	2.89
PYO-84	8336441	385.15	385.97	1.00	3.03
PYO-84	8336442	385.97	386.41	0.67	2.93
PYO-84	8336443	386.41	391.78	0.13	2.94
PYO-84	8336444	391.78	392.33	1.50	2.91
PYO-84	8336445	392.33	396.66	0.98	2.91
PYO-84	8336446	396.66	402.05	0.10	2.64
PYO-84	8336447	402.25	403.1	0.38	2.86
PYO-84	8336448	403.1	403.8	0.22	2.74
PYO-84	8336449	403.8	404.37	0.15	2.65
PYO-84	8336450	404.37	405.15	0.33	2.79
PYO-84	8336451	405.15	407.5	0.16	2.68

PYO-84	8336452	407.5	410.7	0.33	3
PYO-84	8336453	410.7	413.7	0.55	2.92
PYO-84	8336454	413.7	417.95	0.20	2.74
PYO-84	8336455	417.95	421.3	0.25	2.88
PYO-84	8336456	421.3	422.3	0.09	2.73
PYO-84	8336457	422.3	423.5	0.20	2.67
PYO-84	8336458	423.5	424.9	1.50	2.94
PYO-84	8336459	424.9	427.65	0.29	2.74
PYO-84	8336460	427.65	430.2	0.11	2.69
PYO-84	8336461	430.2	433	0.08	2.72
PYO-84	8336462	433	433.45	0.28	2.87
PYO-84	8336463	433.45	437.3	0.11	2.76
PYO-84	8336464	437.3	441.55	0.20	2.69
PYO-84	8336465	441.55	444.85	4.60	2.99
PYO-84	8336466	444.85	445.95	0.32	2.72
PYO-84	8336467	445.95	447.74	4.08	2.95
PYO-84	8336468	447.74	449.08	3.43	2.79
PYO-84	8336469	450.85	454.65	0.83	2.69
PYO-84	8336470	454.65	456.75	0.25	2.85
PYO-84	8336471	456.75	457.5	2.32	2.72
PYO-84	8336472	457.5	461.5	1.96	2.98
PYO-84	8336473	461.5	462.15	0.87	2.91
PYO-84	8336474	462.15	463.9	0.50	2.76
PYO-84	8336475	463.9	467.05	0.47	2.81
PYO-84	8336476	467.05	467.5	0.20	2.87
PYO-84	8336477	467.5	469.35	10.90	2.92
PYO-84	8336478	469.35	471	0.10	2.68
PYO-84	8336479	471	471.65	0.30	2.92

PYO-84	8336480	471.65	473.24	0.08	2.67
PYO-84	8336481	473.24	476.55	0.12	2.69
PYO-84	8336482	476.55	478.6	0.11	2.65
PYO-84	8336483	479.05	481.8	0.10	2.68
PYO-84	8336484	481.8	482.3	0.14	2.7
PYO-84	8336485	482.3	483.3	0.22	2.82

APPENDIX 5.c. R-2242 geophysical properties, by courtesy of Pyhäsalmi Mine Oy:

Drillcore	*Depth (m)*	*RQD*	*Susceptibility SI-units*	*Conductivity Ωm*	*Specific gravity (kg/dm³)*
R-2242	0	0	10.00	1000000.00	2.8
R-2242	4	100	50.00	100000.00	2.78
R-2242	7	84	20.00	100000.00	2.82
R-2242	10	0	20.00	100000.00	2.88
R-2242	13	36	20.00	100000.00	2.88
R-2242	16	100	1000.00	100000.00	2.77
R-2242	19	63	40.00	1000000.00	2.97
R-2242	22	100	25.00	1000000.00	3.01
R-2242	25	78	25.00	100000.00	2.7
R-2242	28	100	35.00	100000.00	3
R-2242	31	100	30.00	1000000.00	3.02
R-2242	34	89	20.00	100000.00	3.07
R-2242	37	100	30.00	100000.00	2.93
R-2242	40	49	25.00	100000.00	2.87
R-2242	43	100	15.00	1000000.00	2.89
R-2242	46	100	60.00	10000.00	2.71
R-2242	49	10	35.00	100000.00	3
R-2242	52	94	25.00	1000000.00	2.92
R-2242	55	100	25.00	1000000.00	2.9
R-2242	58	76	25.00	1000000.00	2.86
R-2242	61	22	150.00	100000.00	2.71

R-2242	64	92	200.00	1000000.00	2.73
R-2242	67	100	10.00	100000.00	2.79
R-2242	70	100	35.00	1000000.00	3.08
R-2242	73	87	25.00	1000000.00	3.09
R-2242	76	15	30.00	100000.00	2.66
R-2242	79	100	800.00	100000.00	2.74
R-2242	82	91	50.00	1000000.00	2.69
R-2242	85	100	200.00	100000.00	2.73
R-2242	88	100	75.00	100000.00	2.86
R-2242	91	88	300.00	100000.00	2.79
R-2242	94	53	1500.00	1000000.00	2.69
R-2242	97	39	1500.00	1000000.00	2.67
R-2242	100	58	1000.00	100000.00	2.67
R-2242	103	100	30.00	1000000.00	2.94
R-2242	106	57	150.00	100000.00	2.7
R-2242	109	56	150.00	1000000.00	2.69
R-2242	112	91	800.00	1000000.00	2.68
R-2242	115	78	600.00	1000000.00	2.68
R-2242	118	88	15.00	100000.00	2.78
R-2242	121	52	200.00	1000000.00	2.73
R-2242	124	76	1500.00	1000000.00	2.69
R-2242	127	47	850.00	100000.00	2.67
R-2242	130	45	1500.00	1000000.00	2.69
R-2242	133	80	45.00	1000000.00	2.82
R-2242	136	100	35.00	100000.00	2.95
R-2242	139	71	35.00	1000000.00	2.67
R-2242	142	94	20.00	100000.00	2.71
R-2242	145	100	30.00	100000.00	2.98

R-2242	148	100	20.00	100000.00	2.8
R-2242	151	100	150.00	10000.00	2.98
R-2242	154	100	200.00	100000.00	2.73
R-2242	157	100	45.00	1000000.00	2.82
R-2242	160	100	250.00	100000.00	2.75
R-2242	163	51	3000.00	100000.00	2.8
R-2242	166	92	40.00	100000.00	2.91
R-2242	169	100	50.00	100000.00	2.66
R-2242	172	100	100.00	100000.00	2.99
R-2242	175	92	200.00	1000000.00	2.97
R-2242	178	88	55.00	100000.00	3.2
R-2242	181	100	30.00	100000.00	2.97
R-2242	184	100	150.00	10000.00	2.94
R-2242	187	100	40.00	100000.00	2.95
R-2242	190	100	40.00	100000.00	2.99
R-2242	193	94	40.00	10000.00	2.95
R-2242	196	100	90.00	1000000.00	3.02
R-2242	199	100	150.00	100000.00	2.97
R-2242	202	100	45.00	100000.00	2.98
R-2242	205	58	0.00	100000.00	2.64
R-2242	208	100	50.00	100000.00	2.82
R-2242	211	91	1500.00	1000000.00	2.74
R-2242	214	100	90.00	10000.00	3.08
R-2242	217	54	1000.00	1000000.00	2.68
R-2242	220	100	30.00	1000000.00	2.7
R-2242	223	100	400.00	1000000.00	2.7
R-2242	226	65	10.00	1000000.00	2.69
R-2242	229	100	10.00	1000000.00	2.68

R-2242	232	100	0.00	1000000.00	2.62
R-2242	235	100	10.00	1000000.00	2.75
R-2242	238	93	1500.00	1000000.00	2.75
R-2242	241	92	15.00	1000000.00	2.76
R-2242	244	93	70.00	1000000.00	2.75
R-2242	247	81	0.00	1000000.00	2.66
R-2242	250	100	15.00	1000000.00	2.94
R-2242	253	86	5.00	1000000.00	2.81
R-2242	256	65	10.00	1000000.00	2.83
R-2242	259	100	300.00	1000000.00	2.93
R-2242	262	100	30.00	1000000.00	2.93
R-2242	265	72	35.00	1000000.00	3
R-2242	268	100	200.00	100000.00	2.94
R-2242	271	100	850.00	1000000.00	2.9
R-2242	274	100	100.00	1000000.00	3.05
R-2242	277	100	30.00	1000000.00	2.89
R-2242	280	100	30.00	1000000.00	2.96
R-2242	283	74	0.00	1000000.00	2.65
R-2242	286	97	0.00	1000000.00	2.65
R-2242	289	100	0.00	1000000.00	2.63
R-2242	292	100	35.00	1000000.00	2.98
R-2242	295	67	10.00	1000000.00	2.88
R-2242	298	100	150.00	1000000.00	2.96
R-2242	301	100	0.00	1000000.00	2.74
R-2242	304	100	10.00	1000000.00	2.79
R-2242	307	93	1500.00	1000000.00	2.67
R-2242	310	100	0.00	1000000.00	2.67
R-2242	313	100	60.00	1000000.00	2.93

R-2242	316	100	0.00	1000000.00	2.61
R-2242	319	100	20.00	1000000.00	2.88
R-2242	322	100	25.00	1000000.00	2.88
R-2242	325	100	5.00	1000000.00	2.66
R-2242	328	100	0.00	1000000.00	2.63

APPENDIX 5.d. R-2252 geophysical properties, by courtesy of Pyhäsalmi Mine Oy:

Drillcore	*Depth (m)*	*RQD*	*Susceptibility SI-units*	*Conductivity Ωm*	*Specific gravity (kg/dm^3)*
R-2252	3	81	10.00	1000000.00	2.7
R-2252	6	48	1000.00	1000000.00	2.71
R-2252	9	81	550.00	1000000.00	2.74
R-2252	12	95	900.00	1000000.00	2.67
R-2252	15	88	0.00	1000000.00	2.67
R-2252	18	78	350.00	100000.00	2.91
R-2252	21	99	150.00	1000000.00	2.72
R-2252	24	86	5.00	1000000.00	2.71
R-2252	27	100	5.00	1000000.00	2.71
R-2252	30	87	0.00	1000000.00	2.68
R-2252	33	95	15.00	100000.00	2.78

R-2252	36	100	0.00	1000000.00	2.67
R-2252	39	100	0.00	1000000.00	2.74
R-2252	42	100	950.00	1000000.00	2.88
R-2252	45	96	20.00	100000.00	2.79
R-2252	48	0	2000.00	1000000.00	2.78
R-2252	51	83	1000.00	1000000.00	2.69
R-2252	54	92	0.00	1000000.00	2.84
R-2252	57	100	20.00	1000000.00	2.84
R-2252	60	95	30.00	1000000.00	2.7
R-2252	63	94	10.00	1000000.00	2.72
R-2252	66	10	0.00	1000000.00	2.62
R-2252	69	94	0.00	1000000.00	2.62
R-2252	72	94	0.00	1000000.00	2.63
R-2252	75	92	0.00	1000000.00	2.61
R-2252	78	92	15.00	1000000.00	2.94
R-2252	81	86	15.00	1000000.00	2.92

R-2252	84	88	100.00	1000000.00	2.7
R-2252	87	96	250.00	1000000.00	2.67
R-2252	90	85	2000.00	1000000.00	2.89
R-2252	93	96	25.00	1000000.00	2.92
R-2252	96	62	15.00	1000000.00	2.65
R-2252	99	80	100.00	1000000.00	2.62
R-2252	102	83	40.00	1000000.00	2.84
R-2252	105	86	250.00	1000000.00	3.03
R-2252	108	72	80.00	100000.00	2.9
R-2252	111	87	950.00	1000000.00	2.67
R-2252	114	94	5.00	1000000.00	2.65
R-2252	117	20	20.00	1000000.00	2.7
R-2252	120	79	300.00	1000000.00	2.65
R-2252	124	61	35.00	1000000.00	2.94
R-2252	127	95	100.00	1000000.00	3.02
R-2252	130	95	85.00	1000000.00	2.9

R-2252	133	95	35.00	100000.00	3.01
R-2252	136	96	3000.00	1000000.00	2.93
R-2252	139	89	90.00	1000000.00	2.94
R-2252	142	87	3500.00		2.91
R-2252	145	85	0.00	1000000.00	2.61
R-2252	148	50	0.00	1000000.00	2.66
R-2252	151	97	100.00	100000.00	3.04
R-2252	154	100	60.00	100000.00	2.94
R-2252	157	100	40.00	1000000.00	3.01
R-2252	160	89	60.00	100000.00	2.93
R-2252	163	100	100.00	1000000.00	2.89
R-2252	166	95	5.00	1000000.00	2.66
R-2252	169	100	5.00	1000000.00	2.68
R-2252	172	100	0.00	1000000.00	2.67
R-2252	175	100	15.00	1000000.00	2.67
R-2252	178	80	10.00	1000000.00	2.64

R-2252	181	95	45.00	1000000.00	2.76
R-2252	184	95	1000.00	1000000.00	2.72
R-2252	187	96	1500.00	1000000.00	2.72
R-2252	190	87	650.00	1000000.00	2.7
R-2252	193	54	1000.00	1000000.00	2.72
R-2252	196	86	1000.00	1000000.00	2.68
R-2252	199	72	4500.00	1000000.00	2.92
R-2252	202	86	1500.00	1000000.00	2.91
R-2252	205	72	700.00	1000000.00	2.72
R-2252	208	91	1000.00	1000000.00	2.68
R-2252	211	91	15.00	1000000.00	2.68
R-2252	214	86	10.00	1000000.00	2.7
R-2252	217	95	0.00	1000000.00	2.63
R-2252	220	86	0.00	1000000.00	2.59
R-2252	223	95	10.00	1000000.00	2.68
R-2252	226	95	30.00	1000000.00	2.67

R-2252	229	93	10.00	1000000.00	2.68
R-2252	232	85	0.00	1000000.00	2.66
R-2252	235	76	5.00	1000000.00	2.69
R-2252	238	89	20.00	1000000.00	2.67
R-2252	241	100	0.00	1000000.00	2.68
R-2252	244	82	0.00	1000000.00	2.6
R-2252	247	74	15.00	1000000.00	2.74
R-2252	250	93	15.00	1000000.00	2.68
R-2252	253	89	5.00	1000000.00	2.64
R-2252	256	92	25.00	1000000.00	2.66
R-2252	259	58	900.00	1000000.00	2.68
R-2252	262	30	250.00	1000000.00	2.67
R-2252	265	72	450.00	100000.00	2.66
R-2252	268	88	250.00	1000000.00	2.7
R-2252	271	83	0.00	1000000.00	2.64
R-2252	274	100	50.00	1000000.00	2.72

R-2252	277	65	35.00	1000000.00	2.72
R-2252	280	100	10.00	1000000.00	2.7
R-2252	283	93	0.00	1000000.00	2.63
R-2252	286	100	10.00	1000000.00	2.67
R-2252	289	78	10.00	1000000.00	2.71
R-2252	292	100	0.00	1000000.00	2.65
R-2252	295	100	0.00	1000000.00	2.63
R-2252	298	100	10.00	1000000.00	2.71
R-2252	301	100	0.00	1000000.00	2.61
R-2252	304	100	10.00	1000000.00	2.7
R-2252	307	100	5.00	1000000.00	2.68
R-2252	310	54	3000.00	1000000.00	2.93
R-2252	313	93	2000.00	1000000.00	2.92
R-2252	316	88	80.00	1000000.00	2.82
R-2252	319	87	2000.00	1000000.00	2.9
R-2252	322	100	2000.00	1000000.00	2.98

R-2252	325	100	7500.00	1000000.00	2.99
R-2252	328	100	6000.00	1000000.00	2.96
R-2252	331	100	5500.00	1000000.00	2.88
R-2252	334	32	4500.00	1000000.00	2.85

APPENDIX 5.e. R-2394 geophysical properties:

Drillcore	*Sample*	*Sample beginning*	*Sample end*	*RQD*	*Susceptibility SI-units*	*Conductivity Ωm*	*Specific gravity (kg/dm3)*
R-2394		0.94	1		1.24		2.71
R-2394		1.76	1.91		0.50		2.67
R-2394		2.74	2.89		0.57		2.67
R-2394		3.75	3.85		0.55		2.74
R-2394		4.71	4.81		0.20		2.81
R-2394		5.55	5.66		12.60		2.71
R-2394		6.57	6.69		14.50		2.7
R-2394		7.46	7.6		3.50		2.72
R-2394		8.38	8.48		1.70		2.93
R-2394		9.31	9.48		0.45		2.93
R-2394		10.33	10.43		0.80		2.96
R-2394		11.25	11.35		5.20		2.68

R-2394	12.17	12.36	1.20	2.75
R-2394	13.14	13.33	6.00	2.71
R-2394	14.12	14.22	6.00	2.7
R-2394	15.8	15.95	7.40	2.68
R-2394	16.12	16.19	8.80	2.68
R-2394	17.04	17.17	1.00	2.97
R-2394	18.07	18.14	0.19	2.76
R-2394	18.98	19.02	0.30	2.92
R-2394	19.94	20.05	0.28	2.76
R-2394	20.88	20.98	0.15	2.7
R-2394	21.78	21.92	0.20	2.73
R-2394	22.75	22.87	0.60	2.67
R-2394	23.78	23.83	0.31	2.82
R-2394	24.66	24.75	0.15	2.69
R-2394	25.61	25.71	6.00	2.74
R-2394	26.67	26.79	1.00	2.69

R-2394	27.55	27.6	0.34	2.69
R-2394	28.28	28.35	3.52	2.69
R-2394	29.2	29.25	7.95	2.71
R-2394	30.28	30.35	3.08	2.72
R-2394	31.16	31.21	1.28	2.69
R-2394	32.16	32.2	0.26	2.96
R-2394	33.09	33.17	0.10	2.67
R-2394	34	34.12	0.65	2.69
R-2394	35	35.09	0.25	2.77
R-2394	35.89	35.96	0.14	2.67
R-2394	36.75	36.87	0.41	2.7
R-2394	37.8	37.85	0.08	2.66
R-2394	38.7	38.78	0.19	2.71
R-2394	39.4	39.57	4.25	2.69
R-2394	40.57	40.67	4.20	2.79
R-2394	41.02	41.1	0.25	3.07

R-2394	44162	41.45	43.66	10.90	4.71
R-2394	44164	45.35	46.71	2.00	4.73
R-2394	44165	46.71	47.63	1.68	3.06
R-2394	44166	47.63	50.83	1.20	4.58
R-2394	44167	50.83	52.63	0.98	4.73
R-2394	44168	52.63	55.37	4.20	4.69
R-2394	44169	55.37	56.94	5.76	4.66
R-2394	44170	56.94	59.29	3.30	4.83
R-2394	44171	59.29	62.1	4.80	4.71
R-2394	44172	62.1	63.72	1.20	4.85
R-2394	44173	63.72	65.5	0.85	4.69
R-2394	44174	65.5	69.45	0.94	4.84
R-2394	44175	69.45	71.57	0.21	4.81
R-2394	44176	71.57	74.31	1.08	4.72
R-2394	44177	74.31	76.49	0.39	4.71
R-2394	44178	76.49	78.95	0.08	4.84

R-2394	44179	78.95	79.67	3.50	3.18
R-2394	44180	79.67	81.24	8.50	4.84
R-2394	44181	81.24	84.07	0.31	4.78
R-2394	44182	84.07	85.58	16.80	2.97
R-2394	44183	85.58	88.46	0.70	4.79
R-2394	44184	88.46	89.27	1.00	4.9
R-2394	44185	89.27	92.32	1.35	4.85
R-2394	44186	92.32	95.25	0.08	4.85
R-2394	44187	95.25	97.71	0.05	4.85
R-2394	44188	97.71	98.33	0.99	2.87
R-2394	44189	98.33	103.25	0.53	4.81
R-2394	44190	103.25	104	0.93	2.88
R-2394	44191	104	106.18	4.93	4.63
R-2394	44192	106.18	108.38	0.15	4.76
R-2394	44193	108.38	110.62	0.16	4.76
R-2394	44194	110.62	112.39	0.76	4.81

R-2394	44195	112.39	114.31	0.15	4.81
R-2394	44196	114.31	117.46	0.09	4.65
R-2394	44197	117.46	120.1	35.50	4.53
R-2394	44198	120.1	122	0.08	4.85
R-2394	44199	122	125.5	0.09	4.89
R-2394	44200	125.5	129.5	0.08	4.77
R-2394	44201	129.5	133.5	0.11	4.93
R-2394	44203	137.41	141.47	0.12	4.82
R-2394	44204	141.47	143.64	0.12	4.81
R-2394	44205	143.64	146	0.04	4.84
R-2394	44206	146	148.71	0.16	4.83
R-2394	44207	148.71	149.84	16.50	4.82
R-2394	44208	149.84	151.05	2.35	4.87
R-2394	44209	151.05	153.35	0.23	4.86
R-2394	44210	153.35	155.19	1.61	4.54
R-2394	44211	155.19	159.3	0.15	4.75

R-2394	44212	159.3	163.39	0.10	4.82
R-2394	44213	163.39	167.15	0.06	4.93
R-2394	44214	167.15	169.75	0.10	4.71
R-2394	44215	169.75	172.61	0.05	4.8
R-2394	44216	172.61	175.92	0.63	4.79
R-2394	44217	175.92	176.71	1.00	4.57
R-2394	44218	176.71	179.14	1.66	4.63
R-2394	44219	179.14	182.25	0.58	4.64
R-2394	44220	182.25	183.17	0.41	4.6
R-2394	44222	185.69	187.44	0.93	4.7
R-2394	44223	187.44	189.91	4.80	4.83
R-2394	44224	189.91	190.71	2.35	4.69
R-2394	44225	190.71	193.59	5.40	4.66
R-2394	44226	193.59	196.56	0.24	4.89
R-2394	44227	196.56	197.12	0.33	2.86
R-2394		198.31	198.37	4.50	2.66

R-2394	199.34	199.43	3.85	2.69
R-2394	200.07	200.16	3.73	2.68
R-2394	201.09	201.17	5.53	2.68
R-2394	202	202.07	0.33	3.02
R-2394	202.38	202.5	0.65	2.66
R-2394	203.63	203.68	6.83	2.67
R-2394	204.75	204.86	3.21	2.64

APPENDIX 5.f. R-2623 geophysical properties:

Drillcore	*Sample*	*Sample beginning*	*Sample end*	*RQD*	*Susceptibility SI-units*	*Conductivity Ωm*	*Specific gravity (kg/dm³)*
R-2623		0.7	0.89		0.41	1000000.00	2.93
R-2623		1.69	1.82		0.39	>1000000	2.97
R-2623		2.75	2.845		0.59	>1000000	2.95
R-2623		3.77	3.845		1.06	>1000000	2.96
R-2623		4.49	4.68		0.34	>1000000	2.93
R-2623		5.54	5.755		2.03	>1000000	2.96
R-2623		6.54	6.7		0.88	>1000000	2.96
R-2623		7.46	7.64		31.50	>1000000	2.93
R-2623		8.47	8.56		1.01	1000000.00	2.92
R-2623		9.28	9.47		2.51	>1000000	3.02
R-2623		10.31	10.44		0.70	1000000.00	2.96
R-2623		11.18	11.31		7.75	>1000000	2.69

R-2623		12.22	12.28		10.70	>1000000	2.77
R-2623		13.12	13.27		0.20	>1000000	2.72
R-2623		14.12	14.24		0.29	>1000000	2.81
R-2623		14.88	15.09		0.34	800000.00	2.78
R-2623		16.02	16.11		0.33	600000.00	2.96
R-2623		17	17.07		0.53	600000.00	2.94
R-2623		17.77	17.94		1.13	>1000000	3.09
R-2623		18.71	18.88		7.03	>1000000	2.74
R-2623		19.58	19.74		0.18	>1000000	2.71
R-2623		20.35	20.54		0.28	>1000000	2.73
R-2623		21.48	21.66		1.02	>1000000	2.72
R-2623		22.53	22.65		0.45	200000.00	2.91
R-2623		23.35	23.55		7.13	>1000000	2.7
R-2623		24.4	24.53		0.08	>1000000	2.67
R-2623		25.38	25.53		0.30	>1000000	2.7
R-2623		26.3	56.45		0.38	>1000000	2.94

R-2623		27.09	27.37	2.15	800000.00	2.87
R-2623		28.8	28.98	20.24	>1000000	2.8
R-2623		29.16	29.24	0.64	>1000000	2.66
R-2623		30.01	30.12	0.09	>1000000	2.68
R-2623		30.95	31.07	0.23	>1000000	2.83
R-2623		31.85	32.02	0.83	>1000000	2.66
R-2623		32.83	32.96	0.20	>1000000	2.66
R-2623		33.77	33.91	2.20	>1000000	2.72
R-2623		34.8	34.94	2.57	>1000000	2.71
R-2623		35.64	35.74	4.29	>1000000	2.74
R-2623		36.37	36.69	8.51	>1000000	2.68
R-2623		37.55	37.71	6.80	>1000000	2.7
R-2623		38.43	38.57	6.95	>1000000	2.7
R-2623		39.35	39.51	19.70	>1000000	2.77
R-2623	54695	41.5	41.62	17.80	0.60	4.68
R-2623	54696	44.19	44.35	6.00	0.03	4.8

R-2623	54697	46.37	46.52	0.15	0.04	4.71
R-2623	54698	47.19	47.32	1.30	0.60	4.78
R-2623	54699	49.22	49.33	0.16	80.00	3.34
R-2623	54700	50.87	51.11	0.50	0.04	4.69
R-2623	54701	52.55	52.75	9.59	2.00	4.74
R-2623	54702	54.71	54.84	0.20	5.00	4.82
R-2623	54703	56.56	56.73	1.00	0.04	4.76
R-2623	54704	60.47	60.61	3.70		4.73
R-2623	54705	62.95	63.2	24.30		4.64
R-2623	54706	65.35	65.56	2.00		4.8
R-2623	54707	66.07	66.21	1.00		4.78
R-2623	54708	68.29	68.35	1.85		2.9
R-2623	54709	69.73	69.9	0.15		4.87
R-2623	54710	71.39	71.5	0.27		4.81
R-2623	54711	74.2	74.32	0.15		4.73
R-2623	54712	75.52	75.45	0.16		4.85

R-2623	54713	77.52	77.67	4.57	4.87
R-2623	54714	80.35	80.51	0.44	4.87
R-2623	54715	82.03	82.16	2.03	4.88
R-2623	54716	83.87	84.02	1.30	4.76
R-2623	54717	85.11	85.13	0.28	4.57
R-2623	54718	87.69	87.88	0.17	4.8
R-2623	54719	89.95	90.14	2.90	4.88
R-2623	54720	91.42	91.58	0.10	4.83
R-2623	54721	94.71	94.9	0.57	4.62
R-2623	54722	95.35	95.53	1.07	4.81
R-2623	54723	97.04	97.24	1.53	4.58
R-2623	54724	99.6	99.8	4.22	4.65
R-2623	54725	101.25	101.35	0.33	4.77
R-2623	54726	104	104.15	0.18	4.76
R-2623	54727	105.9	106.06	1.67	4.86
R-2623	54728	108.73	108.93	9.56	4.86

R-2623	54729	109.68	109.84	12.10	4.83
R-2623	54730	110.4	111.58	2.07	4.69
R-2623	54731	113.41	113.5	0.12	4.86
R-2623	54732	115.38	115.53	0.06	2.87
R-2623	54733	116.86	117.01	0.42	3.77
R-2623	54734	117.65	117.79	0.27	4.86
R-2623	54735	120.02	120.2	2.62	4.71
R-2623	54736	122.87	123	0.52	4.76
R-2623	54737	124.71	124.86	2.30	4.88
R-2623	54738	125.65	125.79	0.08	4.83
R-2623	54739	127.8	128	0.05	4.92
R-2623	54740	131.04	131.16	0.05	4.93
R-2623	54741	132.56	132.75	0.05	4.93
R-2623	54742	134.2	134.32	0.05	4.93
R-2623	54743	135.98	136.14	0.12	4.92
R-2623	54744	137.98	138.13	0.10	4.89

R-2623	54745	139.53	139.73	0.12	4.9
R-2623	54746	141.65	141.83	0.20	4.68
R-2623	54747	143.56	143.71	0.18	4.9
R-2623	54748	145.45	146.6	0.15	4.87
R-2623	54749	147.5	147.64	1.10	4.83
R-2623	54750	150.13	150.34	1.75	4.8
R-2623	54751	151.34	151.51	1.74	4.73
R-2623	54752	153.22	153.9	0.80	4.74
R-2623	54753	154.49	154.68	0.68	4.78
R-2623	54754	156.86	157.01	0.59	4.81
R-2623	54755	158.84	158.91	0.12	4.95
R-2623	54756	160.83	161	0.14	4.64
R-2623	54757	162.76	162.89	0.15	4.86
R-2623	54758	165.1	165.29	0.54	4.86
R-2623	54759	166.44	166.58	0.54	4.88
R-2623	54760	168.39	168.5	0.12	4.93

R-2623	54761	171.88	172.08	0.75	4.9
R-2623	54762	173.56	173.78	0.16	4.86
R-2623	54763	175.13	175.29	0.23	4.79
R-2623	54764	177.63	177.75	0.31	2.91
R-2623	54765	176.64	179.76	0.15	4.89
R-2623	54766	181.25	181.44	0.13	4.87
R-2623	54767	182.35	182.54	0.14	4.94
R-2623	54768	185.33	185.52	0.09	4.95
R-2623	54769	187.26	187.47	0.14	4.91
R-2623	54770	187.82	188.07	0.14	4.95
R-2623	54771	190.03	190.23	0.16	4.95
R-2623	54772	191.28	191.42	0.30	4.91
R-2623	54773	192.8	193	10.10	4.8
R-2623	54774	195.26	195.38	0.60	4.84
R-2623	54775	196.71	196.38	1.00	4.95
R-2623	54776	198.75	198.87	0.14	4.91

R-2623	54777	200.76	200.92	4.72	4.89
R-2623	54778	204.41	204.56	0.42	4.85
R-2623	54779	205.51	205.76	1.10	4.73
R-2623	54780	207.4	207.56	0.02	4.84
R-2623	54781	209.08	209.2	0.09	4.61
R-2623	54782	211.83	212	1.80	4.69
R-2623	54783	213.04	213.14	0.16	4.79
R-2623	54784	214.77	214.96	63.00	4.62
R-2623	54785	215.25	215.42	29.60	4.55
R-2623	54786	216.26	216.44	13.30	2.94
R-2623		216.65	216.82	8.81	2.85
R-2623		217.49	217.7	15.50	2.69
R-2623		218.59	218.66	7.80	2.72
R-2623		219.59	219.63	4.42	2.68
R-2623		220.37	220.52	0.44	2.75
R-2623		221.3	221.44	2.69	2.76

R-2623	222.24	222.41	2.65	2.73
R-2623	223.09	223.25	0.10	2.71

APPENDIX 5.g. R-2642 geophysical properties:

Drillcore	*Sample*	*Sample beginning*	*Sample end*	*RQD*	*Susceptibility SI-units*	*Conductivity Ωm*	*Specific gravity (kg/dm³)*
R-2642	56426	0	2		0.07		4.93
R-2642	56427	2	4		0.12		4.97
R-2642	56428	4	6		0.13		4.94
R-2642	56429	6	8		0.05		4.98
R-2642	56430	8	9.3		0.06		4.95
R-2642	56432	9.3	11.3		1.83		4.81
R-2642	56433	11.3	12		0.07		4.84
R-2642	56434	12	13.44		0.07		4.82
R-2642	56435	13.44	15.44		0.57		4.92
R-2642	56436	15.44	17.73		0.05		4.81
R-2642	56437	17.73	20.25		0.94		4.64
R-2642	56438	20.25	22.08		1.96		4.67

R-2642	56440	22.08	25.08	2.68	4.66
R-2642	56441	25.08	27.77	2.36	4.83
R-2642	56442	27.77	29.81	18.70	4.74
R-2642	56443	29.81	30.37	0.15	2.63
R-2642	56444	30.37	32.28	0.21	2.69
R-2642		33.12	33.25	0.14	2.73
R-2642		34.17	34.29	0.09	2.68
R-2642		35.06	35.14	1.00	2.96
R-2642		36.09	36.17	2.22	2.69
R-2642		37.1	37.2	12.10	2.69
R-2642		39.02	39.14	0.25	2.86
R-2642		39.96	40.03	0.40	2.96
R-2642		40.98	41.03	6.70	2.75
R-2642		41.45	41.58	0.36	2.94
R-2642		42.41	42.53	0.40	2.94
R-2642		43.49	43.57	8.22	2.74

R-2642	44.22	44.32	0.40	2.98
R-2642	45.2	45.33	0.69	2.9
R-2642	46.24	46.32	8.35	2.68
R-2642	47.13	47.22	11.40	2.69
R-2642	48.05	48.15	14.20	2.7
R-2642	49.18	49.26	1.58	2.76
R-2642	50.1	50.24	13.00	2.69
R-2642	50.83	50.97	1.88	2.69
R-2642	51.98	52.07	1.65	2.93
R-2642	52.96	53.05	11.60	2.7
R-2642	53.73	53.84	10.10	2.69
R-2642	54.57	54.64	11.10	2.68
R-2642	55.38	55.43	9.75	2.69
R-2642	56.51	56.59	16.60	2.69
R-2642	57.58	57.67	12.30	2.71
R-2642	58.42	58.52	8.60	3.03

R-2642	59.25	59.43	9.45	2.75
R-2642	60.25	60.35	0.49	2.88
R-2642	61.35	61.47	12.20	2.75
R-2642	62.34	62.44	0.05	2.6
R-2642	63.29	63.4	10.50	2.61
R-2642	64.17	64.27	0.41	2.96
R-2642	64.62	64.69	5.05	2.63
R-2642	65.43	65.55	14.80	2.62
R-2642	66.38	66.47	1.89	3.07
R-2642	67.66	67.75	0.04	2.64
R-2642	68.55	68.68	0.11	2.62
R-2642	69.41	69.5	0.15	2.68
R-2642	70.4	70.55	13.50	2.68
R-2642	71.41	71.49	11.30	2.7
R-2642	72.34	72.4	0.36	2.9
R-2642	73.27	73.39	5.41	2.82

R-2642	74.32	74.39	4.58	2.71
R-2642	75.25	75.34	5.44	2.81
R-2642	76.21	76.27	0.19	2.65
R-2642	77.07	77.18	0.12	2.61
R-2642	78.06	78.16	0.45	2.93
R-2642	78.86	79	2.73	2.92
R-2642	79.88	80	1.08	2.62
R-2642	80.92	80.98	0.17	2.76
R-2642	81.75	81.9	1.28	2.72
R-2642	82.7	82.86	0.34	3
R-2642	83.83	83.92	0.74	2.7
R-2642	84.82	84.89	5.84	2.71
R-2642	85.77	85.85	9.77	2.71
R-2642	86.72	86.8	9.55	2.7
R-2642	87.6	87.7	7.75	2.72
R-2642	88.56	88.66	5.61	2.72

R-2642	89.52	89.66	3.41	2.74
R-2642	90.52	90.64	3.63	2.72
R-2642	91.39	91.61	5.89	2.7
R-2642	92.51	92.57	0.18	2.75
R-2642	93.42	93.5	0.33	2.73
R-2642	94.32	94.44	0.75	2.95
R-2642	95.2	95.4	0.17	2.68
R-2642	96.11	96.3	0.40	2.96
R-2642	97.18	97.27	0.64	2.73
R-2642	98	98.2	0.19	2.72
R-2642	99	99.18	1.28	2.77
R-2642	99.97	100.12	39.10	2.96
R-2642	100.9	100.05	5.99	2.91
R-2642	101.94	102.03	0.15	2.71
R-2642	102.84	102.98	0.18	2.71
R-2642	103.74	103.93	0.70	2.74

R-2642	104.5	104.62	0.49	2.93
R-2642	105.58	105.73	0.24	2.8
R-2642	106.61	106.71	0.50	2.69
R-2642	107.52	107.66	3.20	2.69
R-2642	108.55	108.63	2.51	2.69
R-2642	109.35	109.56	0.53	2.69
R-2642	110.3	110.45	0.59	2.67
R-2642	111.3	111.51	0.69	2.7
R-2642	112.26	112.42	0.42	2.72
R-2642	113.23	113.41	0.86	2.69
R-2642	114.26	114.35	0.41	2.88
R-2642	115.12	115.29	0.42	3
R-2642	116.1	116.2	0.41	2.9
R-2642	117	117.17	3.60	2.84
R-2642	117.89	118.05	1.52	2.8
R-2642	118.85	119	1.65	2.68

R-2642	119.85	119.95	0.13	2.71
R-2642	120.83	120.93	0.09	2.71
R-2642	121.69	121.85	0.15	2.73
R-2642	122.34	122.48	0.13	2.69
R-2642	123.63	123.7	0.25	2.7
R-2642	124.61	124.67	0.92	2.88
R-2642	125.42	125.64	3.55	2.87
R-2642	126.01	126.12	1.40	2.85

APPENDIX 6. General features of main ore types in Pyhäsalmi VMS deposit (Imaña, 2003):

Ore types	*Ore sub-types*	*Sulphide association*	*Gangue association*	*Sulphide content*	*Primary and diagenetic textures*	*Distribution*	*Deformation*
Massive Pyrite (MP)	Mosaic Cataclastic	py>>po, cpy	cal, tre, ser, qtz	90-95%	Massive, recrystallized, annealed very coarse porphyroblasts 0.22cm. Relicts of host facies.	Core of Deep Orebody	Brittle (cataclasis)
Spotty Massive Pyrite (SMP)	Coarse grained Fine grained	py>>cpy>>sph	cal, dol, tre, act, mt, ant.	70-85%	Colloform, crustified and replacement textures. Fine grained pervasive replacement. Diagenetic banding, breccias and veins. Relicts of host facies.	Stratigraphically above massive pyrite ore	Elongated seggregations boudinage, veins D1-D2 folding.
A_Cu Pyrite (AP)		py>>sph, cpy	bar, cal, wo.	90%	Strongly cataclastic, clast supported breccia, massive. Relicts of host facies.	Transition between SMP and AZ. Tectonized areas.	Brittle (cataclasis) locally, mylonitic and pressure solution mob.
A Zinc (AZ)	Disseminated Banded Brecciated	py, sph>>cpy	qtz, bar, mt, cal, gnt, ank, ser	46-60%	Dissemination, fine grained banded suplhides. Irregular brecciation.	Inner part of the Zn rich solid model. Thicker at fold hinge.	Less recrystallized and deformed unit. Ductile banding.
B Zinc (BZ)	Porphyroclastic Mylonitic	py>sph, >>cpy	bar, cal, anh, sil	>60%	Porphyroclastic breccias, banding mylonitic sulphide horizons.	External part of Deep Ore along main thrust faults.	Strong brecciation, cataclasis.
Remobilised Sulphides (REM)	Cpy-po, silica-cpy-gal-asp, Silica-anhydrite sulphides	cpy, po>>gal, asp, tet, py	qtz, anh, >>act, mt.	50-95%	Veins, veinlets, irregular seggregations, pervasive replacements in rock inclusions.	Randomly, and mainly filling fractures within rock inclusions and adjacent country rocks.	Veining along retrograde shear zones.